THE MATURATION OF BACTERIOPHAGE ΦX174 - THE ISOLATION AND CHARACTERIZATION OF SUBVIRAL PARTICLES

Thesis by

Robert George Rohwer

In Partial Fulfillment of the Requirements

For the Degree of

Doctor of Philosophy

California Institute of Technology

Pasadena, California

1974

(Submitted December 19, 1974)

Acknowledgements

It has been my observation in the course of my education that the human environment of a normal individual is the single most important determinant of his intellectual development. I therefore consider myself fortunate to have had so many excellent teachers from whom to learn, especially about learning, and upon whom I could model my own behavior. From the very first there was my father who could always venture a hypothesis if not an answer to every question. He also ruled (and still does rule) the family dinner table, a daily ritual of family debate and discussion of some contemporary issue, often in the sciences, that formed an important part of my education. A lack of scientifically oriented elementary school teachers was more than compensated for by Ruthy Poston, the mother of a good friend, who encouraged or, in some cases at least, tolerated the unorthodox enquiry into the natural history of the earth and its creatures that only young boys could have devised. Later it was my older friend and constant companion, Buddy Cummings, who served as my mentor in sort of a "peer group teaching" arrangement that was highly rewarding for both of us. We survived the building of radios, airplanes, rockets, robots and bombs together.

Jack Janosek, my high school biology teacher, considered me a natural in the sciences but had to make me into a swimmer - a perceptive and generous action on his part for which I will always be grateful. I shall always admire Hettie Kimble's scholarship and the example of her own self-discipline which I have since discovered is a useful quality for learning other difficult subjects besides Latin.

I was of course exposed to many excellent teachers at the

University of Wisconsin but for the most part under rather impersonal circumstances. For that reason it was especially rewarding to have been a member of Professor Robert M. Bock's research group during my junior and senior years. I am particularly indebted to Steve Leppla with whom I worked my junior year for his excellent instruction in biophysical techniques and his patience with my inexperience.

My long stay at Caltech has been filled with friends and excellent teachers almost too numerous to mention. I was especially fortunate to have experienced the last years of the "torture" fraternity. After the departure of the last of the league giants, Clyde Hutchison, Mike Nesson, and John Sedat, a few of us, Moise Eisenberg, Lloyd Smith and myself, tried to carry on the traditions but we were in the end no match for the rigors of that practice and it seems with maybe a single exception to have died out. I carried out my early experimentation under the watchful tutelage of John Sedat and Marshall Edgell. I am especially grateful to John Sedat for "the rule", "the ropes", and other bits of unusual wisdom. John Kiger and John Newbold also provided valued friendship and advice during those first years. Many enjoyable evenings were spent with the Eisenbergs, Ludwigs, Jamiesons and Preers. John Jamieson will always be a scholar and a scientist regardless of what he does for a living. The Preers should also be acknowledged for their infectious political involvement and the simple political lesson that often one can enormously extend one's franchise merely by expressing one's opinions.

Those first years of my graduate career were also spent in the happy company of my wife, Kathy. But, as is so often the case in our

highly diversified and accessible culture, offering as it does so many possibilities for personal development, we grew and changed but not together and our interests, hopes and desires diverged as we sought fulfillment following the paths closest to our true natures. It is a melancholy, if understandable, thing that this happens so often in our contemporary society.

With the departure of John Newbold I became senior graduate student, a position for which I was groomed, possibly to the chagrin of RLS and others, by Clyde Hutchison. Among many memorable associations in these latter years was an especially enjoyable collaboration with Tony Zuccarrelli in guiding three successive undergraduate laboratory classes through the de novo isolation and characterization of new bacteriophage systems from sewerage in "Andromeda Strain" fashion. I hope that in the end we at least mutually understand our respective arguments on the relationship of science and religion, determinism and free will. Akio Fukuda and I had an occasional opportunity to collaborate in the lab but many more enjoyable collaborations over Saki. Never was a baby's bottle warmed with more care. Akio along with Nicole Truffaut provided a refreshing touch of dignified intellectualism to the laboratory and were the source of many stimulating discussions. Lloyd Smith has always been a reliable source of amazement and the Smithwicks a reliable source of friendship-when-in-need, for which I among many others am very grateful. Then of course there is Uncle Jim who made the Irish conflict understandable if all the more tragic by the example of his own irrepressible if somewhat violent nature. Others that I must mention are the Espelie-Millers and Amy and Paul Lee. Tim

Livermore provided two summers of welcome company and assistance in the lab.

Providing a sense of continuity to Caltech's highly mobile population and a stable perspective on the world in general, Mrs. Johnstone has been, by the example of her life, a humbling point of comparison for my own, and a testimony to the incredible power of love in some human relationships. Maybe when my final exam is over we will finally be able to keep our date to the Roller Derby.

I want to thank Robert L. Sinsheimer for supervising my research with that delicate mixture of guidance and knowing restraint that permits one to discover one's own follies without letting them become disasters, and to relish one's triumphs as one's own. (This is a powerful, if sometimes inefficient, pedigogical method, and it saddens me that it is now being abandoned in the interests of financial expediency.) When brought to bear on one's research problems, his perceptive criticism, combined with a seemingly limitless knowledge of molecular biology, could discover any weakness or untried possibility, a sometimes traumatic experience in group seminar. This critical challenge constituted a high standard against which to measure one's own research and refine one's own scientific perception.

I have also received valuable if sometimes conflicting counseling from Clair Patterson and Dan McMahon. "Pat" has been for me the personification of the pure scientist - a man so in love with knowledge that he cannot even be distracted from its pursuit by his own success. His uncompromising and incorruptible scholarship are for me an example of academia at its best. He has been generous and kind in his advice

and I hope that he will be equally understanding if I am unable to meet his high expectations. Where would we all be without Dan McMahon as advisor, psychiatrist, confessor and friend to help us through difficult times. It was Dan that pointed out to me that an experiment that fails time after time is trying to tell you something.

It was Floyd Humphrey who introduced me to sailing, enabling me to endulge a life long desire if only to whet my appetite. We have become the good friends that only the shared adventure of fast passages, night dives and excellent conversation and drink can make of two people. Later John Smart and I shared many similar experiences, often made all the more exciting by the absence of Floyd's experience. Other good friends in that sailing cameraderie were John Flory, Al Jesaitis, Ellen Elliott, Dave McMurchie, Lois Smith, and when we were fortunate enough to have his company Dr. Beckman, who so generously permitted us to sail the Aries even when his commitments did not permit him to join us.

Unfortunately, the burden of thesis writing must also be shared by those whom we would least have burdened. I owe my deepest gratitude to Ellen for sustaining me throughout with her love.

As must be evident by now I fell in love with Caltech and the people here and it is perhaps no wonder that I have never been in any particular hurry to leave. I have enjoyed my research in part because I have enjoyed my surroundings. I can't be sure that I would ever find it so pleasant elsewhere.

Acknowledgement of Financial Support and Justification of Research

I would also like to acknowledge the patronage of this research effort by the people of the United States of America through the aegis of the National Institutes of Health and the United States Public Health Service. Moreover, because of the public nature of this support and the chronic public impatience with the use of public funds to support the study of esoteric subjects, such as my own, I would also like to take this opportunity to present my own justification for these efforts, hoping to persuade at least the limited public of my own friends and relatives (the people who are most likely to want to see, if not read, this thesis) that it is in the interests of mankind and perhaps even a mandate of our human heritage to conduct enquiries such as these, both for the sake of the knowledge they produce and, for the more pragmatic person, the applications that can inevitably be derived from them.

First I will consider the justification of my own efforts in terms of their application to the solution of human problems. I must emphasize that my own research is in no way unique in its potential relevance to the solution of human problems or in the significance of its contribution to human knowledge. It is only one small part of a much larger effort. By citing the possible future significance of this one small effort I hope to convince the reader that all basic research (much of which is necessarily conducted in small obscure studies such as this) harbors within the framework of a larger ongoing effort a similar promise of applicability.

The virus ϕX174 has no natural impact upon human health. It does not infect people and its beneficial enteric host bacterium easily acquires an immunity to its assault. In fact it is considered so innocuous that it has been approved for injection into infants for the study of their immune response (234). As a consequence it may seem somewhat misguided to have directed such an immense effort at understanding this virus and how it works. However, it is this very harmlessness combined with its small size and simplicity that makes this virus so valuable due to the ease with which it can be studied. Research on ϕX174 has, in the absence of the cumbersome precautions necessary with pathogenic organisms, progressed rapidly to a rather complete understanding of many aspects of its infection process. These studies have then served as models for the investigation of more complex and dangerous viruses by permitting one to proceed more directly to the most fruitful lines of experimentation in more demanding systems.

Several of the experimental approaches developed during the course of my own research on ϕX174 will, hopefully, contribute in this way to a better understanding of viruses of more direct significance to human welfare. The first two years of my graduate study were devoted to a study of the antigenic structure of ϕX174. One of the experimental approaches developed in the course of that research enables one to measure the number of inactivating antigens per phage particle, the antibody-phage association constant and the molecular concentration of inactivating antibody in crude serum. This method is generally applicable to the measurement of these same parameters in other viruses as well, including pathogenic ones and the information so obtained

could eventually be very helpful in the design of vaccines and other antiviral strategies. Other immunological experiments conducted during that study provided some insight into the mechanism by which antibody inactivates virus - another process which, when completely understood, could contribute significantly to the control of viral disease.

The major emphasis of my research, along with that of several others, has been to understand how the new ϕX174 viruses are assembled from their constituent parts. After several years of investigation those of us who have been studying this problem are still at the very beginnings of a complete understanding.

What I have gained in return for many tedious trials and setbacks is an appreciation of the delicate and uniquely viral nature of the morphogenetic process. The viral specific nature of this process in turn suggests that a thorough understanding of morphogenesis could result in potentially far reaching consequences for human health and welfare in the form of viral-specific anti-viral drugs. This is because a useful anti-microbial agent must be able to attack the microbe without damaging the host. This condition can be satisfied most easily if the agent disrupts some microbial process (in this case viral morphogenesis) not shared by the host. Penicillin is an example of an antibiotic drug that works in this way against certain bacteria. The penicillin molecule interferes with a uniquely bacteriological function, cell wall synthesis, and kills bacteria without harming the host. (Animal cells do not have cell walls.)

Unfortunately, there are very few antibiotic drugs that attack uniquely microbial functions. Most common antibiotics disrupt analogous

vital functions in the animal and bacterial cell alike. They owe their effectiveness to the greater susceptibility of the bacteria to the toxic effects of the drug. It is unlikely that drugs analogous to these will ever be discovered for viruses. This is because viruses use the host biosynthetic apparatus to carry out almost all of their own biosynthetic functions. Any drug that disrupts these processes, as many of the existing antibiotics do, will damage the virus and host equally severely. This is undoubtedly a major contributing factor to the lack of safe antibiotic type drugs that are effective against viral infections (204).

What is needed is a unique viral function against which to direct a viral specific drug therapy. As suggested earlier the viral maturation process is a priori a uniquely viral function against which viral specific antiviral agents might be developed. It is my hope that my observations will contribute to the eventual solution of this problem.

Having considered several possible ways in which my own research may eventually contribute to the solution of human problems, it is now necessary to emphasize that I forsaw none of these possibilities at the time I initiated these projects. My original, and in large part continuing, interest in the antigenic structure of the ϕX particle, the mechanism of inacitvation by antibody, and the morphogenetic process has had virtually nothing to do with any hope or expectation of the direct or indirect applicability of the results of these studies to the control of viral disease. These justifications for my research arose after the fact of having already conducted it.

My original interest in ϕX174 was purely academic. ϕX was

considered by many at the time I began my graduate work to be the simplest possible model for living systems. I was sure that the infection process held the greatest promise for the first completely mechanistic explanation of a living form. At the time I joined Dr. Sinsheimer's group I had no idea as to what particular aspect of that problem I would be involved with, but rather only the expectation that I would be a part of a historic effort to understand a living organism totally in terms of physical laws. As a consequence I have been motivated in my work purely by a desire to know how viruses work, not by how this information can be applied. It was only during the last stages of this effort that I realized, quite accidentally, what some of the practical consequences might ultimately be. I was, of course, happy to have thought of these ideas, certainly because they may benefit mankind in some way, but also because they provide a justification for continuing research in this area, an endeavor that I should like to remain a part of.

However, I do not think that such a justification, based upon an expectation of applicability, should be necessary for the continued support of basic research. This is because the basis for this justification may not exist or simply may not occur to anyone at the time that a study is begun. This is often the case. The investigator seldom knows in advance where his enquiry will lead him and yet this does not in any way affect the ultimate applicability of his research to the solution of human problems. For example, the contribution of the study of phage morphogenesis to the eventual chemical interdiction of viral diseases would be the same whether or not we thought of a justi-

fication for that study this year or the year we discover a viral specific disruptive chemical or a particularly weak link in the maturation process which suggests an anti-viral strategy.

Thus the nature of basic research is such that it can only be meaningfully directed at understanding a phenomenon. One can seldom predict what practical rewards may accrue from such understanding, but historically we know that every major technological achievement of our civilization has been founded upon the observations and enquiries of individuals who were, in the tradition of basic research, seeking to understand some phenomenon apart from any application that might result.

To the academician, at least, basic research can be justified without any reference to eventual applicability at all. For these people basic research is conducted in the interest of advancing the realm of collective human experience. It is this contribution to the cultural heritage of man, rather than the eventual applicability of their research to human problems, that is most meaningful to these individuals. They have joined a quest for knowledge which as it continues to grow brings man ever closer to either confronting or assuming control of his own destiny. In this sense basic research is, for those who can appreciate it, a continuing high adventure on the frontiers of human experience, and, as such, these adventures are worthy of collective support from the human community, for it is these continuing quests (not only in science) that give collective meaning and purpose to our existence. We can merely survive or we can grow and evolve by the process of cultural evolution. If we choose the latter course we must try to know all things. As we proceed, we can only hope that what we

learn will lead, as well, to the continued improvement of the human condition and our constantly increasing effectiveness as human beings.

Abstract

A search was conducted for possible intermediates in the assembly of bacteriophage ϕX174. Artificial lysates of ϕX174 infected cells labeled with either amino acids or nucleotides were fractionated by velocity sedimentation and the viral DNAs and infection specific proteins analysed by recentrifugations and electrophoreses. Infection specific proteins were detected by comparing the incorporation patterns of differentially labeled infected and uninfected cells. Many experiments employed ^{3}H, ^{14}C and ^{32}P labels simultaneously and an exact solution to the discriminator ratios equations for three channel scintillation counting was derived to process these data.

A major proportion of the phage structural proteins that had not yet been incorporated into phage was observed in a very unstable 111S particle composed of ϕX proteins F, G and D all three of which are also required for ϕX SS DNA synthesis. The 111S particle does not appear to contain DNA. The D protein, present in large proportional amounts, is not found in whole virions. Depending upon the storage buffer, the 111S particle degrades into 12S (F,G protein), 9S (G protein) and 2.5S (D protein) subunits. These same particles are also observed in whole lysates. However, conditions can be found for which the 9S and 12S particles are not present suggesting that they may be 111S particle decomposition artifacts as opposed to *in vivo* particles. The properties of the 111S particle are those expected of a procapsid although this role in the infection has not been demonstrated. Analysis of the proteins in the 70S region of the gradient revealed that a similar D protein containing particle (distinct from the 70S lysis artifact)

sediments there.

Approximately 10% of the total ϕX replicative intermediate DNA in these gradients sedimented in the 70S - 114S regions. After deproteinization this DNA resedimented at the slower velocities expected for free replicative intermediates, indicating that it may have been associated with ϕX proteins. This associated protein moiety is obscured by the much more extensively labeled pools of whole virus, 111S particle and the 70S lysis artifact. It could, however, be the same as the 111S particle.

A radioimmunoassay was developed for ϕX viral proteins and was employed to show that replicating intermediates in SS DNA synthesis (sedimenting from 20 - 30S), but not the "resting" RF II form DNA, are tightly complexed with a ϕX viral antigen. A major peak (the 20S particle) of infection specific protein also sediments in this region. However any association of the DNA replicative intermediates with this protein peak is too fragile to account for the serum binding result. The concentration of DNA-binding antigen is below the resolving power of the amino acid labeling technique.

The infection specific 20S protein peak contains ϕX gene F protein, lesser amounts of other infection-specific components and a host protein (the major constituent); the host protein is also observed to sediment at 20S in uninfected cells. This protein has a molecular weight of about 67,000 daltons and is one of three ϕX stimulated host proteins with molecular weights greater than that of the largest ϕX coded protein, A'.

The ϕX174 literature is reviewed with an emphasis on those

observations that bear upon the ϕX174 assembly process. A model of the ϕX maturation process incorporating the major features of our present knowledge is proposed as a working hypothesis for future study.

Table of Contents

General Introduction (cont.)

Materials and Methods (cont.)

Materials and Methods (cont.)

Results (cont.)

GENERAL INTRODUCTION

The infection of bacteria by the small DNA phage ϕX174 has been the subject of 15 years of intensive study in numerous laboratories around the world (1,181). Many of the molecular species involved in the infection have been carefully characterized with respect to function as well as structure, with the result that most of the central features of the infection process are now quite well understood. However, there does remain one notably large discontinuity in our conception of the ϕX life cycle and it is the structures and events occurring during this morphogenetic stage of the infection process that have been the subject of this investigation. This introduction will emphasize those aspects of the ϕX structure and function that bear most directly upon the morphogenetic process. For other reviews of the ϕX174 infection process see Sinsheimer (2,3), and for complete reviews and bibliographies on viral morphogenesis see Eiserling (4) and Bancroft (5).

Structure of the ϕX174 Virion

The most obvious and easily purified component of the infection, and therefore, the most thoroughly characterized, is the infective particle or virion. A careful consideration of the structure, physical properties, and biological function of the virion provides important insights into the processes by which, and the constraints under which, it is assembled.

The Virion Proteins

The virion is comprised of a covalently closed, single stranded circle of DNA (13,14,26) which is enclosed in an icosahedral protein shell constructed from four major proteins, F, G, H and J, and several minor ones. The twelve vertices of the icosahedron bear small mushroom shaped projections termed "spikes" (17,18,19). Edgell et al. (16) devised a method whereby the spikes (as identified by electron microscopy) could be selectively removed from the virion by means of a 4 M-urea treatment. Polyacrylamide gel electrophoresis was then used to determine the protein compositions of the spikes and the spikeless virion (termed the capsid by Edgell et al.). In this way the spikes were shown to be composed of G and H proteins. The icosahedral sphere or capsid was shown to be constructed of F protein. The J protein was found with both structures.

The icosahedral symmetry of the virus was originally established by electron microscopy (17,18,19). Since then this symmetry has been shown to be consistent with the stoichiometry of the protein subunits as well. Thus, the molecular ratios of F, G and H proteins are

60:60:12, respectively (8,11,20). It is thought that the 60 gene F proteins constitute the 60 identical structural subunits that are required for construction of the simplest possible icosahedron (6) and that gene G proteins are arranged in pentamers which are located at the icosahedral vertices as part of the spike projection. The twelve molecules of H protein are expected to be located at the vertices as well, one H per vertex.

Burgess (11) noted that the existence of a single H protein per vertex would belie the five-fold symmetry of the spike unless the protein binds one of five equivalent sites in such a way as to sterically prevent additional binding of H protein. In order for this binding to occur without disrupting the five-fold symmetry arrangement between the G protein pentamer and the F protein shell, from which the virion presumably derives considerable structural stability, the H protein binding must either be interior to, exterior to, or in a pore formed at the center of the five-fold symmetry axis of the F and G protein shell. Indirect evidence suggests both an external and an internal exposure for this protein--a property that would be compatible with its location in a pore traversing the virion shell.

Conditional lethal mutants in gene H give rise, when grown under restrictive conditions, to noninfectious particles (7,8,9,10,68, 71) containing infectious DNA (9,10,68). One particle sediments slightly slower, 105S-107S, than the wt infective virion, 114S, and contains unit length viral DNA (7,67) and 80-85% of the DNA infectivity (9). Another particle, derived from the 105S particle (71), sediments at 70S, and eighty-five percent of its DNA is in the form of fragmented

viral single strands (7,67,71). Electrophoresis of the defective particles shows them to be lacking the H protein (8,9). On the other hand, electron microscopy shows the 107S particle to be indistinguishable from infective particles (9). Hutchison, in the absence of molecular weight data for these proteins, interpreted this to mean that the H protein was a minor component of the spike added at a late stage of assembly (9). In fact, gene H protein contributes 27% of the protein mass to a spike constructed of one H protein of MW 37,000 and five G proteins of MW 20,500. (Molecular weights are from 12.) One might expect that the loss of a protein of this relative size would have a significant impact upon the spike morphology, unless, of course, it occupied some interior position in the particle.

Mayol & Sinsheimer (8) observed a relative enrichment in G protein compared to F protein in gene H-defective particles. This could account for their morphological similarity to wt particles if the additional G protein was bound to the spike. However, this enrichment was not observed by Benbow et al. in another gene H mutant (12).

Hutchison has shown that restrictive lysates of am23, a mutant in gene H (15) (which was incorrectly assigned to gene G at the time the experiment was performed) do not contain serum blocking power (9). This suggests that the protein bears inactivating antigens. Presumably the H protein would have to be on the exterior of the particle to elicit an antibody response. [This interpretation is complicated somewhat by the observation that lysates of am9, gene G, also do not contain serum blocking power (9).]

The H defective particle is also incapable of absorbing to bacteria in spite of its seemingly normal morphology (2,7,21,84). By comparison, empty phage coats prepared from infective phage particles absorb efficiently and specifically to the normal ϕX hosts (32). [The limited increases in host range observed for empty coats can be conveniently explained by the change in the electrostatic properties of the virion after the loss of its DNA (32,84).] The inability of the H defective particle to absorb to E. coli argues strongly for an external locus for the H protein as well as its involvement in the host recognition and absorption process.

Jazwinski et al. (22,23) have shown that several molecules of H protein are tightly bound to the viral DNA, such that they are resistant to phenol extraction. The protein label enters the cell along with the infecting single strand DNA and remains associated with the parental RF throughout the infection. However, for an as yet undetermined reason, these researchers have not yet been able to extract the RF-associated label as intact H protein.

An association of the H protein with the virional DNA, as well as the insensitivity of the spike morphology to its loss, would seem to argue for an internal H locus, whereas its association with the spike (loss in 4 M-urea), its possible antigenicity, and its effect on absorption to bacteria would suggest an external exposure. All of these observations could be accommodated by a model in which the H protein resides in a pore at the center of the spike. In this position it could bind DNA on its interior end and be exposed to antibody recognition at its exterior end without

disrupting the five-fold symmetry of the G and F protein interaction. The electron microscopic correlate of such a structure has been observed by Tromans & Horne (19) in relatively crude preparations of ϕX174.

The gene H composition of highly purified phage is somewhat variable (see Results). Gene H is, among the capsid proteins, particularly sensitive to the harshness with which a sample is prepared for SDS acrylamide gel electrophoresis. It completely disappears from the acrylamide gel pattern after exposure to 100°C in 9 M-urea for greater than 10 minutes, whereas this treatment does not seriously affect the other virion proteins (R. Rohwer, unpublished). Zuccarelli et al. (77) and Godson (20) have also noted this variability and Burgess, Mayol & Sinsheimer, and Godson find that gene H is present in slightly less than 12 copies per virion (8,11,20). This sensitivity may account for the handling problems encountered by Jazwinski.

The H protein also electrophoreses in close proximity to the gene A product in SDS acrylamide gels and can only be reliably identified in the presence of markers for each of these genes. It will be shown later that there is approximately one copy of gene A product per virion in highly purified phage. As a consequence, it is possible that these two proteins have been confused in Jazwinski's analysis.

Several efforts to reconstitute infectious particles by in vitro complementation of the gene H-defective particles or capsids derived from 4 M-urea have proved unsuccessful (C. A. Hutchison, III & M. H. Edgell, unpublished results; E. Siden, personal communication).

The behavior of the smallest virion protein, defined by the am6 mutation as a ϕX gene product and tentatively assigned to cistron J

(12) (see discussion below), suggests that it is internally located. After 4 M-urea disruption of the virion, it distributes with both the capsid and spike fractions (16), suggesting that it may leak out of the interior of the particle after removal of the spikes. Its high mobility in several electrophoresis systems suggests a small molecular weight, but just how small has not been accurately determined. Edgell et al. (16) note that it must have a molecular weight larger than 200 daltons, the molecular weight range of the polyamines, or it would elute from their gels during staining. Burgess (11), Benbow et al. (12), and Mayol & Sinsheimer (8), estimate its molecular weight as 5,000, 9,000 and 15,000, respectively. Possibly due to an unusual amino acid composition, the mass contribution of J protein is also variable in the hands of different experimenters (8,11,12,52; R. Rohwer, unpublished). As a consequence of the uncertainty surrounding its molecular weight and its mass contribution of infective phage, the virional stoichiometry of J protein is as yet undetermined. In this regard, it should be noted that there may be viral proteins which function enzymatically or serve to stabilize the DNA, or which are fortuitously trapped inside the virion during maturation that do not contribute to the structure of the icosahedron and therefore do not have to satisfy the stoichiometric expectations of that structure.

Experiments presented in the Results demonstrate that the J protein is very lysine-rich indicating that it may be basic. Small size and basicity in turn suggest that J protein may serve to neutralize the acid charge on the DNA, both in conjunction with some DNA condensation step during ϕX maturation and later intravirionally.

Experiments by Maclean & Hall (17) suggest that the viral DNA that is extruded from disrupted particles is stabilized by protein inasmuch as it has, when observed by electron microscopy, the smooth contours of nucleoprotein as opposed to the less rigid conformation of deproteinized viral DNA. Also the strand width of shadowed preparations of extruded DNA is too great to be accounted for by SS DNA alone.

On the other hand, the observation that infective DNA is packaged into uninfective particles in the absence of J protein (in restrictive lysates of am6) indicates that this protein does not play a significant role in either the maturation process or the structure of the virion, but rather is essential for infectivity. These particles have not been inspected in the electron microscope but their protein composition is normal except for the absence of J protein (12).

Several viruses (4,211,212,213,214,215,216,218) have been demonstrated to undergo proteolytic cleavage of the principal capsid component as a step in the viral maturation process. In the case of ϕX174 a splitting of the gene F peak occasionally is observed during the SDS gel electrophoresis of infected lysates from UV irradiated cells (R. Rohwer, unpublished; L. Miller, personal communication). This splitting could be due to a protease-induced difference in the molecular weight of cytoplasmic and virional F protein. If such a cleavage were to occur during ϕX morphogenesis, the "J protein" might merely be a consequence of that proteolysis rather than the gene J product itself, which, presumably, would have effected the hydrolysis.

In addition to the four main virion proteins several other ϕX proteins, most notably A and D proteins, as well as a few host proteins, copurify with the phage particle in amounts of from 1 to 0.01 copy per phage (R. Rohwer, unpublished). It is not known whether these proteins play a functional role in either the structure of the virion or the early stages of infection, or whether they are instead merely trapped fortuitously within the capsid during phage maturation. It should be noted, however, that proteins present in stoichiometric quantities of less than one may still have some essential role in the infection, as the specific infectivity of purified ϕX174 preparations is seldom greater than 0.2 (11,32,181; Results) and this may be the consequence of a limiting concentration of some essential component.

Organization of the Intravirional DNA

Several lines of evidence suggest that the viral DNA is localized inside the protein coat. The intact virion is insensitive to exposure to DNase or streptomycin sulfate, whereas both of these reagents destroy the infectivity to spheroplasts of the deproteinized DNA (17,19,28,29,30,31,32,33).

Several procedures exist by which the viral DNA can be partially or completely removed from the virion without changing its appearance in the electron microscope (9,17,24,31). One would not expect this to be the case if the viral DNA were a major structural component of the viral envelope. Exposure to high temperature (17,33), concentrated ammonium sulfate (17), storage in Tris buffer (24), or anti-ϕX antiserum (28,29,30; R. Rohwer, unpublished), results in the

loss of infectivity to whole cells and the partial extrusion of the DNA from the virion as indicated by sedimentation behavior, DNase sensitivity, electron microscopy, and infectivity to spheroplasts. Abortive infection of cell wall extracts gives rise to a similar particle, but in this case the extruded DNA has been fragmented and is no longer infectious (25,31). The infection itself gives rise to a completely empty coat (32). The majority of the defective particles from restrictive lysates of cells infected with gene H mutants also contain extruded DNA. It is thought that they arise from an inherent inability of the gene H-defective 105S particle to contain its DNA (7,9).

In all cases that have been checked the virion itself sustains the disruption with no great change in its external appearance in the electron microscope (9,17,24,31). This indicates that the viral envelope per se does not require some internal DNA lattice for its own structural integrity. The spikeless particles prepared by 4 M-urea treatment also retain their morphological integrity even though varying amounts of DNA have been extruded from them (16). This indicates that the structure of the F protein capsid is also independent of the viral DNA. These observations do not exclude the possibility that the viral DNA plays some role in the assembly of these structures, but merely indicates that, once assembled, the DNA is no longer needed to maintain them.

In those disrupted particles that have been well characterized, the extruded DNA amounts to 70-80% of the SS circle, indicating that the bulk of the DNA is not tightly bound to the protein envelope. On the other hand, the extruded SS does not dissociate completely from the

particle, and even after DNase degradation of the exposed DNA tail, a significant proportion of the original DNA remains with the protein particle (7,16,24,25,32,33,130,181). This suggests that a portion of the DNA may be bound rather tightly to the capsid. However, the base composition (25) and sequence specificity (130) of this residual DNA, and its saturation plateau when hybridized against ϕX messenger RNA produced in vitro (7), are identical to those of ϕX viral DNA, indicating that no unique region of the DNA is binding.

ϕX shows a strong, if not exclusive, preference for its own DNA or closely related DNAs in the packaging process. In genomic masking experiments with the filamentous phage fd, only 0.02 to 0.05% of the ϕX phenotypic progeny from mixed infections packaged fd DNA, and only 2 to 4% of the phenotypic fd packaged ϕX DNA, even though both of these phage DNAs are single stranded circles and have very similar molecular weights (37). By comparison, the mixed infections of ϕX174 and the closely related phage S13 produce phenotypically mixed, infectious progeny which presumably package either parental DNA, although this has not been determined explicitly (9,34). ϕX174 and S13 share one small region of highly homologous DNA (4.7% of the genome) and the rest of their DNA shows an average homology of 64% (35; J. L. Compton, personal communication). By comparison, ϕX174 and unrelated fd would not be expected to have homologous DNA sequences. It is conceivable that the highly conserved sequence in the ϕX174 and S13 DNAs results from the interaction of this sequence with phage proteins, possibly in conjunction with phage morphogenesis.

The DNA itself is packed into the particle in such a way that distal parts of the circle are brought into close proximity to each other, such that they can be crosslinked by UV radiation (40). It is not known whether or not identical regions of the DNA are compacted together in all virions.

It is conceivable that the DNA might be organized in some regular way by the H protein. The very strong binding of H protein to SS DNA observed by Jazwinski (22,23) would be expected to occur at specific DNA loci. If these proteins were then associated with the spikes, the H binding loci of the DNA would be fixed to the vertices of the icosahedron, effecting some regularity in the intravirional organization of the DNA.

The spontaneous discharge of the SS DNA, observed as a consequence of the disruptive procedures described above, indicates that the free energy of dissociation of the infectious particle is substantial and that the DNA must be constrained within the capsule. However, the extent of this constraint is apparently very dependent upon the molecular environment of the particle. Dann-Markert et al. (24) could partially reverse the DNA extrusion from defective particles generated by storage in Tris buffer by addition of Mg^{++} to the buffer. This process was itself reversible.

It is still an open question as to whether the phage DNA is injected spontaneously into the cell. Injection can occur in the presence of lethal concentrations of KCN and NaN_3, but the fact that the injected DNA is converted immediately to the double-stranded parental replicative form indicates that the triphosphate pools have

not been exhausted even under these harsh conditions, and that cellular energy, perhaps in the form of minus strand replication, may have assisted the injection (21,42,43,89). When DNA synthesis has been inhibited prior to infection by thymine starvation of a thymine auxotrophic host, the infecting DNA is recovered in the single-stranded form. However, in this case there is no assurance that cellular ATP was not involved (43,47). This same ambiguity is associated with the observation that SS DNA is recovered from certain host strains that are defective in DNA replication (dnaB ts, 122) when the infection is carried out at the restrictive temperature (96,127). It is apparent from these experiments that DNA replication is not required for injection. On the other hand, these experiments do not exclude the possibility that DNA replication is a normal adjunct of this process.

Phage will absorb, eclipse, but not inject cells that have been starved for a carbon source, nor will they superinfect a ϕX-infected cell (43,44). In these cases, the infection is thought to be blocked by some unfavorable condition of the cell wall. De novo protein synthesis is apparently not required as pretreatment of the cells with high concentrations of chloramphenicol (2,72,87,88), or starvation of the host for a required amino acid does not prevent injection or parental RF formation (86). Phage will inject isolated cell wall preparations with high specificity for ϕX hosts, but the DNA does not completely dissociate from the phage, thus leaving open the question of whether or not the complete separation of the DNA and protein requires cell-derived energy (25,31,94).

The failure of heavily UV irradiated phage to infect cells (33,41) is probably due to crosslinking of the DNA (40) rather than to the impediment to DNA synthesis that the UV-induced thymine dimers pose (42). This observation is consistent with the idea that the phage DNA either leaves the virion or enters the cell through a small pore.

Genes of ϕX174

Besides genes F, G, H and J mentioned above in conjunction with the virion structure, the ϕX174 genome contains five additional complementation groups. These nine genes have been organized onto a circularly permuted map by genetic recombination (9,15,34). Most of the genes have also been correlated with their respective gene products, as assayed by SDS acrylamide gel electrophoresis. This technique has also been utilized to obtain the molecular weights of the identified gene products (12,20,52,53). Recently the genetic map of ϕX174 has been correlated with a physical map of the ϕX DNA by utilizing the methods developed by Hutchison & Edgell (54) and Weisbeek (55) for mapping the relative positions of ϕX DNA fragments produced by restriction endonuclease degradations of ϕX DNA (56,132). Although some inconsistencies still remain to be resolved, the greater part of these three maps are in good agreement (Amy Shiu Lee, personal communication).

The small size of the ϕX174 genome suggests that the virus must make extensive use of the host biosynthetic systems for its own replication. On the other hand there is no reason to expect host pathways for the synthesis of single-stranded DNA, as this DNA form is not observed in bacterial cells. As a consequence it is not too

surprising that a large proportion of the ϕX174 genome is implicated in this process. In this section the various genes will be discussed one by one with special emphasis on the role they may play in SS DNA replication or viral maturation.

In several instances, information derived from the closely related phage S13 will be cited to fill in various gaps in the characterization of the ϕX174 system. The validity of this comparison depends upon the degree of similarity between the two phages, which in turn depends upon the level at which they are compared. The great functional similarity between S13 and ϕX174 is best indicated by the fact that they complement each other in almost all combinations of complementary cistrons (9,34). The exceptions are notable for what they imply about the gene functions involved. A comparison of the SDS gel electrophoresis patterns of wt UV lysates of both phages indicates that the major gene products are of very similar, if not identical, molecular weights, and that the various genes are expressed with approximately the same stoichiometries (34,35). The virions are serologically related, though not identical (70). On the other hand, the two DNAs seem to have diverged considerably in that hybridization studies show only 64% average homology between their base sequences and only a small region (4.7% of the genome) of highly homologous DNA (35, J. L. Compton, personal communication).

Gene A

It is still uncertain whether or not gene A function is required for SS DNA synthesis or viral assembly. The only published experiment

addressing this question suggests that it is not (57), but the interpretation of this result has been confused by the subsequent discovery that cistron A codes for two different proteins. The function of at least one of the proteins (which is as yet undetermined) is absolutely required for ϕX progeny RF synthesis (2,57,63,87). Whether the other protein is also involved in RF synthesis or some other function is not known. The smaller protein is associated with completed phage particles at concentrations of approximately one copy per virion (R. Rohwer, in preparation). This suggests that it may be functionally involved with virus maturation. Alternatively, it may play some role in introducing the viral DNA into the host. However, it must not be essential for this process, inasmuch as deproteinized SS DNA is able to infect spheroplasts without it.

The relationship between the two gene products of cistron A has been worked out by Linney et al. (45,46). Using SDS acrylamide gel electrophoresis to monitor ϕX proteins in UV irradiated host cells, they noted that when gene A mutant phage are grown in nonsuppressor host strains, am mutations at the N-terminus of cistron A delete a 62,000 MW protein, termed A', whereas those at the C-terminus delete both A' and an additional 35,000 MW protein, termed A. (Note: This nomenclature has been reversed by Henry, 50.) The trypic digest pattern for A protein is included in that for A'. Apparently the entire translation of cistron A gives rise to A' protein, whereas an internal promotor, or ribosome binding site, in that gene gives rise to the smaller A product. A pulse chase experiment, mentioned by Linney but not shown, demonstrates in another way that A does not arise from A'

by proteolytic cleavage (45).

Cistron A function is absolutely required for the second stage of ϕX DNA replication, the synthesis of progeny RF DNA from parental RF (2,57,63,87). However, due to the uncertainty of the map positions of those cistron A mutants that have, so far, been tested for this function, it is still unknown whether it is the A or A' protein, or both, that are required. ϕX*am*30 is the most N terminal cistron A mutant that has been checked explicitly for its ability to synthesize progeny RF (63), but it has not yet been established whether or not *am*30 is inside or outside of the A protein region. Consequently, it is conceivable that only the A protein is required for progeny RF synthesis, and that, once checked, mutants known to be located N terminal to the origin of the A protein (such as *am*86, see Results) will exhibit some other phenotype than that so far observed for cistron A. Should it turn out instead that mutations located exclusively in the A' region do prevent progeny RF synthesis, then an ambiguous situation will remain due to the impossibility of deleting the A protein function independently of A'. In this case the A protein might or might not be involved in RF synthesis. If it is involved then both proteins, A and A', must function as necessary, but not sufficient, ϕX contributions to that process.

Francke & Ray (48,49) have demonstrated that gene A functions *in vivo* by introducing a nick into the viral strand of the ϕX parental RF, and that only a small number of the infecting parental RF molecules are nicked, regardless of the multiplicity of infection and the size of the intracellular pool of parental RF. They postulate that the

nicking activity is restricted to those RF that are associated with the limited number of essential bacterial membrane sites that have been demonstrated to be required for progeny RF synthesis (59,60). This is consistent with the observation of Van der Mei *et al.* that the A' protein is tightly associated with the cellular membrane (51).

Francke & Ray (49) have shown that, in nonsuppressor host strains, specific nicking is also restricted to those parental RF which carry *wt* gene A. This is consistent with the asymmetric complementation behavior of gene A observed by others (2,9,58). From their results, Francke & Ray could not discriminate whether the A' protein promoted the binding of its homologous parental RF to the membrane where nicking was mediated by host enzymes, or whether membrane association was necessary for the transcription and translation of A' protein, which then acted in *cis* fashion to nick the membrane-bound RF which encoded it.

Henry has since shown that purified A' protein introduces a single nick into ϕX RF I, specifically, in the viral strand (50). This *in vitro* activity does not require the presence of bacterial membrane. Therefore, the *in vivo* restriction of A' activity to only certain RF must be a direct consequence of the *cis*-acting property of this gene and only an indirect consequence of the membrane association of the nicked parental RF. In the experiments of Francke & Ray where all progeny RF synthesis is blocked by a host mutation, rep_3^-, apparently only the site-associated parental RF are transcribed and translated, and the resultant A' product reacts only with the DNA molecule which encoded it (49).

Hutchison's experiments on the physiological requirements of ϕX174 complementation also suggest that transcription is limited to those parental RF (and/or their progeny) which are associated with the essential bacterial membrane sites (9). He has shown that ϕX complementation in starved cells which contain only 1 or 2 replication sites per cell (59) occurs only in that subpopulation capable of producing both genotypes of progeny RF, regardless of the multiplicity of infection of each input phage and the resultant size of the intracellular pools of parental RF (9). Truffaut & Sinsheimer have since demonstrated that the progeny RF are the major intracellular substrates for transcription (138). Apparently there is some special property conferred upon the progeny RF which is not shared by the non-site-associated parental RF, and which makes them a suitable transcription substrate, whereas the cytoplasmic parental RF are not. This special property would have to be conferred in cis fashion at the time of synthesis of the new progeny RF and before its release to the cytoplasm. The only ϕX gene whose expression is limited in this way is gene A, thus making the A or A' proteins reasonable candidates for this function.

Gene A function is resistant to suppression by chloramphenicol. Progeny RF synthesis, but not SS DNA synthesis, can occur in the presence of 30 μg/ml chloramphenicol, when overall cellular protein synthesis has been reduced to 2% of normal (72). This was originally interpreted to mean that the A gene product was synthesized in normal amounts in chloramphenicol-treated cells and would be present in relatively greater proportions than in normal cells. This assumption led Levine to search for a chloramphenicol-resistant protein in chloramphenicol-treated

cells (57,73,74). It now appears that functional escape from chloramphenicol treatment is related instead to the numerical requirement of the function for active protein. All protein synthesis is suppressed rather uniformly by chloramphenicol and only those proteins which are required in very small amounts are functionally expressed (8,51). This in turn suggests that the role of gene A function in progeny RF synthesis may be enzymatic and that the protein involved is reused. However, reusability of the protein is not necessarily consistent with its *cis* mode of action or the properties of the *in vitro* reaction of the A' protein. In Henry's preliminary investigation of the purified A' activity, the protein was required in equimolar concentrations to its RF I substrate for quantitative nicking to occur. This indicates that a given molecule of A' may only be able to nick once in the *in vitro* reaction.

A rather weak temperature-shift experiment with ϕX *ts*128, thought to be mutant in both genes A and B, suggested to Levine & Sinsheimer that gene A function was not required for SS DNA synthesis (57). Regardless of the interpretation of this experiment, it is probable that only the A' function was screened, as *ts*128 maps at the N terminus of the A cistron (15). Thus a temperature-sensitive mutant in the A protein region of the gene might have given a more dramatic response. It is also possible that an experiment of this type would not be able to detect the essential role of a *cis*-acting, reusable, protein if the temperature shift was performed after sufficient active protein had already been synthesized to carry the infection.

Levine & Sinsheimer (57) have shown that wild type cistron A product(s) persists in this way. When chloramphenicol, at a concentration sufficient to completely block protein synthesis (150 µg/ml), is added at the time of infection by ϕX174, the infection does not proceed past the synthesis of the parental RF DNA. However, when the same concentration of chloramphenicol is added eight minutes after infection, progeny RF synthesis continues for at least 50 minutes, although at only one half the rate observed before addition of the drug. Presumably, this continued synthesis makes use of gene A proteins synthesized before the addition of chloramphenicol. In the case of a temperature-sensitive mutation in gene A, ones ability to observe this effect would depend upon the nature of the temperature-sensitive lesion. Newbold & Sinsheimer (95) have demonstrated that appropriate mutations do exist, as many ϕX temperature-sensitive strains give rise to proteins that are only inactivated by synthesis at their restrictive temperatures but remain active if shifted to the higher temperatures after synthesis. (They did not test a gene A mutation.)

It is clear that a definitive test of the A cistron's involvement in the process of SS DNA replication has not yet been made. Meanwhile, the strong affinity of both the A and A' proteins for SS DNA, the plus strand specificity of the A' protein, and the association of the A protein with completed particles are all consistent with, and suggestive of, a possible role in SS DNA synthesis.

The assignment of the A' product to a protein in the infected lysates of non-UV irradiated cells, by employing the method of Mayol & Sinsheimer for detecting ϕX-specific proteins (8), has been confused

due to the presence of several host proteins of similar molecular weights whose synthesis is stimulated by the ϕX infection. Data presented in the Results will show that all of these host proteins have molecular weights greater than A' protein, and that their synthesis greatly exceeds and often obscures that of the A' protein.

The large size of the A' protein, estimated variously from 55,000 (51) to 67,000 (12) daltons, is inconsistent with the physical map of ϕX174 derived by Benbow (12). The addition of such a large protein to the phage genome causes the ∿ 228,000 daltons of protein-coding capacity of the phage to be exceeded. However, reassignment of Benbow's A, B and C proteins in the light of more complete characterizations of these cistrons (46,61,62), and the knowledge that both A' and A arise from the same gene, as well as the discovery that the putative gene I mutant (H532 in A) does not define a new complementation group but was assigned to one as the result of a complementation artifact (M. Hayashi, personal communication), restores the known protein output from the genome to within the limits of its coding capacity (Table 1).

Gene B

Many gene B mutant phages have altered thermal stabilities compared to wt ϕX174 (2,9). The thermal instability of gene B phage was originally taken to mean that B protein was a virion component. However, SDS acrylamide gel electrophoresis of highly purified virions (R. Rohwer, in preparation) demonstrates that gene B protein is present in far less than one copy per phage, when using either Siden's (61) or Benbow's (12) B protein assignment. Apparently the mutant B protein

affects the thermal stability of the phage as a consequence of some nonstructural role that it plays in phage assembly.

Siden has provided more direct evidence that gene B functions in the assembly process (61). Under his conditions, ϕX-infected lysates contain a ϕX-specific particle that sediments at 12S. Upon storage, the 12S particles gradually dissociate to equimolar quantities of 6S and 9S particles previously characterized as containing only F or G protein, respectively (65; R. F. Mayol & R. L. Sinsheimer, unpublished). Siden deduced that the 12S particle is equivalent to a single capsomeric subunit of the virus composed of five F and five G proteins. In the absence of gene B function this 12S particle pool disappears. Apparently gene B product either promotes the formation of the 12S particle directly from 6S and 9S subunits, or it is essential for the construction of some structure from which the 12S particle later arises by decomposition.

Whatever the origins of the 12S particle, Siden has shown that the structure formed as a consequence of B function is a direct precursor of the phage particle. In temperature-shift experiments with ts mutants in cistron B, SS DNA synthesis continues for a short time at the restrictive temperature and phage are matured, but only from pre-existing protein pools. In the absence of B function, nascent virion protein is prevented from entering the pool of precursor structures from which phage are being assembled. This precursor pool does not include the large pools of cytoplasmic 6S G pentamers and the 9S F pentamers, inasmuch as neither of these structures require any other ϕX gene for their formation (65). Therefore the protein source for

this residual phage synthesis must either be the 12S structure favored by Siden, but present in very small quantities in the lysates of other researchers (this thesis; Mayol & Sinsheimer, unpublished; Tonegawa & Hayashi, 65), or the much larger pools of 20S, 70S and 111S ϕX-specific subviral particles which are the subject of this thesis.

As indicated above and as originally characterized (63), gene B function is also required for SS DNA synthesis. If it is absent from the time of infection as is the case in a nonpermissive infection with an amber mutant, SS DNA synthesis is apparently never even initiated (71). If the B protein is inactivated during SS DNA synthesis by a "shift up" of a ts mutant, then SS DNA synthesis occurs for only a short time until some phage precursor structure is used up. This is just one of many examples indicating the interdependent nature of SS synthesis and the phage assembly process. It is conceivable that gene B functions directly at the level of SS synthesis but, if this is so, it must function after the DNA is already committed to its phage protein in order to be consistent with Siden's findings. For example, B protein might serve to introduce the nascent SS DNA into a procapsid which later is matured into a form that gives rise to 12S capsomers when disrupted.

Using amber mutations, Siden has identified the gene B product in highly resolving SDS acrylamide gels as a peak migrating between G and D proteins and closer to D. Prior assignments of this protein have been by a process of elimination utilizing the assumption that it was a phage component (8,12). Siden's assignment corresponds to the protein tentatively assigned to gene E by Benbow et al. This protein has a

MW of 17,500 daltons (12).

The experiments presented in the Results show that the B protein (as assigned by Siden) accounted for 4-5% of the ϕX-specific labeled leucine incorporation after pulses of from 18 to 90 minutes. If the labeling period is extended to several hours, the relative incorporation often drops to 1 or 2%, indicating that B protein may be used up or is especially labile to intracellular proteases. Mutants from either end of the gene A cistron give rise to a two-fold enhancement of relative B protein synthesis when grown under restrictive conditions. The cause of this phenomenon is uncertain, but it is unlikely that it is related to Godson's observation that charged t-RNA migrates in this region of the gel (20), as the host labeling pattern observed under identical conditions does not show any distinct peaks in this region of the gel which could account for this effect (Results).

Gene C

The C cistron is defined by a single ochre mutation site in ϕX174 (67) and an ochre and opal site in S13 (62,69). These mutants are very leaky, a property which Funk & Sinsheimer attributed to an enzymatic function requiring very few active copies of the gene product (67). Alternatively, it is just as conceivable that gene C product is not essential for successful infection but merely expedites it.

This gene is apparently required for normal SS DNA synthesis. When the C mutant is grown in nonpermissive cells the early events of the infection occur normally, but SS DNA synthesis and phage production are greatly retarded. DNA isolated from these cells during the period

in which SS DNA is being synthesized at a very slow rate has the sedimentation behavior characteristic of the replicative intermediates of SS synthesis. Very little RF II form DNA is present in these lysates whereas this is the most prevalent conformation in the normal infection. Since it is not clear whether C protein is essential for SS DNA synthesis or whether it merely facilitates it, one does not know, in the absence of pulse chase data, whether these intermediate structures are producing the SS DNA that eventually ends up in the phage, or whether they are an accumulating pool of inactive "dead end" molecules. In the latter case, the residual SS synthesis would be occurring normally, utilizing normal gene C product rescued by translation errors. However, this normal synthesis would be obscured by the large pool of inactive aberrant DNA forms. In the former case, where these intermediate structures are the precursors of SS DNA and phage, the effect of the C protein would be to shift the rate limiting step (93) in SS DNA synthesis from the initiation of a new strand on the "resting" RF II molecule to the completion of the new SS and its release from the replicating intermediate.

By analogy with gene B function, one cannot exclude the possibility that the C function is only indirectly related to SS DNA synthesis. It is conceivable that C protein promotes some step in viral assembly, such as the formation of a precursor structure which is essential if SS synthesis is to continue beyond the stage at which the replicating intermediates accumulate. The effect of the C mutation on the intracellular pools of virion subunits has not been investigated.

By preparing the gene C mutant phage in several different

suppressor strains, each inserting a different amino acid at the ochre mutation site, and then comparing the thermal stability of the resultant phage with wild type ϕX, Funk was able to show that none of the insertions gave rise to virions with altered thermal properties. As the likelihood is great that one of these insertions would create a temperature-sensitive gene product, it appears that the C protein is not a structural element of the virion (67). This result would have been more certain if Funk & Sinsheimer had established the temperature-sensitivity of the ochre C infection in these same suppressor strains.

Barras et al. (62) have been able to assign the S13 gene C product to a particular peak in an SDS acrylamide gel pattern by the stringent criterion of a shift to greater mobility in restrictive lysates of the gene C suppressible mutations. This peak runs faster than gene D product and corresponds to Benbow et al.'s tentative gene A assignment. Benbow et al. determined the molecular weight of this protein to be 13,500 daltons (12).

Gene D

Gene D product is synthesized, in the normal infection, in greater molar quantities than any other ϕX protein. It is present at almost twice the concentration of the major virion protein, F (Results; 12). It also accounts for approximately 12% of the mass of intracellular ϕX protein as monitored by a radioactive leucine label. In UV irradiated cells it is the largest mass constituent. The preferential synthesis of this protein is consistent with its position at the beginning of a

polycistronic message defined by a gradient of polarity extending at least as far as gene H in the order D, E, F, G, H (12). Its assignment to a 14,500 dalton peak in SDS acrylamide gels is generally agreed upon by all authors, although the most rigorous requirement for assignment, the demonstrated appearance of a D fragment coincident with the disappearance of D protein, has not yet been met (12,20,52,53).

In spite of its intracellular prominence, the function of this gene remains obscure. When D mutants are grown under restrictive conditions progeny RF synthesis and host synthesis terminate at the usual time but no SS synthesis commences (63,71). It is therefore one of the five ϕX174 genes absolutely required for SS DNA synthesis, but as is probably the case for several other genes, its involvement in the replication process per se may be rather indirect. It does not bind strongly to DNA, as indicated by its behavior on SS DNA cellulose columns (D. Gelfand & E. Linney, personal communication; 46), and it is only a minor component of the virion, present in from one to two copies per particle (R. Rohwer, in preparation).

Until now, it has been found intracellularly only as the free monomer, sedimenting at approximately 2S (65; R. Mayol & R. Sinsheimer, unpublished data). Van der Mei et al. (51) have shown that it is a cytoplasmic rather than membrane-bound protein. Experiments presented here (Results) will show that, after lysis at low temperature in the presence of Mg^{++}, a large proportion of the D protein is associated with ϕX-specific complexes sedimenting at 111S, 70S and perhaps 20S, as well as the 2S monomer peak. At least one of these complexes, 70S, contains replicating DNA but at least one other does not. Weisbeek &

Sinsheimer have recently discovered gene D product in association with an infectious ϕX particle sedimenting at 140S in lysates prepared in 0.25 M-Tris and saturating EDTA (165). It seems quite likely that the D protein is involved in the assembly of some particle that is required for the synthesis of SS DNA rather than in DNA replication per se.

Jeng et al. (34), in their investigation of ϕX174-S13 complementation, have provided, contingent upon the complete characterization of the phage mutants used in their analysis, indirect evidence that gene D function involves some interaction of D and F proteins such as might be expected if D protein were involved in phage assembly. Of all of the gene combinations tested (Gene J was not yet known. Genes C and D were known only in S13 and ϕX, respectively, so the crosses were performed in only one direction. Gene E of ϕX was not tested.) only gene D protein in S13 and gene F protein in ϕX were shown not to complement.

Of the two most obvious explanations for this complementation failure, the simpler, if less interesting one, is that the S13 gene F mutant used in the test, su68, is in fact a double mutant in genes F and D. In this case, active gene D product would have been lacking in the mixed infection. It has not been possible to detect a double mutant of this type in S13 by complementation procedures as no gene D mutants have yet been identified in this phage. On the other hand, the gene D protein is observed in SDS acrylamide gels of lysates of S13 infected cells (34) and, as a consequence, a hidden gene D mutation should be detectable by this method. However, experiments of this type have not

yet been performed and, as a consequence, this explanation cannot yet be excluded. (Jeng *et al.* also assayed S13 gene F mutants *su*39 and *su*52 against an unidentified ϕX D mutation with the same negative results. However, because these mutants were not used in any other complementation assays, their failure to complement the ϕX gene D mutant cannot be assumed to be a specific effect. This is because S13 gene F mutant *su*39, and another unidentified F mutant, were found by Hutchison (9) not to complement any ϕX cistrons, apparently due to their very poor absorption to the *E. coli* C host used in the complementation assay.)

A more interesting explanation for the gene F-gene D complementation failure can be advanced if it turns out that S13 strain, *su*68, contains only a single mutation in gene F. In this case, the mixed infections with ϕX gene D mutants H81 and H119 would have failed to produce progeny phage even though four configurations of active virion proteins were possible, including a wild type configuration (see Table 2, Complementation I), and active gene D product was supplied by the S13 gene F mutant. Other complementation tests (II and III in Table 2) demonstrate that these same configurations of virion proteins do give rise to infective particles in other mixed infections. This indicates that the failure to produce infective particles in complementation I (Table 2) was not due to a structural incompatibility of the virion proteins *per se* but rather an incompatibility of one of those proteins, F, with the nonhomologous D protein. Complementations IV and V (Table 2) demonstrate that this incompatibility does not arise from the relationship of D protein to H and G gene products. Together, the data

suggest that there is some direct and essential involvement between the F protein and either the homologous D protein itself, or, conceivably some other homologous molecular species produced as a direct consequence of the *cis* functioning of D protein. An example of the latter case might be the interaction of F protein with its homologous SS DNA, which perhaps can only be synthesized in the presence of active, homologous D protein. In this case, only the F and D homologous SS DNA would be expected to be matured into particles. Unfortunately the genetic composition of the progeny phage was not monitored, so these two possibilities cannot be distinguished on the basis of these data alone. However, in either case the expression of F function is shown to involve a strong and essential interaction with some ϕX-specific molecular species other than the virion proteins.

Genes E and J(?)

Mutant phage from the gene E complementation group are unable to lyse nonpermissive host cells. In the absence of lysis, all but one of them, *am6*, produce very high titers of infectious virions which are physically indistinguishable from wild type phage in all comparisons conducted to date (9,12,20,52,63,76). The production of apparently wild type phage without cell lysis has been taken to mean that the E function is exclusively lytic and that the absence of this function has little substantive effect on the rest of the infection process. The gene E lysis-defective mutants have, as a consequence, been a great boon to ϕX research, both in enabling one to study the late events of the infection process without the complication of lysis, and in preparing

high titer phage stocks. Most of the experiments in this thesis were conducted with the gene E mutant am3.

Even though the gene E function may be exclusively lytic (and this is now questionable), lysis itself is probably not the exclusive consequence of gene E expression. Hutchison & Sinsheimer (76) have demonstrated, and one can infer from Siegel & Hayashi (7), that some mutations in gene H are also lysis-deficient. If the am6 mutation defines a new cistron J (see discussion below), then this cistron may also be required for lysis. Apparently genes E, H and J(?) are, when taken one at a time, necessary but not sufficient for the lytic event.

The exclusively lytic nature of the gene E function is now open to question due to the pleiotrophic behavior observed for the putative gene E mutation, am6 (12). Am6 is lysis-deficient like the other E mutations, its complementation behavior places it in the E cistron (Table 3, data from 9); and it maps in the E region (9). However, unlike other gene E mutations, am6 produces very few infective virions (76). Instead, it packages infective DNA into a phage-like particle lacking only the low molecular weight protein component (12). If the am6 mutation is in cistron E, these properties suggest that the E protein, like the H protein, may be an essential virion component as well as an essential element in the lytic process. One can speculate that other gene E mutations, like am3, are located close to the C-terminal end of the cistron, giving rise, in nonpermissive hosts, to fragments with molecular weights so similar to that of the wt protein, that the differences cannot be discriminated by the methods utilized so far. These small changes must then be sufficient to destroy the

lytic function of the E protein but not its structural function in the phage.

The fact that both gene E (am6) and gene H mutations produce phage-like uninfective particles as well as a lysis deficiency suggests that the intact virion may be the lytic principle. This is refuted by the observation that mutations in several other cistrons produce lysis in the absence of any particle production or even SS DNA synthesis (9, 63,71). Therefore lysis cannot be mediated by the phage particle per se. This also suggests that the lytic and structural roles of any of the genes involved in lysis are apparently operationally segregated, even though they may be very similar functionally. For example, it is conceivable that the E protein is stabilizing when incorporated into virions but destabilizing when incorporated into cell membranes.

The phenotypic differences between am6 and the other gene E mutations, the effect of a ϕX deletion mutant on the virion composition, and an analysis of the acrylamide gel electrophoresis patterns of proteins from mutant infections of both types, led Benbow et al. (12) to tentatively assign am6 to a new cistron, J. The new cistron was located between genes E and F [map order -- D, E, J (am6), F, G...] on the basis of the close linkage of am6 to the gene E mutant am3 during three factor crosses. These crosses were, due to the low recombination frequencies, poorly resolved but suggested that am6 was located C terminal to am3. [It was also stated that am6 could be resolved from gene E mutant am27 in three factor crosses. The map order--D, E am27, E am3, F..., was previously established by Benbow et al. (15) by means of two factor crosses. Unfortunately, this critical experiment was

not presented and it must be assumed that am6 was found to map N terminal of am27 to give the map order favored by Benbow et al. (12) (i.e., ...D, E (am27), E (am3), J am6, F...).]

The placement of the am6 mutation between genes E and F contradicts Benbow et al.'s (15) previously published data for two factor crosses which clearly locates the am6 mutation at the N terminal end of cistron E. The data for these crosses are given in Table 4 and strongly supports a map order of [...D, J (am6), E, F...]. This order was obtained for crosses from three separate loci adjacent to the E cistron and, due to the unique problems associated with the three factor crosses presented in reference 12, would appear to be based upon the more compelling data.

If the am6 mutation is located at the N-terminal end (12) of the gene E complementation group, several alternative explanations can be advanced for its pleiotrophic effects other than its assignment to a new cistron.

An N-terminal locus is consistent with, and suggestive of, the interpretation advanced above -- that cistron E codes for a low molecular weight protein that functions both in the lytic process and as a phage structural component. In this case is it necessary to postulate that the latter function is unaffected by small deletions from the C-terminal end.

It is also conceivable that the low molecular weight phage component arises as a secondary consequence of gene E function. For example, the E protein may be a highly specific protease that generates the low molecular weight phage component from a ϕX precursor during the

phage maturation process. Many examples of this kind of reaction are known (211,212,213,214,215,218). The same activity might also be directed against specific host proteins with similar structures, thus accounting for its role in the lytic process as well.

It is also possible that, as proposed by Benbow et al. (12), am6 defines a new cistron J which codes for the low molecular weight phage structural component. Benbow et al. have postulated that this gene functions both in lysis and as a phage structural component. However, as long as the hypothetical cistron is located N-terminal of cistron E, this pleiotrophy need not be explained in terms of functional duality. In this case, the J protein itself would not necessarily have a lytic function. Rather, the lysis deficiency could be the consequence of a strong polarity of the am6 mutation for the E gene. This polarity could not be too strong, however, inasmuch as the F, G and H proteins are made in normal amounts in the am6 infection. The protein to which gene E was originally assigned by Benbow et al. is actually synthesized in greater rather than lesser amounts in the am6 infection. This is probably an indication of an incorrect protein assignment rather than a refutation of a polarity affect.

Perhaps the strongest evidence for a separate cistronic identity for the am6 mutation is Zuccarelli's finding that synthesis of the low molecular weight phage component is unaffected by lysis deficient ϕX174 deletion mutants missing as much as 7% of the wt DNA complement (77). Inasmuch as the gene E function is the only one known that is not essential for the production of infective particles, it is assumed that these deletions must be in the E cistron. Benbow et

al. (15) estimated the genetic size of the E cistron as 5.5% of the genome. Thus, if in fact these deletions are gene E-specific, it is unlikely that only a C-terminal portion has been deleted, leaving a functional N-terminal region. Even if this were the case, such a large deletion would surely be noted as a change in size of the low molecular weight phage component, if in fact this were the E protein.

Several unresolved anomalies serve to temper the otherwise compelling nature of this observation. As yet, the deletion mutations have not been correlated with the loss of any ϕX-specific protein from deletion phage infections. This is not too surprising, inasmuch as it has not yet been possible to identify the gene E product utilizing suppressor mutations either (12,20,52,53). However, it does detract from the significance of the observed conservation of the "J" protein in these same infections. This result becomes more auspicious when combined with the observation that both in vivo RF isolated from the deletion mutant infection and in vitro RF II prepared from deletion phage DNA produce perfectly normal fragment patterns after cleavage with various restriction enzymes (Amy Shiu Lee, unpublished data). One would expect a disappearance or a substantial alteration in the behavior of the DNA fragment normally carrying the deleted DNA (105). On the other hand, a normal pattern is the expected consequence of a randomly distributed deletion. Apparently the ϕX deletion mutants may be more complicated than their preliminary characterization has indicated, and until these latter observations are understood, it would be premature to assign the am6 mutation to a new cistron on the basis of these data. At present the cistronic identity of the am6

mutation remains in doubt. It could plausibly define the N-terminus of the E cistron, expanding our concept of the role of that gene, or it may be the sole representative of a new cistron coding for the small virion protein. Regardless, it is associated with a particular protein and for the sake of convenience, but without any commitment to its unique cistronic identity, this smallest virion component will be referred to as the J protein.

It is somewhat surprising that a definitive identification of the gene E product has not been made in the SDS acrylamide gel systems. Inasmuch as the E cistron is the second or third in the chain of polarity extending from gene D to gene H, one would expect it to be synthesized in large amounts, i.e., at a molecular concentration between those of genes D and F. If the molecular weight of this protein is between those of the D and F proteins (tentative E protein assignments by both Godson (20) and Benbow et al. (12) fall in this region), one would also expect a substantial mass contribution ranging from at least half that of the D protein (D protein is synthesized at twice the molar concentration of F protein) to greater than that of the F protein, depending upon the molecular weight of the E protein. However, the G protein is the only other protein in this molecular weight range besides D and F that is synthesized in anywhere near these quantities. The numerous electrophoretic characterizations of suppressor mutations in all of these genes rules out the possibility that the E protein could be concealed by any of these peaks if it is present in the quantities expected (12,20,52,53). Apparently the E protein must have a molecular weight considerably less than gene D product to be present in the

expected stoichiometric amounts. Unfortunately the low molecular weight proteins are, due to diffusion, the most poorly resolved in the SDS acrylamide gel electrophoresis system, and their high mobilities under the experimental conditions used to date place them out of the linear region of the molecular weight calibrations of the gel systems (12,20,53). As a consequence, their molecular weights have not been accurately determined and their intracellular stoichiometries are unknown.

It should be noted that the D cistron utilizes only 6.4% of the ϕX DNA. If, as this analysis has suggested, the E cistron is much smaller than this, it could not by itself contain the 6-7% deletion measured for the deletion mutation (77).

These same arguments would apply equally well to the J cistron, if it exists.

The mechanism by which ϕX lyses the host cell and the role of the E protein in that process is as yet unknown. However, it probably does not involve a conventional lysozyme, inasmuch as repeated attempts to isolate such an activity from ϕX-infected cells have been unsuccessful (78,79,25). Also, more than one ϕX gene [at least E and H, and perhaps J(?)] is implicated in the lytic mechanism. [Lysis is also delayed by mutants in gene A (76) even though those phage proteins that are assayable by SDS acrylamide gel electrophoresis are made in normal amounts in A deficient infections (66)]. Whatever its function, the position of the E cistron in the chain of polarity of the ϕX genes (12,15), indicates that it is made in large amounts and is, therefore, presumably required in high concentrations for function.

The lysis of a ϕX174-infected culture is very gradual, with the time of individual cell bursts extending twenty minutes past the minimum latent period. The lysis of the individual cells is, however, very abrupt, releasing the entire phage burst to the extracellular fluid in less than 30 seconds (75). This lysis can be prevented by stabilizing the cells against osmotic shock with the addition of 20% sucrose (79), or in an unknown way by the addition of 0.2 M-$MgSO_4$ but not $MgCl_2$ (81). Lysis can also be avoided by exposing the cells to UV_{260} radiation (20,52, Results) or to mitomycin C (A. Fukuda, personal communication) prior to infection. Both of these agents prevent further cell growth and division. When infected with a gene E mutant the host cells continue to grow but do not divide. The resulting snake morphology is often encountered in cells metabolically blocked in DNA synthesis (198) and may be the consequence of the displacement of the host DNA from the DNA replicating machinery by the infecting phage. In ϕX wt infections, lysis occurs long before these snakes would have had time to develop. The lysed cells show only local disruptions in the cell wall (79). In the closely related phage, α3, lysis is preceded by a bulge along the fission plane of the cell. This bulge eventually ruptures, freeing the phage to the extracellular environment (83). Taken together, this phenomenology suggests that lysis may be the consequence of an aberrant cell division induced by the ϕX proteins. If this proves to be the case, the responsible proteins may prove useful in the study of cell division or as antibacterial drugs.

Gene F

The gene F product has been unambiguously assigned to a 50,000 MW protein in the SDS acrylamide gel system on the basis of the behavior of the protein fragments produced by the gene F suppressor mutations (12,20,52,53). It has been identified as the structural unit of the capsid by means of the 4 M-urea treatment (53). In the normal infection, F protein is present in the greatest mass concentration (35-40% of a radioactive leucine label) of all the ϕX proteins (Results; 12). Sedimentation analysis of infected lysates reveals that very little of it is present as the F monomer. As the time after infection increases, an ever greater proportion of the F protein accumulates in the completed phage particles. A fixed proportion of the virional F protein is found, after lysis, in the 70S lysis artifact produced by abortive infections of the cell debris (27). The rest is distributed among at least five ϕX-specific subviral particles of varying degrees of complexity, and ranging in S value from 111S to 9S (65; R. M. Mayol, unpublished data; this thesis). These particles will be discussed at greater length below.

The primary function of the F protein as the capsid structural protein is obvious. However, like the other main virion protein, G, functional F is also required for SS DNA synthesis (68,71). Once again this illustrates the strong interdependence of particle assembly and SS DNA synthesis. In the absence of F function, SS DNA synthesis is not even initiated (71). When temperature-sensitive F protein is inactivated late in infection by a temperature shift, SS DNA synthesis stops abruptly (68; E. Siden, personal communication). As discussed in conjunction with gene D, the F function apparently involves some inter-

action with D protein.

Gene F has several other properties that would be expected of a cistron coding for a virion component. In a comparison of the antigenicity of the spikeless ϕX particle produced by means of the 4 M-urea procedure (16) and whole phage, it was demonstrated that phage inactivating antibodies are produced against the F protein or some complex of F proteins (R. Rohwer, in preparation). Several host-range mutants are located in this cistron in S13 (58), and it is supposed that some of the unassigned ϕX host range mutants may also be in gene F (9). However, no ϕX host range mutants have yet been assigned to this cistron. An extension of the host range of the ϕX or S13 virion by mutations in gene F does not necessarily mean that the F protein is directly involved in phage attachment to the bacterial host. It is more likely that this phenotype reflects an altered charge on the entire particle [as indicated by the altered electrophoretic mobility of many host range mutants (85)] rather than a change in the phage absorption apparatus per se (84). Other gene F mutations affect the thermal stability of the mutant virion (9), and possibly its host absorption kinetics as well (84).

Gene G

The ts79 mutation in cistron G gives rise to a gene G product with an altered electrophoretic mobility in non-denaturing gels. This property, in conjunction with the 4 M-urea dissociation procedure, has been used to unambiguously identify the G protein as the second greatest mass constituent of the virion and as a spike component (16). Suppressor mutations in this same cistron eliminate a 20,500 MW protein

from nonpermissive infections, although without generating an observable fragment (12,20,52,53). The G protein is produced at a slightly lower molecular concentration than F product, as is consistent with its position in the polarity gradient (12). Like the F protein, very little of this gene G product exists intracellularly as the monomer (65). The rest accumulates with time in the pool of completed phage or distributes among various subviral particles (65; R. M. Mayol, unpublished data; Results). As is true for gene F, gene G function is also required for SS DNA synthesis and mutant infections in G give rise to the same phenotypes with regard to that process (71,98; E. Siden, personal communication).

Two gene G mutants, ts79 and am9, are known which do not produce serum blocking power under restrictive conditions, suggesting that the G protein harbors inactivating antigens (9,10). One of these mutants, ts79, also exhibits aberrant attachment kinetics to host cells (84) and an altered electrophoretic mobility in non-denaturing electrophoresis systems (16,85). Still others give rise to phage with altered thermal stabilities (9). Weisbeek has employed a physical mapping technique to locate several host range mutants within or very close to the G cistron (64).

Gene H

Although it is a phage structural component, H protein is synthesized in much smaller molar proportions than are F or G (Results; 12). Using suppressor mutations, the H gene product has been identified as a 37,000 MW protein whose disappearance is correlated with the appearance of lower molecular weight fragments in the unsuppressed

infection (12). Because this protein is made in relatively small quantities and possibly (as discussed earlier) because of its unusual sensitivity to manipulation, the intracellular distribution of this protein is still unknown, except, of course, that it does accumulate in phage particles. Jazwinski's finding that it binds tightly to the phage SS DNA, in conjunction with an antibody binding experiment to be presented in the Results section, suggests that the H protein might be associated with the replicating SS DNA. However, unlike the gene F and G proteins, gene H function is not required for SS DNA synthesis and, as noted above, a phage-like particle can be assembled in its absence.

Like the other virion proteins, gene H product is also required for the normal production of serum-blocking power (9) and normal absorption to host bacteria (84). Curiously, both isolated capsids and spikes can absorb to bacteria in a non-specific way, but the gene H-defective particle does not attach at all (84). Other cistron H mutants have altered thermal stabilities and possibly host ranges as well (9).

Unassigned Infection-Specific Functions

All of the known ϕX genes have now been associated with some function in the infective process, but not all of the infection-specific functions have yet been correlated with the action of specific ϕX genes. Thus, several ϕX genes must be, as yet, undiscovered or several of the known genes must have more than one phenotype. In the case of each of these unassigned functions there is at least one gene that has not yet been screened for its effect upon the given process, and an untested

gene may therefore be responsible for the function. Alternatively, in the case of pleiotrophic genes, it may be that the mutations utilized for the screening were not stringent enough. If, for example, the am6 mutation is in gene E, then only half of the E phenotype is revealed by the lysis mutations at the C-terminal end of the cistron. Consequently, the am6 mutation should be screened for its effect on these processes, regardless of whether or not it is in gene E or J. The cistron A, A'-protein presents a special screening problem due to the complication that it cannot be deleted without simultaneously affecting the A' protein. It is also conceivable that many of the host responses to the infection are the result of synergistic effects of several ϕX genes and are not therefore altered by mutations in single genes. The infecting DNA, by itself, may be responsible for inducing some of the host changes.

Perhaps the most intriguing phenomena still to be correlated with a gene activity are the events surrounding the transition from the "early" stage of the infection, parental and progeny RF synthesis, to the late stage of infection, SS DNA synthesis and phage maturation. During this transition, host DNA synthesis ceases (67,90), progeny RF synthesis is reduced to a very low rate (63,71,91,93,97,98), DNA replication shifts from the membrane to the cytoplasm (93), and SS DNA synthesis and phage maturation commence. As noted earlier, genes B, D, F and G are required for the initiation of SS DNA synthesis, and C is required for this process to occur normally. However, none of the gene functions yet tested are required for the termination of host DNA or ϕX progeny RF synthesis. Genes B, C, F and G have been tested for

their role in the shut-off of host DNA replication (67,90), and B, C, D, E, F, G and H for their role in the cessation of progeny RF synthesis (51,63,67,71,91). It is suspected that both of these processes may be terminated by the same mechanism, in which case only A and J have not been tested. It is unlikely that gene A is involved, as it is required for progeny RF synthesis. Also, gene A function continues to be expressed in the presence of 30 μg/ml chloramphenicol, whereas the shut-off mechanism for ds-DNA synthesis is inactivated at this concentration (57,72,73,76,90,91,92). This chloramphenicol effect indicates that ϕX proteins are required for shut-off and that they must be present in fairly large amounts. Addition of chloramphenicol at any time prior to 15 minutes after infection prevents the shut-off of RF synthesis. Addition of chloramphenicol at even later times causes a renewed synthesis of RF after a delay (57,76,91). Apparently, continued protein synthesis is required to maintain the obstruction to ds-DNA synthesis.

Superinfection exclusion is another unassigned function that can be blocked at early times or partially reversed at later times by the presence of 30 μg/ml chloramphenicol. Again, continued synthesis of large amounts of some protein must be required for expression of this phenotype (44). The exclusion is established from 5 to 10 minutes after infection (44,76), with the consequence that subsequent infections are aborted at the level of eclipse (21,43). Apparently the cell membrane has been altered in some way so as to prevent injection of the viral DNA (43). It is known that gene E function is not required, in spite of its presumed interaction with the host membrane (44,76). As yet the other ϕX cistrons have not been screened for their effect on this process.

Assay of the infection-specific proteins from non-UV irradiated cells by the method of Mayol & Sinsheimer (8) reveals the presence of two and sometimes three high molecular weight host proteins that are apparently induced by the infection (8; Results). These proteins are not labeled during infection of UV-pretreated cells, indicating that their de novo synthesis is not required. As yet, this induction has not been correlated with the expression of particular ϕX genes, nor is the function of these proteins known.

Razin has shown that there is a cytosine-specific DNA methylase associated with the ϕX174 infection. This activity can be demonstrated in infected host cells that do not normally have this methylation specificity. It has not yet been established whether ϕX induces or modifies an existing host enzyme or whether it codes for the enzyme itself (162). In the former case, it may be that one of the ϕX-stimulated host proteins mentioned above is an induced methylase. In any case, the gene responsible for this activity has not been identified.

Single Strand DNA Synthesis

All lines of evidence suggest that SS DNA synthesis and ϕX maturation are highly interdependent processes. In the absence of functional B, D, F or G protein, SS synthesis is not initiated (63,68,71,91,98). Even when it is allowed to begin, it can be efficiently terminated by a shift to the restrictive temperature in temperature sensitive infections with mutants in any of these four cistrons (Siden, E., personal communication). Just how these four genes function in SS synthesis is still unclear. None of them appear to be directly involved in the replication event. Two are major structural components of the virion and the other two have been implicated in the assembly process. Apparently, the replication of SS DNA cannot occur in the absence of some intermediate structure in the phage assembly. One might expect that this intermediate is rather complex as all four of these genes are apparently involved in its construction. As a consequence of the interrelatedness of these two processes, a study of ϕX morphogenesis must necessarily consider the process of SS DNA replication as well.

In the normal infection, SS DNA synthesis begins rather abruptly 10 - 13 minutes after infection (76,90,100,151). The commencement of SS synthesis marks the beginning of the "late stage" of the infection process and this transition is accompanied by several other notable changes in the infection physiology. In particular, host DNA synthesis ceases (67,90) and ϕX progeny RF synthesis is reduced to a very low rate (63,71,91,93,97,98). At the same time the site of DNA replication shifts from the cellular membrane to the cytoplasm (93).

How these events are interrelated and whether or not they are the consequence of a single ϕX gene function has not been determined. They are uncoupled from SS DNA replication to the extent that ds DNA synthesis will terminate even in the absence of SS synthesis (9,67,90,91,98, 100).

Precursors to SS DNA Synthesis

SS synthesis is preceded in the early stage of the infection by the accumulation of a pool of approximately twenty progeny RF molecules per cell (76,95,96,100,152). This pool of progeny RF is derived by semiconservative replication of one or a few parental RF molecules associated with an essential bacterial replication site located on the host membrane (59,60,88,129,151). Once synthesized, the majority of the evidence suggests that the progeny RF do not participate further in DNA replication until the late stage of infection when they become the templates for SS synthesis (59,60,88,99,145,146,147,148,150,151). (A contrary interpretation has been advanced by Iwaya and Denhardt for their data (149). However, their results do not necessarily contradict the idea of a unique role for the parental RF in progeny RF synthesis (82). Nevertheless, a definitive experiment may not yet have been performed.)

Under the same conditions in which the parental RF is found associated with the host membrane, the progeny RF are found free in the cytoplasm as a mixture of the RF I and RF II forms (60,63,71,93,95, 96,97,100,101,102,152,154). The relative proportions of each form apparently depends upon the isolation procedure. The RF II form is preferentially lost to the phenol phase during phenol deproteinization

unless the lysate is first treated with pronase and detergent (71). One interpretation of this preferential loss is that the RF II form is complexed with a protein which carries it into the phenol phase. Both the RF I and RF II forms are however, precursors to SS DNA synthesis (93,95,97,100,152).

SS synthesis is also preceded by an accumulation of the ϕX gene products. With respect to the proteins that can be monitored, either by antiserum precipitability (10) or by SDS acrylamide gel electrophoresis (8,20), there does not seem to be any early or late class of ϕX protein. Rather, all proteins seem to be made at the same relative rates throughout the infection. Thus, the temporal sequence of expression of various ϕX specific functions (superinfection exclusion, ∿ 5 minutes; shut-off of host DNA synthesis, ∿12-15 minutes; initiation of SS DNA synthesis, ∿12-15 minutes; lysis, ∿20 minutes) is probably a consequence of the time required to accumulate sufficient material for activity rather than of some "early" - "late" control mechanism at the level of transcription or translation.

The pools of precursor proteins can be greatly expanded by carrying out the early stage of the infection at 15°C. Under these conditions SS DNA synthesis is blocked due to some cold sensitive step in that process. However, other aspects of the infection develop normally though at a lower rate. Thus, both the shut-off of host DNA synthesis and lysis occur eventually. Progeny RF accumulate to approximately 50 molecules/cell and over two hundred phage equivalents of serum blocking power are synthesized. If, after the accumulation of these pools, the infection is shifted to 37°C in the presence of 100 μg/ml

chloramphenicol up to 70 pfu/cell can be matured without any additional protein synthesis. After the shift to 37°C, 40% of the progeny RF DNA accumulated at 15° is transferred to viral single strands. These experiments demonstrate that the progeny RF are precursors of SS DNA and that concomitant protein synthesis is not required for SS DNA synthesis or phage assembly (95).

In the normal 37°C infection the ϕX protein pools established prior to SS DNA synthesis are apparently not nearly so extensive inasmuch as the addition of chloramphenicol just prior to or during the late stage of infection blocks the synthesis of any additional infectious particles (72,76). From this continuing need for protein synthesis, one can infer a continuing need for transcription as well. Puga et al. (159) have shown, in phage S13, that even though the "structural" half life of the virus messenger RNA (measured as the ability of the in vivo message to hybridize to viral DNA) is much longer, 10 minutes (a similar half life has been observed for the ϕX message (225,226)), than the half life of the E. coli message, 2 minutes, the functional half life (measured as the ability of the in vivo message to give rise to new gene F product) remains short, 1.5 minutes, throughout the infection. As a consequence, phage messenger synthesized at early times in the infection cannot be responsible for protein synthesis at late times. Thus during the late stage of the infection, some portion of the intracellular RF must be engaged in the transcription process as well as in SS DNA synthesis. It is not known whether or not RF molecules freely exchange between these two functions, whether some RF are sequestered for protein synthesis alone, or whether both processes can occur

simultaneously on the same DNA template.

Mechanism of SS DNA Synthesis

Pulse chase experiments performed in numerous laboratories have unambiguously established the progeny RF as the immediate precursors of SS DNA synthesis (93,95,97,100,152). There is also general agreement that synthesis of the SS DNA proceeds by an asymmetric displacement of the plus strand from an RF II molecule by a newly replicating plus strand (93,96,97,100,101,142,152,153). This synthesis mechanism is known as the rolling circle model of DNA replication (102). Most investigators find that the nascent plus strand is covalently attached to the old plus strand giving rise to a continuum of replication intermediates, RI, comprised of unit-length, closed, circular minus strands and linear viral strands of from once to twice unit length (93, 96,101,102,142).

Yokoyama et al.(103) have observed that some of the nascent plus strand DNA is also of less than unit length prompting them to propose a discontinuous model of SS DNA synthesis more in accord with the discontinuous mechanisms established for many other replication systems (155,156,157,158). Nascent plus strand fragments can also be observed in the data of others (96,97,101,102,142). However, the significance of this material is still uncertain as Yokoyama et al. could not rigorously exclude the possibility that the fragments were the consequence of an artifact of sample preparation (103).

No investigator has reported nascent viral strands of greater than twice unit length. (It should be noted, however, that the methods so far employed would not distinguish a molecule of slightly greater

than twice unit length as proposed in Gilbert and Dressler's formulation of the rolling circle model (102).) It is thought that after a unit length of SS DNA has been displaced from the RF II template this SS tail is cleaved off to be matured into an infectious particle thus freeing the RF II moiety for another round of replication. Because pulse label accumulates in this RF II species, it is thought that initiation of a new round of synthesis represents a rate limiting step in the normal replication process (93).

Origin of Replication - Nicks and Gaps

Several investigators have demonstrated that these "resting RF II" molecules contain a nick or a short gap specifically in the viral strand (93,97,104,142). Knippers et al.(93) and Yokoyama et al. (104) have shown that the nick occurs in a unique nucleotide sequence. Johnson and Sinsheimer (105) have utilized the restriction endonuclease fragment assay to demonstrate that in both nicked and the gapped molecules the discontinuity is located within the gene A cistron. Miller and Sinsheimer (38) have shown that the SS linear plus strands isolated from resting RF II can be specifically circularized by a particular restriction endonuclease fragment that includes the A cistron.

It has also been surmised that SS DNA synthesis is initiated at a unique point. Knippers et al. (93) have shown that the displaced viral strand is terminated by a unique 5′ nucleotide, G. Surprisingly, this is not the same 5′ nucleotide, C, that is found at the unique nick in the resting RF II. They suggest that this anomaly may have something to do with the mechanism of circularization of new viral strands. It is assumed however, that the unique 5′ end originated

at the specific nick in the precursor RF II (93). Apparently SS DNA synthesis is both initiated and terminated at a specific DNA locus in the vicinity of the A cistron.

It is not yet known how this specificity is established. On the basis of their limited sequence data Knippers et al. postulated that the nick occurred in a self-complementary region of the viral strand that could provide secondary structure both for recognition by a specific nuclease and for circularization of new viral strands. Fiers and Sinsheimer reported an E. coli phosphodiesterase insensitive discontinuity in viral SS DNA and speculated that it arose from some secondary structure inherent in the free SS (13). Razin and Sinsheimer (106) have demonstrated that the RF II nick is resistant to the 5′ → 3′ exonucleolytic activity of the host Polymerase I enzyme. They speculate that nonspecific nicks in the RF plus strand are translated to the specific site by the nick translation function of Pol I. However, the concomitant conservation of the RF II minus strand circle and the unnicked RF I pool would seem to argue against random nicking as a frequent intracellular occurrence. It has also been shown that the ϕX infection proceeds normally in Pol I$^-$ host cells (107,108) and that the other host polymerases do not have an exonuclease function (133,134,135). Iwaya et al. (164) have reported that ϕX viral strand linear DNA is an efficient template for the T4 DNA polymerase, indicating a self-annealing of the 3′ end of the molecule to some internal region to provide an initiation point. Their data suggest that some of these molecules may be circularized by polynucleotide ligase.

Kato et al. (199) have found that ϕX RF I supercoiled DNA, but

not ϕX RF II DNA or artificially prepared non-supercoiled RF I, is nicked once by a single strand specific endonuclease from Neurospora crassa. Indirect evidence suggests that this nicking may occur at a unique site. They speculate that the stress inherent in the RF I supercoil establishes a small endonuclease sensitive single strand loop on the RF I molecule. Such loops may be similar to the anticodon regions of t-RNAs and serve as recognition signals for various DNA dependent viral functions.

These loops, the result of palindrome sequences in the DNA, are very common in some eucaryotic DNAs (209) and must also exist, at least to a limited extent, in ϕX174 DNA, as well, as ϕX174 DNA is susceptible to Hemophilus influenzae restriction endonuclease R (54) which has been shown to cleave double stranded DNAs at the center of a specific palindrome sequence (208).

Razin et al. (160,161,162) in a continuing study have demonstrated that the ϕX viral DNA contains one 5-methylcytosine residue per DNA molecule. Resting RF II are unmethylated whereas the SS replicative intermediates again contain one 5-methylcytosine per replicative intermediate molecule. Amy Lee (Lee, A.S., personal communication) has recently shown that the 5-methylcytosine residue from viral DNA is located in a specific restriction endonuclease fragment that overlaps both cistrons H and A and, therefore, the junction between these two genes. Although no specific role has been demonstrated for the 5-methylcytosine residue, its association with the replicative intermediate and its location near the origin of replication suggest that it may serve as a recognition signal in the initiation and termination of that process. Razin has proposed a model for the recognition role

of the 5-methylcytosine residue (161).

Other evidence has established that the A cistron is also the origin of parental and progeny RF synthesis (42,136,137). In the case of parental RF synthesis it may be that the origin of replication is indicated by the 5-methylcytosine residue. In the case of progeny RF synthesis it seems likely that the cistron A, A´ protein is responsible for establishing the origin of replication by means of a specific nick in the viral strand of the RF I. However, it remains to be demonstrated that this nick is in the A cistron.

Once SS synthesis has commenced, the replicating RF templates remain in the RF II form for the duration of the infection (93). However, just prior to the initiation of SS synthesis a substantial fraction of the progeny RF are in the RF I form. At least some of this RF I serves as precursor to SS DNA synthesis (93,95,97,152). In this case it is not known how SS synthesis is initiated on these molecules. Again, one might speculate that the A´ protein introduces a specific plus strand nick into the progeny RF I.

This function has not been established, however, and one might infer from the experiments of Francke and Ray(49) that cytoplasmic RF are not suitable substrates for the gene A nicking activity. However, their investigation was limited to a consideration of the cytoplasmic parental RF only, and it appears, from the experiments of Hutchison (9), on limited participation in complementation, and Truffaut on the role of progeny RF in transcription (138), that cytoplasmic parental, and progeny RF are not equivalent molecular species. Apparently, only membrane-site associated parental RF and their progeny can serve

as transcription substrates. (For a more extended discussion, see the section on gene A.) It seems probable that the transcribing cytoplasmic RF might be a suitable substrate for the cis-acting A´ activity.

This activity and its role in SS DNA synthesis might be missed in a conventional screening for gene A function utilizing temperature shift experiments with ts mutants in gene A (57). If the shift were conducted prior to SS synthesis then SS replication could still be initiated on that fraction of the progeny RF pool already in the RF II form. A shift conducted after SS synthesis was underway would have little effect as most of the RF pool would already have been converted to the RF II form.

Circularization

The mechanism by which the newly formed viral strand is circularized has been the subject of considerable speculation. Knippers et al. (93) have postulated a self-complementary region of the SS DNA which would enable the specifically nicked circle to close spontaneously forming a substrate for a ligase activity. Razin and Sinsheimer (106) have discovered a GC rich region of the DNA on the 5´ side of the nick which might serve to establish this secondary structure. Gilbert and Dressler (102) have proposed that a small fragment of minus strand template binds the two plus strand ends together and also serves as an initiator for complementary strand synthesis during parental RF formation in the new infection. Others have postulated that ϕX coat proteins hold the two ends of the new plus strand together for some sort of ligase reaction (103,139).

In every case the expectation is that the discontinuity in the

nascent SS DNA is in a well defined locus. Schekman and Ray (39) have observed that unit length linear plus strands are matured into a large proportion of the virions during infection of a ligase deficient host strain, ts7. It was assumed that these linear molecules represented a normal intermediate in the production of circular viral DNA. Iwaya et al. (164) have since demonstrated that these molecules serve as efficient templates for polymerization by the T4 DNA polymerase, thus indicating that the 3´ end of these molecules is self-annealing to some internal region. From much less convincing experiments they conclude that a small percentage of these molecules are circularized by the polynucleotide ligase reaction. Contrary to expectation, Miller and Sinsheimer (38), by monitoring the efficiency with which specific restriction endonuclease fragments can circularize SS linear viral DNA, have demonstrated that the great majority of the linear viral strands from the ts7 infection are randomly nicked. Using the same procedure they observed a specific circularization (by a particular fragment) of the nicked viral strand from the resting RF II isolated from an infection of the same host. It is apparent that the origin and significance of the randomly nicked viral DNA from the ts7 restrictive infection is as yet undetermined, and it remains to be demonstrated that these molecules are intermediates in the normal circularization process.

It has been reported that the specifically nicked linear viral DNA isolated from RF II molecules (39,140), as well as the linear viral DNA obtained from the ts7 infection (39) has an enhanced infectivity over that expected for randomly nicked SS DNA. In carefully controlled experiments, Miller and Sinsheimer (38) have been able to demonstrate

that, in the cases so far reported, this effect can be explained either by contamination of the plus strand linears by circular molecules or by the adventitious annealing of the plus strand linears to contaminating minus strand linear DNA. Thus a definitive demonstration of this infectivity has yet to be established.

Role of Host Enzymes in SS DNA Synthesis

Prior to the isolation of the Pol I$^-$ strains of E. coli (109), it was reasonably expected that the Pol I enzyme was responsible for ϕX DNA replication. It manifested all of the requisite enzymatic activities (131) and could be used to replicate ϕX in vitro (163). Since that time two additional polymerases, Pol II and Pol III, have been isolated from E. coli (110,111,112), and ϕX has been shown to replicate normally in the absence of both Pol I and Pol II (107,108). This suggests, but does not prove, that the third enzyme, Pol III, is required for all stages of ϕX replication. It is conceivable that a ϕX gene codes for a polymerase activity. However, the only likely candidate is the ϕX gene C product, and the low molecular weight of this protein suggests that, at most, it might serve to modify the activity of an existing host polymerase.

Several groups have utilized the conditional lethality of temperature sensitive mutations to define seven host genes, denoted dnaA through dnaG, that are absoluted required for replication of the bacterial chromosome (113,114,118,119). One of these, dnaE, is the host Pol III gene (115). Host polymerases I and II are not represented by any of these mutations as neither enzyme is absolutely required for bacterial survival (107,108).

Unfortunately most of these mutations do not yet exist in ϕX sensitive E. coli strains. As a consequence, these mutations have been only partially characterized with respect to their role in ϕX DNA replication. The greatest effort has been directed at determining the in vitro requirements for the conversion of ϕX SS DNA to the RF form. The laboratories of J. Hurwitz and A. Kornberg have demonstrated that host dna genes, A, B, C, D, E and G are all required for this conversion in soluble extracts from Pol I⁻ cells. (Wechsler has shown that dna C and dna D are the same gene (141).) Because of the similarity of this requirement to that for host replication, these groups have employed this system as an assay for the purification of the dna gene products (116,117,120,121).

The host genes required for ϕX174 progeny RF or SS DNA synthesis have not been determined so completely. Steinberg and Denhardt (127) as well as Sinsheimer et al. (96), have utilized ϕX174 sensitive mutants in the dna B gene (122) to demonstrate an in vivo requirement for that gene in all three stages of ϕX DNA replication. Taketo (122) has investigated several ϕX174 insensitive dna strains by means of transfections with purified ϕX SS or RF DNA. He showed that dna A and F mutants support all stages of the ϕX174 infection at the restrictive temperature whereas dna E mutants do not. Dumas et al. have undertaken to re-isolate the dna temperature sensitive mutations in an E. coli C strain sensitive to ϕX. To date, they have demonstrated an in vivo requirement for host dna E and dna C during progeny RF synthesis and dna E but not dna C during SS DNA synthesis. Neither the dna E or dna C gene was required for the in vivo conversion of ϕX SS DNA to parental

RF (123,124). The dna C gene has been shown to be required for the initiation of host cell replication (113,125).

It will be noted that there are several discrepancies between the in vitro and in vivo gene requirements for parental RF formation. While dna genes A, C and E are all required for the in vitro conversion of ϕX SS DNA to the RF form, none of these genes are required in vivo. Significantly, the in vitro system is prepared from cells lacking Pol I. Experiments by Greenlee indicate that the discrepancy between the two systems is probably due to the functional overlap between several of these genes and the polymerases I and II. Greenlee demonstrated that, in vivo, the dna E product and Pol I can substitute for each other in the formation of parental RF but that one or the other must be present (126). It is conceivable that Pol I can also substitute for the dna A and dna C functions at this stage of the infection. Greenlee's experiments indicate that Pol I can partially compensate for the dna E function during progeny RF synthesis as well, but both Greenlee and Dumas demonstrated an absolute requirement for the dna E protein during SS replication. The in vivo experiments performed with dna B and dna C mutants were conducted in Pol I^+ cells indicating that the Pol I activity cannot substitute for the dna B gene at any stage of the infection or the dna C gene during progeny RF synthesis.

It is of interest that the in vitro replication systems developed in Hurwitz's and Kornberg's laboratories are soluble systems extracted from the cell cytoplasm. These extracts contain all of the dna A through G gene products and yet the in vivo production of ϕX progeny

RF and the replication of the bacterial chromosome both require some sort of attachment to an essential bacterial membrane site (59,60,143, 144,166,169). Evidently, the "site" genes are not represented by the dna ts mutations nor are the dna gene products structural components of the site. The fact that DNA synthesis does not progress beyond the formation of the first parental RF in these systems suggests that the addition of other components, including presumably, the membrane "site", will be required to obtain progeny RF synthesis. It may be necessary to employ a system such as that of Nusslein et al. for this purpose (128). Inasmuch as such a large proportion of the host replication apparatus is represented by soluble enzymes, the role of this membrane association becomes more intriguing than ever.

The lack of a "site" requirement for ϕX parental RF formation in vitro is in accord with the in vivo observation that at high multiplicities of infection far more parental RF are formed per cell than can ultimately be accomodated at the limited number of essential bacterial membrane sites (60,129). Apparently, association with the essential site occurs after the conversion of the infecting SS DNA to an RF form.

Assembly of ϕX174 Virions

The assembly process itself is one of the least well characterized aspects of the ϕX174 infection. This is, at least in part, a consequence of its complicated nature and inaccessibility to study. As the culmination of the entire infection process, the success of this stage ultimately depends upon the expression of every ϕX174 gene except E. (Gene E may be required as well, if it turns out that the E and J phenotypes are both expressed by the same protein.) Moreover, at least six ϕX genes are directly involved and two others cannot yet be definitely excluded. Thus, by way of summary of the preceding discussion, the four virion proteins F, G, H and J are obviously required as precursors; the B protein has a demonstrable role in the formation of a subunit structure; and the D protein is implicated by virtue of its association with various subviral particles presumed to be assembly intermediates. Gene C product is required for normal SS synthesis but whether its role is at the level of DNA replication or particle assembly has not yet been determined. Gene A has not been adequately screened for a role in this stage of the infection.

Precursors To Assembly

Several lines of evidence suggest that the precursors to assembly are withdrawn at random from common pools. With the exception of mutations in cistron A, most nonallelic combinations of ϕX mutants complement each other in symmetric fashion, though seldom with the same phage producing efficiency as wt (9). In order for complementation to take place, the wt protein of one phage must be able to substitute

for the mutant protein of the other, and vice versa. If one or the other of the mutant proteins is not merely inactive but rather participates in the infection in such a way as to produce aberrant structures or otherwise interfere with the normal functioning of the wt proteins, the efficiency with which new phage are produced will be reduced. Thus, both the fact of complementation itself and the reduced efficiency of the complement infection argue for a freely exchanging pool of intracellular protein.

The phenotypic mixing experiments of Hutchison et al. (85) provide a direct demonstration of the commonality of the precursor pools. These investigators found that when host cells were mixedly infected with two ϕX mutant strains with electrophoretically distinguishable virions, they produced a continuum of progeny phenotypes ranging from the extremes of the parental strains through all combinations in between. The existence of hybrid phenotypes indicates that there has been at least some mixing of the subunit pools of both infecting phage types but one might have expected a completely homogeneous hybrid composition (within the limits of statistical variation) had the subunits been selected entirely at random. Hutchison et al. surmised that this deviation from homogeneity was a consequence of the way in which the infecting genomes were distributed in the host cells as a function of the multiplicity of infection and the limited number of infecting parental types that can participate in the infection of a single cell (59). When these factors were taken into consideration it was found that the distribution of progeny phenotypes and genotypes fit the expectation for particles assembled at random from distinguishable but

equivalent subunits (85).

The concept of common intracellular pools of assembly precursors is also in accord with Newbold's and Sinsheimer's observation that SS DNA synthesis and phage assembly are uncoupled from protein synthesis. When infected cells are shifted from 15°C, a temperature at which they do not undergo SS DNA synthesis, to 37°C in the presence of chloramphenicol, they are able to mature large numbers of phage from the protein pools that accumulate at 15°C (95).

The extent to which precursor pools accumulate during the late stage of the normal infection is still uncertain. Krane (10) has reported that from the time of eclipse to the end of the infection the intracellular pools of ϕX serum blocking power exceed the concentration of intracellular infective particles by a relatively constant factor of thirteen fold. This observation has often been taken to indicate a huge excess of intracellular ϕX protein over that which is ultimately matured into virions. However, it should be noted that the serum blocking power of these lysates was measured as phage particle equivalents. On the other hand, phage stocks of ϕX174 have rather low specific infectivities which rarely exceed 0.3 and are more often on the order of 0.1 pfu/particle (32,181, this thesis). As a consequence, the observation of thirteen phage particle equivalents per infective particle does not necessarily indicate a large excess of intracellular non-vironal protein, since many purified phage stocks are no more active than this.

Hutchison and Sinsheimer (76) observed that infected cells continued to produce infective SS DNA but not infectious particles when chloramphenicol was added at 30 μg per ml at late times. They did not

determine whether this SS DNA was complexed with protein. Nevertheless, inasmuch as mutant infections with at least four ϕX genes are unable to sustain any SS synthesis at all, this result supports the notion of a substantial pool of precursor protein. Morishima et al. obtained a contrary result when SS synthesis was monitored as radioactive thymidine incorporated into mitomycin C treated cells (91). In this case incorporation stopped abruptly upon addition of 30 μg/ml chloramphenicol. It is conceivable that chloramphenicol interferes with thymidine uptake when administered at late times.

Siden and Hayashi (61) have observed that in infections with ts mutants in cistrons F, G, or D, there is an immediate cessation of SS synthesis when the infection is shifted to the restrictive temperature. However, this is not true of gene B mutants which continue to replicate SS DNA for a considerable time after the shift. Surprisingly, this post-shift DNA is not packaged with de novo synthesized capsid proteins, but rather is matured into rapidly sedimenting particles containing protein that pre-existed before the temperature shift. Siden and Hayashi argue that the cell contains a large pool of assembly precursors which require gene B function for their construction. In the absence of gene B protein, SS DNA synthesis and phage assembly can continue only so long as these precursors last.

With regard to this model, one would expect this same precursor pool to be present during the permissive infection with other mutants as well. However, temperature shifts with mutants in genes G and F result in an immediate cessation of SS DNA synthesis. Presumably, this is due to the thermal inactivation of the temperature sensitive G

or F protein pools after the shift up. However, this is not necessarily the case. Newbold and Sinsheimer found that out of six ϕX temperature sensitive mutant proteins that they investigated, only one was inactivated by a shift to the restrictive temperature after being synthesized under permissive conditions. All others, including representatives from cistrons F, B and D, expressed their temperature sensitive phenotype only when synthesized at the restrictive temperature (95). As a consequence, the thermal sensitivity of the mutant phage precursor pools should be substantiated in an independent experiment such as that described by Newbold and Sinsheimer (95).

It it were to turn out that the extant F and G protein pools of temperature sensitive mutants were not inactivated by temperature shifts, then a more complex assembly mechanism would be indicated. Siden has demonstrated that the gene B mediated precursor is composed of capsomeric subunits of the F and G protein (see discussion in conjunction with gene B function). Nascent F and G proteins must, then, necessarily enter the maturation pathway prior to the gene B mediated step. However, in order to explain their immediate effect upon SS synthesis in the event that the extant proteins are not denatured by a temperature shift in a temperature sensitive infection, it would be necessary to postulate that they again enter the pathway at a stage subsequent to gene B function but in some role (initiation of SS DNA synthesis?) in which they would not contribute label to newly constructed virions.

Direct observation of infected lysates prepared at late times reveals that there are substantial pools of non-virion associated virion

proteins in the form of various subunit structures that will be discussed below (65, Mayol, R.M., unpublished data, Results). As the course of the infection progresses an ever increasing proportion of this protein accumulates in phage particles. The phage particle and 70S lysis artifact begin to dominate the intracellular distribution of ϕX protein shortly after the end of eclipse. Once again this suggests that Krane's serum blocking power result merely monitored the specific infectivity of the intracellular phage particles.

Mayol and Sinsheimer have observed that the subunit structures involving the F protein are synthesized throughout the infection at approximately the same rate as new virions, whereas those involving G and D proteins diminish in rate (during the first thirty minutes after eclipse) to about half their post-eclipse values (Mayol, R., unpublished data).

The Relationship of ϕX174 Assembly to SS DNA Synthesis

Although it is clear that normal SS DNA synthesis is tightly coupled to phage assembly it is not necessarily true that assembly is coupled to SS synthesis. The fact that the ϕX virion can package small but significant amounts of nonhomologous fd DNA suggests some autonomy in this process (37). In vitro reconstitution of a phage represents the most unambiguous proof of uncoupling. In this regard Takai (179) has reported a spontaneous association between a soluble extract of ϕX proteins and purified ϕX viral DNA. With the reservation that he did not present all possible controls, it was shown that these complexes did not form with E. coli SS DNA. They were also reported to be nuclease

resistant and would attach to E. coli. With the exception of one preparation, which formed a distinct peak at approximately 110S, the complex sedimented very heterogeneously often in excess of 200S.

Knippers and Sinsheimer (98) have observed the uncoupling of phage assembly from normal SS DNA replication in their in vivo study of the abortive infection of a gene G mutant, ts79. When the ts79 infection is conducted at the restrictive temperature, a pool of progeny RF accumulates but there is no SS DNA synthesis. If the infection is then shifted to the permissive temperature at some time after the end of the normal latent period, infective plus strands from these progeny RF are matured into infective particles by an abnormal process in which the negative strand is degraded. This experiment reveals a striking specificity of the assembly process for a particular SS DNA when presented with two choices that should be equivalent in all properties except their sequences. The absence of SS replication during this aberrant maturation demonstrates that this process is not always required for assembly.

The Intracellular Form of the SS DNA Precursor Pool

This autonomy from SS DNA replication suggests that it may be possible for ϕX proteins to package free SS DNA. This suggests in turn, at least from these limited considerations, that newly synthesized ϕX single strands might enter the assembly process via a pool of free SS DNA circles. Such a pool has been observed by several investigators (39,71,165, Results, this thesis). However, free SS DNA is not always present (72,93,98,99). This conflict has apparently been resolved

by Weisbeek and Sinsheimer (165) who have demonstrated that the particulate form of the intracellular infectivity, and the presence of free SS DNA, is highly dependent upon the lysis conditions. After lysis in a low ionic strength, Tris-EDTA buffer (the procedure utilized by Schekman and Ray (39) and Iwaya and Denhardt (71)) the ϕX infectivity is distributed fairly evenly between a 140S and the usual 114S particle, and free SS DNA is present in the lysate. After lysis in the same buffer, but with the addition of 1.0 M NaCl, the infectivity is recovered exclusively as 114S particles and there is very little free SS DNA. The 140S particle can be converted to phage by exposure to Mg^{++}. Presumably, lysis in the presence of Mg^{++} would also give rise exclusively to 114S particles. In most of the experiments presented in the Results sections of this thesis, lysis has been performed in the presence of Mg^{++}.

The relationship of the 140S particle to the SS DNA pool also suggests that the intracellular SS DNA is normally associated with either the 140S or the 114S particle. Since the culture can be lysed under some conditions (high salt) in which virtually no free SS are found, and, since it is unlikely that this is a consequence of a very rapid maturation of the free SS pool into phage during lysis in this particular buffer, the experiments of Weisbeek and Sinsheimer suggest that the SS DNA pool observed after the low ionic strength procedure is a lysis artifact derived from a large intracellular pool of 140S particles. They note that <u>in vitro</u>, the 140S particle will decompose to 70S particles and free SS DNA when stored in low ionic strength buffer (165).

Whereas these experiments seem to have resolved much of the former controversy regarding the experimental observation of free SS DNA, it should be noted that these authors did not investigate the intracellular location of pulse labeled SS DNA, and there may consequently still be a legitimate question as to whether the immediate product of SS synthesis exists as a free molecule. However, the stringent requirement of SS replication for functional virion proteins makes it highly unlikely that this is the case. This dependency must be a consequence of either a direct interaction between the virion proteins and the replicating SS DNA or feedback inhibition from some latter SS DNA-ϕX protein interaction that is expressed through an intracellular SS DNA pool. If the latter were the case, we would expect that, in the absence of one of the essential viral proteins, this pool would have to be synthesized before the inhibition could be established. Such synthesis is not observed, suggesting that the interaction is a more direct one.

The Specificity of Assembly and the Nature of the ϕX174 Protein - DNA Interactions During Assembly

The nature of this presumed interaction is one of the more intriguing questions concerning the ϕX infection and has been the subject of considerable speculation (71,93,102,103,139). It has been suggested that the nascent SS DNA must be rapidly coated with protein in order to protect it from intracellular single strand nucleases. Alternatively, a protein association might be established to prevent minus strand synthesis (102,139). In this regard the Knippers and Sinsheimer result with the ts79 mutant (98) indicates that not only is

phage protein capable of blocking minus strand synthesis, but it can also completely displace the minus strand from an RF molecule. It may be that this same mechanism is at work in a more orderly fashion during normal SS DNA replication. Quite possibly, the association of viral protein with the 5′ plus strand end is a requirement for initiation of the displacement of the new SS DNA (71,103,139). Several authors have noted that such an attachment might serve an analogous functional requirement during SS synthesis to the membrane attachment of ϕX RF during ds DNA replication (71,102). Others have suggested that the emerging SS serves as a nucleation point for the orderly condensation of the viral proteins into a phage particle (93,103).

Each of these models suggest that there is a strong affinity between one or more of the essential proteins F, G, B and D, and SS viral DNA. However, B protein is not directly involved at the level of SS DNA synthesis. The behavior of D protein on DNA cellulose columns (Gelfand, D.; Linney, E., personal communication) suggests that it does not bind to DNA; and the spontaneous ejection of the SS DNA from the virion indicates that the F and G proteins do not bind strongly to DNA either. Apparently none of these proteins are good candidates for a DNA coating agent, suggesting that some other mechanism may be involved.

The fact that all of these proteins are required to initiate SS DNA replication suggests that they act in a concerted fashion This in turn suggests that they may function as a single particle. If so, one might expect this particle to be quite complex, inasmuch as four proteins are involved in its construction. Such a particle was discovered in the course of this thesis research and will be described in

the Results section.

Similar particles composed of the virion proteins and a large excess of a maturation protein have been demonstrated to be intermediates in the head morphogenesis of phages P22 (219,220) and T7 (224). Procapsid structures are also observed in T4 and λ infections. These particles contain non-virional phage proteins but not in the large mass and stoichiometric quantities observed for φX, P22 and T7. In the cases of P22 (220) and T4 (197), in vivo experiments have demonstrated that the nascent phage DNA is replicated into these procapsid structures. Assuming similar packaging mechanisms for all of these phages, then DNA replication is not a necessity for packaging as phage λ can be completely reconstituted in vitro from phage heads, phage tails, and DNA (221,223). T7 phage proheads also package DNA in vitro (224).

By analogy with the tailed phages one might expect that φX SS DNA is replicated into a procapsid structure as well, and that the existence of this structure as a receptacle for the new single strand is an obligatory requirement for SS DNA synthesis. As such it could serve to protect the nascent SS DNA from nuclease or complementary strand synthesis and, by analogy with the essential membrane "site", as an essential point of attachment from which to initiate the displacement reaction during the "rolling circle" replication of the SS DNA (71,102).

Lerman has demonstrated a possible mechanism by which phage DNAs may be sequestered into small particles for which they show no intrinsic binding affinity. He has demonstrated that several double stranded phage DNAs undergo a cooperative transition from an extended

viscous form to a compact rapidly sedimenting conformation when shifted into a high ionic strength environment in the presence of high concentrations of a neutral polymer, polyethylene oxide. The sedimentation values of the most rapidly sedimenting DNAs indicate that they form particles close to the size of the phage heads from which they were derived. Lerman interpreted this behavior to be the consequence of a competition for solvent space between two nonattracting polymers which results in a phase separation on the part of single DNA molecules. Lerman notes that his in vitro conditions mimic the intracellular molecular environment and that these compact structures may represent the usual conformation of intracellular DNA (168).

One might speculate that interactions of this type may serve to stabilize the phage DNA during its intracellular packaging into the virion and its precursor structures. In addition the procapsid structure may represent a localized environment in which the viral DNA is especially likely to undergo the transition to a compact state. Since the maintenance of this conformation requires a high ionic strength environment (physiological), one might suppose that subsequent to lysis the intravirional DNA becomes destabilized as the occluded ions diffuse away into the low ionic strength extracellular environment. The DNA must then be stabilized by the external constraints imposed by the mature virion. If the extracellular virion is subsequently disrupted by means of various physical or chemical treatments, or by interaction with a bacterial absorption site, the DNA is spontaneously ejected.

The sedimentation behavior of bacterial chromosomes isolated from cells lysed in the presence of 1.0 M NaCl (166,167,169) is in

agreement with Lerman's expectation of a compact conformation for intracellular DNA. Once isolated this DNA retains a compact configuration in both low and high ionic strength solutions indicating some mechanical constraint against its relaxation. This constraint is RNAse sensitive and appears to be in the form of RNA "bridges" between distal parts of the molecule (167,169). One might surmise from Lerman's work that these RNA "bridges" serve as constraints only as a consequence of the *in vitro* environment and do not necessarily function as such *in vivo*. However, their fortuitous existence, regardless of their function, provides an indication of the intracellular conformation of the bacterial DNA.

Pettijohn (227) has noted that the extracellular bacterial chromosome is organized into numerous independent domains of supercoiled DNA. Others have speculated that the intravirional DNA is also highly supercoiled (170,171). However, supercoiling is not a meaningful concept in terms of ϕX174's SS viral DNA, and DNA condensation mechanisms involving supercoils probably would not be applicable to this system. In this regard, direct electron microscopic observations of the encapsulated DNA from several phages has not revealed supercoils (173), and Lerman *et al.* (172) do not observe supercoiling in their *in vitro* preparations of compact phage DNAs. It is therefore unlikely that supercoiling plays a major role in compacting the DNA for assembly.

The observations in the preceding paragraphs lead one to the expectation that ϕX SS DNA is packaged into a protovirion constructed of, or by, the F, G, B and D gene products. However, it is difficult to imagine how, in the aberrant *ts*79 assembly observed by Knippers and

Sinsheimer (98), such a particle could, by itself, confer the remarkable specificity with which the assembly mechanism selects for one strand of DNA (+) over another (-) from a molecule (RF I) in which both strands are chemically equivalent except for their sequences. On the other hand, this specificity is even more incompatible with a model in which the DNA substrate for assembly is selected by coating it with protein. This type of reaction requires that the protein subunits have a non-specific affinity for SS DNA since they must bind along the entire length of the molecule, over a great range of possible sequences. As a consequence, the high degree of specificity that is observed in the assembly process is more likely determined by a specific, localized nucleotide sequence on the plus strand DNA. In some way this sequence must effect the preferential introduction of the plus strand into the protovirion, either by virtue of its primary sequence, its secondary structure, or its interaction with some intermediary protein.

This protovirion model is in apparent contradiction to the observation of a strong association between replicating ϕX SS DNA and a ϕX antigenic protein (93, Results). However it will be shown in the Results that this protein must be present at concentrations of only a few copies per DNA molecule and therefore, could not possibly be "coating" the DNA as proposed in some models. Also the identity of this protein has not yet been determined and it may not be the gene F or G product. One might speculate that this protein serves to specifically introduce the viral plus strand into the protocapsid as proposed above.

Takai's (179) report of a spontaneous <u>in vitro</u> association of ϕX proteins with ϕX DNA would seem to argue for a generalized affinity of

ϕX proteins for SS DNA. However, the specificity of this system for ϕX SS DNA, as opposed to denatured E. coli DNA, again suggests a more restricted interaction. Perhaps the highly specific association of one or a few proteins with the ϕX SS DNA serves to nucleate a much more generalized condensation of the rest of the proteins. Certainly, this in vitro system merits reinvestigation while monitoring both its DNA and protein components. (Takai followed only a ^{32}P DNA label.)

Subviral Particles From the ϕX Infection

From the circumstantial evidence presented so far, one would expect to find that the lysates of ϕX infected cells contained at least one subviral particle composed of F, G and possibly D and B protein (the protovirion) and possibly precursors and degradation products from this structure and other assembly intermediates as well. At least twelve different subviral particles and two non-viral infectious particles have now been observed in conjunction with the normal ϕX174 infection. In order to facilitate discussion of these structures, Table 5 has been constructed listing the various particles and their more important properties. Unambiguous precursor-product relationships have been worked out for only a few of these. They will be discussed in the order of their complexity, the simplest structures first.

Three and sometimes four ϕX specific peaks are found at the top of sedimentation velocity gradients of lysates of infected cells. The particles represented by these peaks have been thoroughly characterized by Tonegawa and Hayashi in cells irradiated with UV_{260} light prior to infection in order to suppress host protein synthesis (65). This technique, while it resolves ϕX specific proteins very well, has the

disadvantages that ϕX induced host proteins are not labeled and, as evidenced by the low phage yields from these infections, many of the cells are abortively or aberrantly infected resulting in a distortion of the normal patterns of particle production. As a practical matter, ϕX specific as well as host incorporation of radioactive amino acids is greatly reduced.

Mayol and Sinsheimer (8) have circumvented these problems by differentially labeling infected and uninfected cultures, then mixing the lysates, and after SDS acrylamide gel electrophoresis or velocity sedimentation, determining the ϕX specific increment of the infected label. This procedure has been used to confirm the existence of these low molecular weight particles in the normal infection (Mayol and Sinsheimer, unpublished; Results). This double label procedure has been modified in the Results section to permit the simultaneous visualization of the ϕX DNA. The UV and non-UV systems vary principally with respect to the proportions in which the ϕX specific material is distributed among the various particles. (See the Results section for the distribution in non-UV irradiated cells.)

2.5S Peak - The Monomeric Proteins - The top of a velocity sedimentation gradient of a lysate of ϕX wt infected, UV pretreated cells is dominated by a broad peak centered at 2.5S and containing what are apparently the monomers of the A, B, C, D, F, G and H proteins (65, Results) as assigned in the earlier discussion of the gene products. The A′ protein is not observed but may not be resolvable. The identity of the smallest molecular weight component as either C or J protein is uncertain. The UV system reveals at least one, and possibly two, unassigned peaks. These could either be the result of residual host

synthesis or perhaps unassigned E protein.

In the non-UV system, the 2.5S peak accounts for a several fold smaller proportion of the ϕX specific protein label compared to the UV system. It is composed principally of D protein and the smaller protein, either C or J. Compared to the UV system it contains much smaller proportions of the other proteins, including F and G. It is likely that these differences are due to a high proportion of abortive infections in the UV culture which result in the accumulation of monomeric proteins which otherwise would be associated with more complex structures. Most of the host proteins in the non-UV system also sediment in this region of the gradient thereby limiting the power of the double label procedure to resolve the smaller quantities of minor ϕX components that are found in the 2.5S peak (Results).

The 6S and 9S Particles - The 6S and 9S peaks represent particles composed solely of G protein and F protein respectively. These peaks are removed from the sedimentation pattern only by mutations in their homologous cistrons, suggesting that no other gene product is required for their formation. On the other hand, when the monomers from either of these cistrons are recovered from the 2.5S region of the gradient they show only a very limited ability to form these particles in vitro. It is unlikely that this is a consequence of a mass action equilibrium because non-UV irradiated cells contain much smaller pools of F and G monomers relative to the 6 and 9S particles than do UV irradiated cells. It may be that their self-assembly is promoted by some host component or, most likely, that some necessary intracellular environmental condition has not been met in vitro.

However, this latter possibility again fails to explain why significantly larger pools of F and G monomer exist in the intracellular environment of UV irradiated cells.

The 6S particle is antigenic and has been observed previously by means of an immunoprecipitation technique (174) and the serum blocking power assay (10).

The 12S Particle - The 12S particle is composed of both F and G protein (65, Mayol and Sinsheimer, unpublished) in the same proportions in which they exist in the virion (61). Siden has suggested that this particle is a capsomeric subunit of the virion and is consequently composed of an F pentamer joined to a G pentamer. Upon storage the 12S particle decomposes to 9S and 6S particles suggesting that these particles are also pentameric structures. On the basis of its sedimentation value, Tonegawa and Hayashi had previously deduced that the 9S particle was an F protein trimer. Apparently the conformation of this particle deviates markedly from the spherical one assumed for the calculation. The 6S particle was,on the other hand, calculated to be a pentamer, indicating an approximately spherical conformation.

Siden and Hayashi (61) have shown that the 12S particle is not formed in the absence of functional gene B product. As discussed earlier (see sections on gene B function and the precursor requirements of phage assembly) they have also observed that, after shifts to the restrictive temperature in ts B mutant infections, SS DNA replication and phage assembly continue for a short time while using up some precursor pool that requires gene B function for its formation. Radioactive amino acids added at the time of the temperature shift are not

incorporated into the phage matured after the shift. This indicates that the B dependent precursor contains the major virion components F and G. Since the 6S and 9S particles do not require B function for their formation, these particles apparently enter the assembly process prior to the B dependent step and are not the B dependent precursors. Since the 12S particle contains both F and G protein and its formation is B dependent, Siden and Hayashi have proposed that this is the immediate precursor to phage assembly and that it is supporting the residual 40°C assembly. However, under the conditions employed by Tonegawa and Hayashi (65), Mayol and Sinsheimer (unpublished) and in the experiments presented in the Results, the small intracellular proportions of this particle could not possibly account for the extent of 40°C synthesis that is observed. It is unlikely that the small pool size observed by these authors is merely the consequence of degradation to 6S and 9S particles at the time of lysis, as the particle decomposes only slowly when stored in these same buffers (61,65). Also, neither the 12S nor 9S particle is observed after a low temperature lysis in the presence of Mg^{++}, indicating that neither of these particles exist as such *in vivo* (Results). It seems more likely that the 12S particle is itself derived from the degradation of some larger, B dependent structure. This could be either the immediate product of B function or an assembly intermediate from some latter step in the pathway. The 111S particle described below and in the Results section could be such a particle.

All of these authors (61,65, Mayol and Sinsheimer, unpublished) have attempted to establish the precursor product relationships of

these particles by means of pulse chase experiments. In this regard it is important to note that, whereas this type of experiment, in the form in which it has been conducted so far, is capable of demonstrating that the proteins observed in various particles are ultimately incorporated into phage, it does not discriminate whether or not the particles observed are the actual in vivo precursors of that assembly. For example, particles such as the 12S or 20S structures will chase into phage whether they are themselves the immediate precursors to phage assembly or merely the decomposition products of some more complex particle which constitutes the actual in vivo precursor. The only materials that will not chase are the decomposition products of the phage itself and protein that is trapped in dead end or by-product pathways. Noting these limitations, it has been demonstrated that the 12, 9, 6 and 2S peaks can all be chased in part into ϕX particles (65; Mayol and Sinsheimer, unpublished). However, none of these authors have demonstrated a quantitative chase of any of these structures.

Mayol and Sinsheimer (unpublished) were puzzled by the chase of the 2.5S peak which, in the non-UV irradiated cell, contains very little phage structural protein. It seems likely in retrospect that they were observing the incorporation of D protein into the 111S and 140S subviral structures described below.

The 20S Peak - The 20S peak has been the subject of an extensive characterization in the Results. This particle cosediments with the SS replicating intermediates suggesting that it may be involved in the replication of SS DNA and is, perhaps, being carried to this region of the gradient by virtue of some complex with the

replicating DNA forms. Two additional lines of circumstantial evidence have served to bolster this contention. First, the replicating DNA from this same region is strongly bound to ϕX antigens - presumably virion proteins - which serve to mediate the binding of the RI DNA to anti-ϕX antibodies prepared against whole phage (93,Results). It was presumed that the 20S particle was the source of these antigens. Second, the major protein component of this particle has a high molecular weight suggestive of the A´ protein, the only strong candidate for a ϕX coded protein that plays a direct role in DNA replication.

However, in accord with the fallibility of circumstantial evidence, it will be shown in the Results that even if the 20S particle is associated with the replicative intermediates, this association is not required for the sedimentation velocity of either the protein or DNA moiety and is much too fragile to account for the serum binding behavior of the replicating DNA. In addition, a careful analysis of the 20S particle proteins reveals that the major mass constituent (54% by mass) is a high molecular weight host protein (arbitrarily termed U_3), rather than the ϕX A´ protein. It is followed in importance by ϕX gene F protein (12% by mass) and a low molecular weight component (12% by mass). At least six additional infection specific minor constituents copurify with the 20S peak.

A 20S peak is also observed in uninfected cells. The uninfected 20S peak is also dominated by the host U_3 protein, but to a much lesser extent than in the infected peak. There is, of course, no gene F component and the other host proteins do not correspond to the minor constituents observed in the infected peak. In fact these

other host components are barely in evidence in the particle isolated from infected cells. A comparison of the host protein contribution to both the infected and uninfected particle indicates that the host U_3 protein is present in four to seven fold greater concentration in the infected versus the uninfected particle. Apparently the synthesis of this protein is stimulated by the ϕX infection.

Mayol and Sinsheimer (unpublished) also observed 20S peaks in both infected and uninfected cells. In contrast to the experiments described above they observed that both particles had identical protein compositions, consisting of host U_3 protein, two additional high molecular weight proteins, and small amounts of low molecular weight components. In an experiment conducted to resolve this discrepancy (Results) it was found that, under the conditions of lysis and sedimentation employed by Mayol and Sinsheimer, the gene F protein accounts for a much smaller proportion of the 20S protein (5%) than is observed after lysis and sedimentation in the presence of Mg^{++} (the conditions employed in the characterization described above). As such gene F protein would not have been resolved in the SDS acrylamide gel system utilized by Mayol and Sinsheimer. The two high molecular weight proteins that they observed were apparently due to cross contamination from other host particles, as they did not cleanly separate the 20S peak from the bulk of the host proteins sedimenting at the top of the gradient. Still it is surprising that they did not observe a difference in the relative proportions of the three high molecular weight host proteins when comparing the protein compositions of the 20S peaks isolated from infected and uninfected cells.

Tonegawa and Hayashi analyzed the 20S particles isolated from UV irradiated cells (65) labeled after irradiation. As expected the high molecular weight host peak was not observed in the UV system. Instead the pattern was dominated by the "minor" components that are observed in the infected peak from the non-UV system. The F protein represented 18% of the total cpm, but the proportion of F protein relative to the "minor" components was much reduced compared to that observed in the non-UV infected peak obtained after lysis in the presence of Mg^{++}. (The distribution observed in the UV system may be much more in accord with that obtained in the non-UV system after lysis in EDTA, which was the procedure utilized by both Tonegawa and Hayashi, and Mayol and Sinsheimer. However, the existing data are inadequate to resolve this possibility.) Surprisingly, none of the "minor" components coelectrophoresed with ϕX proteins, thus indicating that they were of host origin. One would have expected the residual host incorporation to appear in proportionately greater amounts in the greatest host mass constituent of the particle. In the non-UV system this is the high molecular weight U_3 protein described above. However, there was no indication of the U_3 protein in the UV system. It is possible that, in the gel electrophoresis system employed, this protein did not enter the gel (see reference 65).

When Tonegawa and Hayashi investigated a restrictive infection with a C-terminal suppressor mutant in gene F, they found that the 9 and 12S particles disappeared as expected, but that incorporation into the 20S particle was enhanced. Subsequent electrophoresis of this material revealed that the gene F fragment accounted for over 85% of the labeled

protein.

Tonegawa and Hayashi (65) also observed that the 20S particle could be formed at low efficiency in vitro from F monomer and other proteins found at the top of their sucrose gradients. The in vitro particle had a composition identical to that of the in vivo particle except that the ratio of F protein to the minor components was approximately doubled. Tonegawa and Hayashi interpreted this in vitro assembly to mean that the 20S particle was a lysis artifact. They also observed a small amount of in vitro assembly of 9S and 6S particles from the same peak of monomer proteins. In this case they calculated that the efficiency of the in vitro formation was far too low to account for the presence of the 9S and 6S particles in lysates. Using their data and these same arguments one can calculate that the same is true for the 20S particle which is present in the infected lysate in a three fold greater concentration than can be accounted for on the basis of its spontaneous formation under the in vitro conditions utilized.

One would expect particles having discrete sedimentation velocities to have well defined structures. As a consequence, the variations in the relative proportions of the components of the 20S peak, in infected compared to uninfected cells, and after lysis under different conditions, suggest that this peak is comprised of several different particles which are only fortuitously associated by sedimentation velocity. In particular, the fact that the host proteins sediment at 20S regardless of the presence or absence of ϕX proteins, together with the large variations observed in the proportions of U_3 protein and F protein to the other 20S proteins (including each other)

indicates the existence of at least three separate particles, composed of U_3 protein, F protein and the minor host components, respectively. If this interpretation proves to be correct, then it is a remarkable circumstance that these three particles sediment so homogeneously under the wide variety of ionic conditions employed in these experiments and others to be described in the Results.

At present the intracellular existence, as well as the role of the these and other subviral particles so far discovered, has yet to be conclusively demonstrated. Tonegawa and Hayashi (65) have demonstrated that the 20S peak chases into phage; but, as noted above, this result does not demonstrate the existence of these particles *in vivo* or their possible role in the assembly process, but only that the gene F protein that appears in the structure after lysis is not trapped in some dead-end pathway *in vivo*, whether it be in a 20S particle or some other structure.

70S and 111S Particles - Tonegawa and Hayashi as well as Mayol and Sinsheimer restricted their investigations to the slowly sedimenting portion of the cell lysate. In the results two additional particles have been investigated that sediment with greater S values, of approximately 70S and 111S, respectively. Both are unstable under the conditions so far employed and both are obscured by their fortuitous sedimentation in the vicinity of the virion or its lysis artifact (see below). Their existence is demonstrated by indirect means. Both particles contain large relative proportions of gene D product. The 70S particle but not the 111S particle cosediments with replicating intermediates from ϕX SS DNA synthesis. The 111S peak constitutes a large pool of intracellular

ϕX specific protein and readily decomposes to 6S, 9S and 2S particles. Both particles pulse label and it is presumed that they may be intermediates in the ϕX assembly process.

140S Infectious Particle - The 114S phage particle has traditionally been considered to be the sole repository of ϕX infectivity to whole cells. However, two additional infectious particles have now been recovered from artificial lysates of ϕX infected cells. Weisbeek and Sinsheimer have discovered an infectious 140S particle in cells lysed under the distinctly non-physiological conditions of 0.25 M Tris and saturated EDTA (165). This particle is not observed in lysates prepared in 1.0M NaCl (165), in the presence of Mg^{++} (Results) or in borate EDTA (Rohwer, R., unpublished). Once isolated, this particle is subsequently quite unstable unless it is exposed to Mg^{++}, in which case it is quantitatively converted to the 114S particle, or to 1.0M NaCl, in which case it is partially converted to phage. The *in vitro* instability of this particle, when stored in its lysis buffer, is reminiscent of that observed by several other workers for storage of ϕX 114S particles in Tris buffers (24,32, Zuccarrelli, A., personal communication; Rohwer, R., unpublished). As a consequence, the relationship of this particle to its preparation in Tris buffer should be examined more closely.

The protein composition of the 140S particle is identical to that of phage except that it also contains ∿80 molecules of D protein per particle. Because it can be converted to phage by exposure to Mg^{++}, and because of the large intracellular proportions in which it is observed in the Tris EDTA lysis, Weisbeek and Sinsheimer argue that

it is an assembly intermediate to the 114S particle and may constitute the normal intracellular conformation of the virion. On the other hand, one might expect the intracellular state of the infection to be better represented by lysates prepared in buffers that more closely resemble the intracellular environment. The striking resemblance between this particle and the 111S particle (that lacks DNA) suggests a precursor product relationship between the two.

The Infectious Low Density Particle - When φX174 infected cells are lysed artificially in borate-EDTA buffer, a variable portion of the infectivity is found in a particle, ILDP, that bands at a lower density than φX during sedimentation to equilibrium in CsCl (Rohwer, R., in preparation). The protein and DNA composition, as well as the specific infectivity and sedimentation velocity of this particle are identical to those of phage. Upon storage in borate and EDTA it is slowly converted to phage density with no apparent loss of any DNA or protein component. Apparently the molecular species responsible for this density shift is not labeled in these experiments. The only biological materials that are compatible with such a density shift in the absence of any change in sedimentation velocity are lipids. Thus it is postulated that this particle contains lipids.

The biological significance of this particle is unknown but several observations suggest that it is not merely a lysis artifact. First, the infectivity from a borate-EDTA lysate can be recovered quantitatively in this form if the infection is conducted in the presence of 5 μg/ml mitomycin C. However, mitomycin C is not a requirement for ILDP formation as these particles are a constituent of normal

lysates as well. Second, this mitomycin C facilitation is observed only in HCR^+ but not in HCR^- hosts, suggesting that the mitomycin C effect is a consequence of its interaction with the HCR system rather than some nonspecific effect of its methylation activity (210). Apparently, a mitomycin C disruption in the host cell replication apparatus promotes the formation of the ILDP. (Rohwer, R., in preparation).

The 70S Lysis Artifact - In routine preparations of $\phi X174$, the most conspicuous intracellular particle other than 114S virion is a relatively stable, uninfective, contaminant of all ϕX lysates that sediments in a broad peak centered at approximately 70S (14,25,27,33,181). The protein composition of this particle is identical to that of the infective virion (Rohwer, R., unpublished), but it contains only one sixth to one twelfth as much DNA (25, Rohwer, R., unpublished). This DNA is plus strand in character and heterogeneous in sequence (7,25,130). A particle with very similar properties can be prepared in vitro by subjecting the intact virion to various disruptive procedures that destroy its infectivity (17,24,28,29,30,33). When observed in the electron microscope, these particles appear morphologically identical to whole virions except for a trailing fragment of DNA (17,24). The structure of the 70S particle and the ease with which its analogue can be produced in vitro by disrupting whole phage suggests a product rather than a precursor relationship to the 114S particle.

The relative proportion of 70S particle to ϕX in any given lysate is highly dependent upon the lysis conditions. By titrating the extracellular Ca^{++} and Mg^{++} at the end of the latency period with EDTA and then lysing in 0.05 M borate, 0.005M EDTA the 70S concentration

can be reduced to a few percent relative to phage (42, Zuccarrelli, A., personal communication). In other lysis procedures the ratio of 70S particle to ϕX can be as high as 8 to 1 (25,181). Bleichrodt and Knijnenburg (27) have shown that this difference is not just a consequence of the preferential loss of 70S particles in some purification procedures but reflects real differences in the 70S particle concentration in different lysates. This dependence of the 70S particle concentration on the lysis procedure along with the structure of the particle, and the ease with which it can be produced in vitro suggests that this material is an artifact of the lysis procedure. Reconstruction experiments in which purified ϕX are mixed with bacterial cell wall fragments demonstrate that this is the case as 70S particles are produced with high efficiency in this system. Apparently, the newly released phage in a lysing bacterial suspension attempt to reinfect the bacterial debris resulting in abortive injection of their DNA. The protruding DNA tails are then fragmented by nucleases resulting in the production of a 70S particle (27,31,78,94,181).

A different 70S particle was described earlier as a possible intermediate in phage assembly. This particle is a transient, unstable intermediate in the infection process and is not usually observed. To distinguish these two particles, the one produced as a consequence of the lysis event will be referred to as the "70S lysis artifact".

Particles Generated Extracellularly by the Infecting Phage - Newbold and Sinsheimer (32) have characterized three subviral particles that are the by-products of the host invasion process. These particles are, consequently, extracellular in origin and, when differentially labeled can be easily distinguished from the de novo products of the

infection. Two of these, the spontaneously detached abortive particles and the borate-EDTA eluted eclipsed particles, are very similar to the 70S lysis artifact and may originate in much the same way. The third particle is the empty phage coat. To recover this particle, it must be eluted from the cells with borate-EDTA. It is devoid of nucleic acid, both by the criterion of residual nucleic acid label and sedimentation to equilibrium. It sediments in velocity gradients as a homogeneous peak at 72S. A comparison of the sedimentation velocity of whole phage with that of the 70S lysis artifact and the empty phage coat illustrates the importance of configuration as well as mass on the DNA contribution to the S value of a hybrid particle composed of both DNA and protein.

The ϕX174 Virion - The most conspicuous intracellular particle is the phage itself. The reader is referred to Part I of this introduction for a discussion of its structure.

TABLE 1

The molecular weights of the ϕX174 gene products as established by various authors

ϕX Gene Products in Order of Descending MW	MW in Daltons	MW Assignment (Reference)	Gene Assignment (Reference)
A'	62,000	3	3,4
F	50,000	2	1,2,3,7
H	37,000	2	1,2,3,7
A	34,000	2	4
G	20,500	2	1,2,3,7
B	17,500	2	5
D	14,500	2	1,2,3,7
C	13,500	2	6
J	5,000	1	2
E	?	?	?
Sum minus A*	222,000		
Total coding capacity of the genome	∿228,000		

References:
1. Burgess, A. B. (1969) Proc. Nat. Acad. Sci. 64, 613-617.
2. Benbow, R. M., Mayol, R. F., Picchi, J. C., Sinsheimer, R. L. (1972) Virology 10, 99-114.
3. Godson, G. N. (1971) J. Mol. Biol. 57, 541-553.
4. Linney, E., Hayashi, M. N., Hayashi, M. (1972) Virology 50, 381-387.
5. Siden, E., personal communication.
6. Borrás, M. T., Vanderbilt, A. S., Tessman, E. S. (1971) Virology 45, 802-803.
7. Gelfand, D. H., Hayashi, M. (1969) J. Mol. Biol. 44, 501-516.

*Gene A protein is not included in the sum as its contribution to the genome is already included in A' protein (4).

LEGEND TO TABLE 1

Gene assignments and molecular weight assignments were made to the various ϕX specific proteins recovered from lysates of infected cells on the basis of the most convincing experiments (listed). No convincing assignment has been made for gene E, but the sum of the assigned molecular weights falls 6,000 daltons short of the total coding capacity of the genome, leading one to predict that gene E product is a small protein.

TABLE 2

Complementation of ϕX174 and S13 taken from Jeng et al. (34)

	Complementation Tests ϕX174		S13	Configurations of Virion Proteins				Viable Progeny
I	(D^-F^+)	x	(d^+f^-)	$H^+G^+F^+$	$h^+G^+F^+$	$H^+g^+F^+$	$h^+g^+F^+$	-
II	(H^-F^+)	x	(h^+f^-)		$h^+G^+F^+$		$h^+g^+F^+$	+
III	(G^-F^+)	x	(g^+f^-)			$H^+g^+F^+$	$h^+g^+F^+$	+
IV	(D^-H^+)	x	(d^+h^-)	$H^+G^+F^+$ $H^+G^+f^+$		$H^+g^+F^+$ $H^+g^+f^+$		* - +
V	(D^-G^+)	x	(d^+g^-)	$H^+G^+F^+$ $H^+G^+f^+$	$h^+G^+F^+$ $h^+G^+f^+$			* - +

*Complementation I demonstrates that these protein configurations in conjunction with protein d^+ do not give rise to progeny.

LEGEND TO TABLE 2

Data are from Jeng et al. (34). S13 genes and gene products are denoted by lower case letters, ϕX174 genes and proteins by upper case letters. Minus indicates an inactive gene and plus an active gene under the conditions of the complementation. Genes not indicated are active. For simplicity, J protein has not been included in the possible configurations for virion proteins.

TABLE 3

Complementation of *am6* and *am3*[*]

Infecting Phage Strain	Complementary Phage Strain	
	am3	*am6*
am3	0.01	0.02
am6	0.02	<0.001

Yields are expressed relative to a *wt* control.

[*] Data are taken from C. A. Hutchison III, (1969) Ph.D. Thesis, California Institute of Technology, Pasadena, California, Table 20, p. 99.

TABLE 4

The location of ϕX mutant am6 on the genetic map of ϕX174*

Two factor recombination frequencies between the mutants indicated:

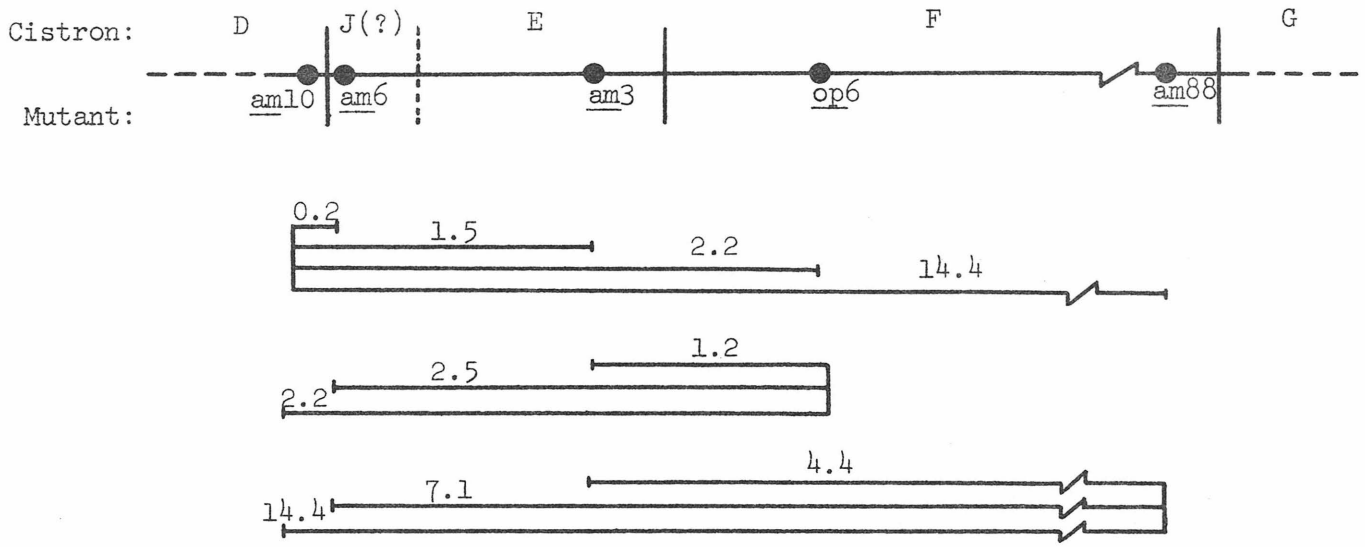

*Data are from Benbow, R. M., Hutchison III, C. A., Fabricant, J. D., Sinsheimer, R. L. (1971) Virology 7, 549-558, Table 2, p. 552.

TABLE 5

Subviral particles of ϕX174

Particle Particles from the normal infection	S Value	Infectivity	Protein Composition	DNA	Comments Structural relationship to origin, etc.
2.5S Peak	1-4S	0	D,J(?),(F),(H),(G),(B), others	none	Monomers or small multimers of ϕX proteins
6S	∿6S	0	G	none	G protein pentamer
9S	∿9S	0	F	none	F protein pentamer
12S	∿12S	0	F,G	none	F-G pentamer--a capsomeric subunit of the phage
20S Peak	∿20S	0	Host U_3,F,others	RI	Circumstantial cosedimentation with RI, at least 3 different particles are present
30S	∿30S	0	Unknown	none	Decomposition product of 111S particle
70S lysis artifact	∿70S	0	Virional	SS frag.	Originates from abortive infections of cell debris at lysis
70S *in vivo* particle	∿70S	0	F,G,D,others	RI	Replication intermediate?
111S	∿111S	0	F,G,D,(B),others	none	Procapsid? Decomposes to 2S, 6S, 9S, & 30S particles
114S	114S	+	Virional-F,G,H,J,others	SS crcl.	The normal infection product-density 1.42
ILDP	114S	+	Virional	SS crcl.	Infectious low density particle density 1.39
140S	140S	+	Virional plus D	SS crcl.	Infectious provirion? Unstable-decomposes to ϕX & 70S particles
Mutant Particles					
107S H^-	105S-107S	0	Virional minus H	SS crcl.	DNA is internal-not trailing
70S H^-	70S	0	Virional minus H	SS frag.	Decomposition products of 107S H^-
J^- particle	∿114S	0	Virional minus J	SS crcl.	
Extracellular Particles					
Abortive particle	∿70S	0	Virional	SS crcl. & SS frag.	Spontaneously detaches from cell during attempted infection
Eclipse particle	∿70S	0	Virional	SS crcl. & SS frag.	Irreversibly altered virion from early stage of the infection-must be extracted from cell wall
Empty coat	72S	0	Virional	none	Must be extracted from cell wall-density 1.32
Artificially Produced Particles					
50S particle	∿50S	0	F,J	SS crcl.	Spikeless capsid, produced with 4 M-urea
Chemically or thermally disrupted particles	50S to 70S	0	Virional	SS crcl. & SS frag.	Virions trailing DNA - the more intact the DNA the lower the sedimentation value

MATERIALS AND METHODS

Materials

(a) Bacterial strains

Escherichia coli H502 is a thy$^-$, uvrA$^-$(hcr$^-$), endoI$^-$, su$^-$, ϕX^S host strain constructed by Dr. Hoffmann-Berling.

Escherichia coli HF4714 is a su$^+$, amber permissive strain used to titer ϕX174 amber mutant strains.

Escherichia coli C is a su$^-$ strain used to prepare ϕX174 amber mutant phage stocks.

(b) ϕX174 strains and preparation of stocks

ϕX174 wt is the wild type strain characterized by Sinsheimer (181). The stock used was the gift of Dr. Lois K. Miller. The amber mutations were isolated by Hutchison (9).

ϕX174 am3 is a lysis deficient mutation in gene E. The stock suspension was cultured from a single plaque isolated on suppressor host, E. coli HF4714. The plaque contents were taken through two passages on E. coli HF4714. The phage were concentrated after each step by the polyethylene glycol procedure of Yamamoto et al. (192). The final concentrate was used to infect E. coli C. The phages were released from a 100X concentrated suspension of this nonpermissive host by incubation at room temperature with 500 µg/ml lysozyme, 0.05 M-sodium tetraborate, 0.4% EDTA. The plaque forming activity was purified from this lysate by sedimentation to equilibrium in a CsCl gradient followed by neutral sucrose velocity sedimentation. Both centrifugations were performed in 0.05 M-sodium tetraborate,

0.005 M-EDTA. The resultant stock was dialyzed against 0.05 M-sodium tetraborate and stored in that buffer at 4°C. The final titer was adjusted to 1.0 x 10^{12} pfu/ml with a specific infectivity of 0.13 pfu/particle and a reversion frequency of 2 x 10^{-5}. Electron microscopic examination of the SS DNA isolated from this stock revealed no detectable deletion DNAs (A. Zuccarelli, personal communication). There has been no loss in titer in over four years of storage.

ϕX174 am18 and ϕX174 am86 are gene A mutations mapping at the C and N terminal ends of the cistron, respectively (15). Stocks were cloned from single plaques and grown to >10^{11} pfu/ml on E. coli HF4714. The polyethylene glycol concentrates of the crude lysates were used as stocks. The reversion frequencies were 1 to 5 x 10^{-5}.

(c) Media

TPG was prepared by dissolving 8.0 g KCl, 0.5 g NaCl, 1.1 g NH_4Cl, 0.8 g sodium pyruvate, 11.4 g Tris-HCl, 3.32 g Tris-OH in 1.0 liter of water, then adding 1.0 ml of 1.0 M-$MgCl_2$, 1.0 ml of 0.23 g/ml KH_2PO_4, 1 ml of 1.0 M-$CaCl_2$ and 1.0 ml of 0.16 M-$NaSO_4$. This solution was brought to pH 7.4, if necessary, with concentrated HCl and autoclaved. Before use 2.0 ml of a sterile solution of 10% glucose in water was added to each 100 ml.

TPG-low P was prepared identically except that 1.0 ml of 0.023 g/ml KH_2PO_4 was substituted for 1.0 ml of 0.23 g/ml KH_2PO_4.

Tryptone was prepared by dissolving 10 g Bacto-Tryptone and 5 g KCl in 1.0 liter of water and then adding 0.5 ml of 1.0 M-$CaCl_2$ followed by autoclaving. There was no precipitation as long as $CaCl_2$ was added after the other ingredients were in solution.

TM is 0.05 M-Tris-OH, 0.05 M-KCl, 0.008 M-$MgSO_4$ brought to pH 7.2 with concentrated HCl and autoclaved.

TE is 0.05 M-Tris-OH, 0.005 M-EDTA, pH 7.2. TG is 0.05 M-Tris-OH, 0.005 M-EGTA, pH 7.2. Both TE and TG were brought to pH 7.2 with concentrated HCl and sterilized by autoclaving.

TE-Azide and TG-Azide are TE and TG buffers, respectively, supplemented with freshly prepared NaN_3 to a final concentration of 0.01 M.

The compositions of other buffers and media are given in conjunction with the method or experiment being discussed.

(d) Biological chemicals

Calf thymus DNA (type I, sodium salt) was obtained from Sigma Chemical Company, St. Louis, Missouri. When used as a carrier for TCA precipitations the DNA was prepared in 1 mg/ml solutions of TE. When used as a carrier and competitive inhibitor of *E. coli* DNase activities, a 1 mg/ml solution in TE was extracted several times with phenol, degraded by sonication and sedimented through neutral sucrose. The fractions with S values of 15 to 30 were pooled, dialyzed against TE and adjusted to 1 mg/ml in the stock solution.

Transfer RNA (type III, from Baker's yeast) was obtained from Sigma Chemical Company. The stock solution was 1 mg/ml in 0.05 M-Tris, pH 7.2.

Bovine serum albumin, BSA, was obtained in crude form as bovine albumin powder (Fraction V from bovine plasma) from Armour Pharmaceutical Company, Chicago, Illinois, for use in the radioimmuno-

assay. High purity BSA, bovine albumin (Pentex, crystallized) was obtained from Miles Laboratories, Inc., Kankakee, Illinois, for use as a carrier for ϕX proteins isolated in the presence of Mg^{++}.

Lysozyme (from egg white, Grade I) was obtained from Sigma Chemical Company. All lysozyme solutions were prepared just before use.

Pronase (B grade, nuclease free) was obtained from Calbiochem, San Diego, California. The stock solution was 10 mg/ml in TE and was self-digested for 45 min at 37°C before use.

RNase A from bovine pancrease (Type 1-A, 5X crystallized, protease free) was obtained from Sigma Chemical Company. The stock solution was 10 mg/ml in TE incubated for 20 min at 80°C to inactivate residual DNase. This stock was diluted 10X into TM buffer before use.

DNase I from bovine pancrease (RNase free, electrophoretically pure) was obtained from Worthington Biochemical Corporation, Freehold, New Jersey. The stock solution was 2.5 mg/ml, 0.1% BSA (Pentex), in H_2O. This solution was diluted 10X into TM buffer prior to use.

(e) Chemicals

Tris-HCl, tris(hydroxymethyl)aminomethane hydrochloride, and Tris-OH, tris(hydroxymethyl)aminomethane, were obtained as Trizma HCl and Trizma Base, respectively, from Sigma Chemical Company. EDTA, ethylenediaminetetraacetic acid (disodium salt, Sigma grade); EGTA, ethyleneglycol-bis-(β-aminoethyl ether)-N,N'-tetraacetic acid and pyruvic acid (sodium salt, type II) were obtained from the same source.

Bacto-Tryptone was obtained from Difco Laboratories, Detroit, Michigan.

Brij 58, polyoxyethylene (20) cetyl ether, was obtained from Atlas Chemical Industries, Inc., Wilmington, Delaware.

Sarkosyl, sarkosyl NL 30, was obtained from Geigy Industrials Chem.

SDS, sodium lauryl sulfate (specially pure), was obtained from BDH Chemicals, Ltd., Poole, England through Gallard-Schlesinger Chemical Mfg. Corp., Carle Place, Long Island, New York.

Acrylamide, bis-acrylamide (N,N'-methylene-bis-acrylamide), and TEMED (N,N,N',N'-tetraethylenediamine), all electrophoresis purity, were obtained from Bio-Rad Laboratories, Richmond, California.

2-Mercaptoethanol was obtained from Matheson, Coleman and Bell, Norwood, Ohio.

Dichlorodimethylsilane used in early experiments was obtained as dimethyldichlorosilane (a 1% solution in benzene) from Bio-Rad Laboratories. Later experiments employed dichlorodimethylsilane, 99%, from Aldrich Chemical Company, Inc., Milwaukee, Wisconsin.

Benzene, analytical reagent was obtained from Mallinckrodt Chemical Works, St. Louis, Missouri.

Molecular sieves (Type 4A, effective pore size 4 Å, 8 to 12 mesh beads, grade 514) were obtained from Fisher Scientific Company, Fair Lawn, New Jersey.

TCA, trichloroacetic acid (analytical reagent) was obtained from Mallinckrodt Chemical Works.

Sodium azide (SX299) was obtained from Matheson, Coleman and

Bell.

Phenol (Analar, analytical reagent) was obtained from BDH Chemicals Ltd.

Cesium chloride (optical grade powder) was obtained from the Harshaw Chemical Company, Solon, Ohio.

Angio Conray (an 80% solution of sodium iothalamate) was obtained from Mallinckrodt Pharmaceuticals, St. Louis, Missouri.

PDI, propidium diiodide (A grade) was obtained from Calbiochem, San Diego, California.

Urea (ultrapure grade) was obtained from Schwarz/Mann, Division of Becton, Dickinson and Company, Orangeburg, New York.

Nitrosoguanidine (N-methyl-N'-nitro-N-nitrosoguanidine) was obtained from Aldrich Chemical Company.

Chloramphenicol (B grade) was obtained from Calbiochem, San Diego, California.

Ammonium persulfate (reagent) was obtained from J. T. Baker Chemical Co., Phillipsburg, New Jersey.

Bromphenol blue was obtained from Matheson, Coleman and Bell.

(f) Radiochemicals

^{3}H-thymidine, [methyl-^{3}H]thymidine (>10 C/m-mole); ^{14}C-thymine, [methyl-^{14}C]thymine (20-50 mc/m-mole); ^{3}H-leucine, l-[4,5-^{3}H]leucine (2 C/m-mole); ^{14}C-leucine, l-[^{14}C]leucine (270-320 mc/m-mole); ^{3}H-lysine, l-[4-^{3}H]lysine (1-5 C/m-mole); and ^{14}C-lysine, l-[^{14}C]lysine (270-300 mc/m-mole) were obtained from Schwarz/Mann, Division of Becton, Dickinson and Company, Orangeburg, New York.

^{32}P, $H_3{}^{32}PO_4$ (carrier free, 30 to 60 mc/ml) was purchased from International Chemical and Nuclear Corporation, Irvine, California.

The specific activities used in each experiment are given in the Results.

(g) Scintillation fluors

TL is 160 ml of Liquifluor scintillator (New England Nuclear, Boston, Massachusetts) mixed with one gallon of analytical reagent grade toluene.

TLNCS is by volume, 90.5 parts TL, 9.0 parts NCS solubilizer (Amersham/Searle Corporation, Arlington Heights, Illinois) and 0.5 parts water. For rapid dissolution the water should be added last.

Dioxane scintillator for use in room temperature Beckman Instruments LS200 or LS233 scintillation counters is 173.8 g napthalene (scintillation grade, Eastman Kodak Company, Rochester, New York), 289.6 ml methanol (analytical reagent), 11.6 g PPO (2,5-diphenyloxazole, New England Nuclear), and 3 kg p-dioxane (Eastman Kodak Company).

Aquasol Universal L.S.C. Cocktail was obtained from New England Nuclear.

(h) Other materials

Glass shell vials (15 x 45 mm, one dram) were obtained from Kimble, Owens-Illinois Laboratory Glass, Toledo, Ohio.

Glass Pasteur pipettes (disposable capillary pipettes) were obtained from VWR Scientific, Los Angeles, California.

Plastic "disPo Beakers" and caps (2 ml, conical) were

obtained from Scientific Products, Evanston, Illinois.

Disposable plastic test tubes (12 x 75 mm and 17 x 100 mm) were obtained from Falcon Plastics, Oxnard, California.

Three kinds of plastic scintillation vials were used in conjunction with the radioimmunoassay. The type used in each experiment is specified. Polyethylene vials were obtained from Packard Instrument Company, Inc., Downers Grove, Illinois. Linear polyethylene vials were obtained from Nuclear Associates Inc., Westburg, New York. Nylon Spectravials were obtained from Amersham/Searle Corporation.

Cellulose nitrate and polyallomer centrifuge tubes were obtained from Spinco Division, Beckman Instruments, Inc., Palo Alto, California. Before use, centrifuge tubes were soaked overnight at room temperature in 0.20 M-EDTA and then exhaustively rinsed with distilled water and dried.

Heavy wall, 12 ml Pyrex tubes were obtained from Ivan Sorvall, Inc., Norwalk, Connecticut. These tubes can withstand routine centrifugation to 15,000 revs/min in the SS-1 Sorvall centrifuge rotor.

Whatman Glass Fiber Paper GF/A filters were used for spotting radioactive samples to be dried and counted in TL scintillator without further treatment. Whatman Glass Fiber Paper GF/C filters with a smaller pore size than GF/A were used to collect TCA precipitated samples by filtration. Whatman Filter Paper 3 MM Qualitative discs were used to spot radioactive samples for batch elution with TCA (see below). All Whatman filters were obtained from W & R Balston, Ltd., England.

Millipore filters with syringe fittings (Swinnex-25 Filter Unit, sterilized, 0.45 μ) were obtained from Millipore Corporation, Bedford, Massachusetts.

Parafilm was obtained from American Can Company, Neenah, Wisconsin.

(i) Apparatus

Centrifuges: Ultracentrifugation was performed in Beckman Instruments L-2, L2-65 and L2-65B preparative ultracentrifuges employing Beckman Instruments rotors as designated in the experimental descriptions. Low speed centrifugation was performed in a Sorvall Superspeed RC2-B (Ivan Sorvall, Inc.) or when indicated in an International Refrigerated Centrifuge Model PR-6 (International Equipment Company, Needham Heights, Massachusetts).

Scintillation counters: Beckman Instruments Liquid Scintillation Systems LS200 (2 channel) and LS233 (3 channel) were employed for room temperature counting. Updated Nuclear-Chicago Liquid Scintillation System 720 series (3 channel) were used for refrigerated counting.

Evapo-Mix vacuum evaporation device is produced by Buchler Instruments, Fort Lee, New Jersey.

Coulter Counter (Model A) particle counter is produced by Coulter Electronics, Chicago, Illinois.

Mickel Gel Slicer for fractionation of polyacrylamide gels is produced by The Mickel Laboratory Engineering Co., Mill Works, Gomshall, Surrey, England.

Technicon Auto Analyzer Proportioning Pump is produced by Technicon Corporation, Tarrytown, New York.

Methods

(a) Preparation of markers

(i) ^{32}P-labeled ϕX RF I and RF II DNA: *E. coli* H502 was grown at 37°C to 4 x 10^8 cells/ml in 40 ml of TPG-low P supplemented with 5 µg/ml thymine. At time zero the culture was infected with ϕX*am*3 at a multiplicity of 7. Eight minutes later, chloramphenicol was added to 35 µg/ml. Fifteen minutes after infection, 5.60 mc of carrier free $H_3{}^{32}PO_4$ was added to the culture to give a specific activity equivalent to one ^{32}P atom per ϕX RF DNA molecule. One hundred and twenty minutes after infection the culture was cooled to 0°C, washed twice in TG, resuspended in 1 ml of the same and lysed at 37°C by the addition of 20 µl of 10 mg/ml t-RNA in 0.05 M-Tris, pH 7.2; 50 µl of 1 mg/ml lysozyme in TG, and 100 µl of 5% Brij in water. The debris was pelleted by centrifugation for 15 min at 15,000 revs/min in the Sorvall SS-1 rotor. To the supernatant was added 100 µl of 0.13 M-EDTA in 0.1 M-Tris, pH 7.4 and 50 µl of 1 mg/ml RNase A stock solution. After 15 min of incubation the lysate was deproteinized by addition of 250 µl of sarkosyl and 20 µl of pronase stock solution and additional incubation for four hours at 37°C. The lysate was then sedimented for 13 h at 5°C at 40,000 revs/min through isokinetic sucrose gradients prepared in TE buffer supplemented with 1.0 M-NaCl in an SW40 rotor. The RF I peak was pooled, dialyzed against TE buffer and

resedimented in the same system. The preparation was converted to 50% RF II by incubating at 100°C for 5 min.

(ii) ^{32}P-φX*am*3 and ^{32}P-φX SS DNA: *E. coli* H502 was grown, infected and labeled as in the preparation of ^{32}P RF DNA except that chloramphenicol was omitted. Lysis was achieved according to procedure I given below. After removing the cell debris by low speed centrifugation the phage were isolated by neutral sucrose velocity sedimentation. In latter experiments this step was preceded by an initial purification by glass bead column chromatography (see Gschwender *et al.*, 193). ^{32}P-φX*am*3 were dialyzed and stored in 0.05 M-sodium tetraborate. For the preparation of ^{32}P-φX SS DNA this stock was dialyzed against TE buffer and extracted twice with redistilled phenol equilibrated with the same buffer. The aqueous phase was then dialyzed and stored in TE.

(b) Growth, infection and radioactive labeling of *E. coli* H502

In all experiments a refrigerated culture of H502 in TPG medium supplemented with thymine, not more than two days old, was inoculated into fresh TPG medium plus thymine at 2 to 3 x 10^7 cells/ml. The culture was aerated vigorously at 37°C and the growth monitored by means of a Coulter Counter. All experiments were begun after one or more generations of exponential growth when the cell titer reached 3 x 10^8 cells/ml. Unless otherwise stated, infections were performed at a multiplicity of seven, adjusted to the plating efficiency of *wt* φX174 on H502 relative to the suppressor strains on which the φX suppressor mutations are assayed. Incubations were continued at 37°C

with vigorous aeration until the end of the experiments. E. coli H502 has a generation time in TPG medium supplemented with either 1 µg/ml or 5 µg/ml of thymine or thymidine of 70 min. The stock was cloned from time to time and monitored for thymine auxotrophy. Long term storage was on agar slants at 4°C.

Radioactive pulses were administered by rapid injection from hypodermic syringes with virtually no interruption of the culture. When indicated pulse labeling and cell growth were terminated by pouring the entire culture into an Erlenmeyer flask of 10 to 20 times the culture volume, containing sufficient 1.0 M-NaN_3 to give a final concentration of 0.1 M, and equilibrated with a dry ice-methanol bath. Ice was observed in the culture within five seconds of its addition to the flask. The culture could be added to the bath within five seconds of its removal from the aeration system. When indicated the culture was thawed at 0°C by incubating for several hours in an ice bath.

Where indicated, the culture was washed by repeated centrifugations. The cells were pelleted by bringing the culture to 12,000 revs/min in the SS-1 rotor of a Sorvall centrifuge and then decelerating the rotor with the brake on. The supernatant was decanted and the cells resuspended and repelleted as desired.

(c) Suppression of host cell lysis with $MgSO_4$

In long term labeling experiments with ϕX174 am18 and am86 in non-UV irradiated H502 host cells, cell lysis was suppressed by the method of Gschwender & Hofschneider (81). The procedure described above for growth and infection of E. coli was modified only by the

addition of $MgSO_4$ to the culture at a final concentration of 0.2 M when the cells had reached 1.2 x 10^8 cells/ml. This has the effect of terminating cell growth for two hours after which growth resumes abruptly at its former rate (Fig. 1). The subsequent infection and labeling of the culture appears to be normal as evidenced by the incorporation of radioactive leucine into ϕX proteins (Fig. 28; Results). Lysis does not occur in over 120 min of incubation and the cells are resistant to artificial lysis. The cells were lysed by resuspending the culture pellet in 0.05 M-sodium tetraborate, 0.05 M-EDTA with lysozyme and SDS and dialyzing against TP buffer (see legend to Fig. 28; Results). Lysis occurred in the dialysis bag.

(d) Lysis

(i) Rapid: The cells were washed one or more times in TE buffer and then resuspended in as little as 1/50 of the original culture volume of TE. Quantitative lysis was affected by the addition of lysozyme to 100 µg/ml from a freshly prepared solution at 1 mg/ml in TE. Lysis was complete after 1 to 5 min of incubation at room temperature.

(ii) Lysis in the presence of Mg^{++}: The cells were washed one or more times with single culture volumes of TG-Azide and finally resuspended in one tenth or greater of the culture volume in TG-Azide. To a 20 ml culture resuspended in 250 µl of TG-Azide was added 80 µl of 1 mg/ml t-RNA in TM buffer and 20 µl of freshly prepared 1 mg/ml lysozyme in TG-Azide. This mixture was incubated for 30 min at 0°C, usually without any loss in turbidity or increase in viscosity. This incubation was followed by the addition of 20 µl of 0.1 M-$MgSO_4$

followed by 40 µl of 5% Brij. The mixture was then alternately frozen and thawed three times in a dry ice-methanol bath and a 37°C water bath. The mixture was agitated vigorously during its exposure to 37°C and when only a sliver of ice remained placed in an ice bath for the final thaw. Often this mixture was stored overnight at -20°C before a final thaw and centrifugation. The final lysate although viscous was never as clear and viscous as that produced by method 1.

When indicated the cell debris was pelleted from these lysates by a 15 min centrifugation at 15,000 revs/min in the SS-1 Sorvall rotor. The lysate supernatant was separated from the pellet with a siliconized Pasteur pipette.

(e) Special problems associated with the use of Mg^{++}

Many of the experiments described in the Results section were performed in the presence of Mg^{++}. In the course of these investigations it was discovered that Mg^{++} promotes the specific loss of some ϕX particles by absorption to the various containers employed in the experiments. In particular, in the absence of the precautions described below, the 111S ϕX protein particle described in Results is almost quantitatively lost upon exposure to cellulose nitrate centrifuge tubes, dialysis tubing, or plastic collection vials. It was found that recoveries of this material could be greatly enhanced by avoiding unnecessary exposure to plastics, collecting fractions into dichlorodimethylsilane coated glass vials, using silane coated Pasteur pipettes for transfers, and using BSA as a carrier.

(i) Inhibition of nuclease: Nuclease activity is also promoted by

the presence of Mg^{++}. To minimize this effect, E. coli H502 which is deficient in endonuclease I was used as the host. Also t-RNA (from 50 µg/ml in sucrose gradients to 500 µg/ml in crude lysates) and calf thymus DNA (50 µg/ml to 200 µg/ml) were added to Mg^{++} containing lysates as carriers and protection against nuclease. The calf thymus DNA as purchased was re-extracted several times in phenol, degraded by sonication and the fractions sedimenting from approximately 15 to 30S collected as carrier. Experimental material was also kept at $\leq 4°C$ in part to inhibit nuclease activity.

(ii) Preparation of silane coated shell vials and Pasteur pipettes: In early experiments a 1% solution of dimethyldichlorosilane in benzene purchased from Bio-Rad Laboratories was used for the procedure below. A preferable reagent, from the standpoint of both cost and purity, used in latter experiments, was a 1% solution of dichlorodimethylsilane prepared from 99% dichlorodimethylsilane (Aldrich Chemical Company, Inc.) and reagent grade benzene dried over 4 Å molecular sieves for several weeks. This solution was heated to 60°C in a large glass vessel with a heating mantle. Washed, dry, glass shell vials or Pasteur pipettes, prewarmed to 60°C, were filled with or immersed in the silane solution for 5 to 10 min, then drained, allowed to air dry, and baked in a dry oven at 250°C for two hours. Vials or pipettes were rinsed with distilled water and then sterilized in a dry oven.

(iii) Dialysis: In experiments performed in the presence of Mg^{++}, dialysis was avoided wherever possible. Cell lysates were sedimented directly without dialysis and low molecular weight radioactivity was subsequently removed by washing the samples prepared for scintillation counting with TCA. Resedimentations were often performed by diluting

rather than dialyzing the original sample to reduce the sucrose content.

(iv) BSA carrier: BSA had the most pronounced effect on reducing losses from nonspecific binding. Table 1 presents the effect of BSA carrier (Pentex) on absorption to both cellulose nitrate centrifuge tubes and silane treated shell vials. As can be seen, the percent of unbound ^{14}C protein label increases dramatically with increasing BSA concentration. In this experiment the ^{3}H-thymidine label is associated with virions and it is apparent that the non-virion associated protein is preferentially bound. In the case of both ^{3}H and ^{14}C cpm there is a reduction in the total recovery of both bound and unbound input cpm as the concentration of BSA is increased. The cause of this effect is not understood as control experiments showed that these concentrations of BSA had no effect upon the counting efficiencies of either of these isotopes. For most experiments BSA carrier was added to a final concentration of 0.01%.

Table 1 also shows that a substantial reduction in both ^{3}H and ^{14}C binding is affected by merely presoaking the cellulose nitrate centrifuge tubes in 0.10 M-EDTA followed by thorough rinsing with distilled water. Polyallomer tubes and plastic collection vials were also investigated and found to bind much more strongly than cellulose nitrate or glass.

(f) Deproteinization

The pooled fractions from a sucrose gradient containing 50 µg/ml t-RNA and 0.01% BSA as carrier were dialyzed against two 3 liter

changes of TE buffer. The retentates were collected into glass Sorvall centrifuge tubes and brought to 50 µg/ml calf thymus DNA carrier, 0.5% SDS and 100 µg/ml Pronase followed by 4.5 h of incubation at 37°C.

Redistilled phenol was equilibrated with TE buffer supplemented with 0.1 M NaCl and 0.5% SDS by means of a 1 h incubation at 60°C followed by overnight storage at 4°C. The mixture was brought to pH 7.0 by the addition of 5.0 M-NaOH while monitoring with pH paper.

One sample volume of phenol was added to each fraction, then several thicknesses of parafilm were pressed onto the top of each tube and the mixture rocked gently back and forth for 10 min at room temperature. The resulting emulsion was cooled to 0°C for 10 min and then centrifuged at 2°C for 5 min at 3000 revs/min in the swinging bucket rotor of an International Refrigerated Centrifuge. The lower phenol phase was removed by means of a siliconized Pasteur pipette. The aqueous phase was then re-extracted in the same manner as before. Total changes in the volume of the aqueous phase was less than 10%.

The aqueous phase was transferred to a polyallomer centrifuge tube suitable for the Beckman SW27 rotor and 1/10 volume of 3.0 M-sodium acetate, pH 5.0, and 2 volumes of isopropyl alcohol added. This mixture was incubated overnight at -20°C. Subsequently the tubes were filled to the brim with -20°C isopropyl alcohol and the DNA pelleted by means of a 30 min centrifugation at 27,000 revs/min in an SW27 rotor at 0°C. The alcohol was then decanted and the pellets redissolved in TE and dialyzed against the same buffer overnight at 4°C. The retentates were transferred to siliconized glass tubes, RNase A was added to 15 µg/ml and the mixtures incubated at 37°C for

15 min. Subsequently, the samples were frozen at -20°C until used.

(g) Velocity sedimentation

(i) Linear gradients: Linear sucrose gradients were formed in the usual way from a two-chambered vessel connected at the bottom by a small passage. The density ranges and compositions of the buffers varied in each case and are given with the descriptions of the experiments in the Results. The initial volumes of each sucrose solution were determined as described by Noll (195) so as to give the same pressure head in both chambers of the apparatus. The gradient itself was formed at a controlled rate by means of a Technicon pump.

(ii) Isokinetic gradients: Isokinetic gradients were prepared as described by Noll (195,196) for the sedimentation of a molecular species of density 1.7 at constant velocity in Beckman SW40 or SW41 rotors. The reservoir contained a solution of 37.8% sucrose. The volume of 5% sucrose to be placed in the mixing chamber depends upon the sample volume and is 14.2 ml for a sample of 200 µl. The gradient was introduced into the bottom of the centrifuge tube with a glass capillary and formed at a controlled rate with a Technicon pump. Buffer compositions are given with the descriptions of the experiments.

All gradients were formed at room temperature and then cooled to 4°C in a refrigerator before application of the samples. When indicated the gradients were formed on top of a dense layer of CsCl or Angio Conray designed to prevent the pelleting of fast sedimenting material. When used these dense layers were formed by dissolving CsCl or Angio Conray in the denser of the two sucrose solutions forming

the gradient.

Unless otherwise indicated, collection of both linear and isokinetic gradients was by tube puncture from the bottom. The centrifuge tube was restrained in a close fitting lucite holder with a screw cap such that the tube was pressed firmly into a rubber pad at the bottom and a rubber gasket at the top. A hypodermic needle centered in a screw could then be forced through the rubber pad and bottom of the tube in a controlled manner. The flow rate was regulated by attaching the top of the centrifuge tube to a 50 ml glass syringe whose plunger could be moved in small increments by a screw device.

(iii) Parallel sedimentations: Some experiments employed a direct comparison of differentially labeled infected and uninfected lysates sedimented separately through parallel neutral sucrose sedimentation gradients. To assure uniformity the linear gradients were formed sequentially using a single tube of the Technicon pump to deliver carefully measured volumes from a gradient maker. Equal volume samples were applied to each of two gradients and centrifuged as described in the results. After centrifugation the two gradients were collected sequentially with the same piece of Technicon tubing. The tubing was flushed with distilled water between collections. The gradients were collected from the bottom by inserting a glass capillary from the top of the liquid column to the bottom of the centrifuge tube. Fractions were taken at timed intervals. In every experiment the same number of fractions were obtained from each gradient.

(h) Sedimentation to equilibrium in CsCl-propidium diiodide

The intercalating dye propidium diiodide, PDI, can be used to separate ϕX RF I, SS and RF DNA forms as well as intermediate structures in sedimentations to equilibrium in CsCl (229, 230; Results). In a non-wetting plastic test tube, 5.010 g of CsCl were dissolved in 5.850 g of liquid sample in TE buffer plus 150 µl of 5 mg/ml PDI in water (store in the dark). The resulting solution was then transferred to a polyallomer centrifuge tube suitable for the type 65 rotor being careful not to wet the top edges of the tube. The tube was capped and filled to the top with bayol oil. Centrifugation was for 40 h at 5°C at 40,000 revs/min. The centrifuge tube was pierced from the bottom for the collection of fractions.

(i) TCA precipitation

Precipitation by trichloroacetic acid was used to separate radioactively labeled high molecular weight proteins and nucleic acids from acid soluble low molecular weight radioactive precursors in order to quantitate incorporation into the polymeric structures.
(i) Single samples: Up to 0.5 ml of sample was added to 5.0 ml of 10% TCA in water followed by two drops (approximately 100 µl) of 1 mg/ml calf thymus DNA carrier. This mixture was stirred and then incubated at 4°C for at least 30 min before collecting the precipitate by vacuum filtration on a Whatman GF/C glass filter. The incubation tube was rinsed once with 5 ml of 10% TCA at 4°C. The filter was then rinsed three or more additional times, depending upon the expected

concentration of soluble cpm. Two final rinses with 100% ethanol at 0°C were used to remove the TCA. The filters were then dried and counted as specified in the Results.

(ii) Batch precipitation: When it was necessary to TCA precipitate an aliquot from every fraction of a centrifugation gradient, each aliquot ($\leq$ 100 µl) was spotted separately onto numbered Whatman 3MM paper filter discs. The wet filters were then dropped sequentially into 300 to 600 ml of 10% TCA at 4°C and swirled gently for 5 to 10 min. The TCA was then decanted and replaced with fresh TCA. The volume and number of rinses was adjusted such that all of the soluble radioactivity would be eluted assuming the maximum possible soluble cpm in the original sample and a uniform redistribution of the soluble radioactivity during each rinse. Several blank filters were placed in each batch to monitor the progress of the elution. TCA itself was removed by two additional washes in 100% ethanol at 0°C. Occasionally there was one final rinse with anhydrous ether at room temperature. After the last rinse the filters were dumped onto aluminum foil, separated with forceps, dried and counted in TL scintillator. All discs were oriented with the sample side up.

The batch elution procedure was also used to remove PDI dye, CsCl, or sucrose from the samples of a gradient when uniform quenching was required for all fractions. For this purpose two TCA rinses sufficed.

(j) SDS polyacrylamide gel electrophoresis

Two different procedures were used for SDS polyacrylamide

gel electrophoresis. The first is a modification of the method of Mayol & Sinsheimer (8). The second adapts the separation gel from the first procedure to the SDS stacking gel system of Laemmli (211) to produce a much more highly resolved and reproducible system. The sample buffer used in procedure II is that suggested by Ward (S. Ward, personal communication). Deviations from these procedures are noted in the experimental descriptions.

Solution A was prepared by bringing 48 ml of 1 N-HCl, 36.6 g of Tris-OH, and 0.23 ml of TEMED to 100 ml with H_2O. The pH was 8.9.

60% acrylamide was prepared by placing 0.25 g of bis-acrylamide and 30 g of acrylamide in a 50 ml graduated cylinder with 20 ml of water. The mixture was incubated at 37°C until dissolved and then brought to 50 ml.

30% acrylamide was prepared in a similar way by dissolving 0.40 g of bis-acrylamide and 15 g of acrylamide in a final volume of 50 ml.

0.14% and 0.40% ammonium persulfate solutions were prepared just before use with water degassed by boiling or by evacuation.

TG' is 144 g/l glycine, 30 g/l Tris-OH. The pH should be 8.5.

TGS is TG' buffer diluted 1/10 in 0.1% SDS. The pH should be 8.3.

1/5-TGS is TG' buffer diluted 1/50 in 0.1% SDS. The pH should be 8.3.

Prerun buffer is 45.8 g/l Tris-OH, 0.1% SDS brought to pH 8.9 with concentrated HCl.

16-TP is 57.0 g/l Tris-OH brought to pH 6.9 with concentrated

H_3PO_4 (approximately 17.5 ml).

TP is a 16-fold dilution of 16-TP buffer.

The tracking dye is a saturated solution of bromphenol blue in 0.05 M-Tris, pH 7.6.

Solution A and both acrylamide solutions were filtered through Millipore HA 0.45 micron filters and stored at room temperature in brown bottles.

Unless otherwise indicated the gels were formed in clean, dry Pyrex glass tubes of 0.7 mm I.D. and 11 cm long for procedure I and 13.5 cm long for procedure II. To form the separation gel one end of the tube was sealed with multiple overlays of parafilm. The tube was then held vertically in a stand and filled with 3.5 ml of polymerizing solution to give a gel column 9 cm long.

(i) Procedure I: To prepare 20 ml of 15% acrylamide polymerizing solution, 2.5 ml of solution A, 5.0 ml of 60% acrylamide and 2.3 ml of H_2O were added to a clean, dry 30 ml test tube, gently mixed, and then aspirated for 2 to 2.5 min to remove dissolved air. Then 200 µl of 10% SDS and 12.5 µl of TEMED were added and mixed gently. To initiate polymerization 10 ml of 0.14% ammonium persulfate was added and the mixture rocked gently back and forth three or four times to mix. Three and one half ml aliquots of this solution were then dispensed as rapidly as possible to the polymerization tubes and overlaid with a 0.5 cm column of degassed H_2O. When the solution had gelled (10 to 15 min) the water overlay was decanted, the top of the gel was flushed with prerun buffer, the parafilm was slit with a razor blade to equalize pressure, then removed, and the gel was introduced into the electrophoresis

apparatus. Prerun buffer was placed in both reservoirs of the apparatus and the gels electrophoresed at 6 ma/gel for 1-4 h. The prerun buffer was then decanted and replaced by 1/5-TGS buffer.

To prepared 12% acrylamide gels this same procedure was followed except that 4.0 ml of 60% acrylamide and 3.3 ml of H_2O were used in the formulation above.

Electrophoretic samples were dialyzed against pH 7.6 Tris buffer and if necessary concentrated by aspiration to dryness on an Evapo-Mix. The Tris concentration was adjusted so that upon re-elution of the sample with the denaturing agents the final Tris concentration was 0.05 M. This method gave good recoveries of material whereas lyophilization to dryness and re-elution did not. The dialyzed, concentrated samples were denatured by the addition of SDS and 2-mercaptoethanol to final concentrations of 1% and glycerol to 10%. The samples were then incubated for 2 min at 100°C, cooled, mixed with 1 to 3 µl of tracking dye transferred in the tip of a 100 µl capillary pipette, and carefully layered onto the gel surfaces with the same pipette.

The electrophoresis apparatus consisted of two lucite cylinders nested one on top of the other with electrodes at the center and as many as twelve gels disposed equidistantly from the electrodes. The current was regulated at 2 ma/gel until the tracking dye had penetrated at least 1 mm into the separation gel after which the current was advanced to 4 ma/gel. Electrophoresis was from anode to cathode.

(ii) Procedure II: The separation gels for procedure II were prepared as described for procedure I except that 13.5 cm glass tubes were used. After polymerization, the water overlay was decanted from the tube and the top of the gels flushed with stacking gel solution prepared as described below but without TEMED.

To prepare 10 ml of stacking gel solution, 1.0 ml of 30% acrylamide, 1.25 ml of 16-TP, 2.65 ml of H_2O, 100 µl of 10% SDS, 5 µl of TEMED and 5.0 ml of 0.4% ammonium persulfate were mixed gently in a clean dry test tube. Immediately after mixing 0.8 ml of this solution (giving a 2 cm stacking gel) was introduced into each gel tube and overlaid with degassed water as before. Polymerization was complete in $\leq$ 20 min. The water overlays were decanted and the gels placed in the electrophoresis apparatus. The reservoirs were filled with TGS and the top of each gel flushed with TGS.

Electrophoretic samples were dialyzed against TP buffer and then brought to final concentrations of 2% SDS, 3.3% 2-mercaptoethanol and 10% glycerol. After a 2 min incubation at 100°C they were applied to the gel columns and electrophoresed as described for procedure I. In this case the current was not advanced until the tracking dye had traversed the stacking gel and entered the separation gel.

Unless otherwise indicated, all gels were run until the tracking dye was within 1 cm of the bottom. After electrophoresis the gels were removed from the glass tubes by rimming with a fine needled hypodermic syringe containing 0.1% SDS. Stubborn gels were ejected by applying hydrostatic pressure at one end of the tube. This can be done without damaging the gel if it is ejected into a large vessel of

water. The free gels were rinsed with distilled water, placed in glass test tubes and laid horizontally on a block of dry ice until thoroughly frozen. If the test tubes were sealed at this stage (after freezing) with a tight fitting serum bottle stopper, the gels could be stored frozen for several weeks without shrinking or desication

The frozen gel was fractionated into 1 mm sections with a Mickel Gel Slicer. A strip of wet filter paper was placed on the movable stage. The frozen gel was placed on the filter paper and a bead of water delivered around the edges. Powdered dry ice was heaped upon the stage to freeze the gel to the apparatus. Dry ice was then cleared away from the leading edge of the gel which was allowed to soften slightly before slicing.

Each slice was placed in a scintillation vial with 5 ml of TLNCS scintillator and incubated at room temperature with slow agitation for at least 18 h before counting. In the case of procedure II the stacking gels were removed from the separation gel and counted as one fraction. In no instance were significant cpm observed in either the stacking gel or the region between the tracking dye and bottom of the gel. As a consequence all data has been plotted with fraction one as the top of the separation gel. The last fraction plotted indicates the middle of the tracking dye band.

In control experiments with procedure II it was shown that the separations of ϕX proteins are identical for total sample volumes of 50 to at least 500 µl and total concentrations of BSA and DNA carriers of at least 500 µg and 200 µg respectively.

(k) Triple label counting

Many of the experiments presented in the results employ ^{3}H, ^{14}C, and ^{32}P radioactive labels concurrently. For this reason an exact solution to the discriminator ratio equations for three labels was derived and utilized in a computer program that separates three-channel scintillation counter output into its three isotopic components. With careful, uniform preparation of standards and samples the program does an excellent job of separating the three isotopes without the tremendous losses in counting efficiency that necessarily result from methods requiring minimal overlaps from one channel to another.

Unknowns and three standards, ^{3}H, ^{14}C and ^{32}P, must be prepared with uniform quench such that all samples generate identical overlaps from one channel to another for any given isotope. Each standard is then used separately to maximize its counting efficiency in one of the three channels of a scintillation counter and minimize it in the other two by means of gain and discriminator adjustments. However, great sacrifices in counting efficiency for the sake of minimizing overlaps is not necessary. With relatively unquenched samples, such as those prepared in the Aquasol system discussed below, it is often possible to count all isotopes at better than 70% of their maximum efficiency in the same system, while the overlaps from high energy emitters to low energy channels are $\leq$ 20% and the overlaps from low energy emitters to high energy channels are $\leq$ 5%. The samples should be counted to high statistical accuracy in all channels and the isotopic composition of the sample computed as follows.

(i) Derivation of the discriminator ratio equations for the separation of triple label scintillation counter data into its isotopic constituents.

Definitions:

Channels 1, 2 and 3 of the scintillation counter are maximized for counting ^{3}H, ^{14}C and ^{32}P respectively.

H, C and P are the final corrected values for the separated isotopes, ^{3}H, ^{14}C and ^{32}P, respectively. Depending upon how the overlap ratios are defined, H, C and P can represent either the total dpm or the total cpm for each isotope in the sample respectively; or they can represent the corrected cpm for the respective isotope in its respective counting channel only (see below).

M_1, M_2 and M_3 are the net cpm observed in channels 1, 2 and 3 respectively. They represent the raw scintillation counter output for a given sample.

K_1, K_2 and K_3 are the background cpm from channels 1, 2 and 3 respectively.

N_1, N_2 and N_3 are the net cpm minus background observed in channels 1, 2 and 3 respectively.

a_1, a_2 and a_3 are the fractions of corrected ^{3}H, "H", found in channels 1, 2 and 3 respectively.

b_1, b_2 and b_3 are the fractions of corrected ^{14}C, "C", found in channels 1, 2 and 3 respectively.

c_1, c_2 and c_3 are the fractions of corrected ^{32}P, "P", found in channels 1, 2 and 3 respectively.

The values assigned to a_i, b_i and c_i depend upon the desired form of the final result, H, C and P. If the final concentrations of the isotopes are to be expressed in dpm, then appropriate standards of known dpm must be prepared and the ratios a_i, b_i and c_i are then the counting efficiencies of the corresponding standard in each of the three channels. When the final isotopic concentration is to be expressed as the total cpm of a given isotope in all three channels, then the ratios must be expressed (using the appropriate standard), as the cpm observed in channel i dividied by the sum of the cpm from all three channels. The equations assume their simplest form when the results are expressed as the total contribution of a given isotope in its corresponding channel only. In this case the ratios a_i, b_i and c_i are computed relative to the count rate of the corresponding standard in its respective channel. As a consequence, a_1, b_2 and c_3 assume a value of 1.0. Each of these three forms of the equations are interrelated by simple multiplicative factors of H, C and P with the consequence that any of these results can be easily interconverted after the calculation.

Derivation:

For any given sample the net cpm minus background cpm, N_i, that is observed in each channel is related to the cpm contribution of each isotope to that net cpm by the expressions:

$$\text{Channel 1} \qquad N_1 = a_1H + b_1C + c_1P$$

$$\text{Channel 2} \qquad N_2 = a_2H + b_2C + c_2P$$

$$\text{Channel 3} \qquad N_3 = a_3H + b_3C + c_3P$$

These three equations can be solved for the three unknowns

H, C and P by means of the determinants:

$$H = \frac{\begin{vmatrix} N_1 & b_1 & c_1 \\ N_2 & b_2 & c_2 \\ N_3 & b_3 & c_3 \end{vmatrix}}{\begin{vmatrix} a_1 & b_1 & c_1 \\ a_2 & b_2 & c_2 \\ a_3 & b_3 & c_3 \end{vmatrix}} \qquad C = \frac{\begin{vmatrix} a_1 & N_1 & c_1 \\ a_2 & N_2 & c_2 \\ a_3 & N_3 & c_3 \end{vmatrix}}{\begin{vmatrix} a_1 & b_1 & c_1 \\ a_2 & b_2 & c_2 \\ a_3 & b_3 & c_3 \end{vmatrix}} \qquad P = \frac{\begin{vmatrix} a_1 & b_1 & N_1 \\ a_2 & b_2 & N_2 \\ a_3 & b_3 & N_3 \end{vmatrix}}{\begin{vmatrix} a_1 & b_1 & c_1 \\ a_2 & b_2 & c_2 \\ a_3 & b_3 & c_3 \end{vmatrix}}$$

The denominators, D, in each case are identical and reduce to:

$$D = (a_1b_2c_3 - a_1b_3c_2 - a_2b_1c_3 + a_3b_1c_2 + a_2b_3c_1 - a_3b_2c_1)$$

Substituting D for the denominators, the expressions for H, C and P become:

$$H = [N_1(b_2c_3 - b_3c_2) - b_1(c_3N_2 - c_2N_3) + c_1(b_3N_2 - b_2N_3)]/D$$

$$C = [a_1(c_3N_2 - c_2N_3) - N_1(a_2c_3 - a_3c_2) + c_1(a_2N_3 - a_3N_2)]/D$$

$$P = [a_1(b_2N_3 - b_3N_2) - b_1(a_2N_3 - a_3N_2) + N_1(a_2b_3 - a_3b_2)]/D$$

In the experiments which follow these expressions were used in their simplest form giving the corrected count rate of each isotope in its respective channel only. This is, perhaps, the form that is most useful when considering the actual cpm available for further manipulation of a given sample when subsequent counting will be performed under the same conditions. In this case the ratios a_1, b_2 and c_3 are set equal to 1.0 as all overlaps are calculated relative to the counting standard's activity in its own channel. This results in the following simplifications of these expressions.

The expression for D reduces to D',

$$D' = 1 - a_2b_1 - a_3c_1 - b_3c_2 + a_3b_1c_2 + a_2b_3c_1,$$

and the expressions for H, C and P become:

$$H = [N_1(1 - b_3c_2) + N_2(b_3c_1 - b_1) + N_3(b_1c_2 - c_1)]/D'$$

$$C = [N_1(c_2a_3 - a_2) + N_2(1 - a_3c_1) + N_3(a_2c_1 - c_2)]/D'$$

$$P = [N_1(a_2b_3 - a_3) + N_2(a_3b_1 - b_3) + N_3(1 - a_2b_1)]/D'$$

Finally, if H, C and P are to be computed directly from the scintillation counter output, then $(M_1 - K_1)$, $(M_2 - K_2)$ and $(M_3 - K_3)$ must be substituted into the above expressions for N_1, N_2 and N_3 respectively so that background cpm will be considered.

These equations will work equally well for any three isotopes having β emission energies that are sufficiently different to be discriminated by a liquid scintillation counter, for example ^{3}H, ^{35}S, ^{32}P or ^{3}H, ^{33}P, ^{32}P.

Because these computations involve considerable manipulation of the data and because much is often made of data involving low count rates (the natural conclusion for most radioactivity experiments) and, finally, because the rather lengthy calculations involved were to be performed by computer; the extent to which the statistical counting error is amplified by these computations was investigated by deriving the standard deviations for H, C and P. This was accomplished by applying the expressions for propagation of the standard error to the statistical error associated with the counter output. The resultant expressions are presented in Appendix A.

Some typical scintillation counter output and its reduction to H, C and P are presented in Table 2 along with the fractional standard deviations computed for the raw and corrected values of each isotope. Inspection of the table shows that the effect of the H, C and P calculation on the value of the fractional standard deviation is not great. The increase in the fractional standard deviation due

to the calculation varies roughly as the ratio of the uncorrected to corrected cpm in a given channel. As expected, the low count rate data are the most strongly affected by the calculation, reflecting the uncertainties in the backgrounds which make a negligible contribution to high count rates. This treatment demonstrates only that the statistical counting error does not generate large uncertainties in the final result during the data processing. It does not consider the effect of systematic errors such as those arising from incorrect values of the overlap obtained from non-representative standards. Experience has shown that these errors, if present, can completely overshadow the effect of the statistical counting error. Thus considerable attention must be given to preparing samples and standards with uniform counting efficiencies and overlaps.

(ii) Sample preparation: For most of the experiments in this thesis the following two methods of sample preparation sufficed to give the required level of uniformity. Examples of data obtained with each method are given in Table 2. In the case of CsCl gradients containing PDI or any sample containing unwanted low molecular weight radioactive precursors, identical aliquots of sample were spotted onto numbered Whatman 3MM filter discs which were then washed by the batch TCA procedure described above.

A much simpler method giving rise to even more uniform results was utilized in the absence of TCA-soluble radioactivity or PDI. In this case identical aliquots were added to Aquasol-H_2O (10:1), mixed and counted. This scintillator counts with very uniform efficiencies and overlaps over the 5 to 20% sucrose concentration

range of the typical sucrose gradient (Table 3). Similar results are obtained if the total concentration of H_2O relative to Aquasol is kept within the range of 1:9 to 1.5:10, volume to volume. When lower concentrations of water are used, efficiencies and overlaps become strong functions of sucrose concentration. When higher concentrations are used these values remain relatively insensitive to sucrose concentration but the counting efficiency of the system declines.

CsCl gradients may also be counted in this system if the concentration of H_2O in the system is kept high. TLNCS also counts much more uniformly with the addition of .5 to 1.0% H_2O. However, this is usually not a practical scintillator for aqueous samples. The dioxane scintillator continues to show a strong sensitivity to added sucrose even after the addition of water.

(iii) Computations: To simplify the use of the triple label equations a Fortran IV program, "TRIPSEP", was written for use with the California Institute of Technology IBM Batch Processor. The raw scintillation counter output is accepted as punch cards, one card per line of output. An auxiliary program, "LIST," can be used to convert paper punch tape output to punch cards. Once the data exists as punch cards it can be arranged and manipulated with ease. The TRIPSEP program, utilizing the required standards and backgrounds, computes the corrected values for ^{3}H, ^{14}C and ^{32}P, along with the respective standard deviations for each fraction. The data are organized into data sets corresponding, for example, to all of the fractions in a single centrifugation gradient or polyacrylamide gel. The total ^{3}H, ^{14}C and ^{32}P cpm in each data set is then computed and from that the

percent distribution of the label across the data set. These percentages, along with the corrected isotopic concentrations and their standard deviations, are tabulated by data set along with the total amount and the maximum and minimum values of each isotope. The program also provides for the optional CALCOMP (Calcomp, Anaheim, California) plotting of either the count distribution or the percentage distribution of each isotope in the gradient. Either one, two, or three isotopes may be plotted per data set.

(1) Computation of infection specific radioactivity (Delta cpm)

A procedure described by Mayol & Sinsheimer (8) was employed to resolve radioactively labeled ϕX infection specific proteins (proteins that are synthesized exclusively or in greater proportions in infected compared to uninfected cells) from radioactively labeled host proteins in the same non-UV irradiated culture. In this technique parallel cultures of infected and uninfected host bacteria are differentially labeled with ^{14}C and ^{3}H labeled amino acids. After fractionation of the proteins (by electrophoresis, sedimentation, or other means), the positions and quantities of the infection specific proteins are revealed by computing the net cpm of each fraction in the infected gradient that cannot be accounted for by the expected incorporation due to host proteins. The expected incorporation is determined by comparing the ratio, R, of the infected and uninfected labels at some region of the gradient where no ϕX proteins are known to exist. In the absence of an infection one would expect to observe this same ratio for all fractions. The validity of this expectation

is born out by the constancy of the ratio of the amino acid labels observed in Figure 4a showing an SDS acrylamide gel fractionation of two uninfected E. coli H502 cultures labeled separately with ^{3}H and ^{14}C lysine and mixed after lysis.

Once the ratio, R, of the host incorporation in the infected, compared to the uninfected cultures has been determined (this is usually the minimum ratio of infected/uninfected cpm observed in the fractionation system), then the infection specific incorporation for any fraction, delta cpm, can be computed as follows:

(delta cpm) = (cpm from infected cell) - R(cpm from uninfected cell)

$$\Delta \text{ cpm} = \text{delta cpm}$$

In some of the applications that follow, the infected and uninfected lysates were mixed together prior to fractionation as described by Mayol & Sinsheimer (8). In other experiments, the computation was applied to the parallel sedimentation gradients described above. In this case similar fractions from each gradient were compared. When parallel gradients are utilized the radioactive labels do not have to differ unless they are to be mixed at some subsequent stage.

To facilitate computation of this kind of data, a Fortran IV program, CNTSEP, was written for use with the California Institute of Technology IBM Batch Processor. This program utilizes the discriminator ratios procedure to compute the isotopic compositions of double labeled samples. It also computes the standard deviations and percent total gradient cpm for each fraction. These calculations are performed

analogously to those described previously in conjunction with the TRIPSEP program. In addition the ratios of the infected/uninfected labels in each fraction (or in the case of parallel gradients, the equivalent fractions in each gradient) are computed and arranged in order of increasing values. In this way a minimum value of R can be easily selected for the delta cpm calculation, which, when a ratio is specified, is also computed. The program can also be directed to perform the delta cpm calculation with the minimum ratio obtained a priori, or with the ratio corresponding to a given fraction number. If so directed, the data are plotted in one or more of several formats by means of a Calcomp plotter.

(m) Suppression of host cell protein synthesis with UV_{260} radiation

The differential labeling technique described above for the detection of infection specific proteins can be circumvented by exposing the host cells to lethal doses of UV_{260} radiation prior to infection with ϕX174 (20,52,53). When this is done only ϕX proteins are synthesized and labeled during the subsequent infection. As a consequence, only one radioactive label is needed to reveal the ϕX proteins. This technique has the disadvantages of distorting the incorporation patterns of the normal infection of non-UV pretreated hosts, of not labeling ϕX infection specific host proteins, and of incorporating radioactive label at a much reduced rate compared to non-UV infections (see below and Results, especially Table 18).

Several experiments were performed to establish the optimum

conditions for labeling UV irradiated cells and to characterize the UV irradiated system. In each experiment E. coli H502 (hcr$^-$) was grown to 3 x 10^8 cells/ml as described above. Fifty ml of cells were then transferred to a sterile glass petri plate (14 cm diameter) and irradiated at room temperature, for the time period specified, with two General Electric germicidal lamps (G8T5) delivering 19 ergs/mm^{2}sec (12). The petri plate was located 30 cm below the lamps and the culture was swirled vigorously during irradiation. Under these conditions the colony forming ability of E. coli H502 is reduced to 7 x 10^{-4} of the input in the first 30 seconds of irradiation. After irradiation the cells were transferred to a fresh culture tube and aerated for 10 min at 37°C before infection and labeling.

The experiment in Figure 2 demonstrates the effect of UV irradiation on the total incorporation of ^{3}H-lysine into both infected and uninfected cells. A culture of E. coli H502 was irradiated for varying lengths of time as described above. The cells from a given exposure period were divided in half and one portion infected with ϕXam3. Both portions were then labeled with ^{3}H-lysine and incorporation monitored as TCA precipitable cpm. A comparison with unirradiated controls demonstrated that the first three minutes of irradiation reduces ^{3}H-lysine incorporation by 88 and 99% in infected and uninfected cultures respectively. Inspection of Figure 2 reveals that in the case of all UV dose levels tested, most of the residual host incorporation has ceased by 30 min after the addition of label. By comparison infected cells continue to incorporate label at the initial rate until 60 min after infection and at a lesser but significant rate

from 60 to 90 min. This difference in the incorporation behavior of infected and uninfected cells can be exploited to enhance the relative incorporation into ϕX proteins. The optimum UV_{260} dose and lysine labeling period were selected from Table 4. Unless otherwise indicated, a 5 min UV_{260} exposure and a labeling period of 30 to 90 min were employed in the experiments presented in the Results.

Figure 3 presents an SDS polyacrylamide gel electrophoresis of the mixed lysates of ϕX wt infected and uninfected E. coli H502, UV irradiated and labeled as described. (ϕX wt does not lyse UV irradiated cells.) Assuming that the residual host proteins are synthesized in the same relative proportions in infected and uninfected cells (This is true in non-UV treated cells with the exception of two or three high molecular weight proteins which are not in evidence here. See Results.) then a comparison of the infected and uninfected patterns reveals very little evidence of host incorporation in the infected cells. In particular the two peaks between G and D are present in far greater quantities than could be accounted for by residual host synthesis. (Compare the ratio of uninfected/infected incorporation in the region immediately preceding G protein to estimate the host contribution to the peaks between G and D.) As a consequence, these two peaks most likely represent infection specific proteins as opposed to charged t-RNA as suggested by Godson (20).

Figure 4 presents the results of SDS electrophoreses of UV and non-UV irradiated, uninfected, host cells, revealing, in addition to the quantitative differences discussed above, qualitative differences in the incorporation patterns in the two systems. Figure 4a

presents a coelectrophoresis of separately and differentially labeled, non-UV irradiated host cultures. The ratio of lysine incorporation in the two non-UV cultures is constant over the entire protein spectrum thus serving as a control on the reproducibility of the methods. By comparison when a non-UV host culture is coelectrophoresed with a UV irradiated culture, the two patterns vary considerably and the ratio of UV to non-UV incorporation increases as a roughly linear function of decreasing protein molecular weight (assuming linearity of the gel). This is the result that would be expected if the UV induced lesions are distributed pretty much at random and a lesion anywhere in a gene prevents its ultimate expression. Under these circumstances larger genes would be more susceptible to damage than smaller ones. Figure 4b does not reveal the presence of any high molecular weight UV resistant protein such as might account for the A' protein (see Results).

(n) Radioimmunoassay for φX174 antigens

A radioimmunoassay (RIA) modeled after that of Catt & Tregear (180) for human hormones was developed for φX174 antigens. In this method a small amount of specific antibody is used to uniformly coat the walls of a plastic scintillation vial. If radioactive antigen is then introduced into the vial it is also bound to the vial via the antibody intermediate. Subsequently all unbound radioactivity can be washed from the vial and the bound antigen monitored by scintillation counting after the introduction of scintillation fluor.

The serum-coated vials can be used to monitor the presence of antigens in two ways. First, the concentration of unlabeled antigen

can be measured by competition for binding sites with a standard amount of radioactive antigen mixed with it. A comparison of the resultant reduction in binding of the radioactive species with a standard curve correlating loss of binding with known antigen concentrations will reveal the concentration of the unknown antigen. In this way the assay works much like the classical serum blocking power assay (10) but it is not limited only to detection of phage antigens giving rise to phage inactivating antibodies.

Alternatively, the existence of labeled antigen in a radioactive sample of unknown composition can be determined directly by comparing radioactivity bound in a serum-coated vial with that bound in a control vial treated identically but lacking serum. This procedure has an advantage over immunoprecipitation (86) in that it can detect monovalent antigen without the addition of large amounts of carrier antigen and a careful determination of the equivalence point conditions. On the other hand, this direct method can only provide minimum values for the concentrations of the bound antigens unless it is known for certain that the total antigen concentration in the sample is far below the saturation point of the assay. The direct detection of proteins provides an additional complication due to the high level of nonspecific binding of protein to the control tubes. In the experimental section this method has been used to detect stable complexes of ϕX DNA with ϕX antigenic proteins. In this case only the DNA is labeled and its binding to the serum-coated vials is monitored. Deproteinized DNA has a very low affinity for the vials, therefore the DNA must bind via a ϕX antigenic protein that is com-

plexed with it.

(i) General procedure for the radioimmunoassay: Anti-ϕX antisera prepared in rabbits with highly purified ϕX were diluted to the appropriate level (see below) in 0.05 M-sodium tetraborate and 2 ml aliquots were introduced into the bottoms of plastic scintillation vials. Care was taken not to wet the sides of the vial. After a ten min incubation at room temperature the antiserum was removed by aspiration. The vials were then washed twice with three ml of 0.15 M-NaCl and finally with 4 ml of 1.0% BSA (Armour), dissolved in 0.15 M-NaCl, 0.01 M-NaN_3. All washings were removed by aspiration. Control vials were prepared in an identical fashion except that the first incubation with dilute serum was omitted.

Radioactive samples were diluted into 0.05 M-Tris phosphate, 0.01 M-KCl, pH 8.0, and 2 ml aliquots were distributed to duplicate serum-coated and control vials. After 12 to 24 h of incubation at 37°C with gentle agitation the vials were aspirated to dryness, then washed twice with 3 ml of 0.15 M-NaCl. 5 ml of an appropriate scintillation fluid were then added to each vial and the vials monitored for bound radioactivity.

(ii) Optimum serum concentration and antibody binding conditions: Curiously, the binding efficiency of the assay is not linearly related to the serum concentration used to coat the vials but must be determined experimentally for each serum used. A typical curve is shown in Figure 5. In this instance a two-thousand-fold dilution of the serum provides optimum binding to the assay tube. Apparently the serum equilibrates very rapidly with the vial as the incubation time

for serum absorption is not critical.

According to Catt & Tregear the only requirement for serum binding to the assay tube is incubation in a pH 9 buffer. Once bound, the antibody is amazingly intractable to removal by either mechanical or chemical means (180). The assay was performed under a wide variety of ionic and pH conditions without dramatically affecting binding efficiency. Neither dioxane scintillator or additional washes with 0.15 M-NaCl release more than 1% of the phage counts once they have been bound.

If the vials are tightly capped after the last aspiration they can be stored at least six months without losing activity.

(iii) Substrates for serum binding: Several types of plastic scintillation vials were investigated for their suitability for the assay. Of these, all polyethylene vials gave similar results, including those constructed from linear polyethylene. Earlier experiments were performed in Packard Scintillation Vials and later experiments in Nuclear Associates Scintillation Vials made from linear polyethylene. Linear polyethylene vials are preferred because they do not swell when used with the toluene based scintillator TLNCS that gives the best counting efficiency for ^{3}H. Serum did not bind efficiently to Nylon Vials, and does not bind at all to glass. The assay can also be performed by binding antiserum to small styrene beads (Dow Styrene Divinylbenzene Copolymer Latex, Particle Diameter 6 to 14 μ) but only by increasing the substrate surface area one hundred-fold over that used in the scintillation vial method.

(iv) Measurement of radioactivity: Before the manufacture of linear polyethylene vials the bound radioactivity had to be monitored with dioxane scintillator as toluene based fluors caused regular polyethylene vials to swell and jam in the scintillation counter advance mechanism. The introduction of linear polyethylene vials permits the use of toluene-based TLNCS which is the preferred scintillator due to its 2-fold greater counting efficiency for ^{3}H (Table 5). Use of TLNCS also results in greater recoveries of bound ^{3}H cpm (86%) than does dioxane (64%). (Recoveries are computed relative to the total input cpm as measured with the same scintillator.) This effect is probably due to the release of bound ^{3}H counts into the TLNCS solution resulting in a better exposure to the fluor. In dioxane the radioactivity remains bound to the vial even after long periods of incubation. The combination of these two effects results in a 2.7-fold greater ^{3}H efficiency when counting with TLNCS. Samples should be counted as soon as possible after the addition of TLNCS as this mixture slowly generates quenching substances from the vial.

(v) Incubation buffer: The assay is compatible with a wide range of buffering conditions. The binding efficiency is relatively constant for KCl concentrations from 0.005 M to 1.0 M and for pH values from 8.0 to 6.0. Nonspecific binding is enhanced at lower pH values, so this condition should be avoided if possible. The assay has also been performed with normal binding efficiencies in TM buffer and in tryptone broth with the addition of 0.01 M NaN_3 to suppress bacterial growth.

(vi) Suppression of nonspecific binding by BSA: The BSA wash is used to suppress nonspecific binding of radioactivity by absorbing

BSA to reactive sites on the polyethylene that have not been occupied by antibody or other serum protein and might otherwise react later to bind nonantigenic radioactive proteins. It is apparent from Table 6 that BSA also reduces the serum binding efficiency by 30% but that this is more than compensated for by a six-fold greater reduction in the nonspecific binding. By washing the vials with BSA before adding antibody we can show that these molecules are binding to the same sites. In this case the binding efficiency is reduced to 3% of normal. By preparing the vials with mixtures of BSA and antiserum this effect can be used to lower the saturation point and range of the competition assay for detection of lower concentrations of antigen.

Various molecular species were monitored directly for their ability to bind to serum or BSA-coated vials. By way of comparison the relative binding of ϕX to BSA-coated control vials is 0.04 of its binding to the serum-coated vial (Table 6). However, if we consider its nonspecific absorption relative to the total input phage counts, it is only 0.008. In experiments such as that in Table 5 where the binding efficiency of the assay approaches 90%, the nonspecific absorption of ϕX approaches this lower limit. Purified E. coli DNA and RNA bind at levels of 0.0017 and 0.0005 if their input counts respectively. Nonspecific absorption of proteins is much more variable and dependent upon the source, ranging from phage-like values to several percent (2 to 3 percent for leucine-labeled uninfected E. coli). It is for this reason that non-serum controls should accompany every determination of direct binding of antigen.

(vii) Kinetics of phage binding to RIA assay tubes: Binding of ϕX to the assay vial was measured as a function of time and the results are presented in Figure 6. Maximum binding is attained between 24 and 48 h, after which time there is a slow reduction in the counts bound, probably due to the gradual degradation of both phage and antibody. Incubation at 4°C drastically lowers the rate of binding and gentle agitation increases it by 20% over the same period.

(viii) Saturation level of the assay and preparation of standard binding curves: The saturation point of the assay was determined by incubating increasing concentrations of unlabeled ϕX*am*3 with a constant amount of ^{3}H-labeled ϕX*am*3 in standard vials and observing the reduction in binding efficiency accompanying increasing phage concentration. This procedure generates a binding curve that can be employed in a competition type of assay for unlabeled antigens. The curve presented in Figure 7 has a useful concentration range of over two decades. This compares very favorably with the 1 to 1.5 decade range of the serum blocking power assay (10). The assay system shows the first signs of saturation at 2.5×10^{9} particles/ml and binding efficiency has been halved at 1.0×10^{10} particles/ml. The Packard and Nuclear Associates Vials yield very similar binding curves.

Though the assay appears to saturate at 2.5×10^{9} particles/ml, the maximum binding efficiency relative to the total input cpm is only 0.12. On the other hand, the data in Table 5 indicate that a binding efficiency of at least 0.64 is attainable when counting with dioxane scintillator and an input antigen concentration of 1.0×10^{9}

particles/ml. In this later experiment the counting conditions were carefully controlled and all data monitored and corrected for quenching. Thus, the greater binding efficiency indicated by this experiment is probably the correct one. The maximum binding efficiency is expected to be substantially below 1.0 due to the mass action equilibrium of the reactants and the finite association constant of ϕX antiserum both with ϕX and presumably with the vial.

TABLE 1

Suitability of BSA as a carrier for ϕX174 proteins

A. Absorption of ϕX174 proteins to cellulose nitrate centrifuge tubes as a function of BSA concentration

BSA Carrier Final Concentration	% of Input cpm Recovered (Bound and Unbound)		% of Recovered cpm not Bound	
	^{3}H-tdr	^{14}C l-leu	^{3}H-tdr	^{14}C l-leu
Untreated tube 0.0%	78	100	53	18
0.0%	74	100	77	28
0.001%	71	87	82	42
0.010%	58	92	100	59
0.10%	44	82	99	76

B. Absorption of ϕX174 proteins to silane-treated shell vials as a function of BSA concentration

BSA Carrier Final Concentration	% of Input cpm Recovered (Bound and Unbound)		% of Recovered cpm not Bound	
	^{3}H-tdr	^{14}C l-leu	^{3}H-tdr	^{14}C l-leu
0.0%	61	81	64	9
0.001%	82	66	86	41
0.010%	81	51	91	81
0.10%	58	47	92	90

LEGEND TO TABLE 1

Identical aliquots of the pooled fractions from under the 114S and 111S peak of an experiment like that in Figure 8a (Results) were incubated for 4 h in the presence of varying final concentrations of BSA in 1/2" x 2" cellulose nitrate centrifuge tubes and 1/2" x 1-1/2" glass shell vials silane-treated as described in the Methods. All of the cellulose nitrate tubes except those designated as untreated had been presoaked in 0.10 M-EDTA and then thoroughly rinsed in distilled water before use. All counting was performed in Aquasol. Appropriate standards were prepared for determining overlaps of the two isotopes. The total input cpm were determined by adding the same aliquot used in the experiments directly to Aquasol. At the end of the incubation period the liquid contents of each tube and the tube itself were counted separately and the sum of these count rates was taken as the total recovery of input cpm. The percentage of recovered cpm that did not bind to the tube was computed from the fraction of cpm recovered in the liquid form compared to the total recovered cpm.

TABLE 2

Typical triple label data and their reduction to H, C and P

Source of Data		Condition of Data	Channel 1		Channel 2		Channel 3	
Fig. No.	Fraction		cpm	σ/cpm	cpm	σ/cpm	cpm	σ/cpm
Group I								
3(b)	18	Uncorrected[1]	110.4	.042	249.6	.028	997.4	.014
		Corrected	63.5	.077	118.7	.062	977.3	.014
2(d)	19	Uncorrected	7046.6	.0053	2487.6	.0090	889.2	.015
		Corrected	6618.3	.0057	2345.8	.0097	851.2	.016
		Bkg. I	16.2	.023	14.0	.025	19.2	.021
Group II								
4(a)	23	Uncorrected	602.8	.018	1085.6	.014	245.2	.029
		Corrected	383.1	.030	1024.0	.015	175.1	.040
2(c)	23	Uncorrected	23638.6	.0029	5335.8	.0061	363.0	.023
		Corrected	22737.8	.0031	4415.4	.0083	116.7	.085
		Bkg. II	12.3	.048	11.8	.049	13.0	.047

Two sets of standards were used for these computations. Set I was used for the computations in Group I and Set II for the computations in Group II. The channel overlaps for the standards are given below.

Standards	Isotope	Overlaps		
		Channel 1	Channel 2	Channel 3
Group I	^{3}H	1.000	.0040	.000020
	^{14}C	.172	1.000	.0079
	^{32}P	.011	.119	1.000
Group II	^{3}H	1.000	.039	.000
	^{14}C	.201	1.000	.053
	^{32}P	.0088	.196	1.000

[1]All samples and standards were counted for 5 min. Group I background was counted for 115 min and the Group II background for 70 min.

LEGEND TO TABLE 2

Typical counting samples are taken from the triple label experiments presented in the Results section, Figs. 2c, 2d, 3b, and 4a. Both the raw data and the computed values of H, C and P, along with their fractional standard deviations, are presented. The samples and standards in Group I are from neutral sucrose gradients and were counted in Aquasol-H_2O (9:1). The samples and standards in Group II are from PDI-CsCl sedimentations to equilibrium and were counted on Whatman 3MM filters after batch elution in 10% TCA. The scintillator used was TL. Count rates were determined using a Beckman Scintillation Counter. The corrected values H, C and P and the standard deviations were computed by means of the TRIPSEP program. All counting efficiencies were greater than 60% of their maximum values under these conditions of sample preparation.

TABLE 3

Counting characteristics of Aquasol-H_2O (10:1)

% Sucrose in Standard	^3H Standard			^{14}C Standard			^{32}P Standard		
	^3H eff.	Overlap to ^{14}C	Overlap to ^{32}P	^{14}C eff.	Overlap to ^3H	Overlap to ^{32}P	^{32}P eff.	Overlap to ^3H	Overlap to ^{14}C
0	.323	.0029	.00007	.677	.227	.0204	.808	.0139	.118
5	.312	.0022	.00001	.672	.243	.0102	.803	.0142	.122
15	.313	.0020	.00005	.675	.242	.0119	.808	.0142	.122
25	.314	.0024	.00003	.672	.241	.0108	.803	.0143	.123

LEGEND TO TABLE 3

To 10 ml of Aquasol and 1 ml of H_2O in a scintillation vial was added 275 µl of either ^3H, ^{14}C or ^{32}P standard containing either 0, 5, 15 or 25 percent sucrose in .05 M-Tris, .3 M-KCl and .005 M-EDTA, pH 7.2. The contents were mixed by shaking and counted in a Beckman LS-233 counter for 5 min, with the results indicated. All values were corrected for background. The ^3H standard contained 2.75×10^5 dpm/aliquot, the ^{14}C standard 6.95×10^4 dpm/aliquot and the ^{32}P standard 1.5×10^5 dpm/aliquot.

TABLE 4

The ratios of ^{3}H-lysine incorporation into infected/uninfected cultures of *E. coli* H502 exposed to varying doses of UV_{260} radiation

UV_{260} Dose Minutes	Incorporation Period Minutes	
	0-90	30-90
0	0.69	0.69
3	2.6	8.6
5	4.8	23.5
7	6.8	12.5
10	2.9	3.6

LEGEND TO TABLE 4

The total incorporation from 0-90 min and from 30-90 min was determined for each of the incorporation curves in Fig. 2 For any given dose rate the infected incorporation was divided by the uninfected incorporation to obtain the ratios presented. In the case of the zero dose sample incorporation was linear for 45 min after which it remained constant due to exhaustion of the label. The 90 min values were therefore obtained by extrapolation.

TABLE 5

Radioimmunoassay - A comparison of counting efficiencies and binding efficiencies in the radioimmunoassay as monitored by two scintillation fluids[2]

Scintillation Fluid	Cpm Added to Vial[1]	Cpm Bound to Vial	Binding Efficiency	% cpm Solubilized by the Scintillator	Counting Efficiency of ^{3}H Relative to TLNCS	
					When Bound	When Soluble
TLNCS	14260	12607	0.86	94.6	1.00	1.00
Modified Bray's	6984	4442	0.64	1.3	0.35	0.49

[1]All cpm are corrected for solvent quenching, backgrounds and nonspecific absorption.
[2]Results are the average of triplicate determinations.

LEGEND TO TABLE 5 - Packard Vials were prepared according to the standard assay procedure. Multiple serum and control vials were then incubated with 2 ml aliquots of ^{3}H-histidine labeled $\phi X174\underline{am3}$ containing 1 x 10^{9} phage particles/ml. After a 48 hr incubation the vials were washed and counted with one of the two scintillation solutions indicated. Aliquots of the ^{3}H-labeled phage preparation were also counted in these solutions and the results corrected for quenching by the phage buffer. After a preliminary counting the scintillator from each vial was transferred to a clean vial to determine the fraction of bound radioactivity that is released by the scintillator.

TABLE 6

Radioimmunoassay-suppression of nonspecific absorption by BSA

Serum-coated and control vials were prepared according to the standard assay procedure except that the concentration of BSA in the last wash step was varied. Identical quantities, 4,500 cpm of ^{3}H-labeled $\phi X174$, were added to duplicate vials of each type. The vials were incubated for 24 hrs before counting the absorbed radioactivity with TLNCS scintillator.

Suppression of nonspecific absorption of ϕXam3 by BSA

Concentration of BSA[1]	Antiserum-Coated Vial		Control Vial		Fraction of Nonspecific Binding[3]
	Cpm bound	Relative cpm bound[2]	Cpm bound	Relative cpm bound[2]	
0	1239	1.00	325	1.0	0.26
0.01	1008	0.81	61	0.19	0.06
0.10	875	0.71	38	0.12	0.04

[1]BSA concentrations are weight/volume
[2]Cpm are normalized to the values for BSA concentration of 0.
[3]Calculated as counts bound in control tube divided by counts bound in the serum-coated tube. The nonspecific binding of phage relative to the total input phage is much lower than this, 0.07 in the absence of BSA.

FIGURE 1

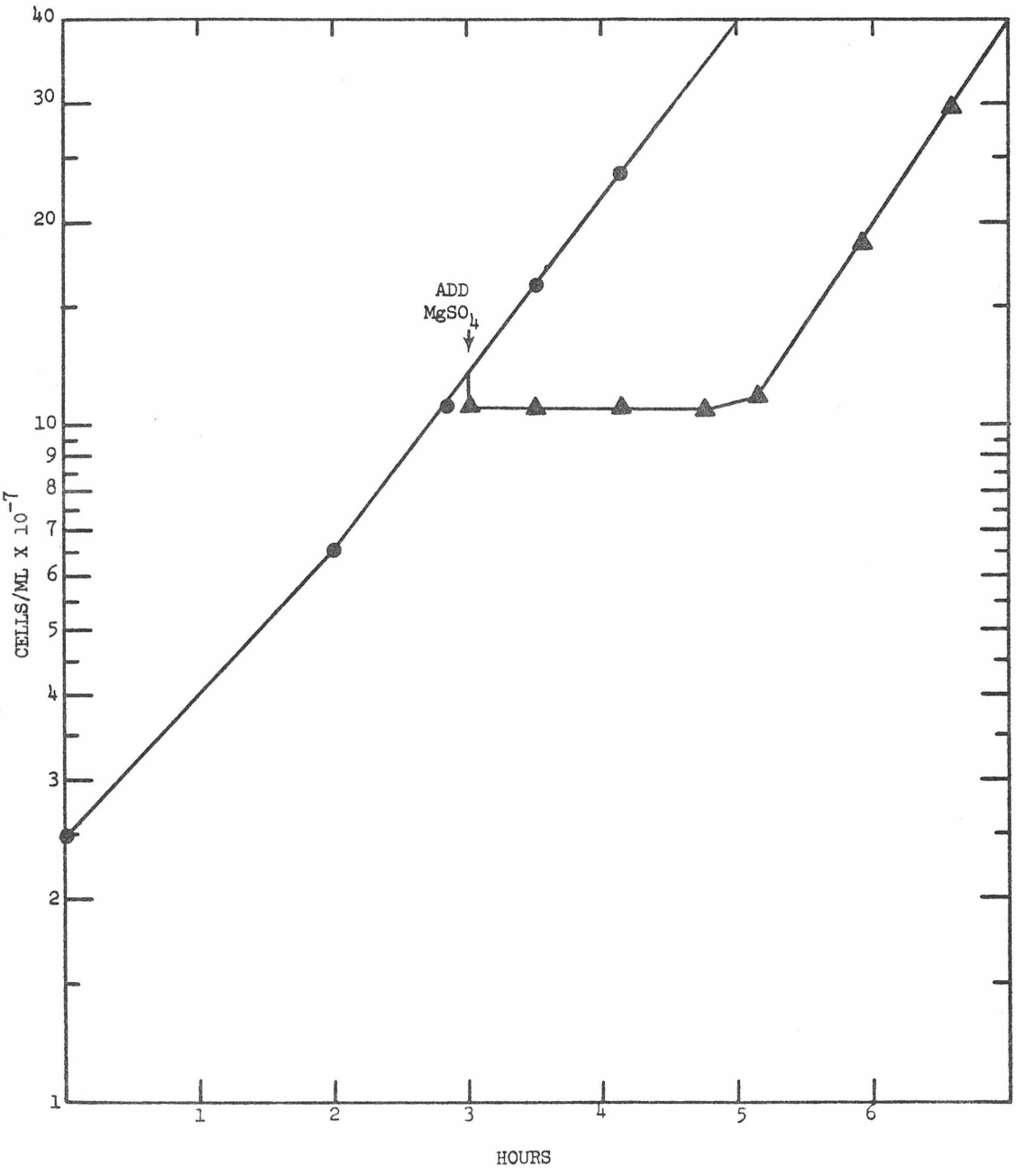

FIGURE 1. The effect of 0.2 M $MgSO_4$ on the growth of E. coli H502.

At time zero E. coli H502 was inoculated into the TPG medium supplemented with 5 g/ml thymidine and subsequently incubated at 37°C with vigorous aeration. Cell growth was monitored with a Coulter Counter. When the cell titre reached 1.2×10^8 cells/ml the culture was divided in half and one portion brought to 0.2 M $MgSO_4$ by addition of 2 M $MgSO_4$ in water. Both cultures continued to be incubated at 37°C with aeration.

The arrow indicates the time of addition of $MgSO_4$

-●- Media without $MgSO_4$

-▲- Media with 0.2 M $MgSO_4$

FIGURE 2

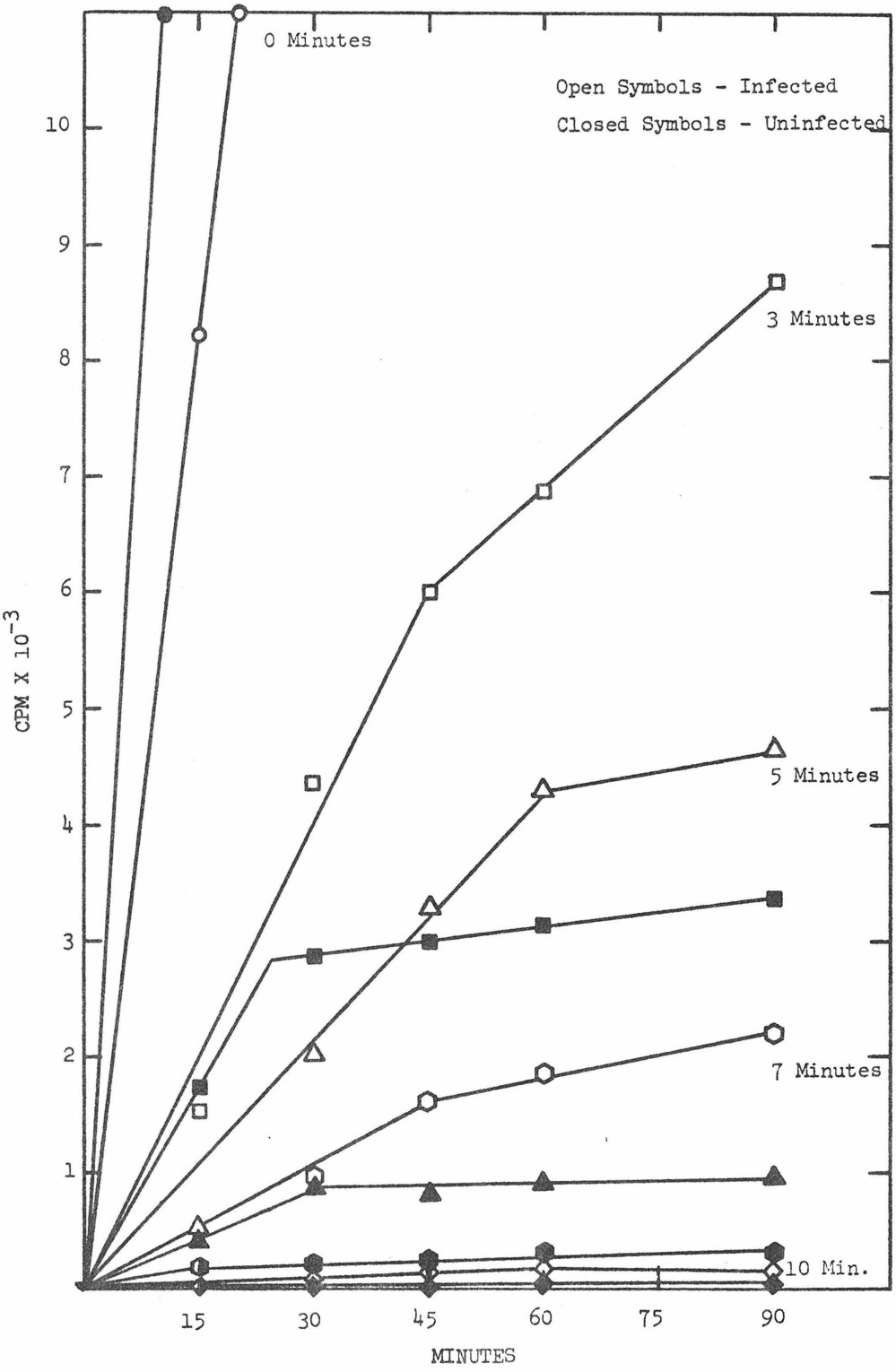
0 Minutes
Open Symbols - Infected
Closed Symbols - Uninfected
3 Minutes
5 Minutes
7 Minutes
10 Min.
CPM X 10^{-3}
MINUTES
1
2
3
4
5
6
7
8
9
10
15
30
45
60
75
90

FIGURE 2. Incorporation of ^{3}H-lysine into infected and uninfected *E. coli* H502 pretreated with varying doses of UV_{260} radiation.

E. coli H502 was grown to 3 x 10^{8} cells/ml as described in the Methods. 50 ml of this culture was placed in a 14 cm diameter glass petri plate and irradiated as described. 10 ml aliquots were withdrawn at times 0, 3, 5, 7 and 10 min, placed in culture tubes and incubated at 37°C with aeration until ten min after the last withdrawal. Each of these cultures were then divided in half and at time zero one half was infected with φX*am*3 at a multiplicity of 7 and both halves were labeled with ^{3}H-lysine at final concentrations of 1.25 μc/ml and 2 μg/ml. 100 μl aliquots were removed from each culture of 15, 30, 45, 60 and 90 min after infection and TCA precipitated and counted according to procedure I. The first point for the zero dose, uninfected culture is off scale and the line is positioned by interpolation.

0 min dose; - ○ - infected, - ● - uninfected

3 min dose; - □ - infected, - ■ - uninfected

5 min dose; - △ - infected, - ▲ - uninfected

7 min dose; - ⬡ - infected, - ⬢ - uninfected

10 min dose; - ◇ - infected, - ◆ - uninfected

FIGURE 3

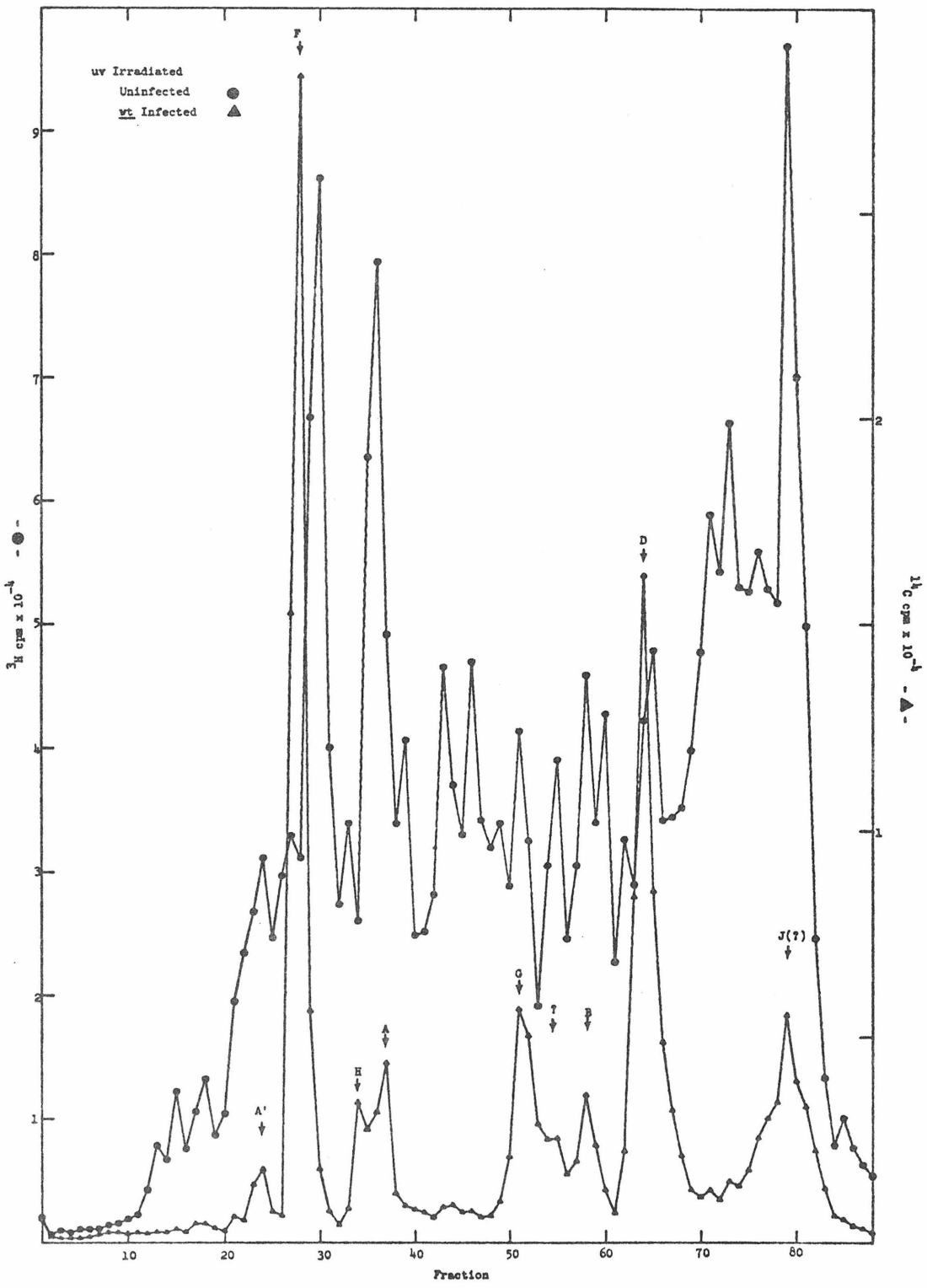
uv Irradiated
Uninfected
wt Infected
F
A'
H
A
G
I
B
D
J(?)
^{3}H cpm x 10^{-4} - ● -
^{14}C cpm x 10^{-4} - ▲ -
Fraction
10
20
30
40
50
60
70
80

FIGURE 3. Coelectrophoresis of ϕX wt infected and uninfected UV-irradiated E. coli H502.

E. coli H502 was grown to 3 x 10^8 cells/ml and irradiated for 7.5 min as described in the Methods. At time zero, one of two 5 ml aliquots was infected with ϕX wt at a multiplicity of 12. 30 min after infection, ^{3}H-lysine was added to the uninfected culture at final concentrations of 20 μc/ml and 2 μg/ml; ^{14}C-lysine was added to the infected culture at 2 μc/ml and 2 μg/ml. 90 min after infection both cultures were cooled to 0°C and lysed according to procedure I. The lysates were then dialysed against TP buffer and 25 μl aliquots mixed, denatured in a final volume of 100 μl, and electrophoresed, fractionated and counted according to procedure II. Peak assignments are on the basis of Table I from the Introduction.

-▲- ϕX wt infected

-●- uninfected

FIGURE 4

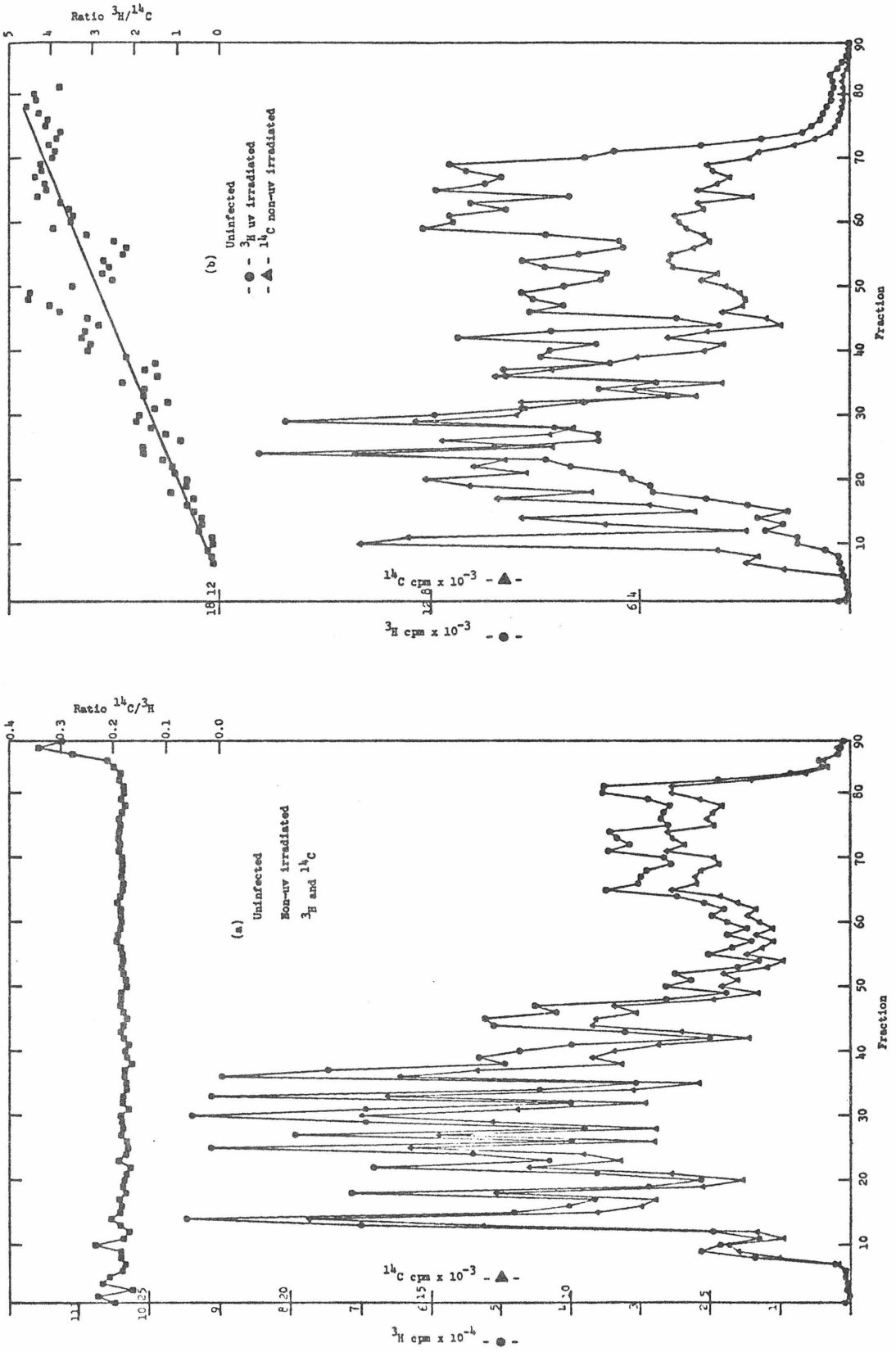
(a)
Uninfected
Non-uv irradiated
^3H and ^{14}C
^{14}C cpm x 10^{-3} - ▲ -
^3H cpm x 10^{-4} - ● -
Ratio $^{14}C/^3H$
Fraction
(b)
Uninfected
^3H uv irradiated
- ● - ^3H uv irradiated
- ▲ - ^{14}C non-uv irradiated
^{14}C cpm x 10^{-3} - ▲ -
^3H cpm x 10^{-3} - ● -
Ratio $^3H/^{14}C$
Fraction

FIGURE 4. A comparison of host cell protein synthesis in UV_{260} and non-UV-irradiated cultures.

(a) E. coli H502 was grown as described in the Methods to 3×10^8 cells/ml. Two 5 ml aliquots were then labeled separately for 90 min with ^3H lysine (20 µc/ml; 2 µg/ml) and ^{14}C-lysine (2 µc/ml; 2 µg/ml), respectively. After 90 min, both cultures were cooled to 0°C and lysed by procedure I. The lysates were dialyzed against TP buffer. A 20 µl aliquot of the ^3H lysate was then mixed with a 10 µl aliquot of the ^{14}C lysate, and the mixture denatured in 100 µl, electrophoresed, fractionated and counted according to procedure II.

(b) A 5 µl aliquot of the dialyzed ^{14}C-lysine labeled, uninfected, non-UV-irradiated lysate from part (a) was mixed with a 50 µl aliquot of the dialyzed ^3H-lysine labeled, uninfected, UV-irradiated lysate prepared as described in the legend to Figure 3. This mixture was denatured in a final volume of 100 µl, electrophoresed, fractionated and counted according to procedure II.

The data from both gels were processed with the CNTSEP program and the ratios of uninfected ^{14}C/uninfected ^3H and of ^3H UV incorporation/^{14}C non-UV incorporation determined in (a) and (b), respectively, and plotted along with the ^3H and ^{14}C cpm. A straight line has been drawn through the ratio plot in (b) to indicate the trend of the ratio values.

All cultures are uninfected.

(a) Non-UV, ^3H-lysine; non UV, ^{14}C-lysine

(b) UV, ^3H-lysine; non UV, ^{14}C lysine

-●- ^3H lysine; -▲- ^{14}C lysine; -■- Ratios

FIGURE 5

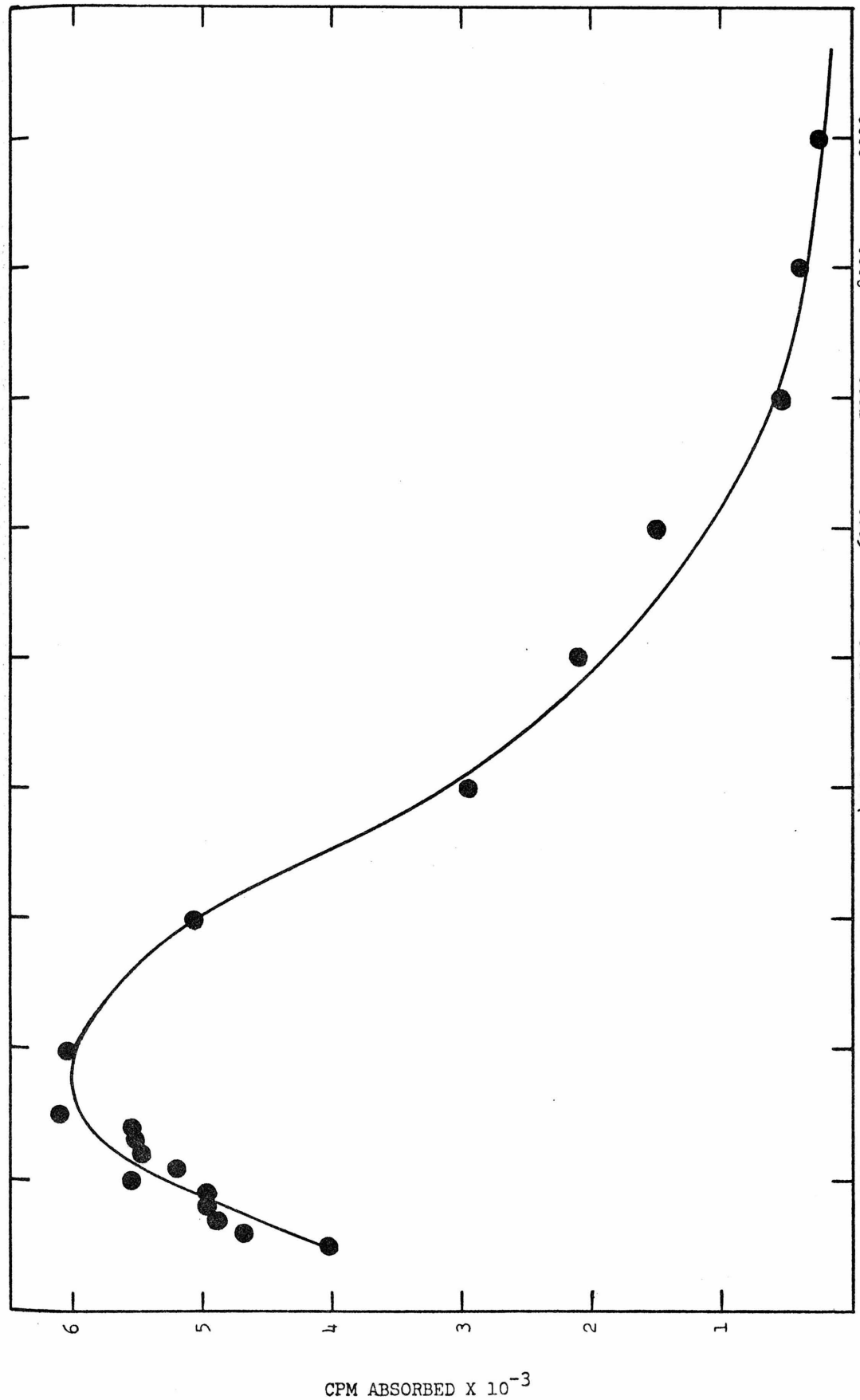
1000
2000
3000
4000
5000
6000
7000
8000
9000
SERUM DILUTION
1
2
3
4
5
6
CPM ABSORBED X 10^{-3}

FIGURE 5. Radioimmunoassay--Optimum serum concentration.

Packard Vials were prepared for radioimmunoassay by the standard procedure except that serum concentrations were varied from dilutions of 10 to 10000-fold. The 10-fold dilution point is from another experiment in which it was determined that the optimum concentration occurred at dilutions greater than 1000-fold. Serum was diluted in 0.05 M-sodium tetraborate and duplicate vials prepared at each dilution. Identical 2 ml aliquots of ^{3}H-thymidine labeled ϕXam3 (1.6×10^{9} particles/ml; 2.5×10^{4} cpm/ml) were added to each vial. All vials were incubated at 37°C with gentle agitation for 16 hrs and then counted in the dioxane scintillator. Maximum phage binding is 0.12 of the input cpm.

FIGURE 6

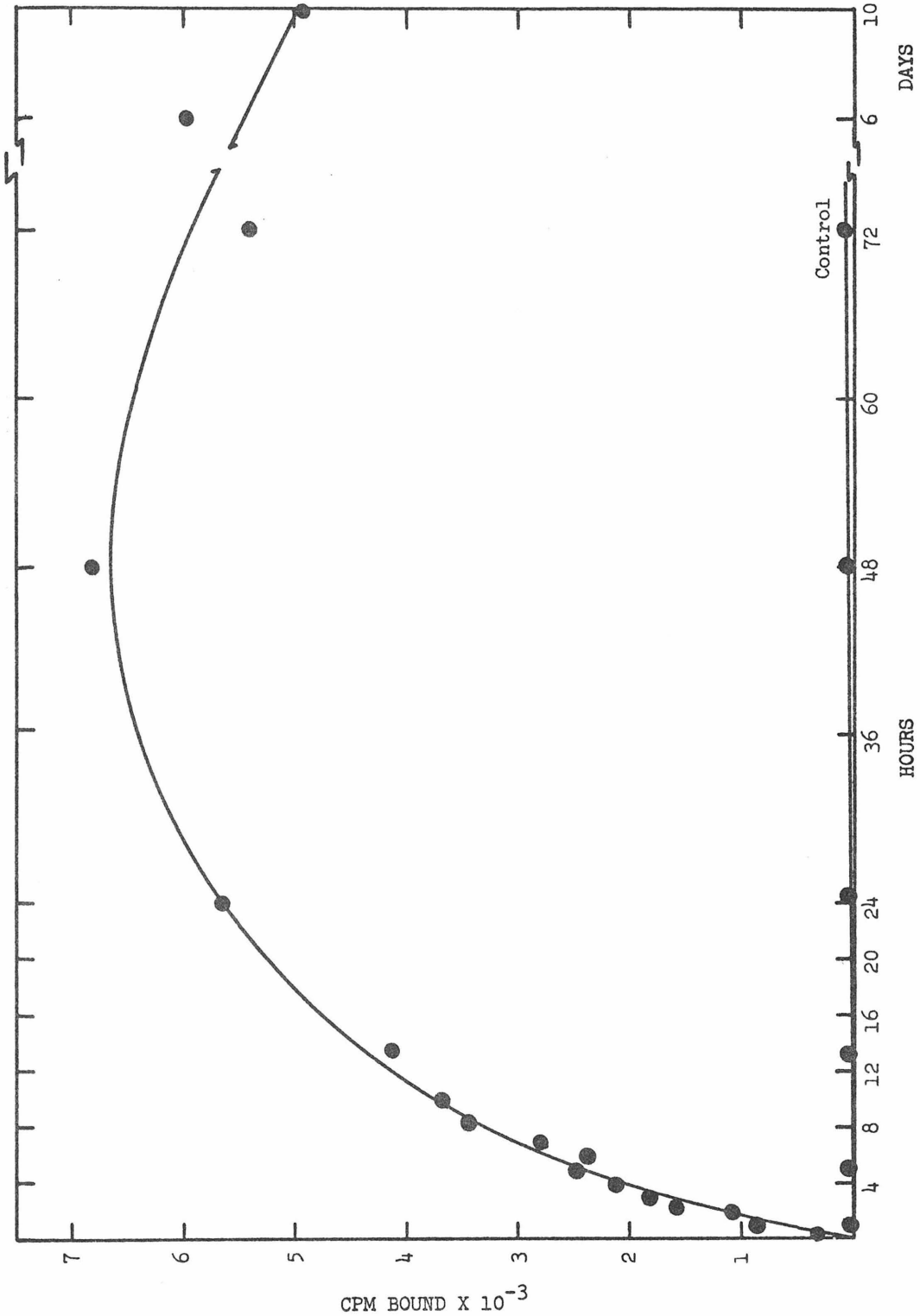
CPM BOUND X 10^{-3}
1
2
3
4
5
6
7
4
8
12
16
20
24
36
48
60
72
Control
6
10
HOURS
DAYS

FIGURE 6. Radioimmunoassay--Kinetics of antigen binding.

Packard Vials were prepared for radioimmunoassay by the standard procedure. Identical 2 ml aliquots of ^{3}H-thymidine labeled ϕX*am*3 (1.6×10^{9} particles/ml; 2.5×10^{4} cpm/ml) were added to each vial. All vials were incubated at 37°C with gentle agitation. At the times indicated on the graph duplicate serum vials, and less frequently control vials, were removed, washed, and counted. Maximum phage binding is 0.14 of the total cpm added.

FIGURE 7

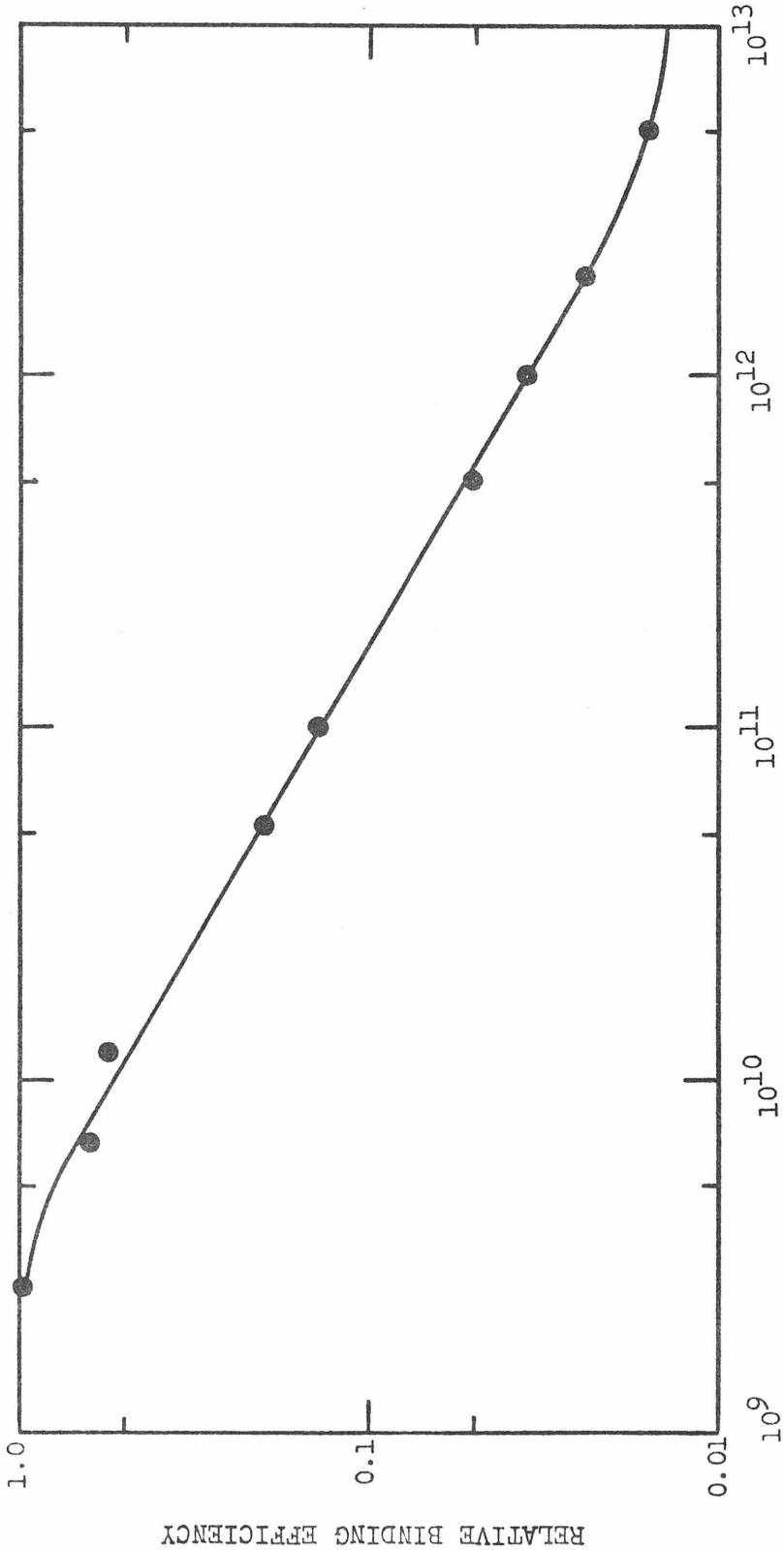
RELATIVE BINDING EFFICIENCY
1.0
0.1
0.01
10^9
10^{10}
10^{11}
10^{12}
10^{13}
PHAGE PARTICLES/ML

FIGURE 7. Radioimmunoassay - The relative efficiency of antigen binding as a function of antigen concentration.

The assay was conducted according to the standard procedure utilizing Packard Scintillation Vials. A constant aliquot of ^{3}H-thymidine labeled ϕXam3 was combined with varying concentrations of cold phage to give the combined concentrations indicated on the graph. Duplicate samples were prepared at each concentration except the two highest ones. The vials were incubated for 16 hrs at 37°C with gentle agitation before washing and counting. A total of 5.0×10^{4} cpm was added to each vial and the maximum binding at the lowest antigen concentration was 0.12 of total cpm added.

RESULTS

Introduction to Results

The structure of the ϕX174 virion and the ϕX174 infection process have been discussed at length in the General Introduction. From the broad picture presented there the following points should be emphasized. 1. SS DNA replication has been well characterized and the entire spectrum of expected intermediates, from RF II to rolling circles with unit length plus strand tails, have been observed. 2. The immediate product of this replication, the new, viral, single strand circle probably does not exist as a free moiety within the cell. 3. SS DNA replication exhibits an absolute requirement for the phage structural proteins F and G. 4. Intracellularly, the F and G proteins have previously been observed only as part of the virion and as several small particles thought to be capsid subunits.

The requirement of the SS replication system for phage structural proteins and the absence of free intracellular SS DNA suggest that DNA replication is coupled to phage assembly in such a way that the nascent single strand is matured directly into a virion or some other highly developed particle at the time of its release from the RF II template. However, as yet there has been no report of any intracellular complex between the SS replication intermediates and the phage structural proteins. The fact that the DNA replication intermediates themselves are observed indicates that this is not because these protein-DNA complexes are so transient that they cannot be visualized by means of the usual pulse labeling regimes.

The study presented here was conducted in an attempt to dis-

cover the *in vivo* process by which the ϕX174 infective particle is assembled from its constituent parts. As a first step in this investigation a search was undertaken to locate, identify, and characterize intracellular subviral structures with the properties expected of maturation intermediates. In particular, the following criteria were established to distinguish a particle of interest and to serve as guide lines for experimental design. The structures should be complex, involving at least the phage structural proteins F and G and the phage DNA, either as a just completed circle or as a replicating intermediate. One might also expect an involvement with the other ϕX proteins, B, C and D that are also required for the late stage of the infection. Finally, the DNA in an assembly intermediate should pulse label. Presumably the maturation structures are transient ones and DNA flows through them at the rate at which new phage are matured.

An attempt was made to anticipate other properties that might be expected of such structures. With reference to the sedimentation values of ϕX, the 70S lysis artifact, the 72S empty viral coat, the 50S 4 M urea particle, SS DNA, RI DNA, and RF DNA, sedimentation values were anticipated in the range of from that of ϕX to that of RF II. It was deemed especially likely that assembly intermediates might sediment in the vicinity of 70S, in as much as the structure of the 70S lysis artifact, containing a complete protein coat but partially external DNA, is similar to that which might be expected of an intermediate at a late stage of assembly.

It was also reasoned that, although the completed phage is adapted to survive in a varied and non-physiological extracellular

environment, this need not be true of maturation intermediates. Thus, another well characterized and exclusively intracellular nucleic acid-protein particle, the ribosome, was selected as an indicator of the possible environmental needs of such structures (175, 176, 177). As a consequence, the search for assembly intermediates was conducted in the presence of Mg^{++}, low salt, low temperature and at physiological pH (see Appendix C for further discussion).

I. The distribution of nascent DNA forms in non-deproteinized lysates of ϕX174 infected cells labeled during the late stage of the infection

A. The relative distribution of pulse and continuous labels in the 70S peak

B. Deproteinization and recentrifugation of the designated fractions of the non-deproteinized gradients in Figure 1a,b

1. Fraction A- The 114S phage peak
2. Fraction B- The 70S peak
3. Fraction C- The replicative intermediates
4. Fraction D- The RF II region

C. Summary

D. Comments

1. Single Stranded DNA fragments
2. Heterogeneity of the DNA populations found in given regions
3. Heavy DNA
4. Marker DNAs
5. Losses to phenol during deproteinization

The following experiments (Figures 1-6, Tables 1-4) were conducted in order to discover the sedimentation positions of possible intermediates in the ϕX174 assembly process and, in particular, to determine whether or not the 70S lysis artifact masks a phage precursor.

Continuous and pulse labels were utilized to differentiate accumulating and nascent, ϕX specific, DNA-containing structures in lysates of ϕXam3 infected cells sedimented without deproteinization. The presence of probable maturation intermediates was then demonstrated in two ways:

A. The ratio of the continuous label in the 70S lysis artifact to the continuous label in whole phage was utilized to determine the extent of 70S lysis artifact formation in a given lysate. A comparison of this number with the ratio of the pulse labels in the same two particles in the same lysate revealed an excess of pulse label in the 70S region indicating a transient particle cosedimenting with the 70S lysis artifact.

B. The DNA from various regions of the non-deproteinized gradients was deproteinized and characterized by recentrifugation. In this way several of the fast sedimenting species from the non-deproteinized gradient were shown to contain SS replicative intermediate DNAs that must have been complexed into more massive or more compact particles in order to have sedimented to the positions observed in the non-deproteinized state.

E. coli H502 was grown and infected with ϕXam3 as described in the Methods. Accumulating, DNA-containing structures such as completed phage and the 70S lysis artifact were preferentially labeled with a continuous exposure to ^{14}C thymine beginning at twenty minutes after infection, well after the end of the eclipse period when host DNA repli-

cation has stopped and progeny RF synthesis has been reduced to a very low level. At this time virtually all incorporation will be into progeny SS DNA and the replicative intermediates in that synthesis (90, 93). Transient, DNA-containing structures such as assembly intermediates were then labeled with five and ninety second pulses of ^{3}H thymidine administered to two equal portions of the culture at fifty minutes after infection. The pulses were terminated by quick freezing. The cultures were then lysed in the presence of Mg++ and the non-deproteinized lysates prepared for centrifugation as described in the Methods and the legend to Figure 1. Centrifugation was through 5-30% linear sucrose gradients for 2.25 hours at 40,000 rpm in an SW 40 rotor. Fractions were collected and counted as described in the Methods and legend to Figure 1. The precautions outlined in the Methods for working with non-deproteinized lysates in the presence of Mg++ were employed at all times. The data are presented in Figure 1a,b. The identities of the various peaks are established in subsequent experiments.

A comparison of the five second and ninety second pulses with the ^{14}C continuous label demonstrates that the DNA label first enters the more slowly sedimenting DNA forms and then flows into the phage peak, labeled A, where it accumulates with time (Table IV). The majority of the pulse label enters the RF II peak, labeled D, and the peak labeled C. In low salt sedimentation gradients of deproteinized DNA, the C peak would be expected to contain RF I, unit length SS DNA, and SS replicative intermediates. Under the sedimentation conditions employed in these experiments, no known ϕX DNA forms sediment faster

than this peak, C, in the deproteinized state (93, see Figures 3 and 4). By comparison, it will be noted that a substantial proportion of the pulse label (12-33%) is found at much higher sedimentation velocities in both of the non-deproteinized gradients presented here. There is also an apparent accumulation of pulse label in the 70S region of the gradient, peak B, during the ninety second pulse.

A. The relative distribution of pulse and continuous labels in the 70S peak

As noted in the Introduction, one might reasonably expect maturation intermediates in the vicinity of peak B. However, peak B is also the expected gradient position of the 70S lysis artifact. To determine the relative contribution of this particle to the 70S pulse label it is necessary to make use of the ^{14}C long term labeling pattern.

By labeling the infected culture from twenty to fifty minutes after infection with ^{14}C thymine, a large pool of ^{14}C labeled phage is established which upon lysis will give rise to the 70S lysis artifact at some ratio R of lysis artifact to phage. If all intracellular phage are equivalent, then all phage in the same culture should produce the lysis artifact with the same efficiency. Thus, the pool of ^{14}C labeled phage can be used as an internal indicator of the efficiency with which the 70S lysis artifact will be generated from pulse labeled phage. Any discrepancy between the amount of pulse label found at the 70S position and that expected from the production of lysis artifact must presumably be due to other pulse labeled species.

The percentage of the pulse label that is found at 70S that

cannot be accounted for by the lysis artifact P is obtained from the expression:

$$P = \frac{B_H - R \cdot A_H}{B_H} \times 100\%$$

where

P = Percentage of the total 70S pulse label that is not due to the 70S lysis artifact

A_C = Total cpm of long term label incorporated into the phage peak

A_H = Total cpm of pulse label incorporated into the phage peak

B_C = Total cpm of long term label incorporated into the 70S peak

B_H = Total cpm of pulse label incorporated into the 70S peak

$R = B_C/A_C$

The cpm were summed under the peaks A and B as indicated in Figure 1. The value of P was then calculated for both the five second and ninety second pulses and the results are presented in Table 1 (experiment 1) along with the values obtained from several additional experiments. It can be seen that from eighty to ninety percent of the five second pulse and from forty to fifty percent of the ninety second pulse cannot be accounted for by the lysis artifact. These percentages are minimum values. The actual ratio of ^{14}C labeled lysis artifact to ^{14}C labeled phage is smaller than R in proportion to the amount of ^{14}C label that the pulse labeled species is also contributing to the 70S peak. This contribution is apparently not very great, as the 70S lysis artifact has already begun to dominate the composition of the 70S pulse label by ninety seconds.

Apparently the additional 70S pulse label is entering some

particle other than the 70S lysis artifact. The fact that this material is labeled by very short pulses indicates that it is actively involved in, or is an immediate product of, SS DNA replication. The fact that it accounts for a diminishing proportion of the 70S pulse with increasing duration of pulse time indicates that it is a transient species and that its existence precedes that of phage (and 70S lysis artifact).

These considerations lead one to the expectation that the 70S pulse labeled DNA is in the form of SS replicating intermediates or new viral SS DNA. The following experiments were conducted in order to check this possibility and characterize the DNA in other regions of the gradient as well.

B. Deproteinization and recentrifugation of the designated fractions of the non-deproteinized gradients in Figure 1a,b

The fractions indicated under A_1 through D_2 in Figure 1a,b were pooled separately and the DNA extracted according to the procedure given in the Methods. In each case ^{32}P labeled ϕX RF I and RF II DNA, as well as ^{32}P labeled virions, were added to the samples prior to phenol extraction. Each step of the extraction procedure was carefully monitored for losses and the final recoveries are given in Table 2. In every case, except A_1, there was a preferential loss of the ^{3}H pulse labeled counts. In this and other experiments the 114S phage peak was always least susceptible to loss. This difference was enhanced if the pronase digestion step or SDS was ommitted from the procedure. When this was done, the 114S DNA was recovered at fifty to sixty percent, whereas recoveries from peaks B, C and D did not exceed twenty percent. If more than one phenol extraction was performed, then recoveries of

both labels from the second extraction were much greater than those for the first, indicating that some phenol soluble subpopulation may have been selectively removed by the first extraction. The preferential loss of pulse labeled DNA versus long labeled DNA and of replicative forms versus phage DNA suggests some special property of replicative form DNA that enhances its solubility in phenol. Presumably this might be due to a strong association with some protein moiety.

Separate aliquots of the deproteinized DNA from each peak were analyzed by sedimentation to equilibrium in the presence of the intercalating dye, propidium diiodide (PDI), and by velocity sedimentation through isokinetic sucrose gradients in the presence of high salt. (See Methods for both procedures.) In each case internal ^{32}P markers indicated the positions of ϕX RF I, RF II and SS circular DNA. After PDI centrifugation to equilibrium, fractions were collected directly onto numbered filter paper discs. The PDI was removed by sequential batch elutions with $0^{o}C$, 10% TCA and the fractions counted in TL as described in the Methods. The velocity sedimentations were fractioned directly into scintillation vials and counted in Aquasol-water, 9:1. In both instances the isotopic composition of each fraction was computed by means of the TRIPSEP program. Recoveries of all three labels from both centrifugation procedures was close to 100% in every gradient.

The data are presented in Figures 2 through 5. In the PDI sedimentations to equilibrium the positions of the internal markers are indicated by arrows. Figure 6 presents a PDI sedimentation to equilibrium of differentially labeled marker DNAs. This centrifugation was conducted in order to unambiguously assign the three peaks of ^{32}P

activity constituting the internal markers in the other gradients to their appropriate DNA forms. The internal markers in the velocity sedimentation experiments are plotted with the other data.

The distribution by DNA species, single strands, replicative forms and heavy DNA (discussed below), of the pulse labels in Figure 1 can be computed from the PDI sedimentation to equilibrium data in conjunction with the percentage distribution of the total pulse label in Figure 1. This calculation is summarized in Table 4a,b which gives the molecular distribution into regions A through D in Figure 1.

1. Fraction A- The 114S phage peak- Figure 2a,b,c,d presents the results of the PDI banding (a,c) and velocity sedimentation (b,d) of the five second (a,b) and ninety second (c,d) pulses into the 114S sedimentation peak. As expected for the phage peak, eighty-five to ninety percent of the long term label is in SS DNA by both PDI banding and velocity sedimentation criteria. However, a small but significant proportion of the counts, six percent, are in other forms as well. This material bands heterogeneously between RF II and SS DNA in the PDI gradient and sediments between RF II and SS DNA on the velocity gradient. Both of these behaviors are expected for replicating intermediates of SS DNA synthesis. A small fraction, one percent, of the long term label bands at a position denser than RF I in the PDI gradient. The patterns of long term label from both the five second and ninety second pulses are identical, demonstrating the uniformity with which the samples were prepared.

The five second pulse distributes itself almost equally between the SS region and the replicating RF region of the PDI gradient. A

significant fraction of the pulse label, seven percent, enters the dense peak. The sedimentation velocity confirms this distribution except that there seem to be fewer cpm in the RF II and RI regions of this gradient, twenty-eight percent, compared to the banding, thirty-nine percent. However, it may be that a significant fraction of the replicative intermediates are cosedimenting with the SS peak thus accounting for this difference.

As the pulse is lengthened to ninety seconds a much larger proportion of the counts enter the SS DNA pool. The pulse pattern observed in the PDI gradient is almost indistinguishable from that of the long term label. If the non-single stranded material in this region represents precursors to phage, then this rapid approach to the long term labeling pattern indicates a very small pool size for these structures. Again there is a small amount of incorporation, two percent, into a "heavy" DNA form.

The sedimentation velocity gradient of the ninety second pulse shows a broad tail extending to low S values. From the PDI gradient it is apparent that only ten percent of this material can be accounted for by various replicative form DNAs. The rest is apparently fragmented SS DNA. The origin of this fragmentation is unclear as neither the ^{32}P DNA marker nor the ^{14}C SS DNA peak show any fragmentation. Whatever the source of these fragments, whether adventitious nuclease or some other more subtle (and more interesting) cause, the fact that they are associated exclusively with the pulse label indicates that there is something unique about the structure or environment of this DNA relative to the long term labeled DNA.

2. Fraction B- The 70S peak- The results of the recentrifugations of the deproteinized 70S DNA are presented in Figure 3a,b,c,d. As expected for the 70S lysis artifact, the long term label bands as a broad peak at the position of SS DNA. Four to five percent bands at the the position of heavy DNA and another five to six percent in the position expected of replicating intermediates. Sedimentation velocity reveals a distinct peak of unit length SS DNA accompanied by the heterogeneous distribution of fragmented DNA expected of the lysis artifact. Again the ^{14}C patterns are identical for both pulses even with respect to the shape of the fragment distribution in the velocity sedimentation.

The five second pulse bands at the intermediate positions expected of replicative intermediates. The majority of the pulse bands slightly denser than RF II. Another peak is present at a density midway between RF II and SS DNA. A third peak bands somewhat lighter than the SS DNA marker. Over eighteen percent of the pulse is in the peak of heavy DNA that bands denser than RF I. The velocity sedimentation also shows a prominent peak at the RF II position trailing to the higher sedimentation velocities indicative of replicating intermediates. There is no evidence of fragmented SS DNA in the five second pulse patterns. It should be noted that in the non-deproteinized state, virtually none of the five second pulse labeled DNA sediments faster than the SS DNA marker.

As expected, a much greater proportion of the ninety second pulse bands at the position of SS DNA. Only eighteen percent bands at the positions of RF II and RI DNA forms and another seven percent at the position of heavy DNA. The velocity sedimentation pattern is dom-

inated by the heterogeneous distribution of DNA fragments and consequently obscurs the sedimentation of the more interesting DNA.

3. Fraction C- The SS replicative intermediates- The recentrifugations of the deproteinized DNAs from region C of the original velocity gradient are presented in Figure 4a,b,c,d. In a sedimentation velocity centrifugation of deproteinized DNA from ϕX infected cells one would expect to find SS DNA, replicative intermediates, and RF I DNA in this region of the gradient (96). The remarkable thing about these recentrifugation patterns is that they are so similar to those observed for the 70S DNA, including the presence of fragmented single strands.

As was true for the 70S region, most of the long term label bands at the position of SS DNA with a slightly greater proportion, twelve to fifteen percent, at the intermediate densities of replicative intermediates. The heavy DNA peak again accounts for three or four percent of the ^{14}C label. Velocity sedimentation shows virtually the same distribution of ^{14}C label, a distinct peak of unit length SS DNA and heterogeneous distribution of fragments, as was observed for the 70S lysis artifact. Unit length SS DNA would be expected to be associated with this region of the gradient in its free state. Fragmented SS DNA would, on the other hand, have to be associated with some particle or bigger molecule to attain this sedimentation position.

The five second pulse is again distributed between a peak slightly denser than RF II, a clearly resolved peak at the intermediate density between RF II and SS DNA, and a peak banding at a position slightly less dense than the SS DNA marker. Once again approximately eighteen percent of the five second pulse enters the heavy DNA peak.

The velocity sedimentation again shows a prominent RF II peak trailing to the higher S values indicative of replicative intermediates. However, in this case, there is significantly less material sedimenting at the highest S values indicative of intermediates with unit length or nearly unit length tails (93, 96, 97). There is no indication of fragmented DNA in the five second pulse label.

The ninety second pulse pattern is qualitatively the same as that for the 70S region, but with a much greater proportion of label in replicative DNA forms. The peak that bands slightly heavier than RF II accounts for thirty-one percent of the pulse, that at the position between RF II and SS DNA for nine percent, and the heavy DNA peak for fourteen percent. Over forty percent of the pulse bands at the density of SS DNA. This suggests that this DNA may constitute a pulse labeled pool of free single strands. However, once again the velocity sedimentation reveals that virtually none of this SS DNA has the mass necessary to sediment to this position in the free condition.

Although it is most likely that these SS DNA fragments have been produced by a limited nucleolytic degradation of free SS DNA or the single strand tails of replicative intermediates at some time subsequent to lysis, there are several observations that appear inconsistant with this origin. First, there is the striking similarity of the sedimentation patterns of the fragmented long term label from all four gradients, Figures 3b, 3d, 4b, 4d. The trimodal distribution observed is not what one would expect for a totally random degradation of unit length ϕX DNA. Second, the large proportion of replicative intermediates which survive at least partially intact indicates that the extent of any nuclease

degradation must be rather limited. Also the reproducible distribution of replicative intermediates into three rather well defined peaks in the PDI banding system would seem to argue against the randomization of these molecules by nuclease (Figures 3b,d; 4b,d).

Depending upon the ultimate resolution of the structure of the dense DNA species observed in PDI equilibrium centrifugations, the integrity of this material may serve as an internal control for nuclease activity. If this DNA species fails to bind dye for the same reasons as RF I DNA (228) then the surviving molecules cannot have sustained any nucleolytic attack (see Discussion). In the case of region C almost nineteen percent of the DNA is in this form (see Table 3). Assuming the most extreme case, that one hundred percent of the pulse label was originally in this form, one can use the Poisson distribution to calculate that there could have been at most an average of 1.6 single strand nicks per molecule that were introduced in the course of the purification. In a random nicking process this average would be distributed evenly over the entire DNA molecule. Thus a rolling circle type of structure with a unit length tail would receive on the average only one half nick per molecule in the single stranded region. Nicks in the double stranded region would not presumably affect its sedimentation velocity.

It is also noteworthy that there are no single strand fragments observed in conjunction with any of the five second pulses (Figures 3a,b; 4a,b). However, this may only be a consequence of not having labeled any single stranded DNA in the course of such a short pulse (see Discussion).

There is also no evidence of degradation in any of the ^{32}P

marker DNAs. However, these markers were not added to the samples until just prior to deproteinization. They would not have been subjected to nuclease in the interval between the velocity sedimentation and deproteinization steps in the procedure. Also the SS DNA marker was added in the form of whole phage.

The C regions of the original velocity gradients are also the expected positions for RF I form DNA. However, in as much as there is little if any de novo synthesis of RF I during the late stage of the infection, this DNA would not be labeled. A small amount of progeny RF synthesis does occur during the late stage of the infection, apparently as a consequence of some residual synthesis by the "site" associated parental RF (63, 93). These membrane bound molecules are most likely discarded with the bacterial debris after the first low speed centrifugation of the lysate.

4. Fraction D- The RF II region- PDI sedimentations to equilibrium of the material from region D are presented in Figure 5a,b. In contrast to the data from regions A, B and C, the long term label is distributed differently in the two gradients. In the five second pulse gradient the long term label is distributed approximately equally between the RF II peak and as a broad SS DNA peak. By the end of a ninety second pulse the ^{14}C RF II peak has essentially disappeared but without a concommitant increase in the SS DNA peak.

The disappearance of the ^{14}C RF II with increasing pulse time is apparently a consequence of the displacement of the thymine DNA precursor pool by thymidine at the time of the pulse. This is born out by experiments (not presented) on the kinetics of incorporation of radio-

actively labeled thymidine or thymine in the presence of the other unlabeled precursor. In the initial period (two to three minutes) after adding thymidine to a culture of a thymine auxotroph growing on exogenous labeled thymine, the rate of labeled thymine incorporation is suppressed. By comparison, the initial rate of incorporation of labeled thymidine is relatively insensitive to the presence of up to two μg/ml of exogenous thymine. Apparently, thymidine, when present, is preferentially incorporated by the cell to the exclusion of thymine. Experiments by other researchers have verified this preference in other E. coli strains (183, 184).

In the case of the ^{14}C labeled RF II molecules from region D of the gradient, only the plus strands are labeled, as the ^{14}C label was added after the period of progeny RF DNA synthesis was over. The plus strands are constantly being displaced from these molecules as a consequence of SS DNA replication. When thymidine is added at the time of the pulse, it becomes the prefered precursor to DNA synthesis. As a consequence, relatively little ^{14}C label is incorporated after the pulse has begun, and the ^{14}C that is present in the RF II pool is displaced out by the new SS DNA synthesis. The fact that the ^{14}C label is displaced so completely indicates that virtually every previously labeled RF II molecule undergoes one round of synthesis in the course of the ninety second pulse.

In general, the ^{14}C patterns found in the other regions of the original velocity gradient (Figure 1a,b), as well as the SS DNA pool observed in region D, have been invariant with pulse time. This invariance indicates either that the molecular species involved are no

longer metabolically active (phage, 70S lysis artifacts, dead end by products), or that the molecular pools represented by the ^{14}C label are very large such that only a small fraction of the molecules are actively involved in their metabolic roles during any ninety second pulse period.

Both the five and ninety second pulses from region D enter primarily into RF II DNA. There is also some incorporation into the peak of intermediate density material, nine percent, and into the heavy DNA peak, seven percent. With time, some of the pulse also appears in the SS DNA region. In this case, free SS DNA could only sediment in this region of the gradient as fragments, as unit length DNA will sediment farther than this. The origin of these single strands is not known.

C. Summary

The experiments presented in this section demonstrate that substantial quantities (approximately 10%; Table 4b) of the replicating ϕX DNA isolated late in the infection sediment in non-deproteinized gradients with velocities far greater than those observed for the same molecules when deproteinized. Most of these fast sedimenting replicative intermediate DNAs are obscured during longer labeling periods by the accumulation of phage particles and the 70S lysis artifact which sediment in the same region of the gradient. The rapidity with which the high molecular weight pulse labeled pools become dominated by the phage and the 70S lysis artifact indicates that the pools of fast sedimenting replicative intermediates are small. On the other hand, the temporal sequence of appearance of the pulse label into fast sedimenting replicative intermediates followed by virional single strands

suggests that these fast sedimenting DNAs are precursors to the completed phage. In order for these replicative intermediate DNA forms to sediment with the velocities observed they must be complexed in some way - presumably with ϕX proteins. Thus both the labeling kinetics and the sedimentation behavior of these DNAs suggests that they may be associated with assembly intermediates.

D. Comments

1. Single stranded DNA fragments- Fragmented, single strand DNA was expected in the 70S region of the gradient in conjunction with the lysis artifact. Surprisingly, it was observed in varying amounts in all other regions of the gradient as well. In the phage region it was associated only with the ninety second pulse label. In the 70S, the replicative intermediate, and RF II regions of the gradient it always constituted the majority of the long term label, a significant proportion of the ninety second pulse label, and little if any of the five second pulse label.

Excepting the reservations noted below, the most likely source of these fragments was nucleolytic attack subsequent to lysis. This would not be too surprising in as much as all steps prior to deproteinization were carried out in the presence of Mg++. The absence of degradation in the marker DNAs could have been a consequence of having added them to the samples just prior to deproteinization and having added the ^{32}P SS DNA marker in the form of whole phage.

A comparison of the continuous and pulse labeled fragments suggests different origins for the two moieties. It was noted above that whereas the long term label and the ninety second pulse label

show fragmentation, the five second pulse label does not. This behavior is consistent with the idea that only SS DNA that has been displaced from the double stranded RF II template is subject to degradation. During the five second pulse, ^{14}C labeled DNA is displaced from the RF II template by the growing pulse labeled end. Subsequent to lysis the ^{14}C labeled but not the pulse labeled DNA is susceptible to nuclease attack. The data in Figure 5 indicate that by the end of a ninety second pulse most of the RF II pool has been through at least one round of synthesis. The displaced plus strands are then labeled with ^{3}H which subsequently can be degraded to SS DNA fragments.

The data also indicate (see earlier discussion) that by the end of a ninety second pulse the ^{14}C thymine label has been largely displaced from the replicative form DNAs (presumably into virions) due to the preferential incorporation of the thymidine pulse label. As a consequence, the ^{14}C labeled SS DNA observed after the ninety second pulse could not have been derived from the degradation of the SS tails of the replicative intermediates. At the same time, the great similarities, both qualitative and quantitative, between the non-random, trimodal distributions of the ^{14}C labeled SS DNA fragments from both the five second and ninety second pulses (regions B and C, Figure 1a,b) suggest a pulse insensitive common origin for both ^{14}C labeled fragment pools, in which case nucleolytic degradation of the SS tails of the RI molecules could not have contributed significantly to the pool of ^{14}C labeled SS DNAs observed after the five second pulse either.

As a consequence the long term labeled SS DNA fragments seem to have an independent origin from the pulse labeled SS DNA fragments.

In the 70S region this pool is easily accounted for by the SS DNA fragments associated with the 70S lysis artifact. In region C of the gradient such a pool could be comprised of free sedimenting unit length single strands. These single strands would then have to have been degraded between the centrifugation and deproteinization steps. The SS DNA found with the RF II peak (region D) would, if uncomplexed with other molecules, have to have pre-existed as SS fragments before deproteinization.

The origin of the ^{14}C labeled SS DNA in region C and D and its relationship to the pulse labeled fragments observed there is uncertain. The fact that the ^{14}C label accumulates in this form could mean either that the SS DNA pool is formed by degradation of completed phage particles or late assembly intermediates, or that it represents a very large intracellular pool of free SS DNA. The latter possiblity contradicts the bulk of the circumstantial evidence (see General Introduction for a complete discussion), as well as more direct experiments by Weisbeek and Sinsheimer (165) who have shown that the observation of free SS DNA in cell lysates is a function of the lysis conditions and that conditions can be found in which no detectable SS DNA is observed. This indicates that a free SS DNA pool is not a normal <u>in vivo</u> occurrence during the infection. Therefore, it seems likely that the long term labeled SS DNA found in regions C and D of the original velocity sedimentations is due to the breakdown of some structure accumulating late in the assembly process. One such structure is the 70S lysis artifact from which continuously labeled SS DNA is ejected during the abortive events that lead to its formation. Another candidate is the unstable

140S particle observed by Weisbeek and Sinsheimer (165) which is known to yield free SS DNA upon its decomposition. Mitigating this possibility is the observation that the purified 140S particle is converted quantitatively to 114S phage particles by the addition of Mg++. Since Mg++ is present in the lysate buffer, this suggests that a similar conversion to 114S particles might take place immediately after lysis, thus accounting for the lack of 140S particles in these experiments. However the lysate environment is not identical to the *in vitro* conditions for conversion (most notably with respect to the presence of nucleases) and as a consequence one might envision an all or none reaction of the 140S particles in which they are either converted to stable 114S particles or are degraded, thereby liberating SS DNA for fragmentation.

Whether or not the SS DNA so liberated was predominantly labeled with ^{3}H or ^{14}C would depend upon the pool size and precursor status of the 140S particle. The incorporation of over 20% of the ninety second pulse label into 114S particles(Figure 1b) suggests that the immediate precursors to phage should be largely labeled with ^{3}H after a ninety second pulse and could not therefore be the source of the ^{14}C labeled SS DNA.

On the other hand, a post-lysis conversion to phage of the 140S particle or some other precursor particle (the 140S particle is not a proven *in vivo* precursor) might account for the differential fragmentation of the ninety second pulse labeled 114S DNA while both the continuous label and marker label remained intact (Figure 2d). For example, if the lysate environment resulted in an abnormal exposure of

the precursor SS DNA to nuclease prior to its *in vitro* transformation to a 114S particle an encapsulation of fragmented SS DNA might result.

If, as proposed by Weisbeek and Sinsheimer (165), the ϕX virion exists entirely as the 140S particle *in vivo*, then the pulse and long term labeled DNA in this pool would be equivalent during any post-lysis transformation to the 114S particle and the 140S particle would, when degraded, give rise to SS DNA fragments of either label. However this model is inconsistent with the differential fragmentation of the ninety second pulse labeled 114S DNA. The latter observation suggests that the 114S particle is made *in vivo* and is the ultimate repository of the SS DNA. Regardless of whether or not nuclease is responsible for the fragmentation of the ninety second pulse labeled 114S DNA, there must be something distinctly different about newly matured 114S particles.

Whatever the origin of the SS DNAs observed in these gradients, there are several observations that are inconsistent with their fragmentation by random nucleolytic attack. The reproducible trimodal distribution of the continuously labeled fragments (Figures 3b,d; 4b,d) is unexpected for a random degradation mechanism. There is also no corroborative evidence of nucleolytic activity. There is no indication of double stranded, unit length, linear DNAs (RF III) or small double stranded DNA fragments in any of these gradients (see Figures 3b and 4b) and a substantial proportion of the replicative intermediates survive as molecules with long SS DNA tails. Also, as noted earlier, the conservation of large pools of the heavy DNA species observed in PDI suggests very little nuclease activity. Finally, there is no evidence of degradation in any of the marker DNAs, but, as noted above, this

merely indicates the absence of nuclease activity from the deproteinization step onward.

An alternative explanation for the SS DNA fragments can be derived from the report of Yokoyama et al.(103) that the plus strands from RF II and replicative intermediates isolated from the late stage of infection are fragmented when sedimented in alkali. One might expect that if nicks do exist in the double stranded region of the tailed replicating species they might result in the liberation of SS DNA fragments as a consequence of branch migration of the displaced single strand tail during the manipulation of the DNA subsequent to lysis. In support of this model, Espejo has observed that under some conditions there seems to be a preference on the part of deproteinized replicative intermediates for the configuration in which the displaced 5' end of the molecule has branch migrated back to form a duplex with the minus strand (Espejo, R., personal communication). However, Espejo did not observe a concommitant release of SS DNA fragments, and Yokoyama et al. do not provide a good internal control for nuclease activity, so it is still most probable that the fragmentation observed in these experiments is nucleolytic in origin.

2. Heterogeneity of the DNA populations found in given regions- The structural diversity of replicating DNA isolated from within a narrow range of sedimentation velocities should be rather limited. That this is true for free DNA molecules, is evidenced by the discrete peak of RF II DNA in region D of the non-deproteinized gradients in Figure 1a,b and by the sedimentation of the marker DNAs in Figures 2-5. Likewise, DNA-containing particles should also have discrete sedimentation

velocities that reflect in part the size of the DNA moiety. For example, one might expect that a particle containing RF II DNA would, in general, have a noticeably different S value from similar particles containing replicative intermediates with various length tails. A comparison of the DNA isolated from regions B and C (Figure 3b, 4b) of the non-deproteinized gradient in Figure 1a indicates that there is a greater proportion of replicative intermediates with very long tails sedimenting in the 70S region as compared to region C. However, in both regions B and C these molecules represent only a part of the overall DNA distribution which includes the entire spectrum of replicating intermediates from RF II to molecules with properties expected of "rolling circles" with long SS DNA tails.

One explanation for the apparent insensitivity of the S value of these particles to the size of the DNA associated with them is that the newly displaced single strand tail from the replicative intermediate is hidden from the solution in such a way that it does not contribute to the viscosity of the particle. For example, the displaced plus strand may be replicated into the interior of a protovirion. In this case the viscosity of the system would be determined solely by the shape of the protovirion and the double stranded ring portion of the replicative intermediate associated with it.

Alternatively the structural heterogeneity observed in different regions of the gradient may have arisen from nuclease activity. If this is the case, the various replicative intermediates, either free or in conjunction with particles, must have sedimented to their respective positions in the non-deproteinized gradient as homogeneous populations

of molecules and the heterogeneity must have been introduced prior to deproteinization and resedimentation by a limited nucleolytic degradation of the DNA. As was noted earlier, other lines of evidence also suggest limited nucleolytic attack subsequent to the first sedimentation.

It is especially likely that nuclease is responsible for the presence of RF II molecules in region C of the gradient (Figure 1a,b). Many of the "tailed" molecules would be expected to sediment here in the free state. Free RF II, on the other hand, sediments with peak D. It has also been shown that there is very little protein actually complexed to the DNA in this region (see section IX). It is doubtful that the small amount of protein responsible for the antigenic properties of this DNA could account for this increase in the S value of the RF II. It is more likely that the RF II from region C has been produced by the degradation of the plus strand tails of the replicating intermediates.

As a consequence of the probable limited degradation of the replicating DNAs from these gradients (Figure 1a,b) it is not possible to know how homogeneous the DNA composition of the various particles is in vivo. For example, it is conceivable that the DNA moiety of the 70S particle may consist primarily of replicative intermediates approaching the end of a cycle of replication, and that the small amount of replicating DNA found at the 114S position represents an even later stage in that process. However the presence of nucleases prevents one from discriminating between this possibility and the model presented earlier in which relatively homogeneous sedimentation velocities are achieved for heterogenous replicative intermediates by sequestering the single

stranded portion of the molecule inside a particle.

3. Heavy DNA- Substantial proportions of the pulse label, as well as significant amounts of long term label from the faster sedimenting regions of the gradient in Figure 1a,b were found in a DNA species that bands at a density greater than that of RF I in the PDI equilibrium sedimentation system (Table 3). In regions A through C this material acquires a relatively constant proportion of both the five second and ninety second pulse label that enters RF II and replicating intermediate DNA forms. This suggests that this DNA species is a replicating intermediate rather than a replication product.

Recently, Espejo has shown that this molecule is composed of a twice unit length plus strand and a unit length minus strand circle (Espejo, R., personal communication). As such, it would appear to constitute the end product of one round of SS DNA replication. The disproportionate accumulation of pulse label into this species relative to other replicative intermediates suggests that the release and, possibly, the circularization of the new viral DNA may, like the initiation of a new round of synthesis (93), constitute a rate limiting step in the replication process. Presumably this molecule is constrained in some way to prevent the uptake of intercalating dye. The nature of this constraint is as yet unknown.

A "heavy DNA" has also been observed by Fukuda and Sinsheimer during the period of progeny RF synthesis (Fukuda, A., Sinsheimer, R.L., manuscript in preparation). It is also of interest that, either as a consequence of, or in spite of, nuclease activity, the PDI banding of the pulse label from both the B and C regions of the gradients in

Figure 1a,b reveal the existence of three discrete peaks of replicative intermediate type DNAs.

4. Marker DNAs- All of the recentrifugations presented here (Figures 2-5) were performed in the presence of internal markers. The RF II marker was formed by radioactive decay of ^{32}P labeled RF I DNA. As such, these molecules are expected to contain one or more single strand nicks but no gaps. It will be noted that the in vivo RF II form DNA cosediments with this marker but bands one or two fractions denser. This indicates that the in vivo RF II has more single strand character than the marker DNA. This could be a consequence of either a small gapped region, as observed by Johnson and Sinsheimer (105), or a short single strand tail.

The ^{32}P SS DNA marker was added to each sample prior to the deproteinization step as whole ^{32}P labeled phage. It is surprising, therefore, that without exception, the in vivo SS DNA bands slightly denser than the ^{32}P SS marker and sediments slightly slower (see especially Figure 1a,b,c,d). Presumably these DNAs have been extracted in identical fashion. The difference must, therefore, lie at some earlier step - the growth conditions or perhaps the lysis conditions.

5. Losses to phenol during deproteinization- The consistent loss of pulse labeled vs. long term labeled DNAs during phenol extraction in the absence of SDS and prior treatment with pronase as well as the greater recoveries of pulse labeled DNAs re-extracted a second time strongly suggest a unique association of the pulse labeled moieties with a phenol soluble substance. The high efficiency of extraction of the 1148 phage particle indicates that this association is not retained in

the virion and that the phenol solubility is not a property of SS DNA. The most likely candidate for the phenol soluble substance(s) is some protein(s) involved in the DNA replication or the assembly process. The preferential loss of pulse labeled DNAs has also been noted by others in other systems (231, 232) and in ϕX (71). The specific loss of many DNA species of interest during deproteinization may ultimately be responsible for many of the apparent discrepancies existing in the literature concerning ϕX replication and for the failure of earlier experimenters to observe some of the structures reported here. Unfortunately it is possible that some structures are still being selectively lost as total recoveries are still far from 100% (Table 2). On the brighter side, the selective loss of these structures also suggests a pathway for their selective purification.

II. The distribution of ϕX antigen-DNA complexes in non-deproteinized lysates obtained during the late stage of the infection

A. Results

B. Summary

C. Comments

1. The relationship of sedimentation behavior to the structure of the antigenic moiety
2. The identity of the molecular species bound by the radioimmunoassay
3. The ionic requirements of the radioimmunoassay

The preceding experiments established the existence of a small pulse labeled pool of replicative intermediate DNA forms (approximately 10% of the total pulse labeled RF DNAs; Table 4b) in the 70S and 114S regions of non-deproteinized sucrose gradients. From a comparison of Figure 1 with Figures 3 and 4 it is apparent that none of these DNAs can sediment this rapidly in the deproteinized state. These same experiments also revealed RF II form DNA sedimenting faster than expected for the free molecule. The sedimentation behavior of these various DNAs as well as their resistance to phenol extraction suggests that they are complexed with proteins. The following experiment (Figure 7, Tables 5-7) was performed in order to discover the existence of stable complexes between phage antigens and ϕX DNA and to explore their distribution in velocity gradients of non-deproteinized lysates. ϕX antigen-DNA complexes were detected by means of the radioimmunoassay

characterized in the Methods.

A. Results

E. coli H502 was infected, radioactively labeled, lysed, and centrifuged in the non-deproteinized state in a scaled up version of the experiment in Figure 1b to give the gradient presented in Figure 7. A comparison of Figure 7 with Figure 1b demonstrates the great reproducibility of these procedures. Subsequent to sedimentation each fraction in the gradient was assayed for the existence of ϕX specific DNA-protein complexes by means of the ϕX radioimmunoassay. In this application of the assay, the binding of labeled ϕX DNA to plastic scintillation vials coated with anti- ϕX antiserum was compared with the binding to control vials that had not been coated with antibody. Specific absorption of DNA label to serum coated vials but not control vials presumably must be mediated by antigenic ϕX proteins that are bound to the DNA, as deproteinized DNA does not bind to the vials (see Methods).

In this case, the assay was performed in duplicate (i.e., two serum vials and two control vials). The details are given in the legend to Figure 7. After determining the cpm absorbed to each vial, the net specific absorption was computed separately for each fraction and each isotope by subtracting the average cpm bound to the control vials from the average cpm bound to the serum coated vials prepared from each fraction. In a few instances one of the four assay vials was omitted from the calculation due to a spurious value. In these cases the plotted point has been indicated by an asterisk. The plot of the serum bound ^{14}C label has been displaced to the top of the graph

in order to minimize confusion.

Inspection of Figure 7 reveals three pulse labeled peaks of binding activity that correlate with whole phage, 70S particles, and the replicative intermediates of SS synthesis, respectively. The binding activity coincident with the phage peak and 70S peak is expected on the basis of the established structures of the DNA-protein complexes found at these positions. The serum binding of pulse labeled DNA from the peak of replicative intermediates indicates that ϕX antigenic proteins are also complexed with this DNA. On the other hand, RF II DNA apparently does not bind. The principal distinguishing feature between these two kinds of DNA is the displaced single strand tail associated with the replicative intermediates. It seems probable that the antigen is associated with this feature.

In the previous section it was demonstrated that much of the DNA that sediments in region C of the gradient resediments to the same position after deproteinization (compare Figures 1a,b and 4b,d). The notable exception is the substantial quantity of RF II that is found in this region. However, it is not clear whether this RF II fraction exists prior to sedimentation or is generated subsequently by adventitious nucleases associated with the sample (see earlier discussion). If this RF II fraction is not artifactual in origin, then it may be that it derives its increased sedimentation velocity from an association with phage antigens. Whether or not it is an artifact, the modest increase in S value observed for the RF II molecule found here as well as the limited effect of deproteinization on the S values of other DNA species from this region suggests that the antigenic moiety in these

complexes does not greatly alter the conformation of the DNA molecules with which it is associated.

The long term label also shows distinct peaks of labeling activity at the phage and 70S positions in the gradient. The significance of the ^{14}C binding observed at the lower S values is uncertain due to the scatter in the data and the low count rates involved. However there may be a peak at the leading edge of the replicating intermediates.

It will be noted that there is much more scatter in the data at the lower S values for both ^{14}C and ^{3}H data. It is suspected that this reflects a greater susceptibility on the part of these complexes to thermal and nucleolytic degradation and other forms of disruption due to a relatively less stable and more exposed configuration compared to the ϕX particle or 70S particle during the long incubation involved in the assay. Various forms of degradation may also account, at least in part, for the relatively low binding efficiency of pulse label cpm in this region (Table 5, line 4). By contrast, the relative binding efficiency of the ^{14}C label in this region is computed to be twice that of the ϕX peak. However it is not known whether or not this is significant in as much as the computation is based upon low count rate data.

Table 5 indicates that the net binding efficiency of all samples is low. Due to the triple equilibrium involved in the binding reaction, i.e., antibody to plastic, antigen to antibody, and DNA to antigen, with each step characterized by a finite association constant, one cannot expect binding efficiencies close to 100%. Low binding

efficiencies are also expected when the saturation point of the assay is exceeded. In as much as different regions of the gradient undoubtedly contain different concentrations of antigenic particles, this could also explain the observed difference in relative binding efficiencies.

Table 6 presents the antigen concentration per fraction expected in the various regions of the gradient calculated in various ways and, in the case of the replicative intermediate region of the gradient, on the basis of data not yet presented (see section IX of Results). In the Methods characterization of the radioimmunoassay it was shown that the system saturates at 2.5×10^9 antigenic particles/ml and that the maximum binding efficiency is reduced by one half at a concentration of 1.0×10^{10} particles/ml (Figure 3, RIA). From Table 6 it is apparent that the saturation point has been greatly exceeded in the 114S ($2\text{-}4 \times 10^{11}$ particles/ml) and 70S ($2\text{-}6 \times 10^{10}$ particles/ml) regions of the gradient, the 70S region less so than the 114S region, probably accounting for the greater relative binding efficiency of this material. The flattened shape of the 114S binding curve compared to the 114S sedimentation peak is also consistent with the estimated antigenic concentration for this peak.

Due to the uncertainity surrounding the antigenic structure of the various ϕX specific particles found in the region of the replicative intermediates, the estimates of the antigen concentration in this region vary considerably. In section VIII of the Results a ϕX particle containing gene F protein will be shown to cosediment with the replicative intermediates. Depending upon: 1. whether or not this particle is attached to the pulse labeled DNA (it probably is not under the con-

ditions of the radioimmunoassay), 2. how many particles this gene F protein represents if it is not attached, 3. how many antigenic binding sites exist per DNA molecule, and 4. the extent of any nuclease activity; the antigen concentration in this region of the gradient could be anywhere from 2×10^9 to 3×10^{10} particles/ml, the maximum and minimum values calculated. Both of these concentrations should, however, result in a higher binding efficiency than for phage. Apparently other factors are at play such as nuclease degradation as proposed earlier. In this case the total amount of antigen bound might be unaffected but the quantity of DNA associated with each unit of antigen would be reduced due to multiple cleavages of the DNA.

It is also probable that phage and 70S particles are bound to the vials via antigen-antibody complexes involving at least two different particle proteins, whereas the antigen associated with the replicative intermediates may only contain one ϕX protein. This is because both the spikes and capsids of ϕX particles harbor antigenic sites (Rohwer, R., in preparation). Presumably any anti-phage antibody can bind whole phage to the radioimmunoassay vials whereas only one of them may be able to bind the replicative intermediates resulting in a lower relative binding efficiency for those structures.

The RF II peak contains from 8×10^9 to 4.5×10^{10} single strand equivalents of incorporated ^{3}H thymidine, depending upon whether the specific activity of the thymidine label is calculated from the thymidine concentration alone or the sum of the thymidine and thymine concentrations. As discussed earlier, the former calculation is probably a better representation of the <u>in vivo</u> situation. However, in

either case one would expect a binding efficiency for RF II that was at least as great as that for ϕX if the RF II molecule was complexed with phage antigens. Both the low relative binding efficiency of this peak as well as the shape of the binding profile in Figure 7 argue strongly against the existence of an antigen complex with the RF II.

Differences in the net antigen concentration for different regions of the gradient can explain differences in the relative binding efficiencies observed for various species but they cannot explain differences in the binding efficiencies of pulse and long term labels from the same regions of the gradient (Table 5, line 3). These differences are especially unexpected in the 114S and 70S region of the gradient where the majority of each label is associated with the same particulate species. In as much as the discrepancy observed for both particles is identical (Table 5, line 5), these differences probably reflect a systematic error most likely in the determination of the counting efficiency for ^{3}H. The differences between the binding efficiencies of the pulse and long term label that are observed at the lower S values could reflect real differences in the molecular species involved; for example, less nuclease sensitivity or a greater antigen density for the long term labeled DNA. However, this remains uncertain due to the poor quality of the low count rate ^{14}C data.

The radioimmunoassays presented in Figure 7 were performed in TM buffer supplemented with t-RNA and calf thymus DNA to suppress nuclease activity during the long incubation at 37°C. Reference to the Methods indicates that this is not the usual buffer in which this assay is performed. However, a control experiment employing purified phage

and TM buffer indicates an increased binding efficiency and a reduction in the relative non-specific absorption for this system compared to the standard buffer (Table 7). TM buffer is not usually employed due to the problems associated with nuclease when Mg++ is present.

The experimental result presented in Figure 7 has been reproduced in several other buffer systems including TM buffer supplemented with 0.30 M or 1.0 M KCl, and a buffer composed of 0.05 M Tris, 0.003 M EDTA, 0.25 M NaCl, pH 8 (see reference 93, Figure 8). In each case except the last, where only the peak of replicative intermediates were assayed, three peaks of binding activity have been observed with the 70S peak showing the greatest relative binding efficiency. Apparently Mg++ is not required for the integrity of the antigen complex with the replicative intermediates of SS DNA synthesis. This complex also appears insensitive to KCl concentration.

B. Summary

The preceding experiment demonstrates the existence of stable complexes between ϕX antigens and nascent ϕX DNAs sedimenting at the position of the SS replicative intermediates (region C). Since the antiserum employed was prepared against highly purified phage particles and since SS DNA itself does not bind in the assay system, the antigens in question are presumably ϕX virional proteins. As was elaborated in the General Introduction there is a great body of circumstantial evidence predicting the existence of just such complexes.

C. Comments

1. The relationship of sedimentation behavior to the structure of the antigenic moiety- Unfortunately, the sedimentation velocities

of the DNA-protein complexes cannot reveal much about the masses of the protein components. This is because the sedimentation behaviors of the ϕX DNA forms are equally strong functions of their conformations as well as their masses. For example, two ϕX particles with the same molecular compositions, the phage and its thermal disruption product, sediment at 114S or ∿50S depending upon whether or not the SS DNA component is compacted inside the protein shell or is streaming out from it.

In the case of those ϕX DNA containing species that sediment faster than free ϕX DNA forms, regions A and B, the increased sedimentation velocity of the DNA can be due either to a significant increase in the masses of the complexes with which the DNA is associated or to the organization of the DNA into much more compact structures than those that characterize the unconstrained free molecules. Both of these effects contribute to the 114S sedimentation velocity of whole phage composed as it is of two particles with lesser S values, a 72S protein shell and a 16-23S SS DNA circle. An example of the compacting phenomena acting alone might be a protein that crosslinks distal parts of the DNA preparatory to packaging. It is conceivable that such a mechanism might require very little protein.

The problem of deducing antigenic structure from S value becomes even more hopeless in the case of complexes from region C. The sedimentation of these DNAs is not strongly affected by deproteinization with the exception of the liberation of some RF II DNA and SS DNA fragments. As a consequence not much can be said about the structure of the antigen itself. It could either be one or a few small proteins

carried to this position in the gradient by the DNA or it could be a larger protein particle with an intrinsic sedimentation velocity similar to that of the free DNA but attached at only a single or a few points so as not to affect the viscosity of the DNA.

The data seem less compatible with a model in which the DNA, or some portion of it, is homogeneously coated with some protein. For this to be true the protein would have to contribute to the viscosity of the system in proportion to its mass. (For example, the protein could be extended out into solution away from its point of attachment.) Regardless, this model is not favored for other reasons as such a generalized binding would not, as discussed in Appendix C, be expected to exhibit the high binding coefficient which is indicated by the survival of these particles in dilute solution.

Whatever the structure of the in vitro complexes, it is also important to remember that their relationships to their in vivo precursors are not known. In the General Introduction it was noted that there is reason to expect that several of the viral proteins required for SS DNA synthesis express themselves simultaneously in the form of a single particle. This is, therefore, the expectation for the in vivo composition of the ϕX DNA-protein complex. However the in vitro complexes observed here may only be stable degradation products of more complicated in vivo particles.

2. The identity of the molecular species bound by the radioimmunoassay- The radioimmunoassay indicated DNA-protein complexes in regions A, B and C of the gradient. In section I replicating DNA forms were shown to be present in all three of these regions. In region C

they accounted for all of the pulse label (assuming that the SS DNA fragments originate from the replicative intermediates). Thus it is certain that at least some of the SS replicative intermediates from this region are complexed with phage antigens. However, because of the low efficiency of the assay, it is not known whether or not all of the DNA from this region is uniformly associated with antigen or whether the RIA is only detecting the binding of a subpopulation that is complexed. For example, it could be that only those RF II DNAs that are liberated after deproteinization of this region are complexed with antigen.

It would also be of interest to know whether or not the replicative form DNAs observed in regions A and B are binding. As discussed earlier, these DNA forms must be associated with larger complexes, presumably ϕX proteins, in order to sediment with these velocities. However, again due to the low binding efficiency of the assay, it is not possible to say whether or not these complexes are binding, confirming the expectation of ϕX antigens, or whether the observed activity is merely the result of the selective binding of the subpopulation of pulse labeled 70S lysis artifact (region B) or of whole phage (region A).

3. The ionic requirements of the radioimmunoassay- The experiment presented here was conducted in the same Mg++ containing buffer, TM, employed in the investigation of non-deproteinized ϕX lysates presented in section I and the subsequent sections with the expectation that the binding efficiency might be enhanced or new complexes might be detected compared to those observed previously in other buffer

systems. Instead, the results of the assay are the same with or without Mg^{++} and from 0.05 M to 1.0 M KCl. This kind of stability is that expected for either a very complex particle such as a virion or a very strong and specific binding of a single protein (see Appendix C). These two possibilities cannot be distinguished by this experiment.

III. The distribution of ϕX174 proteins in lysates obtained during the late stage of the infection

In order to visualize the proteins responsible for the antigenic activity of the nascent DNA forms in region C (Figures 1 and 7) and for the rapid sedimentation of the replicative intermediates in the 70S and 114S region, the experimental procedure in Figures 1a,b and 7 was modified to include a protein label. Use was made of the parallel gradient technique described in the Methods in order to resolve the ϕX specific proteins in the infected culture.

At time zero a log phase culture of E. Coli H502 was divided into two equal portions and one portion was infected with ϕXam3. Thirty minutes later the uninfected culture was pulsed for six minutes with ^{3}H leucine. Fifty minutes after infection the infected culture was pulsed for six minutes with ^{14}C leucine and during the last ninety seconds with ^{3}H thymidine. The pulses were terminated and the cultures lysed as described for the previous experiments. Identical volumes of each lysate were applied to separate but identical 5-30% sucrose gradients and then centrifuged and fractionated as described for parallel gradients in the Methods.

In these experiments the nascent ϕX DNA forms are visualized directly as the ^{3}H label in the sedimentation pattern from the infected lysate. However, a comparison of the infected and uninfected lysates is required to resolve the ϕX specific proteins. The procedure developed by Mayol and Sinsheimer (8) for computing the ϕX specific increment of the total incorporation into infected cell protein was employed

for this purpose (see Methods). The ϕX specific increment of the ^{14}C leucine incorporation is referred to as the $\Delta^{14}C$.

The results of two experiments employing long and short centrifugations of lysates prepared in this way are presented in Figure 8a,b. The lysates in 8a and 8b were sedimented for 3.5 hours and 15 hours, respectively, at 27,000 rpm in an SW 27 rotor at 5°C. The 3.5 hour sedimentation resolves the faster sedimenting particles, i.e., phage and 70S particles, whereas the 15 hour sedimentation resolves a particle sedimenting just ahead of RF II and the three small ϕX specific particles described in the General Introduction. The phage position is indicated on the basis of infectivity measurements made in conjunction with another experiment. The RF II position is assigned by analogy with the experiments presented in Figures 1 and 7. The S values indicated in Figure 8b were calculated assuming that a linear relation exists between sedimentation position and $S_{20°,w}$ and that RF II has an $S_{20°,w}$ of 16 (154). These S values serve to correlate the peaks in this gradient with those observed by Tonegawa and Hayashi (65). The percentage distribution of the ϕX specific protein label and ^{3}H thymidine is given at the bottom of each figure.

In the subsequent sections the various protein labeled peaks revealed by this technique are analysed with respect to their protein composition as revealed by SDS acrylamide gel electrophoresis, their stability to resedimentation, and the likelihood of their association with ϕX DNA forms. Special emphasis has been placed upon the previously uncharacterized 111S peak and 70S peak and the partially characterized 20S peak.

IV. Characterization of the 114S and 111S peaks

A. Resedimentation experiments

1. Controlling the loss of the protein label

2. Decomposition products of the 111S particle

B. Protein composition of the 111S particle

C. Relationship of the ϕX RF form DNAs to the 111S proteins

D. Estimates of the stoichiometry of the 111S particle proteins

E. Summary

F. Comments

1. "Stickiness" of ϕX subunit structures

2. Resedimentation

3. Gene D protein

In Figure 8a the peak of 114S ^{3}H thymidine incorporation does not cosediment exactly with the peak of ^{14}C leucine. In another experiment (not shown) the infectivity peak was found to cosediment with the pulse labeled DNA peak rather than the pulse labeled protein peak. Assuming that ϕX has an S value of 114 and that the gradient is linear, then the ^{14}C labeled peak sediments at 111S. These differences between the two pulse labeled peaks suggest that the ^{14}C label may be associated with a non-phage particle. In an attempt to clarify the identities of these two peaks and to establish the Mg++ and ionic strength requirements of the new ^{14}C labeled peak, its stability was monitored by resedimentation in a variety of new ionic environments. As described in detail below, the first attempts at resedimentation were frustrated by the selective loss of a large proportion of the protein label but not

the DNA label in the resedimentation procedures. Once these losses had been controlled, resedimentations could be performed with good recoveries of both labels but no conditions could be found, including resedimentation in the TM buffer used in Figure 8a, that did not result in the extensive degradation of the 111S particle to various combinations of five smaller particles described below.

A. Resedimentation experiments

1. Controlling the loss of the protein label- The 114S and 111S protein peaks isolated from a gradient like that in Figure 8a were pooled and dialysed against various buffers and resedimented under a variety of ionic conditions. In every case, including that of the sample retained in TM buffer, the protein and DNA peaks resedimented coincidently (Figure 9a). However, the ratio of protein label to DNA label diminished seven fold indicating the specific loss of 85% of the protein relative to DNA. This loss was not accompanied by the appearance of any new compensating peaks in the resedimentation gradients. (The small peak at the top of the gradient in Figure 9a represents only a small fraction of the total ^{14}C lost during the resedimentation.)

If it is assumed that the protein/DNA ratio (0.064) observed after these resedimentations represents that of phage alone, and the coincidence of the protein and DNA peaks as well as corroborating experiments in Figure 9 and Table 9 suggest that this is the case, then approximately 85% of the protein sedimenting in the vicinity of the phage in Figure 8a is not phage protein. (For the details of this calculation see the legend to Table 9.) Furthermore, it is this non-phage protein, as opposed to ϕX particles, that is specifically lost in the

procedures used to prepare this material for resedimentation.

The pool of 114S and 111S material isolated from another experiment was employed to determine the source of these losses and to discover ways in which they could be prevented (Methods, Table 1; Table 8). It was found that, irrespective of the presence or absence of Mg++ or of the ionic strength, the protein moiety in this pool has a tendency to adhere to surfaces with which it is brought into contact. This effect is particularly strong in the presence of Mg++ and is more pronounced with plastic than with glass surfaces and can result in the quantitative loss of non-phage protein label from the sample. Several measures were subsequently employed to reduce these losses (see Methods). Dialysis was avoided whenever possible. Glass was used in preference to plastic and fractions were collected and stored in silane coated glass vials. The addition of BSA carrier to both the samples and the sedimentation buffers had the single greatest effect on the recoveries (Methods, Table 1). When all of these precautions were taken the recoveries from resedimentation improved for all labeled species (Table 8), but especially for proteins (four to seven fold).

2. Decomposition products of the 111S particle- A new set of resedimentation experiments were conducted employing these procedures to minimize losses. The results are presented in Figure 9b,c,d. A gradient like that in Figure 8a was prepared except that the sedimentation was through 3-18% instead of 5-30% sucrose. The fractions from the 114S to 111S region were pooled and then diluted 1:1 with TM buffer supplemented with 0.10% BSA in order to reduce the sucrose concentration to less than 10% without dialysis. Identical aliquots of

this mixture were brought to final concentrations of either 0.05, 0.30 or 1.00 M KCl. One sample at each KCl concentration was left at 0.008 M in Mg^{++} and another was titrated by the addition of EDTA to 0.013 M for a net free EDTA concentration of 0.005 M. One aliquot of the 1.00 M KCl-EDTA sample was made 0.5% in Sarkosyl. Each sample was sedimented at 41,000 rpm in an SW 41 rotor for 10.5 to 12.5 hours through a 10-30% sucrose gradient prepared in its homologous buffer supplemented with BSA to 0.01%. Under these conditions all species sedimenting faster than approximately 40S pelleted at the bottom. The gradients were collected and counted as described in the legend to Figure 9.

In every case, including the resedimentation in TM buffer, protein but not DNA was released from the fast sedimenting peaks to the top of the gradient in the form of three or more particles. In the most extreme case, sample 7, only 19% of the total input protein cpm sedimented faster than ∿40S. The ratio of protein cpm/DNA cpm in this fast sedimenting component was 0.068, the minimum observed under any of the resedimentation conditions employed and similar to the 0.064 ratio observed after the resedimentations in the absence of BSA carrier. If it is assumed that this is the ratio of protein cpm/DNA cpm in whole phage, then this phage ratio can be used in conjunction with the ratios observed in the pellet fractions of the other resedimentations to compute the percent of the total gradient 111S protein cpm (exclusive of whole phage) that sediments with the pellet. (For the details of this calculation see the legend to Table 9.) Even under the best conditions, samples 1-4, only 25% of the total 111S cpm sedimented with the pellet. Moreover, since everything with an S value greater than

~40 pellets it is not known whether this residual protein represents intact 111S particles or their breakdown products. In the case of the resedimentations performed in 0.05 M or 0.30 M KCl with or without Mg++ (samples 1-4 in Table 9 and Figure 9b) the resedimentation pattern is qualitatively the same as that observed in the slow sedimenting region of whole lysates (Figure 8b). A 2.5S, a 6.0S and a 9.0S peak are all present. (These S values are used only as indicators of the peak identities in relation to the introductory discussion and Figure 8b. The 12S, 9S, 6S and 2.5S positions are calculated from an internal RF II marker assuming linear gradients and are indicated by arrows.) A comparison of Figure 9b with Figure 8b shows that the 2.5S peak from the resedimentation is much reduced compared to that observed in the whole lysate. On the other hand, the ratio of the 9S and 6S peaks is identical in both the resedimentation and the whole lysate (Table 10). This suggests that these two peaks may originate during lysis as an artifact of the disruption of the more complex particle sedimenting at 111S. It is unlikely that the converse could be true, i.e., that the 111S particle is formed as a consequence of lysis in the presence of Mg++, as this would suppose a very homogeneous artifactual complex that was formed in the exact intracellular proportions of both particles.

When the salt concentration in the resedimentation is raised to 1.0 M KCl with or without Mg++ a new peak appears in the gradient at approximately 30S (Figure 9c). The distribution of cpm into the 9S, 6S and 2.5S peaks does not change under these conditions. However, the total amount of the ^{14}C leucine label in the pellet decreases as does the ratio of protein/DNA cpm in this peak (Table 9). In as much as

everything with an S value greater than approximately 40 is captured in a CsCl shelf at the bottom of these gradients it cannot be known whether the 30S peak is being released from the fast sedimenting complex (possibly residual 111S particles) in the high salt environment or whether the high salt environment merely reduces its sedimentation velocity such that it can be observed after these very long centrifugations.

Figure 9d, sample 7, shows a recentrifugation performed for a shorter period of time, 10.5 hours, in the presence of 1.0 M KCl and EDTA but with the addition of 0.5% Sarkosyl. This pattern is similar to that of the other high salt recentrifugations except that the 9S peak has completely disappeared and in its stead there is a 12S peak. The 30S peak is much better resolved after the shorter centrifugation.

As discussed in the introduction and as will be shown later in conjunction with the analysis of the peaks in Figure 8b, the 9S and 6S peaks are composed of F and G protein, respectively. Siden and Hayashi (61) have shown that these two proteins also comprise the 12S particle in the same ratio observed in whole phage. In other experiments (R. Rohwer, in preparation) the leucine distribution into the proteins of highly purified phage was investigated. The ratio of proteins G and F was found to be 0.35. If one assumes that the structure of the 12S particle observed here is the same as that characterized by Siden and that it is composed of the F protein formerly in the 9S peak in conjunction with G protein formerly associated with the 6S peak, one would expect a loss of 6.2% of the total leucine cpm in the gradient from the 6S peak. A 5.7% reduction is observed (Tables 9 and 10). However, only

60% of the combined losses from the 9S and 6S peaks can be accounted for by the new 12S peak. The rest appear to be sedimenting with the 2.5S peak.

The resedimentation experiment in Figure 9d suggests that the 12S particle, like the 6S and 9S particles, has an artifactual origin in the disruption of a more complex particle. It is curious, however, that the seemingly harsher Sarkosyl environment gives rise to a more complex particle than does the non-Sarkosyl condition.

It was noted earlier that the ratio of the protein and DNA labels in the pellet fraction of the Sarkosyl gradient (sample 7) is the minimum observed under any conditions suggesting that only phage particles remain in this fraction. Since this ratio is the same as that observed after resedimentation in the absence of BSA carrier, in which case only the phage peak was recovered, it implies that all of the non-phage particles observed in the resedimentations in the presence of BSA (Figures 9b,c,d) were quantitatively lost during the preparation and resedimentation of this same material in the absence of BSA (Figure 9a).

The disruption of the 111S particle to the smaller particles usually observed in lysates suggests that these smaller particles may not exist as such intracellularly. An artifactual origin for at least the 12S and 9S peaks is given further credibility by the experiments presented in Figure 11a,b. Uninfected and infected cultures of E. coli H502 were labeled as in Figure 8a,b, except that the ^{3}H thymidine pulse was omitted. The cells from both cultures were then combined before lysis. The combined cells were split into two equal portions and

lysed either by the method of Mayol and Sinsheimer (8) [which is virtually the same as that of Tonegawa and Hayashi (65)], or in the presence of Mg++ as described in the Methods. In this case the Mg++ lysis was modified further by performing the lysozyme incubation in the presence of 20% sucrose to stabilize the resulting spheroplasts. The cells were then gently opened by the addition of 0.5% Brij in the presence of Mg++. Both lysates were centrifuged for fourteen hours through 5-30% sucrose gradients at 40,000 rpm in an SW 40 rotor at 4°C. ϕX specific cpm were computed by the method of Mayol and Sinsheimer (8).

After lysis and sedimentation in TE buffer (Figure 11a), there are four clearly resolved ϕX specific peaks at 2.5S, 6.0S, 9.0S and "20S", respectively. There is also a suggestion of a peak at 12S. The S values indicated in the figures were calculated assuming linear gradients and a value of 6S for the peak so designated. [These S values are used only to assign peak identities by analogy with Tonogawa and Hayashi (65). In particular the "20S" peak of these authors has a much smaller S value in these gradients.] By comparison the culture lysed gently in the presence of Mg++ shows neither a 9S or a 12S peak (Figure 11b). There are proportionately more ϕX specific cpm in the 2.5S peak from this lysate. This could indicate that the proteins found in the 9S and 12S particles after lysis in Tris-EDTA sediment in a monomeric condition at 2.5S after lysis in Mg++. However, SDS acrylamide gel electrophoreses of the particles at 9S, 6S and 2.5S from the Tris-EDTA lysate confirm the expected F, G and D protein compositions, respectively, for each of these peaks (see below, Figure 15 and reference 65), whereas protein analysis of the 6S and 2.5S peaks from the Mg++ lysate

show principally G protein and D protein, respectively, with no indication of the F protein displaced from the 9S peak.

These experiments support the previous result, suggesting that the slowly sedimenting particles observed in infected cell lysates arise as a consequence of degradation during lysis of more complex, faster sedimenting particles such as the 111S particle in Figure 9a. It appears that the gentler the lysis conditions, the fewer simple particles are observed.

On the other hand it should also be noted that, contrary to the expected result if all 6S and 9S particles are derived simultaneously from the decomposition of 111S particles, the gradient in Figure 11b contains a peak of uncomplexed 6S particles without a corresponding peak of F protein. There must, therefore, either be an excess of G protein in these gradients, or the composition of the fast sedimenting component containing the F protein must be different from that observed in Figure 8a. The fact that the 111S particle can be disrupted to either 6S and 9S particles or 6S and 12S particles suggests that there may be as yet unobserved intermediates in its decomposition.

B. Protein composition of the 111S particle

The appearance of a 2.5S peak as a disruption product of the 111S particle upon its resedimentation (above) suggests by analogy with the 2.5S particle from whole lysates (see General Introduction) that the 111S particle may contain gene D protein. This expectation is confirmed by SDS acrylamide gel electrophoresis of the 111S material. The pooled fractions from the 114S to 111S region of a gradient like that in Figure 8a have been electrophoresed in Figure 12. The 114S to

70S region (Fraction A) of the gradient in 8b has been pooled and electrophoresed in Figure 13. Both gels show a prominent peak, 37% and 26% of the total cpm, respectively, of leucine labeled gene D product. Since the phage particle, itself, does not contain more than 0.1% D protein (Rohwer, R., in preparation), the D protein that is observed here is presumably associated with the 111S particle. Upon dissociation of the 111S particle during resedimentation it is liberated to the 2.5S peak at the top of the gradient.

C. Relationship of the ϕX RF form DNAs to the 111S proteins

In none of the resedimentations in Figure 9 is there any evidence of release of ^{3}H thymidine cpm from the 114S peak. One would not expect any of the resedimentation procedures used here to damage phage particles and the persistence of the ^{3}H thymidine label at the 114S sedimentation position under all conditions used (see Figure 9a) confirms this expectation. Apparently the disruption products observed after resedimentation (Figure 9b,c,d) do not originate from phage.

The experiment in Figure 2c,d demonstrates that approximately 10% of a ninety second pulse conducted under these conditions is incorporated into various RF form DNAs in the 114S region. These DNAs are not observed either, but due to the low ^{3}H count rates employed in the resedimentation experiments and the heterogeneity of the S values expected for these DNAs, their presence may be below the limits of resolution of these gradients. This fast sedimenting DNA is presumed to be associated with ϕX proteins. On the other hand, it is not known how much of the 111S protein is associated with this DNA. A comparison of the DNA/protein ratios in the 114S phage peak and 111S peak indicates

that it is unlikely that very much of the protein is associated with the RF form DNAs. In the case of the phage peak, ≥90% of the pulse labeled DNA (Figure 2c) is complexed with 15% of the pulse labeled protein (see earler discussion and legend to Table 9). Unless the remaining ≤10% of pulse labeled DNA is complexed with the remaining 85% of the ϕX protein in proportions of fifty times more protein per unit of DNA than observed in phage, some of the 111S protein must be free of DNA. This would suggest that both DNA and non-DNA containing particles sediment at 111S. If the 111S DNA forms are associated with ≤ a phage equivalent of protein per phage equivalent of DNA, then this protein would contribute only minimally to the disruption patterns observed upon resedimentation assuming that these complexes are disrupted at all. On the other hand if only one kind of disruption product was associated with the DNA complex it might account for 100% of that particular peak upon resedimentation.

D. Estimates of the stoichiometry of the 111S particle proteins

Crude estimates of the stoichiometry of the 111S particle proteins can be obtained by the various methods given below. For the purposes of the calculations it is assumed that the leucine label is distributed uniformly among the particle proteins. The evidence suggesting that this is roughly true in terms of the mass fraction of leucine incorporated into various ϕX proteins is presented in Appendix B along with a discussion of the effect on these calculations of any nonuniformity in the labeling of the precursor particle pools. It is concluded there that, at best, only order of magnitude type estimates are possible but that the ratio of gene D to F and G proteins that is obtained

is most likely a minimum value.

With the reservations enumerated in Appendix B in mind, two approaches can be utilized to estimate the protein composition of the 111S particle. First the stoichiometry can be calculated from the known compositions and proportions of the disruption products observed after resedimentation. When this is done (Table 11) using the average data for samples 1 through 4 in Table 9 and assuming that the 9S, 6S nd 2.5S peaks are composed of only F, G and D proteins, respectively, one obtains an F, G and D stoichiometry of 1 : 4 : 1.4.

Alternatively, one can calculate the molar ratios of these proteins from the SDS acrylamide gel data for the 111S particle. From the change in the protein/DNA ratio observed before and after resedimentation of the 111S peak in the absence of BSA carrier (see earlier discussion) or in the presence of high salt and Sarkosyl (Table 9) one can calculate that the phage contributes 10 - 18% of the leucine label to these gels. Then, knowing the distribution of leucine in purified phage, one can subtract the phage contribution from each peak and compute the molecular composition of the non-phage material from the difference pattern. When this was done for two separate gels, F:G:D ratios of 1.0 : 2.9 : 10.0 and 1.0 : 1.1 : 3.7 were obtained. These ratios would not change greatly even if the fast sedimenting material was composed entirely of the non-phage particle.

Taking into account the limitations of both the gel data and the resedimentation data, one can, nevertheless, obtain a rough idea of the composition of the non-phage peak at 111S. By comparison with the ratios calculated here for the 111S peak, the F:G:D stoichiometry

obtained for highly purified phage continuously labeled with leucine is 1.0 : 0.85 : 0.005 (Table 11; Rohwer, R., in preparation). (This is equivalent to 0.5 D proteins per virion.) It is unlikely that any nonuniformity of the precursor pools could account for the two orders of magnitude difference observed between the phage and 111S values for the D protein concentration, especially when the expected nonuniformities would tend to give a minimum value for the gene D concentration (see Appendix B). Weisbeek and Sinsheimer (165) using similar nonequilibrium data have reported an F:D stoichiometry for the infectious 140S particle of 1 : 1.3.

Irrespective of the accuracy of the calculations of the 111S stoichiometry, the values obtained from the resedimentation data and the electrophoretic data should be the same. Instead the D:F ratio calculated from the resedimentation is four to ten times less than that obtained from the electrophoreses. This suggests that significant quantities of D protein are still being lost during the resedimentation or else remain with the pellet fraction.

E. Summary

The experiments presented in this section demonstrate the existence of a subviral ϕX particle with a sedimentation velocity of approximately 111S that is composed principally of ϕX proteins F, G and D. Its relationship to the small amount of pulse labeled DNA sedimenting in the same region is uncertain. For unknown reasons, the particle is unstable to resedimentation even in the same buffer in which it was isolated. Depending upon the ionic composition of the resedimentation buffer it decomposes to 9S, 6S and 2.5S particles or 12S, 6S and 2.5S

particles. In addition, a decomposition product of approximately 30S is also observed after resedimentations in high salt.

The decomposition of the 111S particle to 12S, 9S, 6S and 2.5S particles suggests that these particles, when observed in whole lysates (Figure 8b), may arise artifactually from the 111S component. This contention is supported by the observation that two of these particles, 9S and 12S, are missing completely from infected lysates prepared by a very gentle procedure.

F. Comments

1. "Stickiness" of ϕX subunit structures- The proteins in the 111S particle are remarkably "sticky". In the absence of BSA carrier they are quantitatively lost presumably by absorption to solid substrates. Since the 111S particle decomposes so readily to 9S, 6S and 2.5S particles it is presumed that all of these subunits must bind separately. The 9S and 6S particles are structural subunits of completed phage and yet this "stickiness" property is not shared by the completed ϕX particle. Apparently the organization of these subunit structures into virions sequesters the "sticky" sites at internal loci where they do not react with surfaces.

In the case of the whole lysate sedimentation (Figure 8a) the 111S particle was observed without the addition of BSA carrier to the gradient. This may indicate that, like phage, the "sticky" sites on the 111S subunit structures are internally located in the intact particle or alternatively that the crude lysate contains sufficient soluble protein to serve as carrier. This is apparently the case in the upper region of the gradient in Figure 8b which contains 9S, 6S and

2.5S particles. Even though the total recoveries of protein label from the whole lysate sedimentations in Figure 8a,b are high, it is not possible (due to their selective stickiness) to know the recoveries of the ϕX subunit proteins in the same gradients. As a consequence the particle distributions observed may still in fact be distorted from those that actually exist in vivo. It is also conceivable that some particles may still be quantitatively lost by this mechanism.

2. Resedimentation- Numerous attempts were made to resediment the 111S particle in the buffer in which it was isolated but without success. The reason for its decomposition remains unknown. However, all procedures utilized required either dialysis or dilution before resedimentation suggesting osmotic sensitivity as a possible source of its instability.

3. Gene D protein- As was discussed at length in the General Introduction, gene D protein is absolutely required for SS DNA synthesis. Indirect evidence suggests that its function involves some interaction with gene F protein. The fact that F and G proteins are also required for SS DNA synthesis suggests that all three of these proteins may act together as a single particle. The 111S particle observed here contains all three proteins and consequently suggests itself as the required precursor to SS DNA synthesis.

V. The protein composition of the 70S particle and peak B in Figure 8b

A. Results

B. Summary and Comments

A. Results

The 70S region of a non-deproteinized velocity gradient of ϕX infected cells contains the 70S lysis artifact with a full complement of the ϕX virional proteins (R. Rohwer, unpublished) as well as some sort of ϕX SS-DNA replication complex (section I). An SDS acrylamide gel of the 70S particles from a gradient like that in Figure 8a yielded a pattern that was qualitatively the same as that in Figure 12 but with a smaller proportion of gene D product (Table 11, part E). The 70S lysis artifact must contribute at least some and conceivably all of the virional proteins observed in the gel pattern. Because of the contaminating presence of the lysis artifact it cannot be known whether or not virional proteins are also associated with the ϕX RF form DNAs. Attempts to separate these two species intact have not yet succeeded. On the other hand the gene D protein observed here can reasonably be expected to be associated with the RF DNA complexes.

In Figure 8b a small peak, B, of ϕX specific protein is observed sedimenting at a position intermediate between that of the pelleted ϕX and 70S peak and the 20S particle. This material was pooled and electrophoresed with the result presented in Figure 14. The pattern is very similar to that observed in the 111S gels and the 70S

gels except that there is a greater proportion of D protein and no gene B product in evidence. This peak by virtue of its sedimentation position cannot be contaminated by either the 70S lysis artifact or whole phage. The molecular ratios of the F, G and D components computed directly from the gel and normalized to F are 1.0 : 3.0 : 7.9 (Table 11). The sedimentation position of this particle is reminiscent of the 30S particle observed after resedimentation of the 111S particle in high salt-EDTA buffer.

B. Summary and Comments

Subviral particles containing F, G and D proteins have now been observed at S values of 111S, 70S and 30S. Varying amounts of ϕX RF form DNA have also been observed at these same loci. It appears that the ratio of particle protein to RF form DNA increases as the S values of the particles increases. This observation suggests that the ϕX RF DNA may be serving as a nucleus for the condensation of ϕX proteins into ϕX particles. As more protein is associated the complex sediments ever faster and the protein/DNA ratio increases.

However, the observation (section IV) that a substantial portion of the 111S particles do not seem to be associated with DNA is not compatible with this model. Conceivably the 111S particles could have dissociated during centrifugation from the DNA substrates upon which they were condensed. But even this mechanism could, at best, account for only a fraction of the 111S particles, in as much as the discussion in section IX indicates that the pool size of the 111S particles greatly exceeds that of replicating RF form DNAs. If this is true, it indicates that the 111S particle must form independently of SS DNA synthesis.

As such it may serve as the F, G, D precursor that is required for SS DNA synthesis. This in turn suggests that the fast sedimenting RF DNAs may all be associated with the same 111S precursor particle. This would account for the similarities in the protein compositions observed for the 70S and fraction B material to that of the 111S particle. The different S values observed for the various fast sedimenting RF containing particles could be due either to mass differences in the RF DNA forms at different stages of replication or to different conformational possibilities for the exposed DNA or both.

If in fact the 111S particle is required for SS synthesis then all in vivo replicating RF may be associated with this particle and those free sedimenting molecules observed after lysis may be the result of an artifactual dissociation. The presence of discrete particle peaks in the velocity sedimentation patterns indicates that this dissociation, if it occurs, does not take place to any great extent during centrifugation.

VI. Characterization of the 9S, 6S and 2.5S peaks

In Figure 8b the 9S, 6S and 2.5S ϕX specific protein peaks have been resolved from a crude lysate by means of the parallel sedimentation of infected and uninfected lysates as described in the Methods. A comparison of Figure 8b with Figure 11 demonstrates the ability of this method to detect ϕX specific components as sensitively as when two lysates are mixed before sedimentation. The ϕX specific proteins in the various peaks in this gradient were identified by pooling the peak fractions from both the infected and uninfected gradients and then subjecting this material to SDS acrylamide gel electrophoresis. The ϕX specific proteins were then resolved from the host incorporation by means of the $\Delta^{14}C$ calculation described in the Methods. This was done for peaks A through F pooled as indicated at the bottom of Figure 8b. For those samples containing ^{3}H labeled ϕX DNA a control gel was run on the infected material only. In every case approximately 50% of the ^{3}H thymidine label did not enter the gel and 90% of the remainder was found in the top ten fractions.

For the best resolution of the entire ϕX protein spectrum, 15% gels were utilized (samples A, B, D, E and F). Twelve percent gels were used for better resolution of the high molecular weight proteins (sample C). Twelve percent gels have the disadvantage that they tend to run the low molecular weight proteins together. The peak assignments were made on the basis of characterizations of the ϕX particle and lysates from mutant infections that have been performed by others (see General Introduction, Table I). Uncertain assignments are indicated by

question marks.

The gels from regions A and B, Figures 13 and 14, respectively, have already been discussed in the previous section. The material in the 20S peak at C will be characterized in a subsequent section. The gels from regions D, E and F are presented in Figure 15. In general, the latter three gels corroborate the findings of Tonegawa and Hayashi (65) for the UV irradiated host cell system, with the majority of the cpm in the 9S, 6S and 2.5S peaks found in the F, G and D proteins, respectively. The G protein found with the 9S peak is probably due to overlap from the 6S peak. Unlike the UV irradiated system and in agreement with Mayol and Sinsheimer (unpublished), the 2.5S peak from unirradiated cells contains only small quantities of the other monomeric proteins besides D and J(?). Other proteins are present, however, indicating that this is a quantitative rather than a qualitative difference between the two systems. It may be that a large proportion of the aberrant infections associated with the UV system do not proceed far enough to permit the monomeric proteins found at 2.5S from functioning as part of the faster sedimenting complexes with which they would normally be associated.

Minor components are also observed in conjunction with the 6S and 9S particles. A significant proportion of a high molecular weight protein with a mobility suggestive of A' protein is found with the 9S particle. Gene B protein is found in mass proportions of 1B : 3G in the 6S peak. It cannot be known from these experiments alone whether or not these minor components contribute structurally to the G and F pentamers which constitute the 6S and 9S particles, respectively.

However, Tonegawa and Hayashi (65) showed that ϕX mutations in genes other than F or G, including B, do not affect the integrity of these particles suggesting no other proteins are involved either structurally or in the formation of either pentamer. Nevertheless, it is noteworthy that the gene B protein, postulated by Siden and Hayashi (61) to play a role in the formation of 12S particles from 6S and 9S precursors, is found in the same mass proportion to G protein in both the 6S peak and in conjunction with the G contamination of the 9S peak. One would expect these proportions to change in the event that B and G were associated with different particles. The molecular proportion of these two proteins, 2.5 to 2.9 G per B, calculated assuming uniform incorporation of leucine label into each and with the limitations in interpretation outlined in Appendix B, is not, on the basis of the known symmetry of the ϕX particle, suggestive of a subunit structure.

VII. Resedimentation of debris

A. Results

B. Summary

C. Comments

A. Results

In all of the experiments discussed so far, the cell debris has been pelleted and discarded after a low speed centrifugation subsequent to lysis, and yet a substantial proportion of the infected ^{14}C leucine label is retained by the debris. The experiment in Figure 10, Table 12, was conducted to determine the nature of the ϕX specific material retained with the debris. This experiment also gives a further indication of the separate identities of the 114S and 111S peaks.

Infected and uninfected cell lysates were prepared as in Figure 8a and the distribution of the total TCA precipitable incorporation between the lysate supernatant and resuspended debris was determined (Table 12). Only 5% of the uninfected ^{3}H leucine remained with the debris whereas 22% of the infected ^{14}C leucine and 9% of the ^{3}H thymidine partitioned there. The difference between the infected and uninfected leucine distribution suggested ϕX specific incorporation into this component.

To investigate this possibility the debris was fractionated by sedimentation through several different buffer systems. Equal aliquots of the resuspended debris (in TM buffer) from the infected and uninfected lysates were brought to the following concentrations of KCl,

Mg^{++}, EDTA and Sarkosyl:

(a) Sample was retained in TM buffer

(b) Sample was brought to 0.30 M KCl, 0.005 M EDTA (net)

(c) Sample was brought to 1.0 M KCl, 0.005 M EDTA, 0.5% Sarkosyl

Infected and uninfected samples with each of these compositions were then sedimented through parallel 5-30% linear sucrose gradients prepared in the same buffers over a dense layer of CsCl to retain any material that resedimented as debris. The ϕX specific fraction of the ^{14}C leucine label was computed from a comparison of the infected and uninfected leucine labels as in Figure 8.

The resedimentation in TM buffer reproduced the pattern observed for sedimentation of the lysate supernatant fraction. (Compare Figure 10a with Figure 8a. The sedimentations in Figure 10 are not long enough to resolve the 9S, 6S and 2.5S peaks.) Twenty-five percent of the uninfected leucine label was released to the top of the gradient whereas 40 to 60 percent of the infected labels were released from the debris (Table 12). Presumably the material which is released merely by resedimentation through the same buffer in which lysis took place was associated with the debris in some artifactual way.

Resedimentation under the conditions in (b) and (c) above released increasing proportions of all labels from the debris fraction. In all cases the thymidine pattern was the same as that characterized in Figure 1, indicating that there was no preferential trapping of any one molecular species. The patterns observed for the resedimented ϕX specific leucine label become more heterogeneous with the harsher conditions. In 0.30 M KCl-EDTA the 111S peak appears to have separated

into two components. In 1.0 M KCl-EDTA with 0.5% Sarkosyl the 111S peak has been replaced by a peak at approximately 100S and there is much more infected cell protein label throughout the gradient. The relationship, if any, between the 111S particle and 100S peak cannot be deduced from this experiment. It should be remembered however that the 111S particle is not stable to resedimentation in this buffer.

Very little of the uninfected protein label sediments at the intermediate velocities between the debris fraction and the top of the gradient whereas a substantial proportion of the infected label is found there. Virtually all of the uninfected protein is released from the debris by the addition of Sarkosyl suggesting that these are membrane bound proteins.

In other experiments proteins in the debris fraction have been examined by SDS acrylamide gel electrophoresis without any detectable differences from the patterns observed for whole lysates. This is probably a consequence of the large proportion of artifactually trapped ϕX material in this fraction which may obscure any specifically membrane associated protein such as the A' protein observed by Van der Mei, et al. (51).

B. Summary

Resedimentation of the cell debris fraction of ϕX infected cell lysates indicates that the association of ϕX specific cpm with the debris is the result of artifactual, nonspecific trapping of ϕX DNA and proteins.

C. Comments

Figures 10b and 10c suggest that the 111S particle is converted

to another slower sedimenting particle or conformation in high ionic strength gradients containing EDTA. It appears that although the use of TM buffer is required for the isolation from whole lysates of a homogeneous 111S peak in high yield (Figure 10a), the particle or what appears to be its ∿100S derivative, is far more stable in high ionic strength-EDTA buffers than might have been expected from the resedimentation experiments in Figure 9. Apparently its stability in any of these buffers including the high ionic strength-EDTA ones, is dependent upon the presence of the rest of the cell lysate. This suggests that there may be some cytoplasmic factor that is necessary for 111S stability which becomes separated from the particle during the first sedimentation.

A comparison of the infected and uninfected cell proteins released upon resedimentation of the debris reveals that the ϕX proteins, unlike the host proteins, resediment largely as particles between the positions of the membrane and the monomer or small multimer peak. The particulate nature of the ϕX proteins may in some way be responsible for the preferential trapping of ϕX versus host proteins in the debris fraction (Table 12). Perhaps many of these proteins were associated with the ϕX DNA forms prior to resedimentation and were trapped by virtue of this association.

VIII. Characterization of the 20S peak

A. The 20S peak from uninfected cells

B. Protein composition of the 20S peak

C. The particles composing the 20S peak

D. Infection specific stimulation of 20S host protein synthesis

E. Resedimentation experiments

1. The effect of the ionic environment and temperature

2. The effect of nucleases

3. The composition of the protein dissociation products from the 20S resedimentations

4. Comments

i. The relationship of the 20S DNA to the 20S proteins

ii. The interrelationships of the 20S proteins

F. The relationship of the 20S U_3^{20} protein to the ϕX induced proteins and gene A' product

1. The four high molecular weight infection specific proteins

2. Assignment of the U_3^{20} protein to an infection specific peak in whole lysates

3. Assignment of the A' protein to an infection specific peak in whole lysates

i. The UV labeling conditions

ii. Characterization of the gene A mutant infection in UV irradiated cells

iii. Assignment of the A' protein

4. The non-identity of the (U_3,I_3,U_3^{20}) peak and the A' protein

5. The molecular weights of the infection specific high molecular weight proteins

G. Summary of the 20S results

Eight percent of the ϕX specific leucine in the infected gradient in Figure 8b sediments as a sharp symmetrical peak at 18 to 19S. Presumably this is the same particle that was reported to sediment at 20S by Tonegawa and Hayashi (65) and Mayol and Sinsheimer (unpublished). Later experiments (Table 15) indicate an S value of 18-20S depending upon the experimental conditions. To avoid confusion this peak will continue to be referred to as the 20S particle here.

In the experiments that follow, the 20S peak is characterized with respect to its protein composition, its stability to resedimentation, its relationship to the ϕX RF form DNAs that cosediment with it and the ϕX antigens associated with this DNA, and its relationship to a host particle that cosediments with it from uninfected cells. It will be shown that the major mass constituent of the 20S peaks isolated from either infected or uninfected cells is a high molecular weight host protein. This protein has an electrophoretic mobility similar to, but distinct from that of, the ϕX A' protein, and its synthesis is stimulated two to ten fold by the infection. Its relationship to the other infection specific proteins found to sediment at 20S (of which gene F protein is the major constituent) is ambiguous with some data suggesting a single complex of host and ϕX proteins while other data suggests separate particles fortuitously associated by S value alone.

In the ensuing discussions it will be necessary to discuss the

SDS acrylamide gel electrophoresis patterns from four different sources of proteins. The following nomenclature will be used to designate specific protein peaks in the electrophoretic patterns. Each source will be identified by a letter as follows:

U = Whole lysate of Uninfected cells

I = Whole lysate of Infected cells, infection specific proteins

U^{20} = 20S particle from Uninfected cells

I^{20} = 20S particle from Infected cells, infection specific proteins

Individual protein peaks will be designated by a subscripted integer, with increasing numbers corresponding to peaks of increasing mobilities in the gel. The only exception will be those peaks in the infected samples which have been assigned to ϕX gene products. They will be labeled by their gene designations A - H and J.

In later experiments the relationships of the proteins from different sources will be established by coelectrophoresis. Once two proteins have been shown to comigrate they will be considered identical and the protein peak in question will be referred to by both of its labels, for example (U_3, I_3).

A. The 20S peak from uninfected cells

Sedimenting just behind the 20S peak from the infected lysate in Figure 8b is a peak of ^3H leucine labeled host protein from the parallel uninfected gradient. Contrasting with this result, Mayol and Sinsheimer (unpublished) observed that the 20S particle from infected cells cosediments with a host particle in mixed lysates. Since the lysates in Figure 8b were not mixed before sedimentation, the 1.5 fraction separation observed between the infected and uninfected peaks may be an

artifact of the parallel gradient technique. The experiments in Figure 11a,b indicate that this is probably the case, in as much as the host and infected particles in these gradients of mixed infected and uninfected lysates cosediment even after a much longer centrifugation than that employed in Figure 8b or by Mayol and Sinsheimer. A lack of coincidence of the infected and uninfected gradients in Figure 8b would not have a great effect upon the ^{14}C discrimination of this particle as there is only a small contribution of host cpm regardless of how one aligns these two peaks (see below).

B. Protein composition of the 20S peaks

Because of the likelihood that the uninfected and infected particles cosediment when mixed, the peak fractions from each particle separately (fraction C, Figure 8b) were pooled for SDS acrylamide gel analysis of their respective protein compositions. Aliquots from each pool, infected and uninfected, were then dialysed, mixed, concentrated, and electrophoresed in the same manner as before (section VI). Twelve percent acrylamide gels were used in order to enhance the resolution of the higher molecular weight components. The results are presented in Figure 16a,b,c.

In Figure 16a infected and uninfected aliquots of fraction C were mixed before electrophoresis. Figure 16b presents the results of an electrophoresis of the infected material alone, demonstrating that the ^{3}H cpm at the top of the gel in Figure 16a are due to ^{3}H thymidine DNA in the infected fraction rather than undissociated proteins from the uninfected aliquot. This is verified by an electrophoresis of the uninfected particle in Figure 16c. Figure 16c contains an internal

marker of ^{14}C labeled RNA polymerase core enzyme. (RNA polymerase was prepared in collaboration with Lloyd Smith.) Other experiments show that RNA polymerase sigma component has a mobility approximately that of host peak U_2^{20}. It can be seen that the major host peak, U_3^{20}, is not an RNA polymerase component.

A comparison of Figures 16a, 16b and 16c reveals that these gels are sufficiently reproducible and well resolved to permit an unambiguous identification of many of the minor components from experiment to experiment. In order to facilitate discussion, the peaks from the uninfected sample have been numbered U_1^{20} through U_8^{20}. Figure 16a shows that the major mass constituent of both the infected and uninfected particle is host protein U_3^{20}. The infected peak moving just ahead of U_3^{20} has the electrophoretic mobility of ϕX F protein and can be seen to coelectrophorese with F protein in Figure 26a,b (see discussion below). The infected peaks, labeled I_1^{20} through I_6^{20}, electrophorese between the positions of F protein and that expected for G protein (G protein electrophoreses between I_6^{20} and I_7^{20}). From Figure 16a it can be seen that I_1^{20} through I_4^{20} have unique mobilities compared to the uninfected pattern and hence must be infection specific proteins. As yet, no attempt has been made to correlate them with ϕX coded proteins. The peak at I_7^{20} electrophoreses slower than the uninfected peak at this position. Other experiments show that it has approximately the same mobility as gene D protein. It cannot as yet be definitely assigned to this protein, however. A comparison of the uninfected with the infected cell patterns either in Figure 16a before the $\Delta^{14}C$ calculation (not shown) or in Figures 16b,c indicates that the infected cell particle is

strongly dominated by the infection specific components as the pattern of minor components from the uninfected cell is barely evident.

C. The particles composing the 20S peak

None of the proteins observed in these gels has a molecular weight sufficient to sediment with the 20S peak as a monomer. Assuming a globular conformation for the 20S particle and utilizing the assumptions and methods of Martin and Ames (182) one can calculate that approximately 6×10^5 daltons of protein would be required to attain this sedimentation velocity. The molecular weight of the host protein U_3^{20} can be estimated as 67,000 daltons from its relative mobility in SDS acrylamide gels compared to ϕX proteins with known molecular weights (Figure 30). The molecular weight of gene F protein is 50,000 daltons (Table 1, General Introduction). Thus, pure F protein or U_3 protein would have to be organized into multimers of at least 12 and 9 subunits, respectively, to acquire this S value.

A quantitative comparison of the infected and uninfected particles is given in Table 13. The data are compiled as averages from three separate gels of each type, infected and uninfected. The differences in the relative proportions of the various components of the 20S peak from infected and uninfected cells suggests that there must be several different particles comprising this peak. At the very minimum there must be at least one host particle composed of the 20S proteins from uninfected cells, and one infection specific particle composed of the 20S infection specific proteins either in combination with each other or with the host proteins. In addition the dramatic change (a four to six fold increase) in the proportion of U_3^{20} protein

relative to the other labeled host proteins in the infected compared to the uninfected peak is consistent with there being either more than one host particle (for example one composed of a U_3^{20} multimer and one composed of the other 20S host proteins) or more than one particle containing U_3^{20} protein (for example an uninfected particle and an infected particle). Unfortunately due to the vagaries inherent in the amino acid pulse labeling data (see Appendix B) these various possibilities cannot be resolved.

Mayol and Sinsheimer (unpublished) did not observe gene F protein in conjunction with the 20S particle from infected cells. The lysate in Figure 11a was prepared and sedimented according to their procedure (0.05 M Tris-HCl, 0.0125 M EDTA). SDS acrylamide gel electrophoresis of the peak fraction of the 20S particle from this gradient revealed only 5% F protein (compared to 19% F protein in the analogous particle from Figure 11b) and a ratio of U_3^{20} to F protein of 13 : 1 as opposed to 4.5 : 1 observed in the infected lysate of Figure 8b and 2.5 : 1 in Figure 11b. Apparently the F protein composition of the particle under these conditions was below the resolution of the gel system used in Mayol and Sinsheimer's experiment. The variability of these ratios suggests that the U_3^{20} and F proteins belong to separate particles.

In summary, a comparison of the proteins comprising the infected and uninfected 20S peaks suggests that the peaks are composed of three or more independent particles fortuitously associated by reason of having very similar S values.

D. Infection specific stimulation of 20S host protein synthesis

The delineation of the 20S peak in the $\Delta^{14}C$ calculations in Figure 8b and 11a,b establishes its identity as an infection specific moeity regardless of whether or not it also exists in uninfected cells. The infection specific increase in incorporation into this peak relative to the host peak sedimenting behind it in Figure 8b or cosedimenting with it in Figure 11a,b can be calculated by analogy with the $\Delta^{14}C$ calculation (see legend to Table 14) and is tabulated in Table 14. In every case there is at least a two fold stimulation of incorporation into the infected cell 20S peak relative to the uninfected peak. Gene F protein and the other infection specific proteins can account for only a small fraction of this increase as they comprise less than 50% of the labeled mass of the infected peak. To account for the rest of the infection specific increase, the major mass constituent of the 20S peak, host U_3^{20} protein, must also be stimulated by the infection either with regard to its synthesis or its organization into 20S particles.

The extent of this stimulation of U_3^{20} protein is computed in several different ways in Table 14. In part A the overall infection specific stimulation of incorporation into the 20S particles has been multiplied by the ratio of the percent composition of the U_3 protein in the infected versus the uninfected 20S peak, as determined by SDS acrylamide gel electrophoresis of each of these particles, to obtain the infection specific stimulation of just the U_3^{20} protein component.

In part B the infection specific U_3^{20} incorporation is computed directly from the SDS acrylamide gel in Figure 16a of the 20S particle from Figure 8b. The first calculation is based upon the mini-

mum ratio of infected/uninfected cpm used in the $\Delta^{14}C$ calculation of the parent velocity gradient in Figure 8b after correcting this value for differences in ^{3}H and ^{14}C counting efficiencies and the different proportions of infected and uninfected sample applied to the sedimentation velocity and acrylamide gel assay systems. By analogy to the $\Delta^{14}C$ calculation, this ratio can be employed in conjunction with a parallel or mixed fractionation of infected and uninfected samples to compute the contribution of uninfected label to the total infected label in a given sample (see legend to Table 14 for details). By dividing the total infected incorporation by the uninfected contribution to this incorporation one obtains the fractional stimulation by the infection.

The second calculation in B is based upon the increase in incorporation into U_3^{20} protein relative to the other host proteins in the infected compared to the uninfected gel patterns of the 20S peak. In this case the same minimum ratio of infected to uninfected incorporation is observed in conjunction with host peaks U_2^{20}, U_6^{20}, and U_8^{20}. This suggests that none of these peaks are coelectrophoresing with infection specific proteins and that this is the ratio of the uninfected incorporation in both the infected and uninfected particles.

Using these various approaches, the host protein U_3^{20} in the infected 20S particle from Figure 8b is found to be present in four to ten fold greater concentration than that expected for an uninfected particle. Apparently the synthesis of the U_3^{20} protein is promoted by the ϕX infection. This will be verified in a more direct fashion below.

E. Resedimentation experiments

The data presented previously suggest that it is perhaps only

a remarkable coincidence that a host protein strongly stimulated by the ϕX infection and the ϕX gene F product (and perhaps other ϕX gene products as well) cosediment with identical S values in a homogeneous peak at 20S. The variability in composition of the 20S peak observed after different lysis and sedimentation procedures suggests that it might be possible to establish the autonomy of these particles in a more direct way by separating the 20S peak into its various component particles by resedimentation in buffers with different ionic compositions from that of the TM buffer in which the peak was isolated. Resedimentation experiments might also clarify the relationship of this particle to the pulse labeled ϕX replicating DNA forms that cosediment with it (Figure 8b) and the antigenicity of this DNA observed earlier (Figure 7). The resedimentation experiments in Figures 18a,b,c and 19a,b were conducted with these questions in mind.

1. The effect of the ionic environment and temperature- In the experiment in Figure 18a,b,c equal aliquots of the 20S peak from the infected gradient in Figure 8b were diluted into TM buffer to reduce the sucrose concentration and then brought to final concentrations of either 0.05, 0.03 or 1.0 M KCl. EDTA was added to one sample at each KCl concentration to titrate the Mg++ and bring the solution to a final concentration of 0.005 M EDTA. BSA and calf thymus DNA carriers were added to all samples. Some samples were incubated for twenty minutes at 37°C while others were kept at 4°C. Just prior to centrifugation a mixture of ^{32}P RF I and RF II marker DNA was added to the samples represented by the gradients in Figures 18b and 18c. All samples were then sedimented through sucrose gradients prepared in homologous

buffers for 12 hours at 40,000 rpm at 4°C in an SW 40 rotor and collected and counted as described in the figure legend.

The sample in Figure 18a was kept at 0°C until just prior to centrifugation when it was diluted with 4°C TM buffer containing protein and DNA carriers and layered onto a precooled sucrose gradient in the same buffer. This centrifugation was performed in conjunction with those in Figure 19a,b (see below) and, as described in the legend to Figure 19, the positions of the RF I and RF II markers were obtained from a parallel sedimentation of these DNAs in the same buffer and centrifuge run. Inspection of Figure 18a shows that under these conditions the bulk of the 20S protein and DNA resediments in a single peak slightly behind the RF I position. A small shoulder of pulse labeled DNA sediments at a slightly slower velocity and some of the 20S protein is released to the top of the gradient. Attempts to reproduce this result in subsequent resedimentations under the same conditions gave rise to a pattern like that in Figure 18b.

Figure 18b presents the results of a resedimentation in TM buffer after incubation of the sample at 37°C for twenty minutes. In this case the nascent DNA peak has separated from the protein peak and shifted to the position of the DNA shoulder in Figure 18a. There remains an unsymmetrical leading edge extending to higher sedimentation velocities. The protein peak continues to sediment in the same position apparently unaffected by the loss of the DNA moiety.

Resedimentations under the other ionic conditions listed above result in patterns intermediate between that in Figure 18b and that in 18c of a resedimentation in TM buffer supplemented with 1.0 M KCl and

EDTA. In all cases the DNA peak is dissociated from the protein peak but with a leading edge extending to the protein mobility. As the KCl concentration is increased the protein peak shifts to lower mobilities until in 1.0 M KCl (Figure 18c) it is only one fraction removed from the DNA peak. The changes in the relative S values of the protein and DNA peaks with changes in the ionic environment are given in Table 15. From Table 15 it is seen that the resedimentation results are insensitive to the presence or absence of Mg++.

2. The effect of nucleases- A comparison of Figures 18a and 18b suggests that regardless of whether or not the 20S protein particle is associated with ϕX DNA in vivo, this association is not required for its sedimentation velocity. This expectation is confirmed by the experiment in Figure 19a,b. In this case aliquots of the pooled 20S peak from Figure 8b were subjected to DNase or RNase digestion prior to resedimentation in TM buffer. A characterization of the nuclease digestion is presented in Figure 17a,b. It is seen that in the presence of the tRNA carrier in the 20S sample, the DNase and RNase degradations plateau at 22.4% and 4.9%, respectively, of residual TCA precipitable cpm compared to input cpm. Control experiments showed that the RNase used in these experiments did not measurably degrade RF I under the conditions of the assay. Figure 19a indicates that RNase has no effect upon the resedimentation of either the protein or DNA moiety. Figure 19b indicates that DNase digestion completely displaces the DNA label to the top of the sedimentation gradient without affecting the sedimentation behavior of the protein.

The insensitivity of the protein mobility to the presence or

absence of the pulse labeled DNA suggests that the DNA and protein moieties of the 20S peak may be only fortuitously associated in sedimentation gradients by virtue of having similar S values. At the very least, these experiments demonstrate that an association of these two species, if it does exist, results in only slight changes in the sedimentation velocities of the component particles. On the other hand, and in contrast to the conclusions drawn from the investigation of the protein composition of the 20S peaks, the continued association of the bulk of the protein components in a single peak over a wide variety of ionic conditions suggests that they comprise a single particle. This contention is strengthened by the following investigation of the protein compositions of the 20S resedimentation products by SDS acrylamide gel electrophoresis.

3. The composition of the protein dissociation products from the 20S resedimentations- In all of the 20S resedimentation gradients there is some evidence of dissociation of the protein moiety. The pattern of this dissociation is relatively invariable with the sedimentation conditions as can be seen from Table 16 where the percent distribution of the leucine label is compiled for each gradient. Much of the small amount of variability that is observed may be the consequence of differences in the sucrose quench sensitivities of the three counting methods employed in various parts of this experiment (see table legend).

In order to determine the protein composition of the various peaks in the redistribution, different regions of the gradient in Figure 19b were pooled as indicated and electrophoresed as described in the legend to Figure 20a,b,c,d,e. Similar fractions were electro-

phoresed from other resedimentations with the same results. An electrophoresis of the 20S protein peak, pool II, from Figure 19b is presented in Figure 20a. The leucine distributions among the 20S particle proteins from three separate resedimentation experiments are compiled in Table 13. A comparison of the 20S particle compositions before and after resedimentation indicates that the proportions of both F protein and component I_7^{20} have decreased somewhat relative to U_3^{20} protein after resedimentation but that the overall composition of the peak is qualitatively very similar to that observed earlier, Figure 16b. There has been no striking loss of any protein component.

Figure 20b is an electrophoresis of the slower sedimenting shoulder, fraction III, of the 20S peak in Figure 19b. The leucine distribution in this gel is also given in Table 13. This distribution is undoubtedly distorted to some extent by the low count rate of the sample and the low sample to background ratio. Nevertheless, it is clear that, compared to the 20S peak *per se*, this peak contains an increased proportion of F protein, and the other infection specific components relative to U_3 protein. It was noted above that the electrophoretic analyses of the resedimented 20S peaks reveals a decrease in the proportion of F protein to U_3^{20} protein relative to the original sample (Figure 8b, Fraction C) whereas the electrophoretic analysis of the 20S shoulder reveals an increase in this proportion. This reciprocal change might suggest a major redistribution of gene F protein in the resedimentation. However, this is not the case in as much as the 20S shoulder accounts for only 4% of the total gradient cpm and only 5% of the total gradient gene F protein, the remainder sedimenting at

20S. As a consequence the change in the proportion of F protein in the resedimented 20S peak remains unaccounted for. Apparently a disproportionate quantity of F protein relative to U_3^{20} protein was lost during the resedimentation (overall recoveries exceeded 90%). The change in the ratio of U_3^{20}/F protein in the 20S peak isolated from the same source is consistent with the idea that these proteins define different particles.

The electrophoretic analyses of the protein peaks at the top and the bottom of the gradient in Figure 19b are given in Figures 20c,d,e and show mainly low molecular weight components. The gel of fraction IV resolves two high mobility peaks suggestive of I_7^{20} and U_8^{20} in the original analysis before resedimentation. However, if these were the peak identities, then the slower of the two would correspond to I_7^{20} and should constitute the principal low molecular weight protein recovered from the total resedimentation. However, this is the only resedimentation fraction containing this peak and it accounts for a very small percentage of the total gradient protein. Apparently this is some easily dissociated slower migrating component that is obscured by the I_7^{20} peak in the electrophoresis of the entire particle.

The analysis of the protein banding in a dense shelf (formed with Angio-Conray) at the bottom of the gradient as well as that sedimenting at the top of the gradient, fractions I and V respectively, reveals only the faster of the two high mobility proteins. This protein has the same mobility as that observed for the high mobility component of the 20S peak in fractions II and III as well. However, because of the poor resolution in this region of the 12% gel system, this similar-

ity in mobility does not necessarily indicate that these are all the same protein. It may be that electrophoresis on higher percentage acrylamide gels would separate these high mobility species into several additional components.

4. Comments-

i. The relationship of the 20S DNA to the 20S proteins- A comparison of the 20S resedimentation presented in Figure 18a, conducted with the least possible manipulation of the sample, with that in Figure 18b, an attempt to reproduce the Figure 18a result with equally gentle conditions, indicates that the DNA and protein moieties in the 20S peak may be associated in an extremely fragile complex that is easily dissociated into its DNA and protein components both of which have S values very similar to that of the original complex. In order for the two subunits to have the same S values as the complex, they would have to be joined in such a way that, as a single particle, they presented the sum of their independent viscosities as well as their masses to the sedimentation system. Such might be the case if a protein particle were attached to the free single strand end of a rolling circle replicative intermediate.

An alternative explanation of the data in Figures 18 and 19 is that the DNA and protein moieties constitute completely independent particles and are only fortuitously associated by reason of their similarities in S value. In this case, the change in the sedimentation behavior of the DNA species after incubation at 37°C compared to 4°C (Figures 18a and 18b), could be explained as a temperature induced change in the DNA conformation alone resulting in a slower sedimentation

velocity. The protein particle would have to be unaffected by this treatment.

Adventitious nuclease activity immediately suggests itself as a mediator of such an *in vitro* change in DNA conformation. However, there is no additional evidence of nuclease activity in these gradients. The gradient fractions were not TCA precipitated before counting so that any low molecular weight material generated by nuclease degradation would still be present (see Figure 19b). There is no evidence of double stranded unit length RF III form DNA indicative of a double strand lesion in the circular ϕX DNA. The only kind of nuclease activity compatible with the observed results would be single strand nicks in double stranded circular DNA. This type of degradation would only cause a change in the sedimentation velocity of these molecules if it resulted in the relaxation of some constrained configuration as in the case of the transition of RF I supercoiled DNA to the RF II form. The earlier analysis of the DNA from this region showed that there was no pulse labeled RF I in this region (Figures 1 and 4). There was, however, a significant fraction, 18%, of dense DNA as assayed by PDI sedimentation to equilibrium. However, far more than 18% of the DNA in these samples is involved in this transition. Apparently some mechanism other than nucleolytic degradation would have to be responsible for the change in DNA sedimentation velocity that is observed.

Whatever the *in vivo* relationship between the 20S DNA and proteins, it is clear from these results that such a complex, if it exists, must be very fragile under the *in vitro* conditions employed here. As a consequence it could not possibly survive the incubation conditions

of the radioimmunoassay and therefore must not be responsible for the antigenicity of the pulse labeled DNA observed in that assay.

ii. The interrelationships of the 20S proteins- Curiously, the protein compositions of 20S particles isolated from original lysates are somewhat variable depending upon the conditions of lysis and whether or not the cultures were infected or not (Table 13). In an earlier section this variability was interpreted to mean that the 20S peak was composed of several cosedimenting but independent particles. By comparison with the first isolation, the 20S peak, once purified, resediments homogeneously as a single entity under a variety of ionic conditions and with or without DNA present. Those protein fractions that do separate from the particle during resedimentation are mostly low molecular weight components which may be associated with the cosedimenting ϕX DNA instead of the protein particle. Contradictory to the interpretation of the protein composition data given earlier, the conservation of the host U_3^{20} and ϕX gene F protein association under the wide range of resedimentation conditions employed here, suggests that these two proteins are complexed in a single particle.

F. The relationship of the 20S U_3 protein to the ϕX induced host proteins and gene A' product

Mayol and Sinsheimer (8) noted that there are two or three peaks of infection specific leucine incorporation with molecular weights greater than that of gene F protein in SDS acrylamide gels of whole lysates of ϕX infected cells. They noted that the summed molecular weights of these proteins were much too great for them all to be coded for by ϕX and therefore suggested that they were host proteins that had

been induced by the infection. Subsequently Godson (20) noted a protein with a molecular weight greater than that of F protein in SDS acrylamide gels of UV irradiated cells. Host proteins do not incorporate label in this system so presumably this was a ϕX coded protein. When lysates from restrictive infections with gene A mutants were examined, this protein was not present. Linney et al. (45, 46) corroborated this result and showed that this high molecular weight protein, denoted A', was one of two gene products synthesized from cistron A. (See General Introduction for a more complete discussion.)

The host protein U_3^{20} observed in conjunction with the 20S particle also has a molecular weight greater than that of F protein and it was demonstrated earlier, Table 14, that its synthesis or at least its assimilation into 20S particles is promoted by the ϕX infection. The following experiments comparing the electrophoretic mobilities of host U_3^{20} protein, the ϕX induced proteins observed in whole lysates and gene A' protein, were conducted in order to clarify the relationships of these proteins to one another.

1. The four high molecular weight infection specific proteins- Figure 21 presents the results of an SDS acrylamide gel electrophoresis of the mixed whole lysates from a ϕXam3 infected and uninfected culture of E. coli H502 differentially labeled with ^{14}C and ^{3}H leucine, respectively. The infection specific incorporation has been resolved by means of the $\Delta^{14}C$ calculation of Mayol and Sinsheimer (8, Methods) and both the uninfected host incorporation and the infection specific incorporation have been plotted. The assignment of the ϕX gene products to the various $\Delta^{14}C$ peaks was made on the basis of Table I from the

Introduction. In this case a 12% acrylamide gel has been utilized to enhance the resolution of the higher molecular weight components. As a consequence the higher mobility proteins have either run together or run off of the bottom of the gel.

Three prominent peaks of infection specific label and a hint of a fourth have molecular weights greater than that of gene F product. These have been denoted I_1 through I_4 and presumably one of them corresponds to the 20S U_3^{20} protein and another to ϕX A' protein. The host pattern in this region is also resolved into distinct peaks which have been numbered U_1 through U_8.

The host pattern is qualitatively the same from experiment to experiment but quantitatively somewhat variable. In particular, incorporation into peak 1 varies from an extreme of that observed here to levels on the order of that observed for peaks U_2- U_4. The $\Delta^{14}C$ discrimination of peak I_1 is also quite variable, usually indicating no peak at this position but at other times showing either a positive or negative infection specific effect. These variations do not seem to correlate with particular ϕX mutants or with the labeling conditions. Because of the erratic behavior of this peak the ratio of infected to uninfected cpm observed here is not used for the $\Delta^{14}C$ calculation even though it often constitutes the minimum ratio. Peak I_1 coelectrophoreses with peak U_1 and as a consequence this position in the gel can now be designated (U_1, I_1).

When a radioactively labeled RNA polymerase preparation is mixed with the host proteins, the sigma factor coelectrophoreses with peak (U_1,I_1) which can consequently be designated (U_1,I_1,σ). The alpha

subunit moves with or slightly slower than peak U_7. This peak or peak U_4 is often used as the minimum ratio point for the calculation of the infection specific incorporation. Such is the case in Figure 21.

The other peaks in the high molecular weight region of the gel behave much more predictably than peak U_1. Peaks I_2 and I_3 are observed in all of the experiments reported here irrespective of the ϕX mutant used in the infection or the labeling regime. Peak I_3 electrophoreses coincidently with peak U_3 , giving (U_3,I_3). Peak I_2 electrophoreses slightly slower than peak U_2. Expression of peak I_4 is dependent upon the experimental conditions and its position with respect to peak U_4 varies, for unknown reasons, from exact coincidence in gene A mutant infections to a slightly slower mobility in am3 infections (see below).

2. Assignment of the U_3^{20} protein to an infection specific peak in whole lysates- In order to establish which of the high molecular weight infection specific proteins from whole lysates corresponds to host U_3^{20} protein from the 20S particle, an aliquot of the ^{14}C leucine labeled 20S particle isolated from the infected gradient in Figure 8b was mixed with the ^{3}H leucine labeled uninfected lysate of Figure 21 and coelectrophoresed (Figure 22b). A parallel gel was run of mixed infected and uninfected whole lysates (Figure 22a). In this case the electrophoresis was allowed to proceed for a longer time than in Figure 21 with the consequence that the gene G and D products have begun to run together at the bottom of the gel whereas the pattern of the high molecular proteins has been somewhat expanded. The various peaks have been numbered as in Figure 21. From Figure 22b it is clear that the 20S host protein, U_3^{20}, coelectrophoreses with host peak U_3. A similar result

was obtained when the ^{3}H labeled uninfected 20S particle from Figure 8b was coelectrophoresed with the ^{14}C labeled infected lysate from Figure 21. The resulting designation is (U_3,I_3,U_3^{20}).

A comparison of Figures 22a and 22b shows that the putative F protein from the infected 20S peak and the F protein from the whole lysate of infected cells electrophorese in the same position relative to the host protein pattern indicating that they are indeed the same protein.

Since the host U_3 protein is expressed in the infection specific pattern of whole lysates, I_3, its synthesis must be promoted by the ϕX infection but whether by induction by some ϕX component of the infected system or some other mechanism is not known. Apparently its infection specific enrichment in the 20S peak is a consequence of this increased synthesis rather than, as proposed earlier, some infection related process that restructures a greater proportion of the intracellular pool of this protein into 20S particles than occurs in uninfected cells.

3. Assignment of the A' protein to an infection specific peak in whole lysates- The electrophoretic position of the (U_3,I_3,U_3^{20}) peak is approximately that described by Godson (20) and Linney et al. (45, 46) for the A' protein. In order to establish the relative electrophoretic mobilities of the (U_3,I_3,U_3^{20}) peak and gene A' product, radioactively labeled ϕX infected lysates of UV irradiated cells were prepared and coelectrophoresed with the 20S peak isolated from Figure 8b and the host proteins from uninfected non-UV irradiated lysates. The UV system is required in order to obtain the ϕX pattern of incorporation

with only one radioactive isotope so that material labeled with the other isotope can be compared with it. The UV labeling system is characterized in the Methods.

i. The UV labeling conditions- In order to enhance the relative incorporation into the A' component the UV pretreated infections were labeled with radioactive lysine rather than leucine, as Linney had observed a preferential incorporation of lysine into the ϕX A and A' proteins (Linney, E., personal communication). Figure 23 presents the result of a coelectrophoresis of ^{14}C leucine labeled and ^{3}H lysine labeled lysates of ϕX wt infected, UV irradiated host cells conducted as described in the Methods and Figure legend. The relative incorporation of each label into the various ϕX proteins is given in Table 17. Inspection of Figure 23 and Table 17 demonstrates that the most dramatic enhancement of incorporation by lysine relative to leucine is in the low molecular weight region of the gel, probably into J protein. This is followed by a 50% enhancement of the A' protein and the H-A peak which, in this case, was not resolved into its component parts. With these exceptions the labeling pattern throughout the rest of the gel is quite uniform for both labels. This indicates that both of these amino acids are distributed relatively uniformly among the ϕX gene products resolved by this gel. The only exceptions would be proteins unusually enriched or impoverished in both amino acids simultaneously. Since this is not very likely, the incorporation of either of these labeled amino acids probably provides a reasonable approximation of the relative protein masses being synthesized.

ii. Characterization of the gene A mutant infection in UV

irradiated cells- The experiments presented in Figure 24a,b were conducted in order to establish the A and A' assignments in this gel system. A lysate of ϕX wt infected, ^{14}C lysine labeled, UV pretreated cells was mixed with similar lysates of am86 or am18 infected, ^{3}H lysine labeled cells and electrophoresed in the SDS stacking gel system described in the Methods. Inspection of Figures 24 and 25 indicates the superiority of this electrophoretic system over that used in the earlier experiments. At least eight peaks of infection specific proteins are clearly resolved in this system. ϕX gene products are again assigned to the various peaks on the basis of Table 1 from the General Introduction. As expected from the work of Linney et al.(46) (see the General Introduction for a detailed discussion) the highest molecular weight peak in these gels is not present in an infection with ϕXam86, a gene A mutant that maps near the N terminal end of cistron A. The lysate of the ϕXam18 infection lacks both the high molecular weight peak and a peak that electrophoreses just ahead of the H protein. This is the expected behavior of mutants like am18 which map at the C terminal end of cistron A.

The average percent distribution of lysine label into the ϕX proteins from the wt, am86 and am18 infections from several different gels is compiled in Table 18. Inspection of Figure 24a,b and the data in Table 19 reveal several additional gene A mediated deviations from the ϕX wt labeling pattern. Most dramatic is a more than two fold enhancement of incorporation into the putative gene B peak. This enhancement has not been reported by others, probably because this region of the molecular weight spectrum is not so well resolved in other systems. It

should be noted that this effect is contrary to that expected for the A, B, C polarity of the genome established by Benbow et al.(12). Of course the assignment of this peak to gene B product can only be considered tentative in the absence of an experiment demonstrating a change in the mobility of this peak in this gel system after infection with an unsuppressed suppressor mutant in B.

The A mutations also cause a 50% reduction in incorporation into the low molecular weight peak at the bottom of the gel. This diminuation was also observed by Benbow et al.(12) and may in part be due to polarity effects depending upon which if any of the unassigned cistrons are represented by this peak. The gene A lysates also show a reduction in the gene D peak.

Because of this plethora of gene A related effects, many of which are at least as dramatic as the suppression of the A and A' peaks, it may still be premature to make a conclusive assignment of the gene A product(s) to the A and A' peaks. However, these experiments do serve to show that the A and A' peak assignments used here are the same as those of Linney et al.(46).

It should be noted that the ϕX stimulated high molecular weight host peaks I_2 and I_3 are not present in the ϕX wt infected UV irradiated lysates in Figures 24-26. This is also true for different labeling regimes and infections with ϕXam3 as well as ϕX wt and cistron A mutant strains. Apparently de novo synthesis of these proteins is not required for ϕX infection. The lack of such synthesis may, however, be a contributing factor to the poor growth of ϕX in UV irradiated hosts (20, 52).

iii. Assignment of the A' protein- In the following experiments (Figures 25 and 26) the A' protein observed in the UV infection is shown to migrate at the position of the small infection specific I_4 peak in whole lysates of am3 infected non-UV irradiated cells. Unfortunately, it was not possible to do this by means of a direct experiment because both the ^3H and ^{14}C protein labels must be used to delineate the infection specific proteins in the non-UV cultures thereby eliminating the possibility of coelectrophoresis with an unknown or standard. This problem was circumvented by coelectrophoresing the A' protein (the ^3H leucine labeled, UV irradiated, ϕX wt lysate from Figure 24) with a whole lysate of uninfected cells (^{14}C labeled, non-UV irradiated). When this was done (Figure 25b), the A' protein migrated slightly slower than host peak U_4 but two fractions ahead of host peak (U_3,I_3,U_3^{20}). Figure 25a (and Figures 21, 27a, 28a, 29a,b,c,d) reveal that the small infection specific I_4 peak migrates in this same position in the non-UV am3 infected lysates. This suggests that the small I_4 peak is composed of ϕX A' protein. However, due to the strange behavior of the I_4 peak in gene A mutant infections it cannot definitely be assigned to the A' protein (see below).

4. The non-identity of the (U_3,I_3,U_3^{20}) peak and the A' protein- The distinct electrophoretic mobilities of the A' protein and the (U_3,I_3,U_3^{20}) peak is confirmed by the clear separation of these proteins in the gels presented in Figure 26 in which the infected 20S particle from Figure 8b has been coelectrophoresed with lysates of ϕX wt infected, UV pretreated cells. Figure 26a employs the wt lysate and 15% acrylamide stacking gel system of Figures 24 and 25. Figure 26b employs a

wt lysate prepared from cells irradiated for a lesser period of time, thus accounting for some residual synthesis of high molecular weight host proteins. The proteins in 26b were separated on a 12% acrylamide gel thus accounting for the greater separation between the U_3^{20} and A' proteins.

Both of the gels in Figure 26 were optimized for the unambiguous expression of both U_3^{20} and A' proteins. To avoid any possible counting artifacts in the discrimination of the U_3^{20} and A' peaks that might be caused by ^{14}C overlap to the ^{3}H channel, sufficient ^{3}H labeled ϕX wt lysate was added to the mixture such that the ^{3}H incorporation in the A' peak would equal or exceed the ^{14}C label from 20S protein. This results in good resolution of these two proteins but, since the A' protein accounts for only 2-3% of the total lysine incorporation into the wt lysate, there is concomitantly a huge excess of ^{3}H label compared to ^{14}C label in the rest of the gradient. As a consequence the ^{14}C gene F peaks and other 20S protein peaks have been distorted due to inaccuracies in the overlap correction at these very high count rates.

5. The molecular weights of the infection specific high molecular weight proteins- By plotting the mobilities of the ϕX174 proteins in an SDS acrylamide gel of a whole lysate of am3 infected cells (Figure 29b) against the molecular weights of these proteins given in Table I in the General Introduction, one obtains a molecular weight calibration of the gel (Figure 30). In other experiments it was shown that the E. coli RNA polymerase components sigma and alpha coelectrophorese with the host peaks U_1 and U_7, respectively, in the same gel system, thus giving two additional calibration points, one at the upper end of the molecular

weight range of interest. The approximate molecular weights of the ϕX-stimulated host peaks in Figure 29b, including host component U_3^{20} of the 20S particle, are obtained by comparing the mobilities of these peaks with Figure 30. It is seen that host component (U_3,I_3,U_3^{20}) has a molecular weight of 67,000 daltons, whereas component U_2 has a molecular weight of 84,000 daltons. Host peak U_4, which migrates only slightly faster than gene A' product (Figure 25), has a molecular weight of 58,000 daltons, suggesting that A' would probably give a lower molecular weight in this system than the 62,000 daltons indicated in Table 1 of the General Introduction.

G. Summary of the 20S results

Both infected and uninfected E. coli lysates contain well resolved sedimentation peaks at approximately 20S. The peak from uninfected cells is composed mostly of a high molecular weight host protein, denoted U_3^{20}, and lesser amounts of several additional host proteins. Synthesis of host U_3^{20} protein is stimulated several fold by the ϕX infection, thereby contributing to a several fold increase in 20S peak production compared to uninfected cells. In the infected cell 20S peak, host U_3^{20} protein remains the major protein constituent followed by ϕX gene F product and lesser amounts of other infection specific proteins. Very little host protein other than U_3^{20} is present. Infected cell lysates also contain ϕX SS replicating DNA throughout the 20S region. Unfortunately the relationships between the various 20S components have not been clearly resolved by these experiments.

The sedimentation homogeneity of the 20S protein peak suggests that the protein constituents are complexed into a single particle. In

addition, the dramatic infection specific increase in synthesis of the 20S particle, in conjunction with its cosedimentation with ϕX replicating DNA and gene F protein, suggests that the 20S proteins may also be complexed with ϕX DNA. As noted in detail in the General Introduction, a large body of indirect evidence points to the existence of just such a complex. The resedimentation experiments are also consistent with this idea.

The most straightforward interpretation of the resedimentation results is that the 20S peak components in the infected cell are organized into a fragile DNA-protein complex that is dissociated into its protein and DNA components as a result of virtually any manipulation, thereby giving rise to protein and DNA disruption products that have S values very similar to those of the complex. In addition the conservation of the 20S protein peak as a single sedimentation species under the variety of resedimentation conditions tested suggests that the 20S proteins (with the exception of a small proportion of low molecular weight proteins) are themselves complexed into a single particle.

In contrast to the resedimentation experiments several other lines of evidence suggest that most of the 20S components are associated only by a fortuitous similarity in S values. Moreover, the resedimentation results cannot exclude this interpretation as it is always conceivable, regardless of how remarkable, that the separation of DNA and protein peaks observed in Figures 18a and 18b was the result of a change in conformation of an independent DNA moiety, and that the protein particles were unaffected by this change by virtue of being unattached and unrelated to the DNA. If, in addition, the sedimentation

properties of the host and infection specific components of the 20S protein peak are affected identically by changes in the ionic environment, then they could also constitute separate particles. Thus there is no impediment, except improbability, to all three of these 20S components being organized into separate particles. This is the 20S peak structure that is indicated by the variations observed in the proportions of the various proteins comprising the 20S peak when comparing the infected and uninfected peaks or the peaks isolated as the result of different lysis procedures. Nevertheless, to be entirely convincing, this model will require a demonstration that the component particles can be separated and then reconstituted back into a 20S peak.

Regardless of the in vivo relationships of the 20S components it is clear that any association between the ϕX replicating DNA and the major protein species observed in these experiments is much too fragile in vitro to account for the antigenicity of this DNA.

The host (U_3,I_3,U_3^{20}) protein is one of four infection specific proteins that have molecular weights greater than gene F product. The presence of this protein in a 20S particle in uninfected cells, U_3^{20}, as well as its sensitivity to UV irradiation establishes its identity as a host protein. There are two other proteins, I_1 and I_2, with molecular weights even greater than U_3, that also seem to be host proteins. Electrophoresing between (U_3,I_3,U_3^{20}) protein and ϕX F protein is a fourth protein, I_4, that is clearly dependent upon gene A for its synthesis in UV irradiated cells, gene A' product, but shows very little sensitivity to A mutations in non-UV irradiated cells. The reasons for this difference in behavior are not known. (Gene A mutant infections of non-UV irradiated cells are characterized in the next section.)

IX. Characterization of the Gene A mutant infection in non-UV irradiated cells

A. 140 minute labeling period

B. 0-18 minute labeling period

C. Other consequences of gene A mutant infections

D. The relationship of the labeling period to the proportion of total ϕX specific incorporation of protein label

E. Summary

1. Gene A mutant infections
2. Variations in the proportion of ϕX specific labeling
3. The high molecular weight infection specific proteins I_1-I_4

F. Comments

1. Functions of the infection specific host proteins I_1-I_4
2. Other infection specific peak resolved by the stacking gel system

Comparison of Figures 21, 22a and 25a with Figures 23 and 24 indicates that the A' product may be expressed much more strongly in UV irradiated hosts than in non-UV irradiated hosts. In fact there is only a hint of incorporation into the A' peak, if any, in Figures 21, 22a and 25a.

A quantitative comparison of the infection specific incorporation into the expected A' position in the non-UV lysate with that into the A' peak of UV lysates is given in Table 18. The ratio of the A' region to F protein incorporation given in Table 19 for non-UV experi-

ments like those in Figures 21, 22 and 25 shows only 1/5 as much A' region protein relative to F protein as in the UV system. This result is independent of any differences in the overall distribution of label in the two systems.

These findings suggest that A' protein may not be present in the normal infection of a non-UV irradiated host. Alternatively, the differences observed may be due to the different labeling periods used in the UV (30-90 minutes) and non-UV (0-140 minutes) experiments. The experiments in Figures 27 and 28 were conducted to explore the effects of gene A mutations and different labeling periods on the normal infection. It will be shown that 0-18 minute pulses do give rise to a well defined peak at the A' locus (similar in prominence to that observed in the UV infection) but that this peak does not behave in the manner predicted for the A' protein in gene A mutant infections. By contrast, pulses of from 0-90 minutes or longer result in only a small, poorly defined peak at the A' locus, but this peak nevertheless behaves in the predicted manner in the presence of gene A mutations. Nevertheless this effect is the least dramatic of numerous other consequences of the A mutant infection.

In both of the experiments presented below (Figures 27 and 28) equal aliquots of an uninfected ^{14}C lysine labeled lysate were mixed with ^{3}H lysine labeled lysates of cells infected with ϕX mutants am3, am18, or am86 and electrophoresed on SDS stacking gels as described in the Methods and legend to Figures 27 and 28. In this case the ϕX specific incorporation was calculated as $\Delta^{3}H$ instead of $\Delta^{14}C$. The cultures in Figures 27 and 28 were labeled from 0-18 minutes and 0-140 minutes after

infection, respectively. By comparison all of the UV irradiated cultures shown in previous experiments were labeled from 30-90 minutes after infection except for those in Figures 23 and 26b, which were labeled from 0-90 minutes. The percent incorporation into the various regions of these gels is given in Table 18 and the ratios of the A' region to F protein incorporation in Table 19.

A. 140 minute labeling period

The SDS acrylamide gel of the 140 minute am3 infection in Figure 28a shows no clearly defined peak in the A' region of the gel but does show a low level of incorporation there. This is only 1/5 the incorporation relative to gene F protein that is observed in am3 infections of UV irradiated cells. Infection with either of the gene A mutants over this same time period reduces this low level of incorporation by another four fold (Figure 28b,c). This result supports the contention that a small amount of A' protein is present at the expected position in infections of non-UV irradiated cells but it must be qualified by the realization that this observation is made at the limits of resolution of this method and constitutes the least dramatic of numerous other changes correlated with the gene A mutant infections (see below).

B. 0-18 minute labeling period

In contrast to the long term labeling result, the SDS acrylamide gel of the 18 minute am3 infection (Figure 27a,b,c) shows a definite peak at the expected A' position and in the same proportion to F protein as observed in the infections of UV irradiated hosts. However, the effect of the gene A mutations on this peak is ambiguous. Am86

reduces incorporation relative to F protein by only 13%, however the position of the peak shifts to a lower molecular weight coelectrophoresing with host peak U_4. This would be the expected result for an ordinary C terminal amber mutation. Am86, on the other hand, maps at the N terminus of the A cistron (15). Its behavior in the UV irradiated system supports this assignment. As a consequence, this mutation should produce only small fragments in the restrictive host and, if the model of gene A behavior espoused by Linney et al.(45, 46) is correct, these fragments should be at least as small as the A protein. The am18 mutation reduces the incorporation into the A' peak relative to F protein to 27% that of the am3 infection. It does not shift the position of the residual incorporation as might be expected for a mutant very close to the C terminal end of the cistron. As was true in the 140 minute infection these effects on the A' peak are among the least dramatic consequences of the gene A mutant infections.

C. Other consequences of gene A mutant infections

In both of the am3 infections (Figures 27a and 28a) the H and A peaks are well resolved although the relative proportion of these two proteins varies with the conditions, gene A protein dominating in the 18 minute infection and gene H protein in the 140 minute infection. This is similar to the relationship of A' to F protein in the two labeling periods and may reflect the accumulation and stabilization of the phage components in completed virions while normal intracellular proteins including the phage A and A' proteins are slowly catabolized. This might also account for the relative impoverishment of the 140 minute am3 infection of B protein (compare Figures 27a and 28a).

The effect of the gene A mutations on this labeling pattern differs markedly from that observed in the UV system. In the case of either gene A mutant and either labeling period the H and A doublet of peaks is replaced by a single peak electrophoresing between these former positions. This change can be monitored sensitively by using the host peaks as reference points. In the am3 infection, host peak U_8 electrophoreses between the H and A peaks (Figures 27a and 28a). After infection with a gene A mutant it comigrates with the remaining peak (Figures 27b,c and 28b,c). In the UV system the A peak is clearly eliminated in the am18 infection but not by am86. The H peak is unaffected by either mutant. In the non-UV system it appears to be the A peak, if any, that is conserved and the H peak that is lost.

As was true in the UV system both gene A mutants appear to stimulate gene B production though not to the extent observed there. In the non-UV infections the am86 mutation appears to have a much stronger effect upon B synthesis than does am18. Am86 also appears to promote incorporation into a peak electrophoresing between gene D protein and the lowest molecular weight protein. This effect was not observed in the UV system.

Both of the 140 minute, but not the 18 minute, gene A mutant infections show a great enhancement of incorporation into the infection stimulated host peaks U_2 and U_3.

In all of these experiments the constancy of the host incorporation pattern serves as an indicator of the high reproducibility of this gel system. In addition the observations made here have been repeated in several other experiments. As a consequence it is concluded that

there are substantial differences in the behavior of the gene A mutants in non-UV irradiated and UV irradiated hosts.

D. The relationship of the labeling period to the proportion of total ϕX specific incorporation of protein label

The experiment presented in Figures 27 and 28 indicates that there can be substantial differences in the infection specific labeling patterns dependent upon the labeling conditions. This is substantiated in Figure 29a,b,c,d which presents the patterns observed for the am3 infection under four different conditions of labeling. The host, the infected, and the infection specific patterns are all plotted. It can be seen that whereas the host patterns remain relatively constant, irrespective of the labeling period, the pattern in the infected cell becomes increasingly dominated by the ϕX proteins as the labeling period increases or is shifted to later times in the infection. By fifty minutes after infection 69% of the total amino acid incorporation in the infected culture appears in infection specific proteins as resolved by the delta cpm calculation. Table 20 presents the ratios of the total infection specific cpm compared to the total cpm of amino acid label incorporated in the infected cultures of Figure 29. The high proportion of infection specific synthesis in infected cultures apparently reflects a displacement of the host from its translation apparatus rather than an increase in total intracellular protein synthesis as the ϕX174 infection has only a small effect on the total incorporation of amino acid labels into infected versus uninfected cells and this effect is inhibitory (Figure 2 from the Methods; references 86, 73).

As was noted earlier, an increase in the labeling period is

also accompanied by a change in the relative proportions of H and A proteins with A dominating in a 0-18 minute pulse and H dominating in longer pulses. The 0-18 minute pulse also labels the A' peak, or at least a protein at the A' position (see earlier discussion), as well as three peaks with mobilities between those of A and G and the two peaks between G and D, including B, much more strongly than do the longer labeling periods. As was noted earlier this may reflect a greater exposure to catabolism of proteins not stabilized by incorporation into the virion.

E. Summary

1. Gene A mutant infections- The gene A mutant infections of UV irradiated cells corroborated the behavior of the A and A' peaks reported by Linney et al. (45, 46) but also revealed several other, previously unreported effects that were at least as dramatic. In particular there was a greater than two fold stimulation of gene B protein synthesis and a two fold reduction in synthesis of the low molecular weight components.

In the non-UV infections with gene A mutants, these "secondary" effects constituted the only clear correlations with the gene A mutants. Neither of the putative gene A proteins was strongly affected by the presence of the mutations. (The H-A doublet peak was consistently reduced to a single peak but by mutations from either end of the cistron and in a manner that appeared to conserve the A protein and delete the H protein instead of the other way around as expected.) As a consequence of the complicated behavior of the gene A mutants in the non-UV system and the lack of correlation with the UV system, the possibility

must be entertained that the UV assignments of the A and A' proteins are an artifact of the radiation treatment. At the very least these experiments suggest that the normal infection, while considerably more vigorous, is also considerably more complex than the UV irradiated one.

2. Variations in the proportion of ϕX specific labeling- The data presented in Figure 29 and Table 20 indicate that with increasing time after infection, ϕX infection specific protein synthesis increasingly dominates intracellular protein synthesis. Since the rate of total protein synthesis actually decreases somewhat in infected vs. uninfected cells (Figure 2, Methods), this means that the ϕX infection is not simply superimposed upon an otherwise normal host metabolism, but must instead interact with it in some way so as to suppress host protein synthesis. Puga et al. (159) mention a similar decrease in host protein synthesis in the S13 infection beginning at twenty minutes after infection. It may be that the decrease in host protein synthesis is related to the shut off of host DNA synthesis that occurs at about this time.

3. The high molecular weight infection specific proteins I_1-I_4- Four infection specific peaks with electrophoretic mobilities less than that of gene F protein are observed in ϕX infected non-UV irradiated cells. They are denoted I_1, I_2, I_3, and I_4 in order of increasing mobilities (Figure 21).

The I_4 peak occupies the locus of the ϕX A' protein as characterized in gels of UV irradiated lysates. However, whether or not the I_4 peak is the A' protein is unclear due to the ambiguous effects of gene A mutant infections on this peak in the non-UV irradiated system.

The I_3 peak corresponds to the host U_3^{20} protein which is the major constituent of the 20S peak isolated from both infected and uninfected cells. This protein coelectrophoreses exactly with host peak U_3 from whole lysates and is presumed to be the same protein, the synthesis of which is in some way enhanced by the ϕX infection.

The I_2 peak is consistently the most prominent of the four high molecular weight proteins. It electrophoreses slightly slower than host peak U_2 and presumably represents a host protein whose synthesis is promoted by the ϕX infection but which is present only as a minor component in uninfected cells and is therefore obscured by host peaks U_1 and U_2 in the uninfected electrophoretic pattern.

The visualization of peak I_1, as well as host peak U_1 with which it comigrates, is, for unknown reasons, erratic. Its relationship to the infection is, nevertheless, of considerable interest, in as much as this peak coelectrophoreses with the host RNA polymerase sigma factor.

F. Comments

1. Functions of the infection specific host proteins I_1-I_4- As yet the functions of the high molecular weight I_2 and I_3 proteins are unknown. The I_3 protein can be assigned to an intracellular locus, the 20S particle, but the function of the particle is also unknown. The I_2 protein has not yet been observed with any particular sedimentation fraction. A successful infection does not apparently require the de novo synthesis of either of these proteins as neither of them are made in the UV infection. Their absence in UV irradiated cells is further evidence that they are, in fact, host proteins rather than undissociated ϕX protein multimers or translation read-through products. However, it

is not known to what extent their absence contributes to the poor growth of ϕX in UV irradiated cells. The mechanism, classical derepression, metabolic feedback, or other, by which their synthesis is promoted in the normal infection is not known. As yet the only known ϕX induced host function is the cytosine specific host methylase observed by Razin (162). It is, therefore, conceivable that one of these proteins is that enzyme or a subunit of that enzyme. As yet there has been no correlation of the presence or absence of any ϕX gene product with the synthesis of either of these proteins.

2. Other infection specific peaks resolved by the stacking gel system- The experiments in Figures 24-29 employed a highly resolving stacking gel system described in the Methods. As a consequence several new infection specific peaks are consistently observed in these gels especially after the shorter pulse times. The B peak (assignment by Siden, 61) is well resolved from G and D proteins along with an unassigned peak migrating between B and G. In addition there are three small peaks between A and G, as well as two and sometimes three peaks between D and J. One of the latter may be the gene C product (62). Assuming a low molecular weight assignment for the C protein that leaves only the gene E product unassigned and none of these peaks fulfill the stoichiometric expectations for gene E production (see General Introduction). Nevertheless, regardless of how the ultimate gene assignments are all made, there are five or six too many peaks (not counting the I_1, I_2 and I_3 peaks) to be accounted for by the eight or nine cistron coding capacity of the ϕX genome. Thus, unless the cistron A-A' phenomenon is widespread, most of these new peaks must

represent host proteins. The ability to visualize host proteins that are apparently involved in the infection process again demonstrates the power of the double label technique.

X. A comparison of the computed and observed DNA/protein ratios of various subviral particles

The resedimentations (Figures 18 and 19) of the 20S peak obtained from lysates of infected cells (Figure 8b) indicate that even if there is some *in vivo* association between the nascent ϕX DNA forms and the ϕX proteins cosedimenting in this peak, this association is not stable enough to account for the radioimmunoassay binding of the nascent DNA from this region. Also the profile of anti-ϕX antiserum binding of ϕX DNA parallels the broad distribution of ϕX replicative intermediate DNAs (Figure 7) rather than the sharp 20S protein peak.

If the phage specific proteins in the 20S peak are not responsible for the radioimmunoassay binding of ϕX DNA, then one must enquire what antigen is responsible and why it is not observed in the protein labeling experiments. Inspection of Figure 8b reveals a substantial background of ϕX specific incorporation into proteins throughout the velocity gradient in the region of the ϕX replicative DNA forms. It is conceivable that the proteins responsible for binding are represented by this background or that they are not visualized at all by the labeling procedure utilized. Such might be the case if, for some reason, the six minute pulse of labeled amino acids did not enter the pool from which the antigenic moiety of the DNA-antigen complex was withdrawn, or if the pulse entered a very large pool of antigenic precursors such that it was greatly diluted (see Appendix B). Alternatively, the antigenicity of the nascent ϕX DNA forms may derive from an association with one or a very few molecules of ϕX protein per molecule of DNA such that

the specific activity of the labeling is inadequate to detect such small quantities of protein.

In order to obtain some idea of the lower limits of detection of the protein labeling procedure used in these experiments, the specific activities of the radioactive leucine and thymidine labels were employed to calculate the intracellular concentration of the nascent DNA forms and the concentration in cpm of leucine label that would be expected to be complexed with the ϕX DNA as the consequence of various hypothetical associations between ϕX DNA and ϕX proteins. The results are presented in Table 22.

The determination of the specific activities of thymidine and leucine labels is hampered by an imprecise knowledge of the size of the intracellular pools of these molecules and the rate at which these pools are replenished by de novo synthesis. However, in the case of both labels indirect evidence suggests that these pools are sufficiently small and, at least in the presence of exogenous label, de novo synthesis is sufficiently limited that, for the sake of an approximate calculation, the specific activities of the exogenous labels provides an adequate estimate of the intracellular values.

In the case of the DNA label, ^{3}H thymidine is added to a culture of E. coli H502, a thymine auxotroph, that is already supplemented with 1 µg/ml thymine. However, this exogenous supply of thymine apparently has only a small effect on the specific activity of the added thymidine label since the rate of incorporation of labeled thymidine into TCA precipitable material is, during the first three minutes of labeling, relatively insensitive to the presence of cold thymine in

concentrations of up to 2 μg/ml (89, 183, 184; Rohwer, R., unpublished results).

An additional indication of the preference of E. coli H502 for the thymidine precursor to DNA synthesis and of the separation of the thymine and thymidine pools is provided by the experiments presented earlier in which a continuous ^{14}C thymine label was shown to be displaced from the pool of late, resting RF II by increasingly long pulses of ^{3}H thymidine.

As a consequence of these observations, the specific activity of the exogenous labeled thymidine was used to calculate the nucleic acid concentrations in Table 22. To the extent that the thymidine specific activity is diluted by the incorporation of cold thymine this value of the specific activity will result in the calculation of minimum values for the DNA concentrations.

The calculations in Table 22 are based upon a ninety second pulse of thymidine label. In the case of the replicating RF DNA molecules, the experiments mentioned above in which the ^{14}C thymine label was displaced from the resting RF II pool by a ninety second thymidine pulse indicate that the replicating DNA species are uniformly labeled in their plus strands with ^{3}H thymidine by the end of ninety seconds. Thus the total concentration of these DNAs can be computed from the pulse label.

The DNA concentrations in Table 22 are expressed as ϕX DNA plus strand equivalents. Since there is very little incorporation of DNA label into minus strands at this stage of the infection (93, 96, 97), one plus strand equivalent represents one molecule of RF II DNA or one

half molecule of replicative intermediate DNA with a unit length plus strand tail. Since most of the X DNA replicative intermediates have short tails (Figure 4), this is a reasonable approximation of the molecular concentration of DNA in this region.

In the case of the 114S region of the gradient, the pulse label can only indicate the amount of DNA accumulating there in a ninety second interval rather than the total concentration of the DNA.

The intracellular specific activity of leucine is uncertain because the E. coli H502 host is not a leucine auxotroph. In one attempt to overcome this problem, several independently isolated leucine auxotrophs of H502 were prepared by means of nitrosoguanidine mutagenesis and a penicillium enrichment technique. However all of these mutants required such high concentrations of exogenous leucine for growth, ≥20 µg/ml, that they proved impractical for use with radioactive leucine due to the loss in specific activity of the added label and the consequent reduction in total incorporation. Rahmanian et al. (185) have recently shown that exogenous leucine represses synthesis of the leucine permease apparatus which results in a high leucine requirement for leucine auxotrophs. A similar repression of the leucine biosynthetic pathway would make use of the use of a leucine auxotroph unnecessary for the determination of the specific activity of intracellular leucine.

The leucine biosynthetic pathway of Salmonella typhymurium has been demonstrated to be under feedback control by leucine which both represses the synthesis of leucine biosynthetic proteins under the control of an operator gene (186) and inhibits the activity of α-isopropylmalate synthetase, the enzyme catalyzing the first reaction in the

leucine biosynthetic pathway (187, 188). A similar organization of the leucine biosynthetic genes into a single operon has now been demonstrated in E. coli strains B/r and K-12 (189, 190) suggesting that similar feedback controls may exist there, although this has not as yet been demonstrated.

The data in Table 21 suggest that the leucine biosynthetic pathways are, in fact, inactive under the labeling conditions employed in these experiments. In Table 21 the extent to which the specific activity of exogenous leucine is diluted by intracellular pools and endogenous synthesis of leucine is estimated by comparing the phage particle yield from infected cells continuously labeled with leucine with the phage particle concentration calculated from the specific activity of the ^{3}H leucine label. It can be seen that the various methods of determining the phage particle concentration all agree within a factor of two of each other, suggesting that for the purposes of a rough calculation the specific activity of the exogenously supplied leucine can be used to compute the incorporated mass of leucine. To the extent that the leucine specific activity is reduced by residual host synthesis the calculated protein masses will represent minimum values.

In Table 22 the protein label corresponding to one phage equivalent of leucine was first determined as described in the Table legend. The leucine contents of the other hypothetical structures were then related to this value as the fraction of one phage equivalent of leucine that they represented. Next, the expected DNA/protein ratio was computed for each hypothetical structure. If the cpm of pulse labeled DNA from any point in the gradient is then multiplied by these fractions,

an estimate is obtained of the cpm of protein label that can be expected for any of the hypothetical DNA-protein associations given.

This estimate is a maximum value in as much as any dilution of the leucine specific activity by endogenous leucine would result in lower levels of incorporation. Dilution of the ^{3}H thymidine specific activity would act in the opposite direction. The maximum dilution that could occur would result from the complete equilibration of the thymidine and thymine pools which would result in a ten fold increase in all of the computed values. Such an equilibration does eventually take place by means of the degradation of the thymidine supply to thymine. However, as evidenced by the change in incorporation rate of thymidine label with time, thymidine label continues to be preferentially incorporated, thus maintaining the input specific activity, until the thymidine pools are completely converted (183, 184; Rohwer, R., unpublished). This does not occur until three minutes after the addition of thymidine under the conditions employed in these experiments (183; Rohwer, R., unpublished). Therefore the thymidine specific activity should be relatively unaffected during the ninety second pulse utilized.

The expected $\Delta^{14}C$ leucine cpm in Table 22 have been computed for the pooled peak of 20S material from the gradient in Figure 8b and for the peak fraction of the RF II peak in the same gradient. The peak fraction of the RF II peak contains the highest DNA count rate of any fraction in the replicative intermediates region of the gradient. As a consequence, the expected $\Delta^{14}C$ cpm computed for this fraction represent the greatest values that can be expected for any fraction in this region.

Inspection of Table 22 reveals that the antigens responsible for the anti-ϕX antiserum binding of ϕX DNA, would, if present in only one or a few copies per replicating DNA molecule, be below the resolving power of the leucine labeling technique employed. A low antigen density per DNA molecule could, therefore, account for the failure of the resedimentation experiments in Figures 18 and 19 to distinguish these proteins and this complex from the rest of the 20S sedimentation peak. An antigenic association of only one or two proteins per DNA molecule would, at best, account for only 1-2% of the phage specific cpm in the 20S peak. As a consequence the DNA antigen may be represented by one of the minor protein components of the SDS acrylamide gel electrophoresis of the 20S peak in Figure 16.

The methods employed in the analysis of the 20S peak in Table 22 can also be used to evaluate the pattern of incorporation of protein and DNA labels into the 114S peak in gradients like that in Figure 8a. With reference to the labeling conditions employed in these experiments, one is, in this case, comparing the amount of DNA accumulated in this peak during the course of a ninety second pulse with the protein accumulated during a six minute pulse rather than the total protein and DNA in this region of the gradient. In the earlier discussion in conjunction with the resedimentation experiments in Figure 9 and Table 9, it was noted that 86% of the protein label originally sedimenting in the vicinity of the 114S peak is lost upon resedimentation. The ratio of DNA/protein observed after resedimentation is considered to be that of the phage free of non-phage protein. From Table 23 it can be seen that the protein content of the resedimented phage peak is seven times less than

would be expected if leucine labeled proteins were associated with the pulse labeled DNA at the specific activity of the added leucine. This result is obtained even though the cells are prelabeled with leucine for 4.5 minutes prior to the addition of radioactive thymidine. Apparently, the pulse labeled protein precursors to phage assembly are diluted by a large pre-existing pool of unlabeled precursors prior to their incorporation into phage particles, whereas the thymidine labeled DNA precursor pools are much smaller. Inspection of Figure 8 and the analyses of the protein compositions of the various protein peaks in these gradients (Figures 12-16) reveal that the greatest proportion of the protein pulse entering structural precursors of the phage particle is found in the 111S peak followed by the 6S, 9S and 20S peaks in that order. It was shown earlier that the 6S and 9S peaks can be generated from the 111S peak suggesting that the 111S structure may constitute an even larger pool <u>in vivo</u> and represent the principle repository of the direct precursors of phage assembly.

XI. Maturation of the ϕX174 virion- a model

A. Known pathways between ϕX174 subviral particles

B. A model for ϕX174 maturation

1. The 111S particle
2. The 12S particle and gene B function
3. The fast sedimenting replicative intermediates of SS DNA synthesis
4. The pulse labeled antigenic DNA
5. The 140S particle
6. Particles unaccounted for in the model

A. Known pathways between ϕX174 subviral particles

Twelve different subviral particles have now been observed in lysates of either wt or lysis deficient mutants of ϕX174. They are listed along with a summary of their properties in Table 5 (Particles from the Normal Infection) of the General Introduction. One of these, the 70S lysis artifact, is a post-lysis breakdown product of whole phage. Another, the infectious low density particle (ILDP) may have a similar origin (Rohwer, R., in preparation). The rest most likely represent in vivo particles or their decomposition products. Figure 31a is a schematic representation of the known pathways between these particles.

Five forward reactions (simpler particles → more complex particles) have been demonstrated. Thus Tonegawa and Hayashi (65) have shown that F and G monomers will spontaneously form into 9S and 6S

particles *in vitro* and require no other gene products for this step *in vivo*. They also showed that a 20S particle will form spontaneously *in vitro*. Weisbeek and Sinsheimer (165) demonstrated the conversion of 140S particles to ϕX whole virions *in vitro*. The considerable literature chronicling the conversion of ϕX RF DNA to viral SS DNA was reviewed in the General Introduction.

The rest of the known pathways are decomposition reactions. The 111S particle decomposition pathways were presented in the Results; Siden and Hayashi (61) showed that the 12S particle degrades to 6S and 9S particles; the 140S particle decomposition was observed by Weisbeek and Sinsheimer (165); and the evidence for the ϕX virion's conversion to 70S lysis artifact or, upon infection, empty shells and SS DNA was reviewed in the General Introduction.

The instability of the more complex particles (12S, 111S and 140S) to storage in the same buffers in which they were isolated, as well as their homogeneous appearance in velocity sedimentation gradients, and their reproducible protein compositions, indicate that they are real *in vivo* particles as opposed to random complexes formed at lysis. Their degradation products provide insight into their structure and may represent the *in vivo* precursors to their assembly.

B. A model for ϕX174 maturation

If one makes the simple assumption that the degradation products observed *in vitro* do, in the intracellular environment, constitute maturation intermediates, then the hypothetical assembly pathway presented in Figure 31b can be constructed as a useful working hypothesis for further experimentation. The fallibility of this approach

is demonstrated by the two alternatives, 1 and 2, for the formation of the 111S particle. The existing data support either pathway. However, since this is the only step for which good alternatives exist, the rest of the pathway represents a reasonable extrapolation from our present knowledge. In addition there is a great deal of indirect evidence supporting various features of this scheme.

1. The 111S particle - The various lines of evidence suggesting the existence of a phage precursor with the composition of the 111S particle were reviewed in the General Introduction. Thus, the F, G and D proteins are all required for the initiation and continuation of ϕX SS DNA synthesis. The 111S particle is composed of these same three proteins and could play an essential role in SS DNA synthesis if, for example, it served as an essential attachment point or reservoir for the 5' end of the displaced SS DNA tail of the replicative intermediate. The complementation failure of certain ϕX and S13 mutants (34) suggests a molecular interaction of ϕX gene F and D proteins and the 111S particle may be the site of this interaction. The structure of the ϕX virion, a stable protein shell surrounding a non-integral DNA molecule (as distinct from a structure like the TYMV virion or a ribosome in which the nucleic acid is intermeshed with the proteins, 233), suggests that a similar protein shell might serve as a precursor to packaging. The sedimentation velocity and decomposition products of the 111S particle are compatible with its being a complex structure with approximately virional dimensions. As such, it might be a procapsid precursor.

2. The 12S particle and gene B function - The existing data

are compatible with two possible origins for the 12S particle either as an assembly intermediate or as a degradation product or both. It is a known decomposition product of the 111S particle and it can itself degrade to 6S and 9S particles. On the other hand, it has never been observed to form spontaneously from these subunits. Under the various lysis regimes employed in the Results, by Mayol and Sinsheimer (unpublished), or by Tonegawa and Hayashi (65), the 12S particle constitutes a very small proportion of the infection specific label compared to the 6S, 9S, 20S and 111S particles. By comparison Siden and Hayashi (61) have reported that lysis conditions can be found for which the proportion of intracellular 12S particles is much greater. They interpreted this result to mean that the 12S particle had been stabilized from further decompositon to 6S and 9S particles by their procedure.

Alternatively, their conditions may promote the disintegration of the 111S particle to 12S particles. The experiment presented in Figure 11b supports this latter interpretation. Under the very gentle lysis conditions employed there, virtually no 12S or 9S particles are observed in the lysate. The total absence of 9S particles means that the absence of the 12S particle cannot be explained by post-lytic degradation to its 9S (and 6S) subunits. (Under these same lysis conditions most of the gene F protein is found at the faster sedimentation positions indicative of 111S particles or whole phage.) As a consequence one can conclude that, <u>in vivo</u> the 12S particle is either nonexistent or constitutes a very small pool. However it should be noted that a small pool size and a post-lytic origin for most of the 12S particles observed in ϕX lysates do not exclude this particle from a

possible role in the in vivo maturation scheme. Such a pathway is presented in Figure 31b - Pathway 2.

Siden and Hayashi (61) also observed that their expanded 12S particle pool did not form in the absence of gene B function. This led them to suggest that, as outlined in Figure 31b - Pathway 2, gene B protein catalyzes the formation of the 12S capsomer from 9S and 6S subunits. However, given that the 12S particle can be a degradation product of the 111S particle, it is equally likely that the B protein catalyzes the formation of the 111S particle from which the 12S particle is later derived by degradation. If the B protein acts exclusively at the level of 111S particle formation (Figure 31b - Pathway 1), then the 12S particle must be a 111S particle degradation product as all precursors to the 111S particle would, in this case, assemble independently of the B function (for example, see the dotted line in Figure 31b - Pathway 2), and the 12S particle requires B function for its assembly. It could also be that B protein acts at the level of both 12S and 111S particle assembly.

Both Siden and Hayashi (61) and Tonegawa and Hayashi (65) have shown that pulse labeled 12S particles can be chased into phage. However, this result would be obtained with either pathway 1 or 2 as long as the 111S particles do not degrade in vivo. The experiment in Figure 11b suggests that they do not.

Gene B protein, like F, G and D proteins, is also required for SS DNA synthesis (General Introduction). However, unlike the latter three proteins, Siden and Hayashi (61) found that SS DNA synthesis and phage production continued for some time after the removal

of B function by means of a shift to the nonpermissive temperature in a temperature sensitive B-mutant infection. After the shift new phage were matured until some pre-existing pool of phage precursor was used up. (Protein label added at the time of the shift appeared in 6S and 9S particles but was not matured into phage.) Because gene B function was also required for 12S particle formation, they proposed that the 12S particle was serving as the pre-existing pool for the post-shift synthesis of phage. However, as noted above, it is quite likely that any intracellular pool of 12S particles is quite small and could not account for the residual synthesis. The experiment in Figure 8 indicates that the largest subviral repository for phage structural proteins is the 111S particle. (As long as the 12S particle is a precursor of the 111S particle as proposed here, then greater incorporation into the 111S compared to the 12S particle can only mean that the 111S pool is larger in spite of the fact that a pulse label was employed.) The analysis in section X of the Results indicates that this pool is much larger than indicated by the pulse labeling regime. It seems likely therefore that this is the gene B dependent precursor pool from which phage are being matured. Nevertheless it should be noted that the 111S particle pool would still be gene B dependent for its synthesis even if B protein acted at the level of 12S particle formation (Figure 31b - Pathway 2). As a consequence neither pathway 1 or 2 can be excluded by this argument.

3. The fast sedimenting replicative intermediates of SS DNA synthesis- The proposal that the 111S particle serves as a precursor to the residual phage synthesized in a gene B deficient infection is

in agreement with the expected behavior of an F, G and D protein-containing particle on the SS DNA replication process. If in fact the 111S particle does interact with the ϕX RF II or replicative intermediate form DNAs, then it may be this DNA-111S particle complex that was observed in the 70S to 114S region of the sedimentation velocity gradients in Figure 1. Depending upon how much of the replicating DNA in such a complex was exposed to the sedimentation environment, the expected sedimentation velocities could range from those of the free replicative intermediates to in excess of the phage velocity.

The physiological investigations of ϕX F, G and D mutant infections (reviewed in the General Introduction) indicates that all stages of SS DNA replication require the participation of the F, G and D proteins. By comparison, the greatest proportion of the replicating DNAs isolated from the non-deproteinized sedimentation gradients in Figure 1 were found at the velocities expected for the free DNA molecules (Table 4b). As a consequence it seems possible that much of this DNA may have dissociated from the F, G and D proteins (the 111S particle?) with which it must presumably have been complexed in vivo. Depending upon the nature of the DNA-protein interaction in this complex (Appendix C) conditions may still be found for which the majority of the ϕX replicative intermediates sediment at the higher velocities. (There is a major peak of ϕX protein, the 20S peak, that sediments in the velocity range of the SS DNA replicative intermediates, but this peak does not parallel the DNA distribution and has not clearly been shown to be attached to the DNA that cosediments with it.)

4. The pulse labeled antigenic DNA- The radioimmunoassay

experiment in Figure 7 shows that at least some of the "free" replicative intermediate DNAs, but not the "resting" RF II DNA, are associated with ϕX antigens. (Unfortunately, the experimental method could not differentiate whether or not all of the pulse labeled DNAs in the binding region were associated with antigen or only some subpopulation. It is noteworthy, however, that the binding curve parallels the pulsed DNA distribution.) This antigenic association could either be a consequence of the disruption of an F,G,D particle-RIA DNA complex or a precursor to that association or both. The idea of an antigen-RI DNA complex as a prerequisite to association with a larger protein particle is in accord with the extraordinary specificity of the ϕX maturation process for the ϕX plus strand DNA over ϕX minus strands or coinfecting phage DNAs of similar size (see the General Introduction for a complete discussion). Such high specificity DNA-protein interactions are characterized by the binding of the protein moiety to a unique locus on the DNA molecule (203, Appendix C). (The more generalized DNA "coating" reactions proposed for some proteins, gene 32 protein from T4 or gene 5 protein from M13, cannot show DNA specificity as the protein must be able to bind at a large number of different sequences.) It is tempting to speculate that such as association may serve to select a DNA which is then introduced into a 111S procapsid precursor. The introduction of the 5' plus strand end of an RF II molecule into a procapsid would then be a prerequisite to SS DNA synthesis thus accounting for the F, G and D protein dependency of that process.

5. <u>The 140S particle</u>- The similarity in protein composition of the 111S particle and the 140S infectious particle suggests a pre-

cursor-product relationship. However, so far neither this relationship or its direction have been demonstrated. Nevertheless in keeping with the basic precept of going from simpler to more complex particles, the 140S particle has been indicated in Figure 31b as the end result of the 111S particle's association with SS DNA. Weisbeek and Sinsheimer (165) have converted the 140S particle to ϕX virions in vitro thereby suggesting that the 140S particle is the immediate precursor to phage. Since, under some conditions of lysis, they recover 100% of the ϕX infectivity in the form of 140S particles, Weisbeek and Sinsheimer have proposed that the 140S particle is the sole in vivo form of the ϕX infectivity and that the virion itself is the product of a post-lysis transformation of this particle. However a comparison of the pulse and long term labeled DNAs isolated from the phage peak in Figure 1 suggests that this is not the case (see section I for the details of this argument).

6. Particles unaccounted for in the model- Several components of the infection are not accounted for in the proposed assembly scheme in Figure 31b. No role has been proposed for the 20S particle or the 30S decomposition product of the 111S particle though conceivably the latter may be an intermediate in 111S particle assembly. If the 111S particle has the complex structure expected of a procapsid then such intermediates in its assembly must exist. The intracellular state of the 6S and 9S particle pools observed after lysis may consist largely of unstable intermediates of this type.

No attempt has been made to identify the level at which the H, J and A proteins are integrated with the virion. However, it should be noted that Jazwinski (23) has identified a phenol resistant, high

ionic strength resistant, association between the ϕX gene G protein and the virional DNA. The same complex may be responsible for the antigenicity of the ϕX replicative intermediates in as much as that antigen-DNA association is also remarkably stable.

As was noted at the beginning of this section, the model in Figure 31b is proposed only as a working hypothesis. Although the circumstantial evidence for many of its features is compelling, most of the pathways proposed have yet to be established by direct experimentation. It is hoped that this task will be easier now that subviral particles filling the entire complexity spectrum from monomer proteins to completed phage have been identified and characterized.

TABLES

TABLE 1

70S particle - The percentage of total 70S pulse label that cannot be accounted for by the 70S lysis artifact

Experiment Number	Duration of Pulse	
	5 seconds	90 seconds
1*	88	52
2	80	43
3	87	47
4	--	46

*Data are from Figure 1 (a,b)

LEGEND TO TABLE 1

Infected cells were continuously labeled during the late stage of the infection and then pulse labeled as described in the legend to Figure 1 (a,b). The ratio of the continuous label in 70S material to that in phage was compared with the ratio obtained with the pulse label. The percentage of total 70S pulse that could not be accounted for by the 70S lysic artifact was computed for four separate experiments. The calculation is described in detail in the Results.

TABLE 2

Phenol extraction - Recovery of pulse and continuous DNA labels after phenol deproteinization

[Samples are from Figure 1 (a,b)]

		Pooled Fractions from 5 Second Pulse			
		A_1	B_1	C_1	D_1
Fractional Recovery	^3H	.98	.62	.65	.62
	^{14}C	.71	.72	.64	.68
		Pooled Fractions from 90 Second Pulse			
		A_2	B_2	C_2	D_2
	^3H	.66	.50	.64	.39
	^{14}C	.81	.65	.74	.58

LEGEND TO TABLE 2

The fractions indicated (A_1 through D_2) in Figure 1 (a,b) were pooled and deproteinized as described in the Methods. The recovery of input DNA label was monitored at the end of the procedure and is expressed as the fraction of input cpm.

TABLE 3

"Heavy DNA" - The distribution of pulse label into the "heavy DNA" species isolated from various regions of the gradients in Figure 1 (a,b)

Gradient position	Region A		Region B		Region C	
Pulse time in seconds	5	90	5	90	5	90
Fraction of total incorporation into heavy DNA	0.071	0.023	0.183	0.076	0.189	0.141
Ratio of heavy DNA incorporation to incorporation into RFII and RI DNA forms	.18	.28	.31	.42	.28	.35

LEGEND TO TABLE 3

The distribution of pulse label into the heavy DNA isolated from regions A, B and C of the gradients presented in Figure 1 (a,b) [identified by PDI banding in Figs. 2 (a,c), 3 (a,c), and 4 (a,c)], was computed as both the fraction of total pulse label cpm incorporated and as the ratio of the "heavy DNA" incorporation to that into the RF II and RI form DNAs in the same gradient.

TABLE 4

φX174 DNA distributions in nondeproteinized lysates

A. The percentage distribution of pulse label and continuous label into various regions of the gradients in Figure 1 (a,b)

Experiment	Region of Gradient			
	A	B	C	D
5 second pulse ^{3}H	4	8	38	36
Continuous ^{14}C	49	13	21	6
90 second pulse ^{3}H	20	11	33	22
Continuous ^{14}C	40	11	30	7

B. The percentage distribution of pulse labeled SS, RF, and "heavy" DNA forms in the gradients in Figure 1 (a,b)

DNA Species	Region of Gradient									
	5 second pulse					90 second pulse				
	Total* Gradient	A_1	B_1	C_1	D_1	Total* Gradient	A_2	B_2	C_2	D_2
SS	8.1	18.5	17.2	46.9	17.3	44.7	38.9	17.4	31.8	11.9
RF	62.8	2.5	7.6	41.1	48.7	32.9	4.9	6.1	40.1	48.9
heavy	11.4	2.6	12.3	63.2	21.9	5.9	6.8	15.3	80.0	0
RF + heavy	74.2	2.6	8.4	44.5	44.6	38.8	5.2	7.5	45.9	41.5

* Percentage of total gradient pulse label in this species

LEGEND TO TABLE 4

A. The total cpm within the regions A, B, C and D of the two sedimention velocity gradients in Figure 1 (a,b) were individually summed for each isotope and the percent of the total cpm in the entire gradient computed.

B. The percentage distributions of pulse labeled SS, RF, heavy and RF plus heavy DNA forms in Figure 1 were computed by multiplying the percentage distribution of total pulse label in each region (Part A) by the fractional DNA composition of that region as determined in the PDI resedimentations in Figures 2 - 5 to give the percentage of the total pulse of each molecular species in each region. The latter values were summed for a given DNA species over all regions to give the percentage of the total pulse label in that DNA form (column labeled "Total Gradient"). The percentage distributions of each DNA form in each region were then computed as the fraction of the percentage of the total pulse label in that DNA form that is found in each region.

TABLE 5

Radioimmunoassay - Characterization of the serum binding pattern observed in Figure 7

Value Calculated	Isotope	Gradient Position			
		A	B	C	D
1. Percentage distribution of centrifuged label	^{3}H	29	8.1	26	28
	^{14}C	64	6.4	8.7	5.9
2. Percentage distribution of serum bound label	^{3}H	30	20	25	6.7
	^{14}C	44	9.2	17	7.5
3. Binding efficiency-Fraction of input label bound by serum	^{3}H	0.022	0.051	0.019	0.005
	^{14}C	0.052	0.11	0.14*	0.097*
4. Relative binding efficiency - serum binding relative to the 11$4$S peak (A)	^{3}H	1.00	2.3	0.90	0.23
	^{14}C	1.00	2.1	2.8*	1.9*
5. Relative binding efficiency of pulse vs. long label - normalized to the 11$4$S peak (A)		1.00	1.1	0.33*	0.12*
6. Nonspecific absorption-ratio of nonspecific ^{3}H absorption to specific absorption	^{3}H	0.16	0.098	0.36	0.36
	^{14}C	0.24	0.11	0.30*	0.30*
7. Relative nonspecific absorption-normalized to 11$4$S (A)	^{3}H	1.00	0.61	2.2	2.3
	^{14}C	1.00	0.45	1.3*	1.3*

*Values are based on low count rate data

LEGEND TO TABLE 5

The total cpm before radioimmunoassay and after radioimmunoassay for both serum and control tubes were summed under each of the four regions designated in Figure 7 [as A, B, C and D by analogy to Fig. 1 (a,b)]. These values were then employed in conjunction with the total gradient cpm of each isotope, and the relative counting efficiencies of the two scintillators used, to calculate the information presented in 1-7. ^{3}H and ^{14}C data were computed separately.

1. Percentage distribution of centrifuged label - The percentage of the total cpm recovered from the velocity sedimentation was computed for each region.

2. Percentage distribution of serum bound label - The percentage of the total cpm bound by the radioimmunoassay was computed for each region.

3. Fraction of input label bound by serum - For each region of the gradient the total cpm bound to serum coated vials was divided by the total cpm added to the vial after correcting for differences in the counting efficiencies associated with the two counting methods employed (see legend to Fig. 7).

4. Specific activity of serum binding relative to the 11$\frac{1}{2}$S peak (A) - The binding efficiency of each region was compared to that of the phage peak by dividing the binding efficiency of each region as calculated in (3) by the binding efficiency of the phage peak as calculated in (3).

5. Relative binding efficiency of pulse vs. continuous label - The relative binding efficiency of pulse vs. continuous label was computed for each region in the gradient by dividing the binding efficiency computed for the pulse in (3) by the binding efficiency computed for the continuous label in (3). These ratios were then compared to that obtained for the ϕX peak by dividing the value obtained in all regions by that obtained for the ϕX peak.

6. Nonspecific absorption - The total cpm that bound to control vials was divided by the total cpm that bound to serum vials in each region.

7. Relative nonspecific absorption - The fraction of nonspecific absorption observed for each region was compared to that observed for the ϕX peak by dividing the values obtained in all regions by that obtained for the ϕX peak.

TABLE 6

Radioimmunoassay - The calculated antigen concentration in antigenic particles/ml of the peak fractions assayed for serum binding from the gradient in Figure 7

Gradient Region	Fraction Number of Sample Analyzed	Antigenic Species Expected in this Region	Computed Antigen Concentration in the Assay Vial (Particles/ml)	Basis for Computation (See legend for detailed explanation)
A	- 10	Whole phage	a. 4.7×10^{11} b. 2.4×10^{11}	Expected burst ^{14}C thymine incorporation
B	- -	70S lysis artifact	a. 5.6×10^{10} b. 2.0×10^{10}	^{14}C thymine distribution between 114S and 70S peak
C	36 36	Replicative intermediates	a. 2.3×10^{9} b. 3.3×10^{10}	Incorporation of ^{3}H thymidine Spec. Act. from thymidine (tdr) Spec. Act. from tdr + thymine
	36 36	20S protein particle	c. 1.2×10^{9} d. 1.0×10^{11}	From Figure 8 (b), Table 22 Particulate F and RI conc. in (a) Monomer F and RI conc. in (b)
	36 36	Total antigens	e. 3.5×10^{9} f. 1.3×10^{11}	Minimum from a and c Maximum from b and d
D		RF II DNA	a. 8.0×10^{9} b. 4.5×10^{10}	Incorporation of ^{3}H thymidine Spec. Act. from thymidine alone Spec. Act. from tdr + thymine

LEGEND TO TABLE 6

The antigen concentrations of four samples selected from the peaks of ^{3}H thymidine incorporation of Figure 7 were calculated in the manner described below and expressed as antigenic particles per ml in the radioimmunoassay sample. (This means that in each case the particle concentration in the gradient has been corrected for dilution into the assay vials.)

Region A a. The phage particles/ml was calculated on the basis of an expected burst of 1000 particles/cell and a 75% recovery under the lysis conditions used. These particles were assumed to be distributed over three fractions in the 114S peak. b. The phage concentration in the peak fraction (10) was calculated from the total ^{14}C thymine incorporation in this fraction and the specific activity of ^{14}C thymine.

Region B The concentration of 70S lysis artifact was estimated from the relative incorporation of ^{14}C leucine into the 114S peak and the 70S peak in the experiment in Figure 8a, assuming the same specific activity of labeling for both particles. It was then assumed that these particles were distributed over five fractions. Values a and b were computed from a and b in region A, respectively.

Region C The concentration of replicative intermediates was calculated as SS DNA equivalents of ^{3}H thymidine incorporation into fraction 36 assuming uniform incorporation into plus strand DNA only. Each DNA molecule was assumed to represent one antigenic particle. The fact that most molecules have more than one SS equivalent

of plus strand was not considered. Values (a) and (b) were calculated assuming, respectively, a ^{3}H thymidine specific activity based upon the thymidine concentration of the media alone or the summed concentrations of thymidine and thymine.

The concentration of ϕX174 20S particle was calculated from the molecular ratio of ϕX specific proteins to pulse labeled DNA in region C of the gradient. This value was computed in conjunction with the experiment in Figure 8b and was obtained from Table 22. The same ratio, 0.52 phage equivalents of phage gene F protein/phage equivalent of SS DNA, was assumed to apply here. Value (c) was calculated assuming the concentration of replicative intermediates given in (a) and that one phage equivalent of gene F protein is associated with each antigenic particle. Value (d) is calculated assuming the concentration of replicative intermediates given in (b) and that only one F protein molecule (1/60 of one phage equivalent) is associated with each antigenic particle.

The minimum value, (e), of total antigen concentration, is obtained by summing values (a) and (c). The maximum value (f) is obtained by summing values (b) and (d).

Region D Although no phage antigens are indicated in this region, the molecular concentration of the RF II was calculated to give an idea of the relative concentration of these molecules and demonstrate that the failure to detect binding probably was not due to saturation of the assay. The concentration of the RF II DNA was calculated as before on the basis of the ^{3}H thymidine incorporation assuming in (a) and (b) respectively that the ^{3}H thymidine specific

activity was a function of the thymidine concentration alone or the summed concentrations of thymidine and thymine.

TABLE 7

Radioimmunoassay - Relative efficiency of the assay in TM buffer compared to the standard assay buffer

	Buffers	
	Standard Assay Buffer	TM Buffer
Percent of input cpm bound to the serum coated tube	37	44
Percent of input cpm bound to the control tube	3	2.5

LEGEND TO TABLE 7

Identical aliquots of highly purified ^{3}H leucine labeled ϕXam3 phage were added to serum coated and control vials prepared according to the Methods and containing the standard radioimmunoassay buffer, 0.05 M-Tris-phosphate, 0.01 M-KCl, pH 8.0 or TM buffer, 0.05 M-Tris-chloride, 0.05 M-KCl, 0.008 M-$MgCl_2$, pH 7.2. Duplicate determinations were made for each value. The incubation was carried out for 20 hr at 37°C with gentle agitation. The vials were then washed and counted as described in the Methods. Nuclear Associates Linear Polyethylene vials were employed and counting was performed with TLNCS fluor.

TABLE 8

BSA carrier - Effect of BSA carrier on percent recoveries from resedimentation experiments

Experimental Conditions	Radioactively Labeled Molecular Species					
	^{3}H-thymidine ϕX174		^{14}C-leucine protein		^{32}P RFI & II form DNA	
	range	average	range	average	range	average
Without BSA	75-88	81	14-20	18	60-95	77
With BSA (.01%)	96-100	100	83-94	90	86-97	90

LEGEND TO TABLE 8

The pooled fractions from the 114S and 111S peaks of experiments like that in Figure 8a were resedimented under a variety of ionic conditions, as described in the text and the legend to Figure 9, either with or without BSA added as carrier. The percent recoveries of total input cpm were computed.

TABLE 9

Resedimentation of the 111S peak - Percentage distribution of protein label after resedimentation of the 114S to 111S peak in various buffers (Figure 9)

	Sample Number and Buffer Composition*							Averages	
	1	2	3	4	5	6	7		
Molarity KCl	0.05	0.05	0.30	0.30	1.00	1.00	1.00	Samples	Samples
Mg^{++} or EDTA*	Mg^{++}	EDTA	Mg^{++}	EDTA	Mg^{++}	EDTA	EDTA	1,2,3 & 4	5 & 6
% Sarkosyl	0.0	0.0	0.0	0.0	0.0	0.0	0.5		
Protein Particle									
Pellet	27.6	27.7	33.9	31.9	25.7	23.4	18.9	30.3	24.5
∿30S	0.0	0.0	0.0	0.0	11.6	13.9	18.7	0.0	12.8
12S	0.0	0.0	0.0	0.0	0.0	0.0	14.2	0.0	0.0
9S	18.4	18.8	15.7	18.2	17.7	16.6	1.4	17.8	17.2
6S	30.2	30.3	29.8	29.4	30.7	29.4	24.2	29.9	30.0
2.5S	5.5	6.4	8.3	8.0	6.1	9.6	17.3	7.0	7.9
Ratio: Protein cpm/DNA cpm in the pellet†	0.190	0.186	0.158	0.145	0.107	0.113	0.068	0.170	0.110
Non - ϕX fraction of pellet	0.64	0.63	0.57	0.53	0.36	0.40	0.00	0.60	0.38
Percent of total gradient cpm in non - ϕX pellet	17.7	17.4	19.3	16.9	9.2	9.3	0.0	18.2	9.3
Percent of total gradient 111S cpm in pellet	24.6	23.9	26.4	23.3	12.2	11.8	0.0	25.0	12.0

*All buffers contain 0.05 M-Tris-HCl, pH 7.2 and BSA at 0.01%. Buffers containing Mg^{++} are 0.008 M in $MgCl_2$. Buffers containing EDTAare 0.008 M in $MgCl_2$ and 0.013 M in EDTA.

†When these experiments were performed in the absence of BSA only the phage peak was recovered and the ratio of protein cpm/DNA cpm was 0.064.

LEGEND TO TABLE 9

The leucine label in each of the peaks in the sedimentation gradients in Figures 9b, 9c and 9d was summed and compared to the total leucine label recovered from the same gradient to obtain the percentage distribution of leucine. The ratio of the ^{14}C-leucine cpm to the ^{3}H-thymidine cpm in the peak at the bottom of each gradient is given at the bottom of the table. It was assumed that the minimum protein cpm/DNA cpm ratio observed in sample 7 (0.068) or after resedimentation in the absence of BSA carrier (0.064) is the ratio in the phage alone. Then, given that the recovery of the thymidine label is close to 100% in each sample (Table 8), that virtually 100% of the thymidine is found in the pellet fractions, and that $\geq$90% of the pelleted thymidine label is in ϕX SS DNA and presumably in phage (see Fig. 2c), the fractional distribution of protein label into the ϕX (whole virus) and non-ϕX (the 111S particle or its breakdown products) components of the pellet was computed by dividing the protein/DNA ratio of ϕX (0.068) by the pellet ratios observed in samples 1-6. Multiplying the percent of total gradient protein cpm that is observed in the pellet by the fraction of non-ϕX protein in the pellet one obtains the percent of total gradient cpm in the non-ϕX pellet component.

A similar calculation can be performed comparing the protein/DNA ratio of whole phage (0.068) with that of the whole sample (0.45) in which case only 15% of the protein label from the combined 114S and 111S peaks in Figure 8a is found to be in phage. This is in good agreement with the results presented here.

The percent of total gradient 111$ cpm (exclusive of phage cpm) that is found in the pellet is computed by dividing the percent of the total gradient cpm in the non-ϕX pellet component by the sum of the percent total gradient cpm in all non-ϕX components.

TABLE 10

Relationship of the 9S and 12S particles in Figure 9

A. A quantitative comparison of the 2.5S, 6S and 9S particles observed after resedimentation of the 111S non-phage particle with those observed in whole lysates

Source of Material	% Distribution of Total Leucine			Ratio
	Particles			
	2.5S	6S	9S	6S/9S
1. Sedimentation of whole lysates (Figure 8b)	27.0	15.7	9.6	1.64
2. Resedimentation of 111S non-phage particle (Figure 9b and Table 9, average nos. 1-4)	7.0	29.9	17.8	1.68
	Proteins			
	D	G	F	G/F
3. Whole phage†	.1	24	69	.35
4. 12S particles*	-	-	-	.35

†(Rohwer, R., unpublished)

*12S particles have the same G/F ratio as phage (Siden, E., & Hayashi, M., reference 61)

(continued next page)

TABLE 10 - continued

B. Computation of the expected redistribution of the 9S and 6S peaks into the 12S peak in Figure 9d and Table 9

	Percent
% of total leucine formerly in the 9S peak	17.8
% G protein required for quantitative conversion of the 9S peak to 12S (17.8)(.35) =	6.2
% of 6S peak redistributed in Figure 9d, Table 9	5.7
% of combined F and G protein expected at 12S position	24.0
% of total leucine incorporation observed at 12S	14.2

LEGEND TO TABLE 10

The ratio of 6S and 9S particles from the whole lysate in Figure 8b was compared with that for the average resedimentation pattern of samples 1 through 4 (Figure b, Table 9) of the 111S non-phage particle, and the ratio of G/F protein in purified phage. This latter value is that expected for 12S particles as well (61). Using this ratio the expected loss from the 6S peak was computed assuming that the 9S peak was quantitatively converted to 12S particles.

TABLE 11

Protein composition of the 111S particle, 70S particle, and particle B from Figure 8b

	Major Particle Components		
	F	G	D
A Purified Phage-continuously labeled†			
Leucine distribution**	69	24	.1
Molecular weight+	50000	20500	14500
Stoichiometry*	1.0	0.85	0.005
B 111S Particle-from decomposition products			
Leucine distribution-total leucine	17.8	29.9	7.0
Leucine distribution-from 9S, 6S and 2.5S peaks only	31.4	52.7	12.3
Stoichiometry	1.0	4.1	1.4
C 111S Particle-from electrophoresis of combined 111S and 114S peaks-Figure 12			
Leucine distribution-total leucine	19.5	17.3	37.2
Leucine distribution-nonphage leucine	12.6	14.9	37.2
Stoichiometry	1.0	2.9	10.0
D 111S Particle-from electrophoresis of fraction A (Figure 8b) - see Figure 13			
Leucine distribution-total leucine	30.6	13.3	25.8
Leucine distribution-nonphage leucine	23.7	10.9	25.8
Stoichiometry	1.0	1.1	3.7
E 70S Particle-from electrophoresis			
Leucine distribution-total leucine	32.7	22.3	17.0
F Particle B from Figure 8b			
Leucine distribution-total leucine	13.1	16.3	30.0
Stoichiometry	1.0	3.0	7.9

†Rohwer, R., unpublished experiments

**Distributions are percents

+Data are from Table 1 (General Introduction) - molecular weights are in daltons.

*All stoichiometries are molar stoichiometries normalized to gene F

LEGEND TO TABLE 11

The composition of the 111S particle was computed from the distribution of radioactive leucine into the degradation products of this particle upon resedimentation and from the protein composition of the combined 111S and 114S peaks from gradients like that in Figure 8a.

A. The percent distribution of a continuous leucine label into the F, G and D proteins of the purified phage , the molecular weight of these proteins and the molar ratios normalized to gene F product are given for comparison. Data are from Table 1, General Introduction, and from unpublished experiments by the author.

B. The composition of the nonphage 111S material was computed from the distribution of leucine label into the degradation products from the resedimentation of the 114-111S peaks. It is assumed that the 9S, 6S and 2.5S peaks are composed solely of F, G and D protein, respectively, and that no material is lost in the resedimentation. The molecular proportions of these three proteins were then computed by dividing the mass distribution between the three peaks by the molecular weights of the appropriate proteins in each peak and normalizing the result to the value obtained for gene F product.

C. The composition of the nonphage particle at 111S was computed from the leucine distribution into the SDS acrylamide gel electrophoresis pattern of the combined 114S and 111S peaks (Figure 12). The phage contribution of total leucine incorporation was taken to be 10% from a comparison of the protein/DNA ratio in the 114S to 111S peaks before 0.65 and after 0.064 resedimentation in the absence of BSA carrier. The 10% phage contribution was then divided among the F,

G and D proteins according to the distribution of leucine label in purified phage (see A above). The phage contributions to the F, G and D peaks were then subtracted from the total distribution which was then taken to be the composition of the nonphage particle.

D. The calculation in C was performed on the gel electrophoresis pattern (Figure 13) obtained from fraction A in Figure 8b. In this case the pattern contained 114S, 111S and 70S particles but the same assumptions were applied.

E. The percentage distribution of the total leucine incorporation into the F, G and D proteins of the 70S particle was determined by SDS acrylamide gel electrophoresis of the pooled fractions from the 70S region of a gel as described for the 114S-111S region in the legend to Figure 12.

F. The percentage distribution of the total leucine incorporation into the F, G and D proteins of the particle at position B in the sedimentation velocity gradient in Figure 8b was determined by SDS acrylamide gel electrophoresis (Figure 14). The molecular ratios of the proteins in this particle were calculated assuming no contamination from other structures.

TABLE 12

Distribution of pulse labels between cytoplasm and debris in Mg^{++} lysed cells. Redistribution after resedimentation of the debris fraction (Figure 10)

Isotope	% of Pulse Label Retained by Debris Fraction			
	Original Lysate	After Resedimentation*		
		a	b	c
Uninfected				
^{3}H-leucine	5	75	68	4
Infected				
^{14}C-leucine	22	55	40	26
Δ^{14}C-leucine		63	22	60
^{3}H-thymidine	9	42	9	9

*The conditions used are those in Figure 10. All samples originated in TM buffer and were adjusted to the ionic conditions below as described in the legend to Figure 10.

(a) TM buffer
(b) TM buffer - 0.30 M-KCl, 0.005 M-EDTA (net)
(c) TM buffer - 1.00 M-KCl, 0.005 M-EDTA (net), 0.5% Sarkosyl

LEGEND TO TABLE 12 - Data are from Figures 10a,b,c. The percent distribution of the total TCA precipitable protein and DNA pulse labels between the debris fraction and the cytoplasm in the initial lysate was determined from TCA precipitated aliquots of both the lysis supernatant and the resuspended debris. The debris fraction was that fraction of the total radioactivity recovered in or on the CsCl shelf at the bottom of the gradient.

TABLE 13

Percent distribution of leucine among the protein components of infected and uninfected 20S peaks

Source of the 20S Peak			Protein Components										
Gradient	Figure	Number of Gels Averaged	Uninfected										
			U_1^{20}	U_2^{20}	U_3^{20}	U_4^{20}	U_5^{20}	U_6^{20}	U_7^{20}	U_8^{20}			
Uninfected lysate from Figure 8b	16	3	1.5	6.6	38.8	1.7	3.3	5.6	13.9	23.9			
Infected lysate from Figure 8b	16	3	Infected										
				U_2^{20}	U_3^{20}	F	I_1^{20}	I_2^{20}	I_3^{20}	I_4^{20}	I_5^{20}	I_6^{20}	I_7^{20}
				1.3	54.1	12.1	3.1	1.9	3.3	1.8	1.8	2.5	12.3
Resedimentations of Infected 20S Peak in Figures 18 and 19													
20S Peak	20a	3			72.8	10.1				[——— 4.0 ———]			4.2
Shoulder of 20S Peak	20b	1			28.2	9.0				[——— 10.6 ———]			19.9

LEGEND TO TABLE 13

The leucine distributions among the protein components of the 20S peaks in Figures 16 and 20 were computed as percent of total leucine recovered from the SDS acrylamide gels. Where possible the averages of several gels are presented. When present the ^{3}H-thymidine contribution to the ^{3}H-labeling pattern in a gel was subtracted before the calculation.

TABLE 14

Infection specific stimulation of 20S particle production and host protein U_3^{20}

	Infection Specific Stimulation*	
	20S Particle Fractional Increase	Protein U_3^{20} Fractional Increase
A 20S Particles from sedimentation velocity gradients		
Source of 20S particles		
1. Figure 8b	6.9	10.1
2. Figure 11a	2.4	2.8
3. Figure 11b	3.2	5.1
B Protein U_3^{20} from SDS acrylamide gel electrophoresis of the 20S particle from Figure 8b in Figure 16a		
Source of minimum ratio (see legend)		
1. Velocity gradient Figure 8b		6.3
2. Host protein peaks U_2^{20} and U_6^{20} from Figure 16a		4.0

*Expressed as infected cpm/uninfected cpm in the species of interest

LEGEND TO TABLE 14

The infection specific stimulation of 20S particle production and the synthesis of host protein U_3^{20} was calculated and expressed as the ratio of infection specific cpm/uninfected cpm in the species of interest. This calculation circumvented the problems associated with differences in specific activities of labeling, counting efficiencies, and the specific number of infected and uninfected cells being compared. By analogy with the $\Delta^{14}C$ calculation of Mayol & Sinsheimer (8, see Methods), the minimum ratio of infected to uninfected label was selected in each of the gradients or gels listed, if possible at the locus of known host proteins or no known ϕX proteins. Multiplying this ratio times the uninfected cpm at any other locus in the gradient gave the host contribution to the infected cpm at that point. To obtain the infection specific stimulation of incorporation at that locus the total infected cpm at that position was divided by the uninfected contribution to that total, i.e.:

$$[\text{infection specific stimulation of incorporation}] = \frac{(\text{infected cpm})}{R\ (\text{uninfected cpm})}$$

where R is the ratio of uninfected label in infected versus uninfected cells.

A. This calculation was performed on the integrated 20S peaks in the figures listed. In Figure 8b the integrated infected peak, fractions 25-30, was compared with the integrated uninfected peak sedimenting just behind it, fractions 27-32.

The stimulation of the U_3^{20} protein component of the 20S particles was computed from the relative percent composition of U_3^{20}

protein in the infected vs. the uninfected particle obtained from SDS acrylamide gels of the particles. The data for the 20S particle from Figure 8b are presented in Table 13.

B. This calculation was performed on the integrated peak of U_3^{20} protein in Figure 16a. The minimum ratio in the first calculation was derived from that obtained from the parent velocity gradient of this 20S particle, Figure 8b, after correcting for the differences in counting efficiencies for ^{3}H and ^{14}C in the two assay systems employed and for the fact that the ratio of infected to uninfected sample applied to the gel was twice that obtained from the sucrose gradient.

The minimum ratio utilized in the second calculation is that associated with host peaks U_2^{20} and U_6^{20} from the SDS acrylamide gel electrophoresis itself.

TABLE 15

The relative sedimentation positions of the protein and DNA components of the 20S peak after recentrifugation

No.	Experimental Conditions				Relative Sedimentation Positions				Approximate S Values	
	Substitutions to TM Buffer†		Incubation at 37°C	Other	RFI	Protein Peak*	DNA Peak*	RFII	Protein*	DNA*
	KCl	EDTA								
1**	0.05	Mg^{++}	-		1.0	0.86	0.86	0.0	20.3	20.3
2	0.05	Mg^{++}	-	repeat	1.0	0.59	0.12	0.0	19.0	16.6
3	0.05	Mg^{++}	+		1.0	0.67	0.11	0.0	19.4	16.6
4	0.05	EDTA	+		1.0	0.71	0.12	0.0	19.6	16.6
5	0.30	Mg^{++}	+		1.0	0.50	0.056	0.0	18.5	16.3
6	0.30	EDTA	+		1.0	0.50	0.13	0.0	18.5	16.7
7	1.0	EDTA	+		1.0	0.29	0.14	0.0	17.5	16.7
8**	0.05	Mg^{+}	+	RNase	1.0	0.79	0.29	0.0	19.9	17.5
9**	0.05	Mg^{+}	+	DNase	1.0	0.72	-----	0.0	19.6	----

*Only the positions of the major peaks sedimenting between the RFI and RFII markers are given.

**These samples do not contain internal RFI and RFII markers.

†All buffers contain 0.05 M-Tris-HCl pH 7.2 and 0.008 M-$MgCl_2$. Buffers containing EDTA are 0.013 M in EDTA.

LEGEND TO TABLE 15

The relative sedimentation positions of the major protein and DNA components of the 20S peak from the infected gradient in Figure 8b were computed after the recentrifugations conducted in Figures 18 and 19. The distance between the RFII and RFI marker DNAs was taken as 1.0 and the separation of the peak fraction of the "20S particle" protein or DNA moiety computed as a fractional distance migrated from the RFII to the RFI position.

Approximate S values for the "20S particle" components were computed assuming S values of 16.0 and 21.0 for RFII and RFI, respectively, under all conditions utilized. It was also assumed that a linear relationship exists between sedimentation position and S value. This is true for samples 1, 8 and 9 for which linear sucrose gradients were employed. However, it is a much poorer approximation for samples 2 through 7 which were sedimented through exponential isokinetic sucrose gradients.

TABLE 16

Percentage distribution of protein label after resedimentation of the 20S peak in various buffers (Figures 18 and 19)

No.	Experimental Conditions					Region of the Gradient				
	Substitutions to TM Buffer†		Incubation at 37°C	Other	Figure	Bottom I*	20S II	20S Shoulder III	Next to Top IV	Top V
	KCl	EDTA								
1	0.05	Mg^{++}	-		18a	1.6	61.5	9.8	6.0	12.2
2	0.05	Mg^{++}	-	repeat		0.5	76.4	6.4	3.2	6.4
3	0.05	Mg^{++}	+		18b	0.6	75.4	7.0	2.5	7.7
4	0.05	EDTA	+			1.1	68.6	7.0	9.9	5.5
5	0.30	Mg^{++}	+			0.3	74.7	6.5	4.2	7.7
6	0.30	EDTA	+			0.6	71.4	7.0	6.1	8.2
7	1.00	EDTA	+		18c	0.05	71.5	8.3	4.3	9.0
8	0.05	Mg^{++}	+	RNase	19a	4.3	75.4	3.9	3.9	5.6
9	0.05	Mg^{++}	+	DNase	19b	2.6	76.5	4.3	3.3	5.2
Average						1.3	72.5	6.7	4.8	7.5

†All buffers contain 0.05 M-Tris-HCl pH 7.2 and 0.008 M-$MgCl_2$. Buffers containing EDTA are 0.013 M in EDTA.

*Numerical designations are those in Figure 19b.

LEGEND TO TABLE 16

The leucine label in each of the indicated peaks in each resedimentation gradient was summed and compared to the total leucine label recovered from the same gradient to obtain the percentage distribution of leucine into that peak. Some of the differences in distribution observed may be the consequence of different quench sensitivities to sucrose of the various counting methods utilized. Sample 1 was counted in a dioxane fluor. Samples 8 and 9 were counted in TL after being spotted and dried on paper filters. All other samples were counted in Aquasol.

TABLE 17

A comparison of the distributions of leucine and lysine in ϕX174 proteins from whole lysates of UV-irradiated wt infected host cells[†]

Gene Product	Percent Distribution		Ratio* Lysine/Leucine
	Leucine	Lysine	
A'	1.6	2.2	1.7
F	30.8	24.5	1.0
H and A	5.9	8.3	1.8
G	19.5	18.3	1.2
D	26.0	24.3	1.2
J region	5.2	10.8	2.6

[†]Data are from Figure 23.

*The ratio is normalized to that for gene F product.

LEGEND TO TABLE 17

The percent distribution of ^{14}C-leucine and ^{3}H-lysine incorporation into the ϕX gene products resolved in the SDS acrylamide gel co-electrophoresis of the differentially labeled lysates of ϕX174 wt infected, UV-irradiated, H502 host cells in Figure 23 is computed on the basis of the total label of each type recovered from the gel.

TABLE 18

The ϕX specific protein composition of whole lysates-The percent distribution of lysine incorporation into infection specific proteins in UV and non-UV irradiated hosts infected with wt, am3, am86, and am18 ϕX strains and labeled for various time periods

Number	ϕX174 Infecting Strain	Labeling Period Minutes†	Number of Gels Averaged	Figures	Protein Peaks from SDS Acrylamide Gel Electrophoresis*															
					I_1	I_2	I_3	A' or I_4	F	H	A	?	?	?	G	?	B	D	?	?	J(?)
	UV-Irradiated Hosts																			
1	wt	30-90	10	24,25,26				2.2	25.0	3.7	4.6	1.0	1.5	1.4	10.1	3.2	4.7	20.9	3.0	5.7	8.3
2	am3	30-90	1	None				1.7	25.5	5.1	3.5	0.6	2.2	0.9	12.2	4.4	4.7	20.2	3.0	5.5	7.6
3	am86	30-90	2	24				0.8	28.4	4.3	5.3	1.1	1.4	0.7	11.3	3.5	12.3	17.1	3.0	3.8	3.9
4	am18	30-90	2	24				1.0	31.5	3.6	1.4	1.4	2.0	0.8	14.7	3.8	10.0	17.3	2.4	2.8	4.2
	Non-UV-Irradiated Hosts																			
5	am3	0-18	2	27		3.6	2.6	2.0	26.5	3.3	5.5	1.8	2.9	0.8	10.6	2.2	5.0	17.1	3.4	5.3	5.9
6	am86	0-18	2	27		4.5	1.8	1.4	21.3	[-2.7	6.0-]	0.8	2.6	1.4	8.1	3.7	8.1	14.3	[-	8.3	-]6.8
7	am18	0-18	2	27		6.3	4.0	0.5	24.3	[-2.2	4.3-]	2.1	3.0	0.9	12.3	2.9	7.2	15.6	3.2	3.2	4.7
8	am3	0-140	2	28		5.0	3.0	0.6	33.4	5.2	3.4	0.5	1.4	0.8	12.4	1.0	2.7	17.3	1.7	[-4.5	5.7-]
9	am86	0-140	1	28	1.6	8.6	5.5	0.1	23.1	[-2.4	4.4-]	2.7	2.6	2.1	9.8	1.6	6.3	15.3	4.3	2.4	4.9
10	am18	0-140	1	28		10.6	7.3	0.1	23.0	[-5.6	5.3-]	2.0	2.7	2.1	11.7	1.9	1.9	15.2	3.1	1.7	4.5
11	am3**	0-90	1	None		2.9	1.7	1.4	43.6	3.8	4.0	0.4	1.6	0.4	11.8	1.5	1.1	11.4	2.3	1.3	5.3

*Peak assignments are those indicated in Figures 24a and 27a. A (?) indicates a peak of unknown or uncertain identity.

Brackets indicate that the two or more peaks included within were not resolved by the gel. If only one number is present between the brackets it indicates that a single peak has replaced the peaks indicated by the bracket.

†Time zero is the time of infection.

**This infection was labeled with radioactive leucine instead of lysine.

LEGEND TO TABLE 18

The percent distribution of radioactive lysine incorporation into infection specific proteins was computed relative to the total infection specific incorporation recovered from the SDS acrylamide gels. In the infection of UV-irradiated cells this is the same as the total incorporation. In the infection of non-UV irradiated cells the infection specific incorporation must be calculated from comparisons of uninfected and infected lysates.

All experiments utilizing the UV system were performed as in Figure 24. Experiments in the non-UV system were performed as in Figures 27 and 28. Experiment number 11 was conducted as in Figure 27 except that radioactive leucine (at the same concentration and specific activity) was substituted for lysine, and the infection was allowed to proceed for 90 minutes.

The peak assignments used in this table are given in Figure 27a. The three peaks indicated by question marks between A and G protein are not always clearly resolved, in which case the cpm at the respective loci were summed anyway. The three peaks between D and J(?) protein and including J(?) protein are usually only resolved as shoulders or assymmetries of the J(?) peak. However, in the case of the am86 infection two well resolved peaks are observed here. In the case of the am86 and am18 infections of non-UV irradiated hosts, only one peak is observed in the H-A region of the gel moving between the H and A peaks but closer to the A peak. In this case the incorporation under the shoulder of this peak at the normal H protein mobility is summed separately. The lack of a distinct peak at the H position is indicated by brackets linking the H and A positions.

TABLE 19

Identification of the A' locus-The relative incorporation of radioactive l-lysine into the A' locus relative to incorporation into F protein as a function of the infecting ϕX strain and labeling conditions

Number	ϕX Infecting Strain	Labeling Period Minutes	Figures	Ratio A'/F	Normalize to No. 1
		UV Irradiated			
1	wt	30-90	24,25,26	.088	1.00
2	am3	30-90	None	.068	.78
3	am86	30-90	24	.028	.32
4	am18	30-90	24	.032	.36
		Non UV Irradiated			
5	am3	0-18	27	.076	.86
6	am86	0-18	27	.066	.75
7	am18	0-18	27	.021	.23
8	am3	0-140	28	.018	.20
9	am86	0-140	28	.0043	.05
10	am18	0-140	28	.0043	.05
11	am3*	0-90	None	.033	.38

Data are from Table 18.

*This infection was labeled with leucine instead of lysine.

LEGEND TO TABLE 19

The ratio of incorporation of radioactive lysine into the A' protein or the A' region of SDS acrylamide gels to that into F protein was computed from the data in Table 18. These ratios were normalized to that for the ϕX wt infection of UV irradiated cells.

TABLE 20

The proportion of infection specific protein label in ϕX am3 infected, non-UV irradiated, host cells labeled for different time periods

Source of Data Figure 29	Labeling Period Minutes	Labeled Amino Acid	Ratio $\frac{\text{Infection Specific Incorporation}}{\text{Total Incorporation}}$
(a)	0-18	lysine	0.31
(b)	0-90	lysine	0.51
(c)	0-140	lysine	0.53
(d)	50-56	leucine	0.63

LEGEND TO TABLE 20

For each of the SDS acrylamide gels in Figure 29 the total infection specific cpm recovered from the gel was divided by the total cpm recovered from the infected lysate.

TABLE 21

A comparison of several methods for determining the phage particle concentration of a ϕXam3 preparation

Basis of the Determination	Concentration of ϕXam3 Particles/ml
I. Direct measurement of pfu*	7.0×10^{12}
II. Expected burst of 200 pfu/cell*	8.1×10^{12}
III. ^{3}H-leucine incorporation and specific activity of ^{3}H-leucine	3.8×10^{12}

*Assume a specific infectivity of 0.20 pfu/ϕX particle.

LEGEND TO TABLE 21

E. coli H502 was grown at 37°C to 3×10^{8} cells/ml in TPG medium supplemented with 5 µg/ml thymine. A 50 ml aliquot was infected with ϕXam3 at a multiplicity of 7 and labeled continuously with ^{3}H-leucine added to final concentrations of 3.9 µg/ml and 60 µc/ml. After a 2 hr incubation at 37°C the culture was pelleted at 4°C and washed two times with 0.05 M-sodium tetraborate, 0.005 M-EDTA and lysed by room temperature incubation in 1 ml of the same buffer containing 100 µg/ml lysozyme. The debris was pelleted by a low speed centrifugation and the supernatant fractionated on a glass bead column (193). The void volume, containing 100% of the ϕX infectivity, was collected and centrifuged to equilibrium in the same borate buffer. The infectivity peaks were collected and dialyzed and the summed infectivities and coincident ^{3}H cpm were employed to compute the values in

the table. The measured and expected infectivities in I and II, respectively, were related to the phage particle concentrations by an assumed specific infectivity of 0.20. The specific activity of the leucine label was assumed to be the same as that of the leucine added to the culture. Appropriate corrections were made for the counting efficiency of ^{3}H-leucine in the system employed.

TABLE 22

DNA/protein compositions of hypothetical 20S structures-

The Δ^{14}C-leucine concentrations expected in a gradient like that in Figure 8b for various hypothetical DNA-protein associations

No.	Hypothetical Protein Bound per SS DNA Equivalent	Fractional Phage Equivalent of Leucine*	Expected Ratio DNA cpm / Protein cpm	Expected Δ^{14}C-Leucine Concentration - cpm**	
				20S Peak†	RFII Peak‡
1	One phage equivalent	1.00	3.27	8200	3000
2	Capsid-i.e., one phage equivalent of F protein	0.69	4.7	5700	2100
3	Spike-i.e., one phage equivalent of G, H and J	0.30	10.9	2460	910
4	Single F protein	0.012	272	98	36
5	Single G protein	0.0040	820	33	12
6	Four H protein	0.010	327	82	30
7	Single H protein	0.0025	1310	20	8
8	Total J protein	0.030	109	246	91
	Observed Values				
1	20S peak (ϕX proteins only)†		3.67	10300	
2	RFII peak‡		502		196

*The leucine content of a given structure divided by the leucine content of whole phage (one phage equivalent).

**The cpm that would be expected to appear in the regions designated in the gradient in Figure 8b as a consequence of one of the given structures.

†These values are based on the sum of the ^{3}H-thymidine cpm found under the 20S peak.

‡These values are based on the ^{3}H-thymidine cpm found in the peak fraction of the RFII region.

LEGEND TO TABLE 22

Using the specific activities of the ^{3}H-thymidine (25.3 c/mmole) and ^{14}C-leucine (312 mC/mmole) labels supplied exogenously to the culture in Figure 8b, the ^{3}H cpm associated with one plus strand equivalent of ϕX DNA (6.42×10^{-6} cpm/viral strand) and the ^{14}C cpm associated with one phage equivalent of protein (1.96×10^{-6} cpm/phage) were computed utilizing the values of 1800 thymidine residues/5500 nucleotides in the viral plus strands (14) and 7.6 mole percent of leucine per whole phage (16). It is also known (16) that the average molecular weight of the virion amino acids is 115 daltons, giving 3.91×10^{4} amino acid residues per virion containing 4.5×10^{6} daltons of protein (181). The counting efficiencies of ^{3}H and ^{14}C in this experiment are 0.04 and 0.57 cpm/dpm, respectively.

The leucine content of other hypothetical structures was computed from the fraction of leucine contained in these structures compared to whole phage. These fractions were computed from the leucine distribution among the proteins of whole phage (R. Rohwer, unpublished experiments), and the stoichiometry of the phage subunit proteins which is given in the General Introduction. The values used here are 60F:12H:60G.

For each of the hypothetical structures listed the ratio of the expected DNA cpm to protein cpm was computed. The $\Delta^{14}C$ cpm that would be expected to be associated with the pulse labeled DNA found at any position in the gradient as a consequence of the DNA-protein association postulated was then computed as: (Observed ^{3}H DNA cpm)(Ratio) = (Expected $\Delta^{14}C$ cpm).

This computation was performed for the pooled 20S peak containing 28,350 cpm of ^{3}H-thymidine labeled DNA and the peak fraction of the "resting" RFII peak containing 9870 cpm ^{3}H DNA. The Δ^{14}C cpm values observed for each of these peaks are given at the bottom of the table.

TABLE 23

DNA/protein ratio of the 114S peak-A comparison of the expected and observed DNA/protein ratios in the 114S peak from an experiment like that in Figure 8a

Source*	DNA/Protein Ratio	DNA/Protein Ratio Normalized to the Calculated Value
Calculated	2.12	1.00
Observed		
Before resedimentation	2.22	1.05
After resedimentation†	15.6	7.4

*Data are from the experiments in Figure 9 and Table 9.

†The ratio used is that observed after resedimentation in the absence of BSA carrier, Figure 9a, or in the presence of 1.00 M-KCl, 0.005 M-EDTA, and 0.5% sarkosyl, Figure 9d.

LEGEND TO TABLE 23

The expected value of the DNA/protein ratio was computed in the same manner as in Table 22 except that the specific activity of the ^{3}H-thymidine label was 16.4 C/mmole. The ^{3}H-thymidine cpm from pooled fractions of the 111S to 114S peak were used to compute the expected cpm of the protein. The observed ratios were obtained from the pooled fractions of the 111S to 114S peaks from the initial sedimentation in TM buffer and after resedimentation of the pooled peak in the absence of BSA carrier (see text).

FIGURES

FIGURE 1

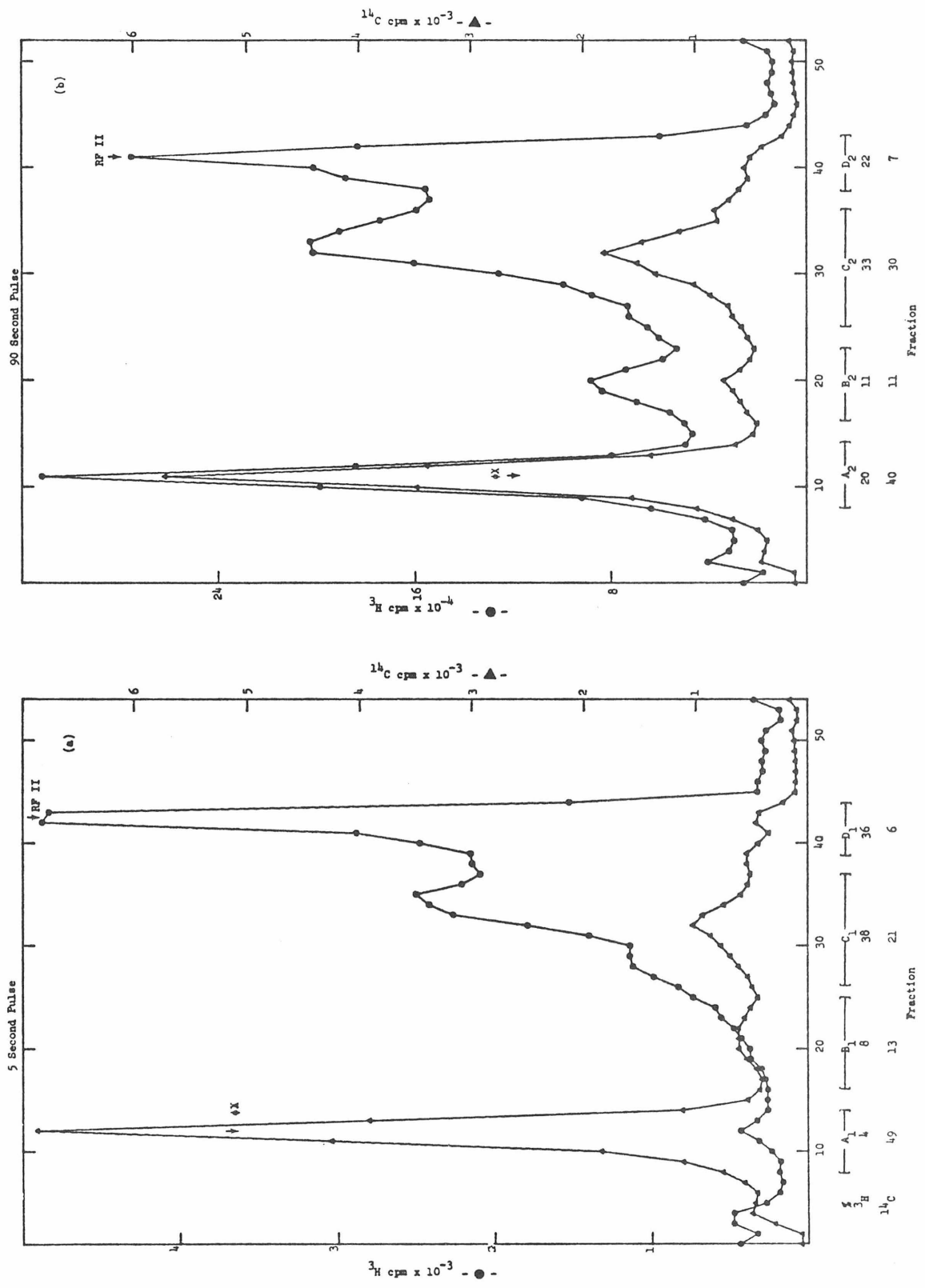
(a)
5 Second Pulse
RF II
ΦX
^{14}C cpm x 10^{-3} - ▲ -
^{3}H cpm x 10^{-3} - ● -
^{3}H
^{14}C
A$_1$
B$_1$
C$_1$
D$_1$
4
8
38
36
49
13
21
6
Fraction
(b)
90 Second Pulse
RF II
ΦX
^{14}C cpm x 10^{-3} - ▲ -
^{3}H cpm x 10^{-4} - ● -
A$_2$
B$_2$
C$_2$
D$_2$
20
11
33
22
40
11
30
7
Fraction

FIGURE 1. The distribution of nascent and continuously labeled DNA species in non-deproteinized lysates obtained from the late stage of ϕX174 infection.

E. coli H502 was grown to 3 x 10^8 cells/ml in 40 ml of TPG media supplemented with 1 μg/ml thymine at 37°C. At time zero the culture was infected with ϕXam3 at a multiplicity of seven. 20 min after infection ^{14}C-thymine with a specific acitivity of 38.3 mc/mmole was added to a final concentration of 0.6 μc/ml. 45 min after infection the culture was divided into two equal portions. 48 min after infection one portion was pulsed for 5 sec with ^{3}H-thymidine. 50 min after infection the other portion was pulsed for 90 sec with ^{3}H-thymidine. In both pulses ^{3}H-thymidine was added (at a specific activity of 23.5 C/mmole) to a final concentration of 0.5 mc/ml. Pulses were terminated, as described in the Methods, by rapid freezing in the presence of 0.1 M-NaN_3. Both cultures were thawed at 0°C and then washed three times by low speed centrifugation with 20 ml aliquots of TG-Azide. The final pellet was resuspended in 250 μl of TG-Azide and lysed as described in the Methods (Mg^{++} procedure). The lysate was stored overnight at -20°C, thawed at 0°C, and the debris pelleted. The cleared supernatant was removed with a Pasteur pipette. One half ml of each lysate was then layered onto a 5-30% linear sucrose gradient formed over a 0.5 ml CsCl underlayer. The gradients were prepared in TM buffer supplemented with 50 μg/ml t-RNA and .01% BSA to inhibit DNase activity and to prevent absorptive losses, respectively. Sedimentation was performed at 40,000 revs/min in an SW40 rotor for 2.25 hr at 4°C. Fractions were collected from the bottom of the tube into precooled, siliconized shell vials. 50 μl aliquots of each fraction were spotted onto

numbered paper filter discs with glass micropipettes. The discs were washed 7X in 300 ml of TCA by the batch procedure. They were then dried and counted in TL as described in the Methods. The isotopic composition of each sample was computed by means of the CNTSEP program. The fractions from the regions indicated by A, B, C and D were pooled for use in latter experiments. The sedimentation positions of ϕX and RF II are indicated for easy reference but do not represent internal markers.

(a) Five second pulse

(b) 90 sec pulse

^{3}H is indicated by -●-

^{14}C is indicated by -▲-

FIGURE 2

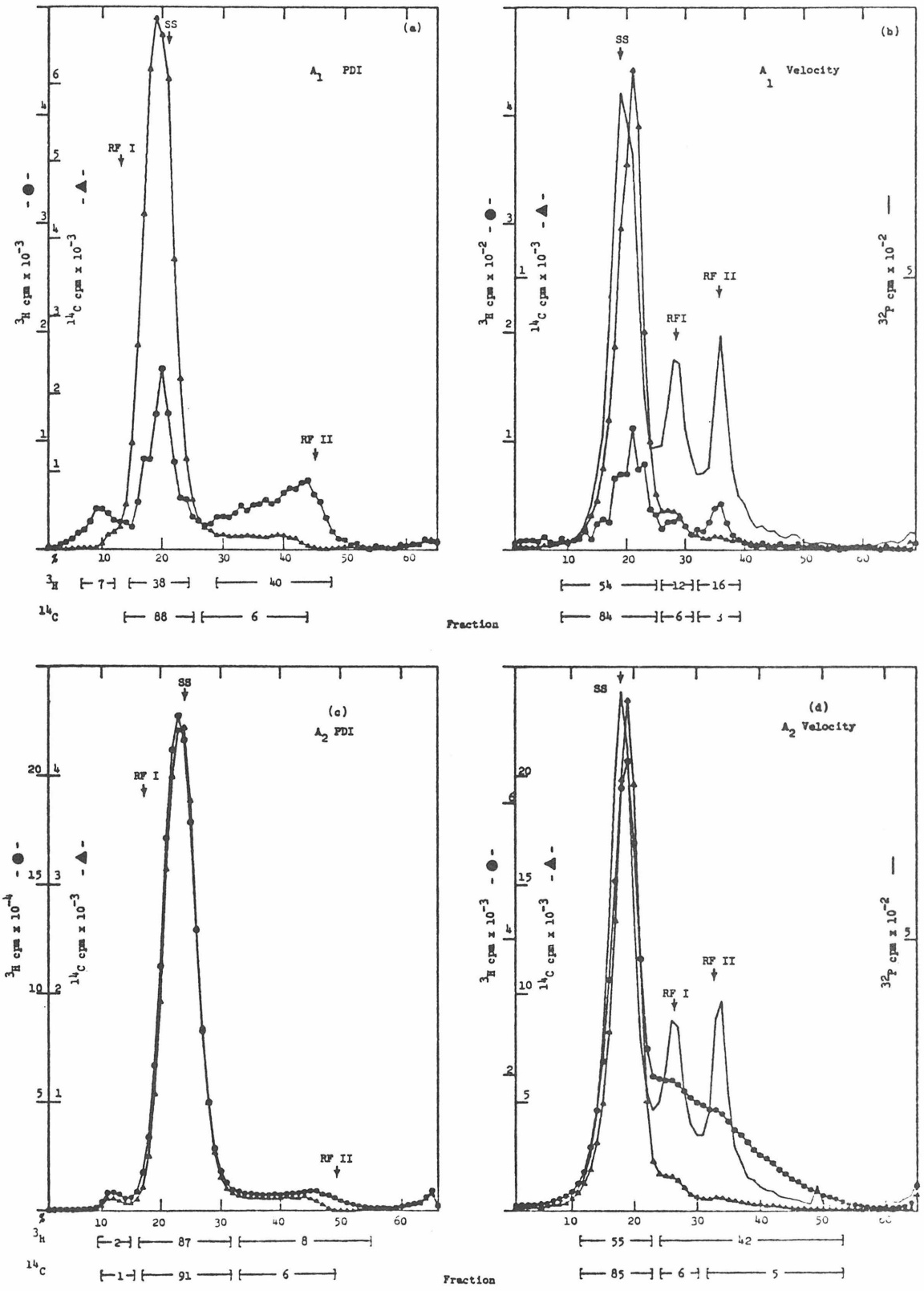
(a)
A1 PDI
SS
RF I
RF II
3H cpm x 10-3
14C cpm x 10-3
3H 7 38 40
14C 88 6
(b)
A1 Velocity
SS
RFI
RF II
3H cpm x 10-2
14C cpm x 10-3
32P cpm x 10-2
54 12 16
84 6 5
(c)
A2 PDI
SS
RF I
RF II
3H cpm x 10-4
14C cpm x 10-3
3H 2 87 8
14C 1 91 6
(d)
A2 Velocity
SS
RF I
RF II
3H cpm x 10-3
14C cpm x 10-3
32P cpm x 10-2
55 42
85 6 5
Fraction
Fraction

FIGURE 2. Region A - PDI sedimentation to equilibrium and high salt velocity sedimentation of the deproteinized material from region A of the gradients in Figure 1.

The fractions from regions A_1 and A_2 of the sedimentation velocity gradients in Figure 1(a,b) were pooled separately and deproteinized according to the methods after adding ^{32}P-labeled RF I, RF II and phage as internal markers. An aliquot from each preparation was then sedimented to equilibrium in PDI, and fractions collected and counted as described in the Methods. Additional aliquots from each preparation were sedimented through high salt, neutral sucrose, isokinetic sucrose gradients. The gradients were prepared in TE buffer supplemented with 1.0 M-NaCl as described in the Methods. 200 µl aliquots were applied to each gradient and sedimented for 10 hr at 40,000 revs/min at 5°C in an SW40 rotor. Fractions were collected from the bottom of the tube directly into scintillation vials and counted in 10 ml of Aquasol:water, 10:1. Data from both the PDI bandings and the sedimentation velocities were processed by means of the TPIPSEP program.

PDI sedimentation to equilibrium

(a) 5 sec pulse

(c) 90 sec pulse

The positions of the marker DNAs are indicated by arrows.

High salt sedimentation velocity

(b) 5 sec pulse

(d) 90 sec pulse

^{3}H is indicated by -●- ^{32}P is indicated by ———
^{14}C is indicated by -▲-

FIGURE 3

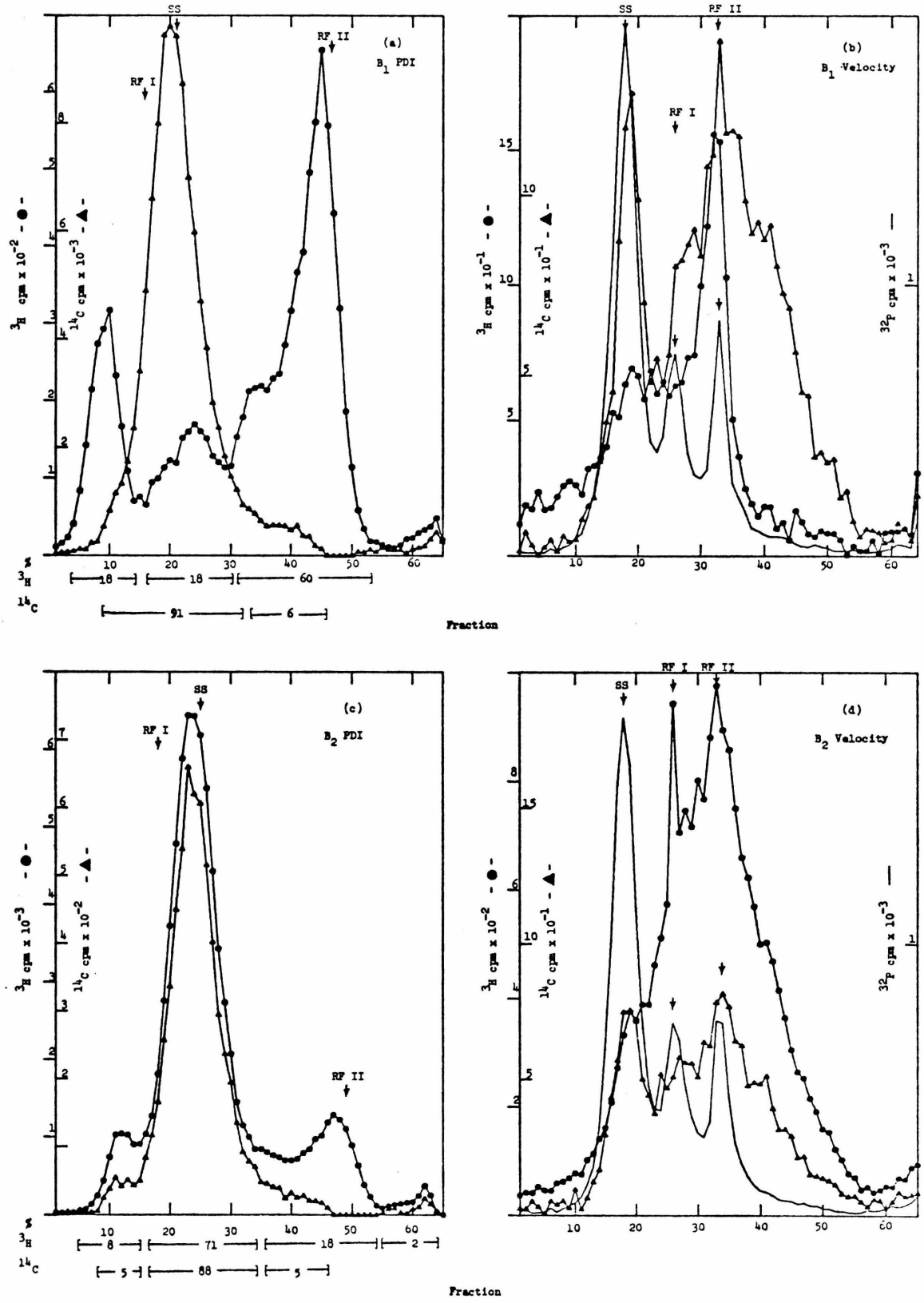
SS
RF I
RF II
(a)
B1 PDI
3H cpm x 10-2 - ● -
14C cpm x 10-3 - ▲ -
% 3H 18 18 60
14C 91 6
(b)
B1 Velocity
3H cpm x 10-1 - ● -
14C cpm x 10-1 - ▲ -
32P cpm x 10-3 —
(c)
B2 PDI
3H cpm x 10-3 - ● -
14C cpm x 10-2 - ▲ -
% 3H 8 71 18 2
14C 5 88 5
(d)
B2 Velocity
3H cpm x 10-2 - ● -
14C cpm x 10-1 - ▲ -
32P cpm x 10-3 —
Fraction

FIGURE 3. Region B - PDI sedimentation to equilibrium and high salt velocity sedimentation of the deproteinized material from region B of the gradients in Figure 1.

The fraction from regions B_1 and B_2 of the sedimentation velocity gradients in Figures 1a and 1b were pooled separately, deproteinized, and recentrifuged as described in the legend to Figure 2.

PDI sedimentation to equilibrium

(a) 5 sec pulse

(c) 90 sec pulse

High salt sedimentation velocity

(b) 5 sec pulse

(d) 90 sec pulse

^{3}H is indicated by -●-

^{14}C is indicated by -▲-

^{32}P is indicated by ———

FIGURE 4

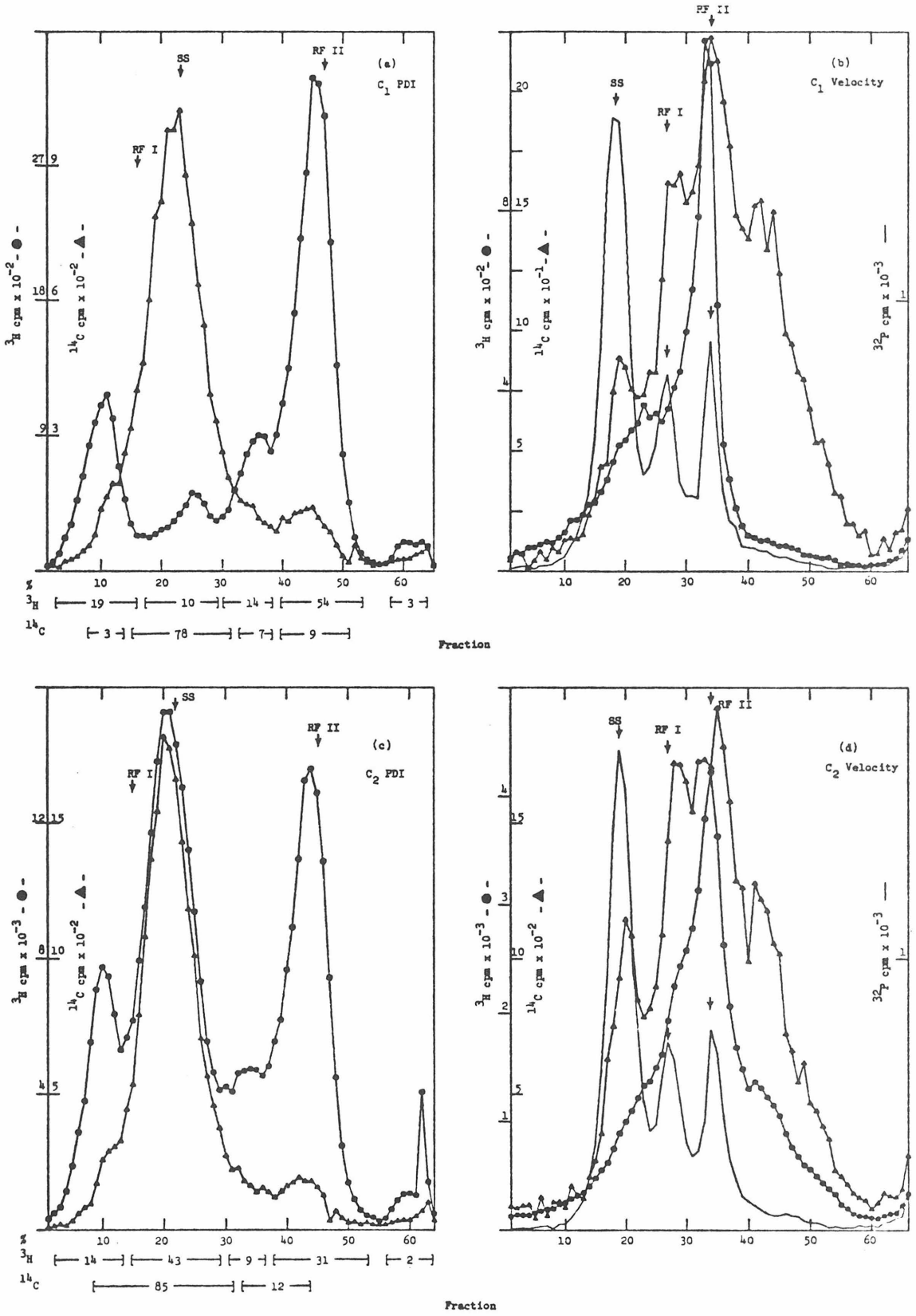
(a)
C1 PDI
(b)
C1 Velocity
(c)
C2 PDI
(d)
C2 Velocity
SS
RF I
RF II
3H cpm x 10-2 - ●
14C cpm x 10-2 - ▲
3H cpm x 10-3 - ●
14C cpm x 10-1 - ▲
14C cpm x 10-2 - ▲
32P cpm x 10-3
% 3H
% 14C
Fraction

FIGURE 4. Region C - PDI sedimentation to equilibrium and high salt velocity sedimentation of the deproteinized material from region C of the gradients in Figure 1.

The fractions from regions C_1 and C_2 of the sedimentation velocity gradients in Figures 1a and 1b were pooled separately, deproteinized, and recentrifuged as described in the legend to Figure 2.

PDI sedimentation to equilibrium

(a) 5 sec pulse

(c) 90 sec pulse

High salt sedimentation velocity

(b) 5 sec pulse

(d) 90 sec pulse

^{3}H is indicated by -●-

^{14}C is indicated by -▲-

^{32}P is indicated by ——

FIGURE 5

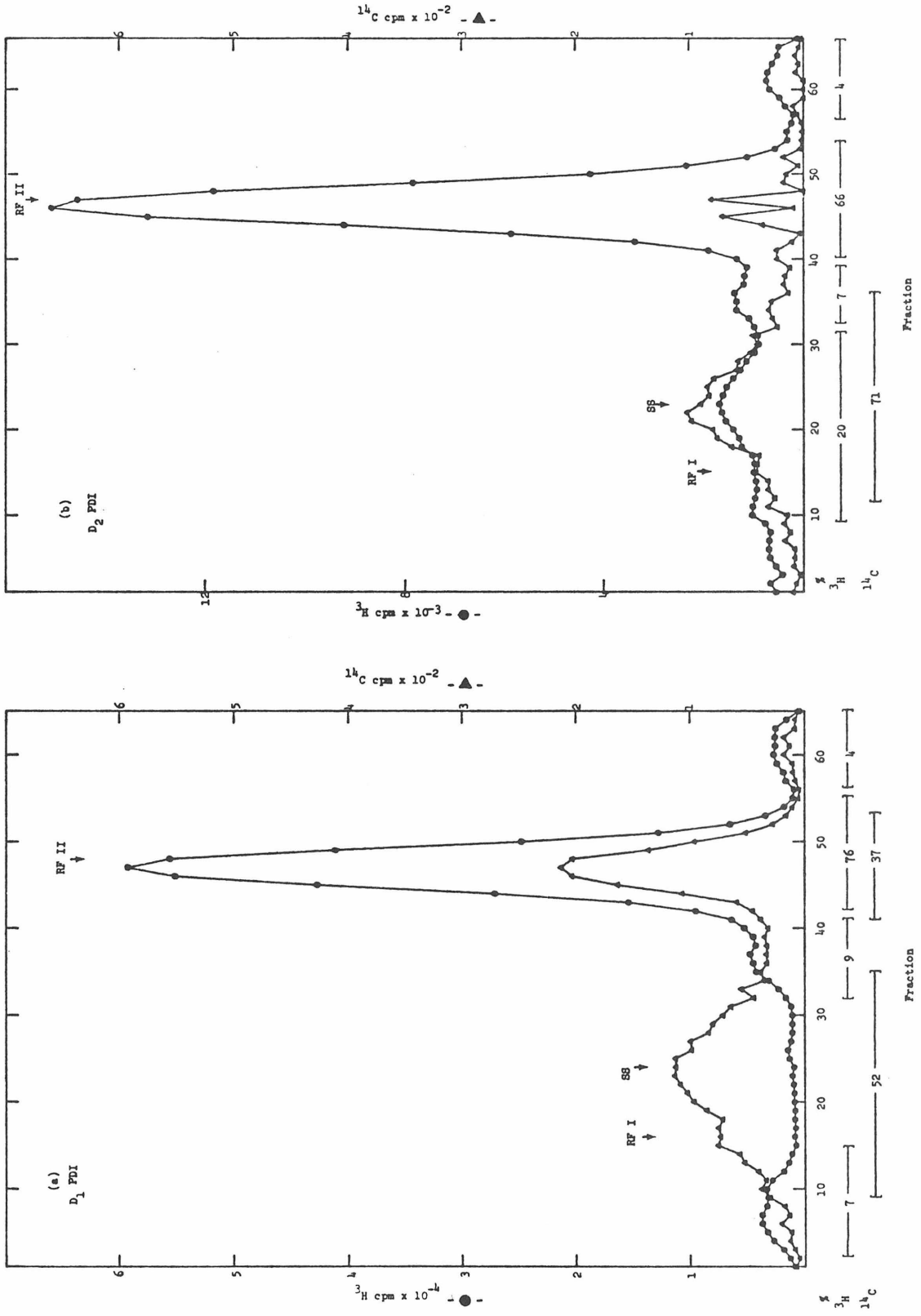
(a)
D_1 FDI
RF II
RF I
SS
^{14}C cpm x 10^{-2} - ▲ -
^{3}H cpm x 10^{-4} - ● -
^{3}H
^{14}C
7
52
9
76
37
4
Fraction
(b)
D_2 FDI
RF II
RF I
SS
^{14}C cpm x 10^{-2} - ▲ -
^{3}H cpm x 10^{-3} - ● -
^{3}H
^{14}C
7
20
71
66
4
Fraction

FIGURE 5. Region D - PDI sedimentation to equilibrium of the deproteinized material from region D of the gradient in Figure 1.

The fractions from regions D_1 and D_2 of the sedimentation velocity gradients in Figures 1a and 1b were pooled separately, deproteinized, and sedimented to equilibrium in PDI as described in the legend to Figure 2.

(a) 5 sec pulse

(b) 90 sec pulse

^{3}H is indicated by -●-

^{14}C is indicated by -▲-

^{32}P is indicated by ——

FIGURE 6

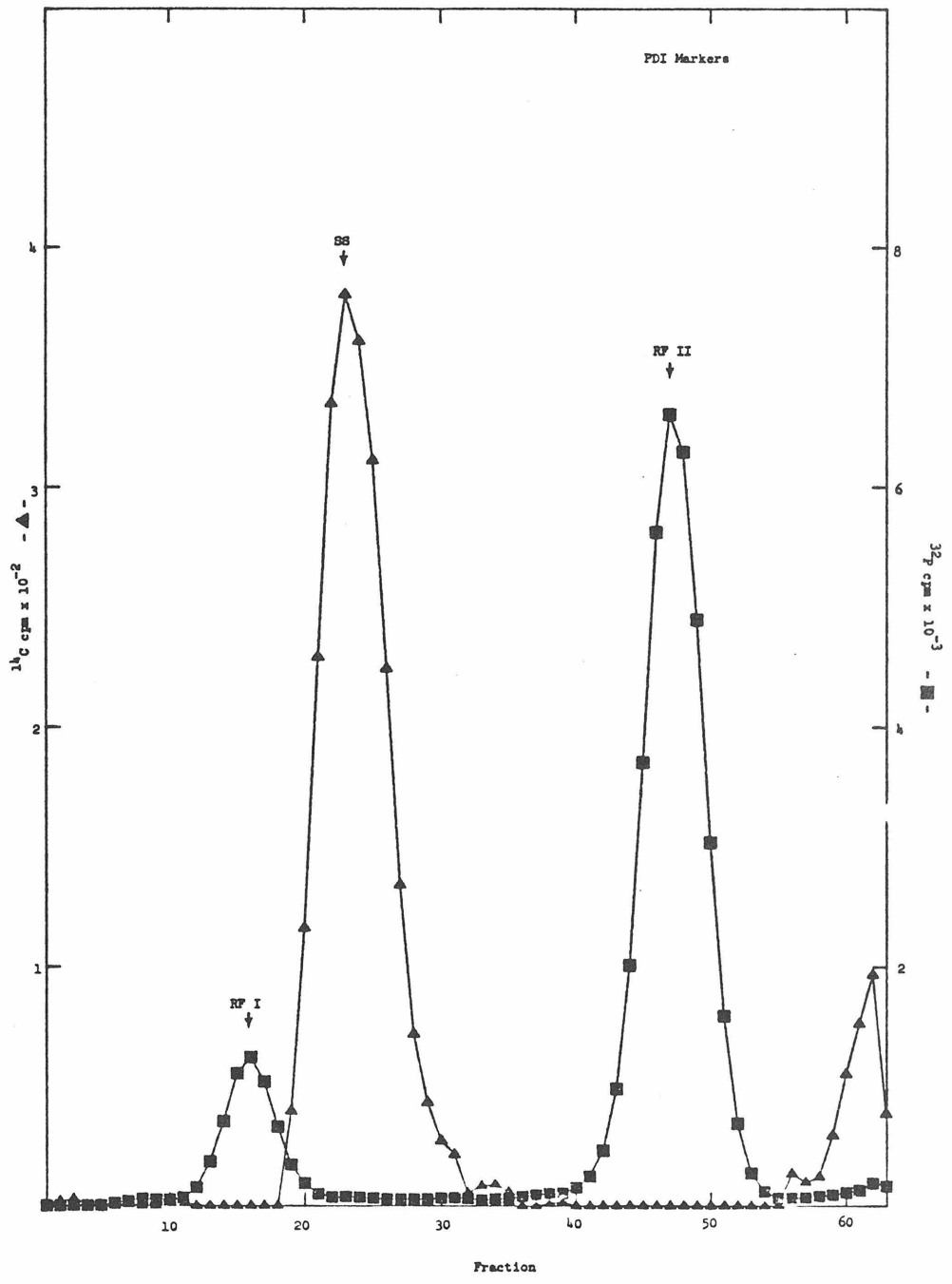
PDI Markers
SS
RF II
RF I
^{14}C cpm x 10^{-2} - ▲ -
^{32}P cpm x 10^{-3} - ■ -
Fraction
10
20
30
40
50
60
1
2
3
4
6
8

FIGURE 6. Control - PDI sedimentation to equilibrium of marker DNA.

A mixture of ^{14}C labeled plus strand circular DNA and ^{32}P labeled RF I and RF II marker DNA was sedimented to equilibrium in PDI and fractions collected and counted as described in the Methods. The RF II marker was derived from ^{32}P decay of the RF I DNA. The data were processed by means of the TRIPSEP program. The assignments of the RF I and RF II positions were made on the basis of the relative proportions of these two molecules as determined by other means.

^{14}C is indicated by -▲-

^{32}P is indicated by -■-

FIGURE 7

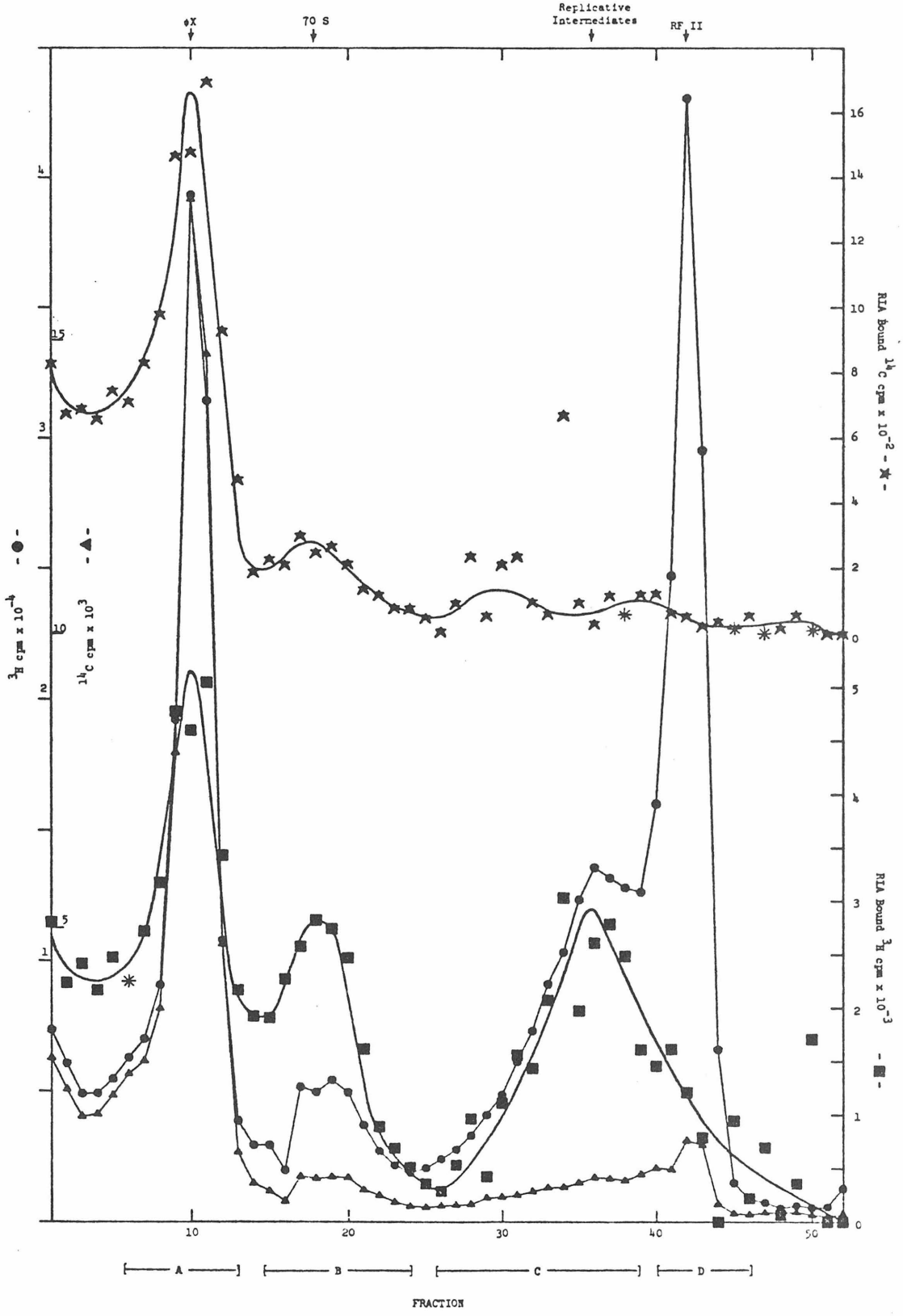
φX
70 S
Replicative Intermediates
RF II
^{3}H cpm x 10^{-4} - ● -
^{14}C cpm x 10^3 - ▲ -
RIA Bound ^{14}C cpm x 10^{-2} - ★ -
RIA Bound ^{3}H cpm x 10^{-3} - ■ -
A
B
C
D
FRACTION

FIGURE 7. Radioimmunoassay - Phage specific DNA-protein complexes from ϕX174 infected cells.

Infection and Labeling

100 ml of E. coli H502 was infected with ϕXam3, labeled with ^{14}C thymine from 20 to 50 min after infection, and then pulsed for 90 sec with ^{3}H-thymidine as described in the legend to Figure 1. Lysis was performed in the presence of Mg^{++} as described in the Methods. The 2 ml of lysate minus debris was layered onto a 5-30% linear sucrose gradient formed over a 1.5 ml CsCl underlayer. The gradients were prepared in TM buffer supplemented with 50 µg/ml t-RNA, 0.1% BSA and 0.01 M-NaN_3. Sedimentation was performed at 27,000 revs/min in an SW27 rotor for 5 hr at 2°C. Fractions were collected from the bottom of the tube into precooled, siliconized shell vials. 50 µl aliquots of each fraction were then washed by the batch TCA procedure and counted as described in the legend to Figure 1.

Anti-ϕX antiserum coated vials and control vials were prepared by the procedure described in the Methods utilizing Nuclear Associates Linear Polyethylene Vials and a 200 µl dilution of a pooled anti-ϕX antiserum with a K value, before dilution, of 1035. To each vial was added 1.9 ml of TM buffer supplemented with 5 µg/ml t-RNA, 10 µg/ml fragmented calf thymus DNA and 0.001 M-NaN_3. Then 4 100 µl aliquots of each fraction from the sedimentation velocity gradient were added to two serum-coated vials and two control vials respectively. The vials were capped and then incubated with gentle agitation for 47 hr at 37°C. After the incubation the supernatant was removed and the vials washed as described in the Methods. 5 ml of TLNCS were added

to each vial for counting. The isotopic composition of each sample was computed using the CNTSEP program. Then, for each fraction and each isotope independently, the average cpm bound to the control vials was subtracted from the average cpm bound to the serum-coated vials to give the net specific absorption to the vials. The net specific-absorption is plotted in the figure. An asterisk indicates that one of the four values was ommitted in the calculation of the net specific absorption for that fraction due to an obviously spurious value for that vial. The ^{14}C serum binding plot is displaced above the other plots to minimize confusion.

^{3}H pulse label cpm -●-

^{14}C continuous label cpm -▲-

^{3}H RIA bound cpm -■-

^{14}C RIA bound cpm -★-

✳ The plotted value was computed from three rather than four measurements.

FIGURE 8

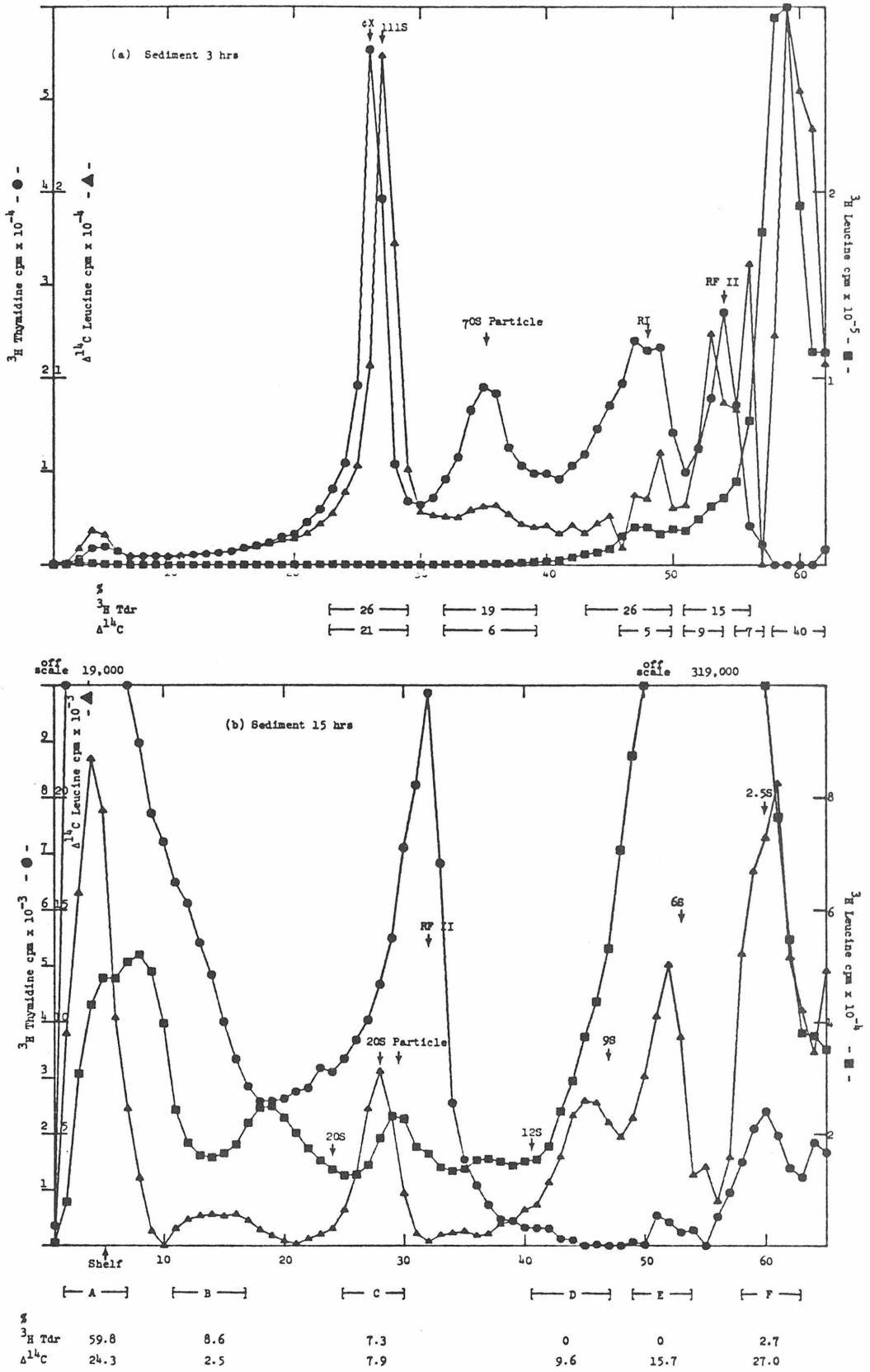
(a) Sediment 3 hrs
ϕX 174
111S
70S Particle
RI
RF II
^{3}H Thymidine cpm x 10^{-4} - ● -
Δ^{14}C Leucine cpm x 10^{-4} - ▲ -
^{3}H Leucine cpm x 10^{-5} - ■ -
%
^{3}H Tdr
Δ^{14}C
26
21
19
6
26
5
15
9
7
40
off scale 19,000
off scale 319,000
(b) Sediment 15 hrs
Δ^{14}C Leucine cpm x 10^{-3} - ▲ -
^{3}H Thymidine cpm x 10^{-3} - ● -
^{3}H Leucine cpm x 10^{-4} - ■ -
RF II
2.5S
6S
9S
20S Particle
20S
12S
Shelf
A
B
C
D
E
F
%
^{3}H Tdr 59.8 8.6 7.3 0 0 2.7
Δ^{14}C 24.3 2.5 7.9 9.6 15.7 27.0

FIGURE 8. Distribution of ϕX specific protein and pulse labeled DNA in lysates from the late stage of infection.

In separate experiments (a and b) 100 ml of E. coli H502 was grown at 37°C to 3 x 10^8 cells/ml in TPG medium supplemented with 1 μg/ml thymine. At time zero the culture was divided in half and one portion was infected with ϕXam3 at a multiplicity of seven. 30 min later the uninfected culture was pulsed for 6 min with ^{3}H-leucine at a final concentration of 20 μc/ml (2.0 C/mmole). At 50 min the infected culture was pulsed for 6 min with ^{14}C-leucine at a final concentration of 2 μc/ml (312 mc/mmole). At 54.5 min the infected culture was pulsed for 90 sec with ^{3}H-thymidine at a final concentration of 20 μc/ml (23.5 C/mmole). The infected cell pulses were terminated together at 56.0 min. All pulses were terminated by quick cooling in a dry ice methanol bath as described in the Methods. The cells from the uninfected and infected cultures were washed and prepared for lysis separately, as described in the methods except that the Brij and freeze-thaw steps were omitted from experiment (a) as lysis was apparent without it. In experiment (b) Mg^{++} was added before lysozyme and brief exposure to 37°C during the freeze thaw steps was necessary to obtain lysis. Subsequent to lysis the cell debris was removed by a 15 min centrifugation at 15,000 revs/min in a Sorvall centrifuge. The cleared supernatants from the infected and uninfected cultures were then layered onto separate but identical 5-30% linear sucrose gradients buffered with TM, supplemented with 50 μg/ml t-RNA, 0.01% BSA, 0.01 M-NaN_3 and formed over a 2 ml shelf of 50% Angio Conray in TM buffer. Samples were centrifuged at 27,000

revs/min in an SW27 rotor at 4°C for 3.5 hr, and 15 hr, in experiments (a) and (b), respectively. After centrifugation identical numbers of fractions were collected from each gradient by introducing a glass micropipette to the bottom of the centrifuge tube and pumping out the contents, fractionating on the basis of time (see Methods). 50 µl aliquots from each fraction were spotted onto numbered paper filters, washed by the batch method with 10% TCA, and counted in TL scintillator. The CNTSEP program was utilized to separate the ^{3}H and ^{14}C cpm in the infected gradient, to compare the uninfected ^{3}H-leucine and the infected ^{14}C-leucine incorporation patterns in the two parallel gradients of each experiment and to compute the ϕX specific ^{14}C incorporation ($\Delta^{14}C$) in the infected gradient (see Methods). The ϕX position indicated in (a) was determined by an infectivity measurement in another experiment. The RF II position is indicated by analogy with Figures 1 and 5. The sedimentation values indicated in (b) were computed assuming a linear gradient and an S value of 16 for RF II (154). The percentage distributions of cpm into various regions of each gradient are indicated at the bottom of each graph.

(a) Sedimentation for 3.5 hr

(b) Sedimentation for 15 hr

^{3}H-thymidine -●-

$\Delta^{14}C$-leucine -▲-

^{3}H-leucine -■-

FIGURE 9

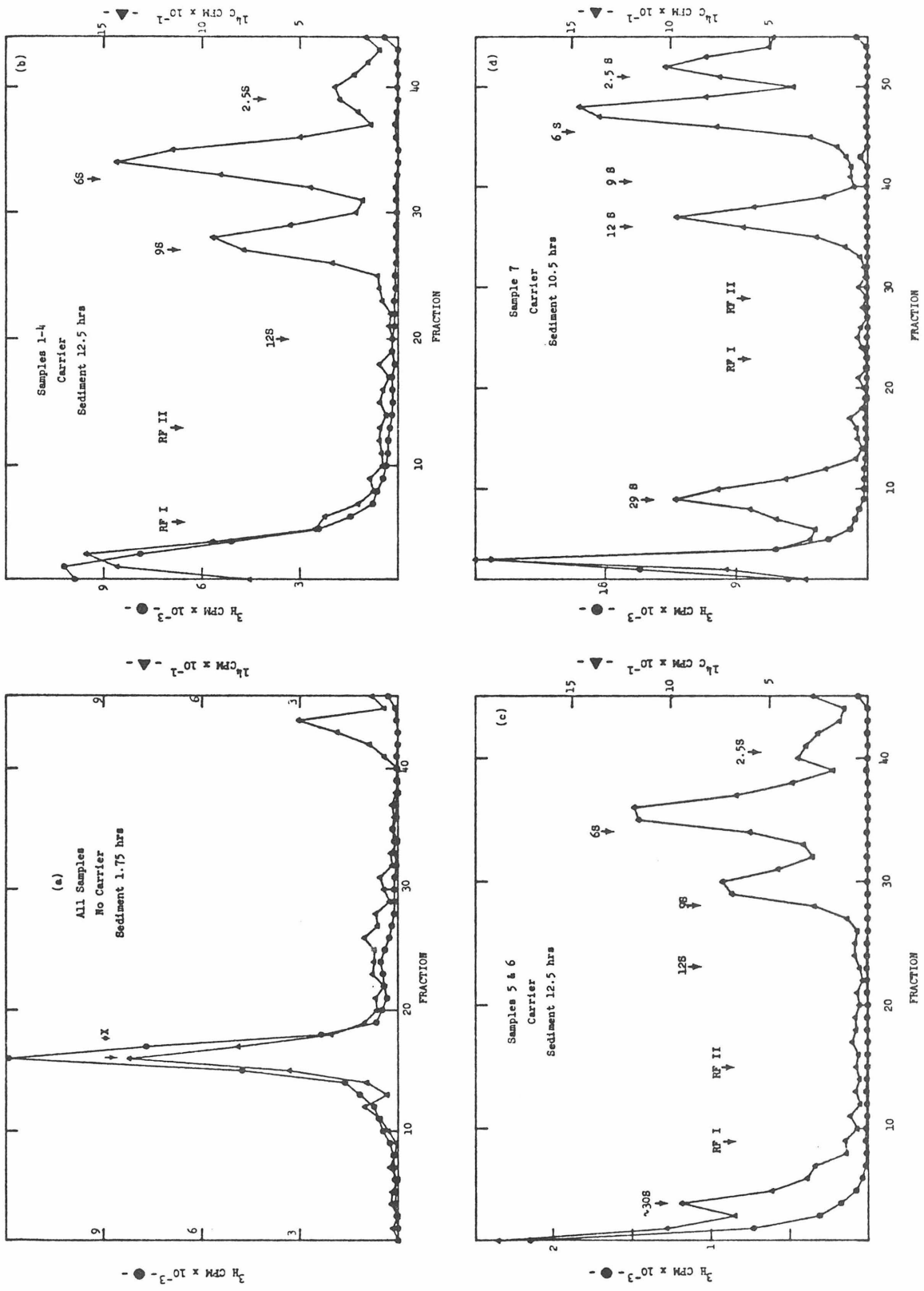
(a)
All Samples
No Carrier
Sediment 1.75 hrs
φX
RF I
RF II
FRACTION
(b)
Samples 1-4
Carrier
Sediment 12.5 hrs
RF I
RF II
6S
9S
12S
2.5S
(c)
Samples 5 & 6
Carrier
Sediment 12.5 hrs
~30S
RF I
RF II
6S
9S
12S
2.5S
(d)
Sample 7
Carrier
Sediment 10.5 hrs
RF I
RF II
29 S
12 S
9 S
6 S
2.5 S
^{3}H CPM x 10^{-3}
^{14}C CPM x 10^{-1}

FIGURE 9. Resedimentation of the 111S particle.

An experiment like that in Figure 8a was performed except that this time the lysates were sedimented through 3-18% sucrose instead of a 5-30% gradient. This permitted a sample from any region of this gradient when diluted 1:1 with buffer to be relayered without dialysis onto 10% sucrose for resedimentation. The fractions from the 114S to 111S region [the ^{3}H-thymidine plus the ^{14}C-leucine labeled peaks] of the infected cell gradient were pooled into a silane-coated glass vial. In separate experiments (a) and (b,c,d) seven 100 µl aliquots of this pool were diluted 1:1 with TM buffer (a) or TM buffer supplemented with 0.10% BSA (b,c,d). Different samples were brought to either 0.05, 0.30, or 1.00 M-KCl by the addition of dry KCl. One sample at each KCl concentration was left at 0.008 M in Mg^{++} and another was made 0.013 M in EDTA for a final EDTA concentration of 0.005 M after titration of the Mg^{++}. One of the 1.00 M-KCl-EDTA samples was made 0.5% in sarkosyl. The compositions of the various samples are given below.

Table A

Composition of Samples for Resedimentation

Sample No.	Final Concentrations*			
	KCl M	Mg^{++} M	EDTA M	Sarkosyl %
1	0.05	0.008	0.005	-
2	0.05	-	0.005	-
3	0.30	0.008	-	-
4	0.30	-	0.005	-
5	1.00	0.008	-	-
6	1.00	-	0.005	-
7	1.00	-	0.005	0.5

*Samples were brought to these concentrations by additions to TM buffer.

All samples were incubated for 2 hr at 0°C and then for 10 min at 37°C just prior to centrifugation for complete chelation of Mg^{++} by EDTA (L. H. Smith, personal communication). 10 to 30% linear sucrose gradients were prepared in each of the buffers indicated in Table A over 0.5 ml, 1.5 g/ml, CsCl shelves at the bottoms of each tube. The gradients in (a) contained no BSA carrier, but contained an internal ^{32}P ϕX marker. Those in (b,c,d) were formed from sucrose solutions supplemented with 0.01% BSA and contained internal ^{32}P RF I and RF II markers. Samples 1 through 7 prepared without BSA carrier were centrifuged for 1.75 hr at 4°C in an SW41 rotor at 41,000 revs/min. The results were the same in each case and are represented by the gradient in (a). Samples 1-6 prepared with BSA were centrifuged for 12.5 hr at 4°C in an SW41 rotor at 41,000 revs/min. The results of samples 1 through 4 were identical (see Table 9) and are presented in (b), the results of 5 and 6 were the same and are presented in (c). Sample 7 prepared in BSA was centrifuged for 10.5 hr at 4°C in an SW41 rotor at 41,000 revs/min. The results are presented in (d). The gradients were collected into siliconized glass shell vials. 50 µl aliquots of each fraction were spotted onto numbered paper filters. The filters were washed by the batch procedure to remove sucrose and then dried and counted in TL. The data were processed by the CNTSEP program. The sedimentation velocities indicated by the arrows were calculated assuming a linear relationship and an S value of 16.2 for the internal RF II marker (154). Percentage compositions of these

gradients are given in Table 9.

(a) Samples 1 through 7 prepared and sedimented without BSA. Sedimentation is for 1.75 hr.

(b) Samples 1 through 4 prepared and sedimented with BSA. Sedimentation is for 12.5 hr.

(c) Samples 5 and 6 prepared and sedimented with BSA. Sedimentation is for 12.5 hr.

(d) Sample 7 prepared and sedimented with BSA. Sedimentation is for 10.5 hr.

-●- ^{3}H-thymidine

-▲- ^{14}C-leucine

FIGURE 10

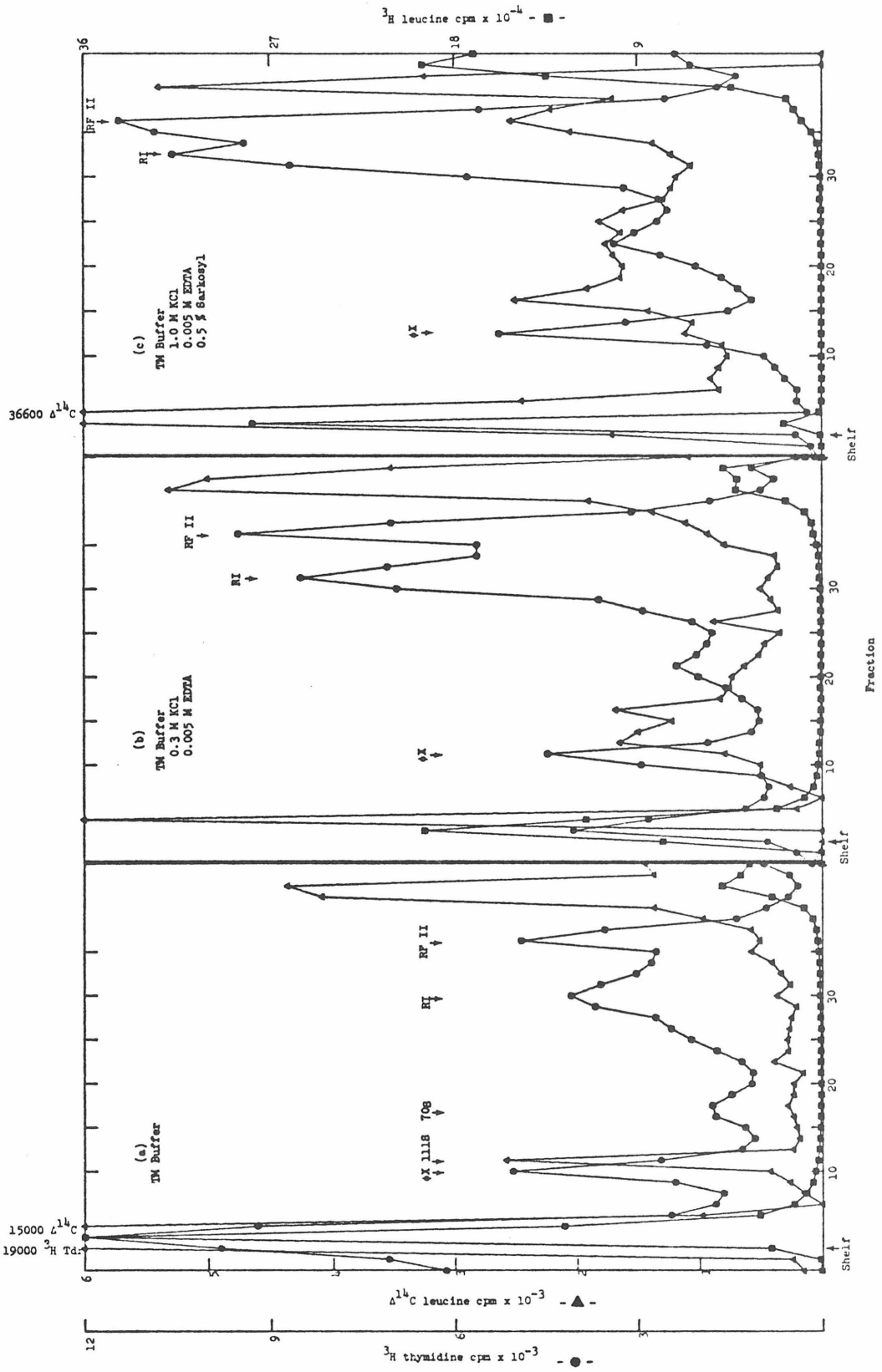
^{3}H leucine cpm x 10^{-4} - ■ -
RF II
RI
(c)
TM Buffer
1.0 M KCl
0.005 M EDTA
0.5 % Sarkosyl
φX
36600 Δ^{14}C
Shelf
RF II
RI
(b)
TM Buffer
0.3 M KCl
0.005 M EDTA
φX
Shelf
RF II
RI
(a)
TM Buffer
φX 1118 708
15000 Δ^{14}C
19000 ^{3}H Td
Shelf
Fraction
Δ^{14}C leucine cpm x 10^{-3} - ▲ -
^{3}H thymidine cpm x 10^{-3} - ● -

FIGURE 10. Resedimentation of the cell debris.

Infected and uninfected lysates of E. coli H502 were prepared as in Fig. 8(a). The cell debris was pelleted from each lysate by a 10 min centrifugation at 0°C at 15,000 rpm in a Sorvall SS-1 rotor. The supernatants were removed with a Pasteur pipet and the debris resuspended in 1.0 ml of TM buffer and 200 µl of 1 mg/ml t-RNA in the same buffer by vigorous vortexing and titurating with a glass pipet. Three 200 µl aliquots of each resuspension were brought to the final concentrations of KCl, Mg^{++}, EDTA and Sarkosyl indicated below:

(a) TM buffer, i.e., 0.05 M-KCl, 0.008 M-MG^{++}, 0.05 M Tris, pH 7.2.

(b) TM buffer brought to 0.30 M-KCl , 0.005 M-EDTA (net).

(c) TM buffer brought to 1.0 M-KCl, 0.005 M-EDTA (net),-0.5% Sarkosyl.

Infected and uninfected pairs of these samples were then sedimented through parallel 5 to 30% linear sucrose gradients prepared in the same buffers and formed over 1 ml CsCl shelves with a density of 1.5 g/ml. Sedimentation was for 1.75 hrs at 41,000 rpm in an SW41 rotor at 4°C. The parallel gradients were prepared and collected in a uniform fashion as described in the methods and the legend to Fig. 8. 50 µl aliquots of each fraction were prepared for counting by the TCA batch procedure, and the resulting data processed by the CNTSEP program. The ϕX position is assigned by analogy with other gradients and does not indicate an internal marker. The CsCl shelf constitutes the first three fractions.

● ^{3}H-thymidine - infected

▲ ^{14}C-leucine - infected

■ ^{3}H-leucine - uninfected

FIGURE 11

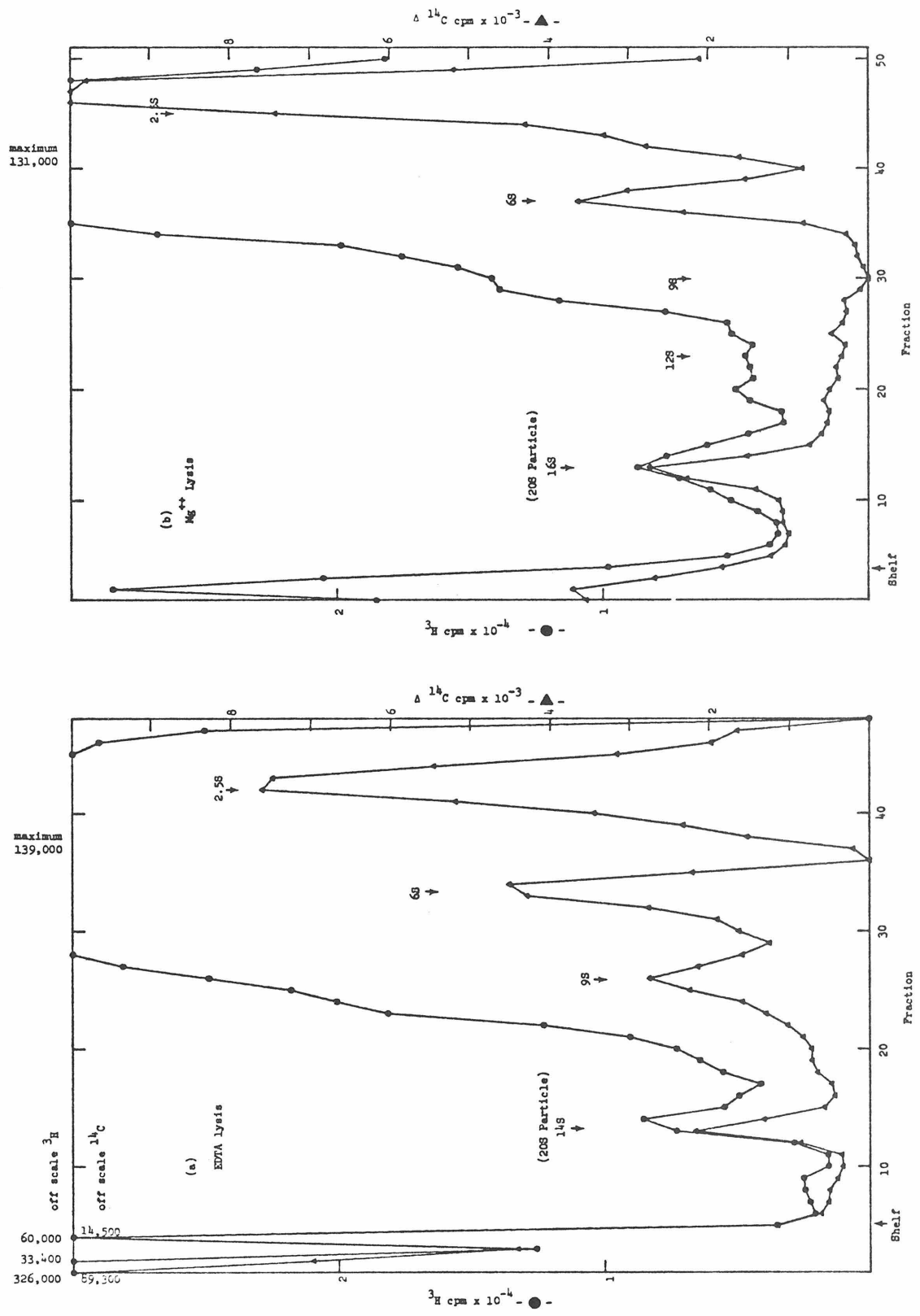
Δ 14C cpm x 10-3 - ▲ -
maximum
131,000
2.5S
6S
9S
12S
(208 Particle)
16S
(b)
Mg++ Lysis
Shelf
Fraction
3H cpm x 10-4 - ● -
Δ 14C cpm x 10-3 - ▲ -
maximum
139,000
2.5S
6S
9S
(208 Particle)
14S
(a)
EDTA lysis
off scale 3H
off scale 14C
14,500
60,000
33,400
326,000
89,300
Shelf
Fraction
3H cpm x 10-4 - ● -

FIGURE 11. Cosedimentation of differentially labeled infected and uninfected cell lysates after "harsh" versus "gentle" lysis.

E. coli H502 was grown to 3 x 10^8 cells/ml at 37°C in TPG supplemented with 2 µg/ml thymidine and divided into two 10 ml portions at time zero. One portion was infected at a multiplicity of 7 with ϕXam3. 25 min later the uninfected culture was pulsed for 5 min with ^{3}H-leucine (2.0 C/mmole) at a final concentration of 20 µc/ml. 45 min after infection the infected culture was pulsed for 5 min with ^{14}C-leucine (316 mc/mmole) at a final concentration of 1.0 µc/ml. Both pulses were terminated by quick cooling in a dry ice methanol bath as described in the Methods. The cultures were thawed at 0°C and washed once with 10 ml of TG buffer supplemented with 20% sucrose. The pellets from each culture were resuspended in 5 ml of the same buffer, combined, and then divided into two equal parts. This mixture of infected and uninfected cells was then lysed and centrifuged according to (a) or (b) below.

(a) The cells were lysed according to the procedure of Mayol and Sinsheimer (8) The culture was washed two additional times with 0.05 M-Tris-HCl pH 8.0 and the final pellet resuspended in 0.20 ml of the same buffer. 25 µl of a 1 mg/ml solution of lysozyme in 0.10 M-EDTA was added and the mixture incubated for 5 min at room temperature before freezing and thawing three times. The resulting viscosity was reduced by repeatedly forcing the sample through a #18 syringe needle. The lysate was dialysed overnight against 0.05 M-Tris-HCl pH 8.0 and then centrifuged through a gradient in the same buffer (see below).

(b) The cells were washed two additional times in TG buffer supplemented with 20% sucrose, and then resuspended in 0.20 ml of the same. 10 µl of a 1 mg/ml solution of lysozyme dissolved in the same buffer was added and the mixture incubated at 0°C for 30 min. Then 10 µl of 0.1 M-$MgSO_4$ and 20 µl of 5% Brij in water were added in that order. The viscosity of the sample was reduced by repeatedly forcing the lysate through a #18 syringe needle. The lysate was dialysed overnight against TM buffer and sedimented through a gradient prepared in the same.

The entire lysates, a and b, were applied to 5-30% linear sucrose gradients preprared in the buffers indicated above and formed on top of 60% sucrose shelfs. Centrifugation was for 14 hrs at 4°C at 40,000 rpm in an SW40 rotor. Fractions were collected from the bottom of the tubes and 100 µl aliquots were spotted onto GF/A glass filters, dried and counted in TL. Data were processed by the CNTSEP program to separate the ^3H and ^{14}C cpm and compute the ϕX specific fraction of the ^{14}C incorporation, $\Delta^{14}C$. S values were calculated assuming a linear gradient and a value of 6S for the second peak from the top.

▲ ^{14}C-leucine

● ^3H-leucine

FIGURE 12

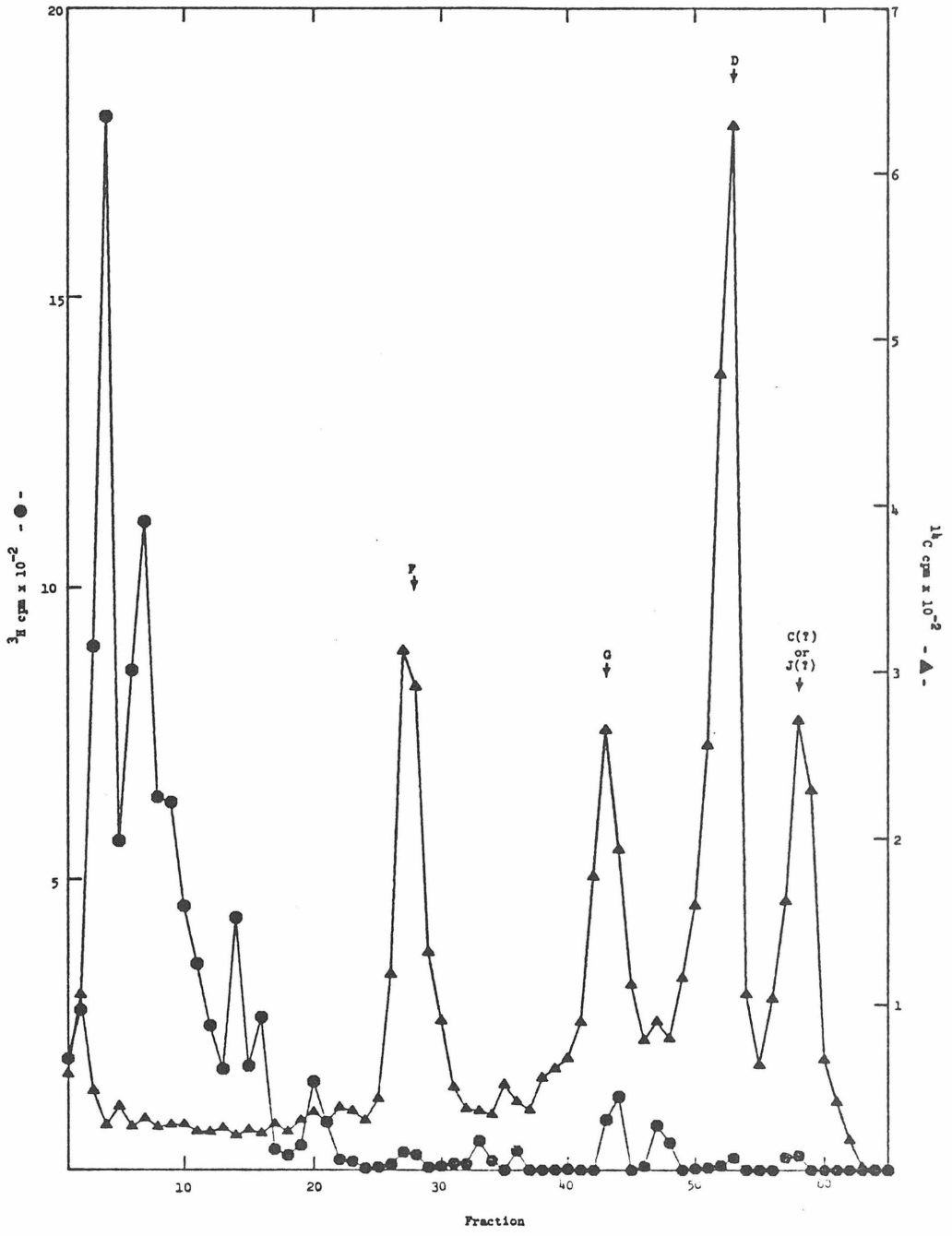
20
15
10
5
7
6
5
4
3
2
1
D
F
G
C(T)
or
J(T)
10
20
30
40
Fraction
^{3}H cpm x 10^{-2} - ● -
^{14}C cpm x 10^{-2} - ▲ -

FIGURE 12. SDS-acryladmide gel electrophoresis of the combined 114S and 111S peaks.

The 114S to 111S region of an infected gradient like that in Fig. 8(a) was pooled and dialysed against 0.05 M-Tris-HCl pH 8.0. The dialysed sample was concentrated by blowing a stream of nitrogen over the sample and then denatured with SDS (0.1%), mercaptoethanol (0.5%) and urea (9 M) and electrophoresed on a 12% acrylamide gel by the method of Mayol and Sinsheimer (8). The gel was fractionated by slicing with stacked razor blades, solubilized in 90% toluene, 10% NCS and counted by the procedure of these same authors. The scintillation counter output was processed by means of the CNTSEP program. Peak assignments are made on the basis of comparisons with other gels.

▲ ^{14}C-leucine

● ^{3}H-thymidine

FIGURE 13

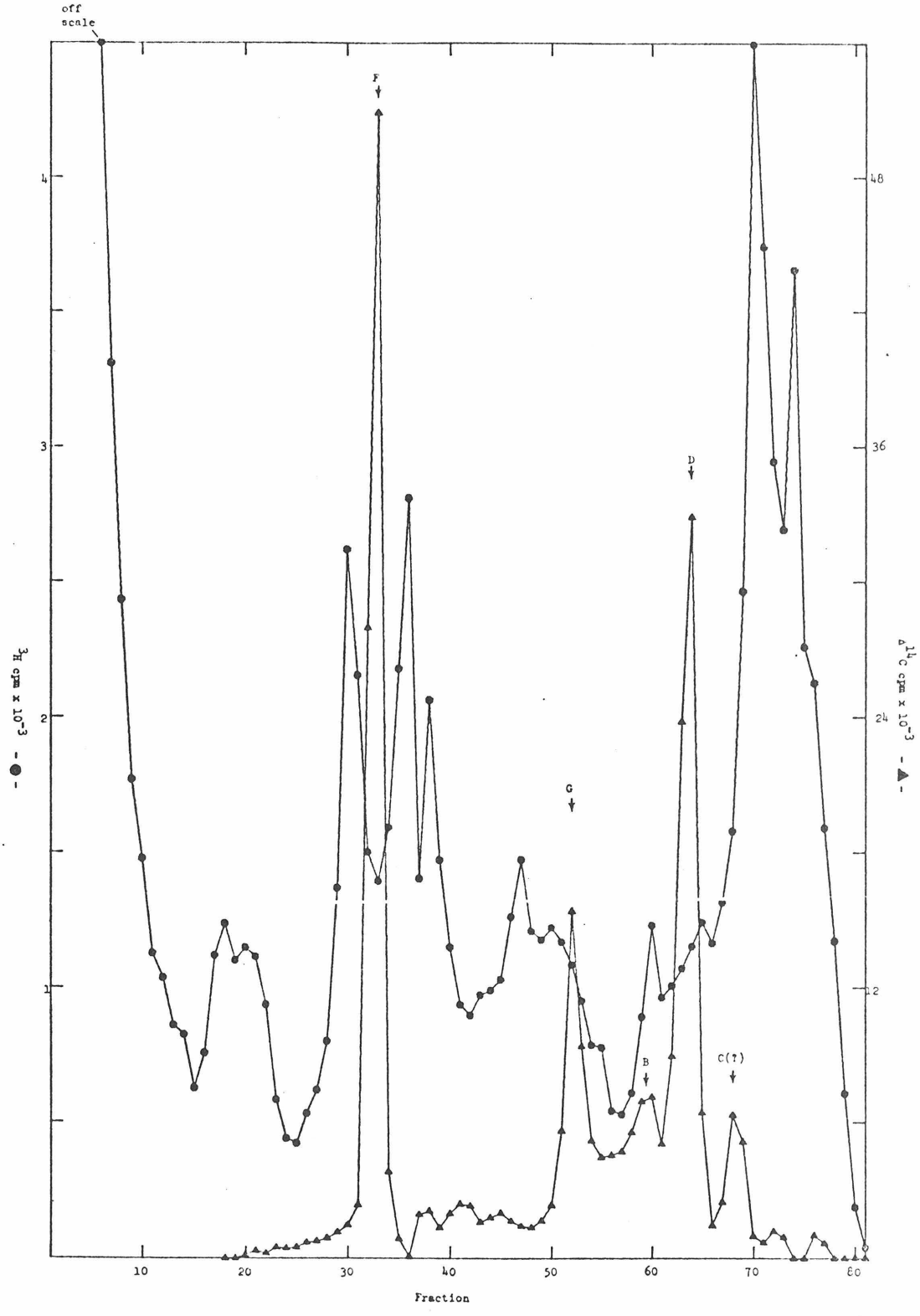
off scale
F
D
G
B
C(?)
4
3
2
1
48
36
24
12
0
10
20
30
40
50
60
70
80
Fraction
^{3}H cpm x 10^{-3} - ● -
$\Delta^{14}C$ cpm x 10^{-3} - ▲ -

FIGURE 13. SDS-acrylamide gel electrophoresis of fraction A from Fig. 8(b).

The fractions indicated from A to F in Fig. 8(b) were pooled separately from the infected and uninfected gradients, brought to 100 µg/ml BSA, 100 µg/ml calf thymus DNA and 0.005 M-EDTA and then dialysed against several changes of 0.01 M-Tris, 0.001 M-EDTA pH 7.4 at 4°C. The retentates were collected into siliconized shell vials and the dialysis bags rinsed with the dialysis buffer and the rinse added to the sample. Recoveries were 50 to 70% for all labels. A 200 µl aliquot of the infected material at A was mixed with 200 µl of uninfected material in a siliconized shell vial and then brought to dryness on the Evapo-Mix. The sample was redissolved in 100 µl of 1% SDS, 1% 2-mercaptoethanol, 10% glycerol and incubated for 2 min at 100°C. The entire mixture was then applied to the top of a 15% 7 x 110 mm gel and electrophoresed, counted, and the ϕX specific fraction of the ^{14}C label, $\Delta^{14}C$, computed as described in procedure I in the Methods. A separate gel was run on the infected fraction alone which as described in the text permitted the assignment of the large peak of ^{3}H label at the top of the gel to ^{3}H-thymidine label. Because of the presence of non-protein ^{3}H label in this region of the gel, the $\Delta^{14}C$ calculation (see Methods) generates negative values under this DNA peak. These values were not plotted. Peak identities are assigned by reference to Table 1 in the General Introduction.

● ^{3}H-leucine, uninfected; ^{3}H-thymidine, infected

▲ $\Delta^{14}C$-leucine

FIGURE 14

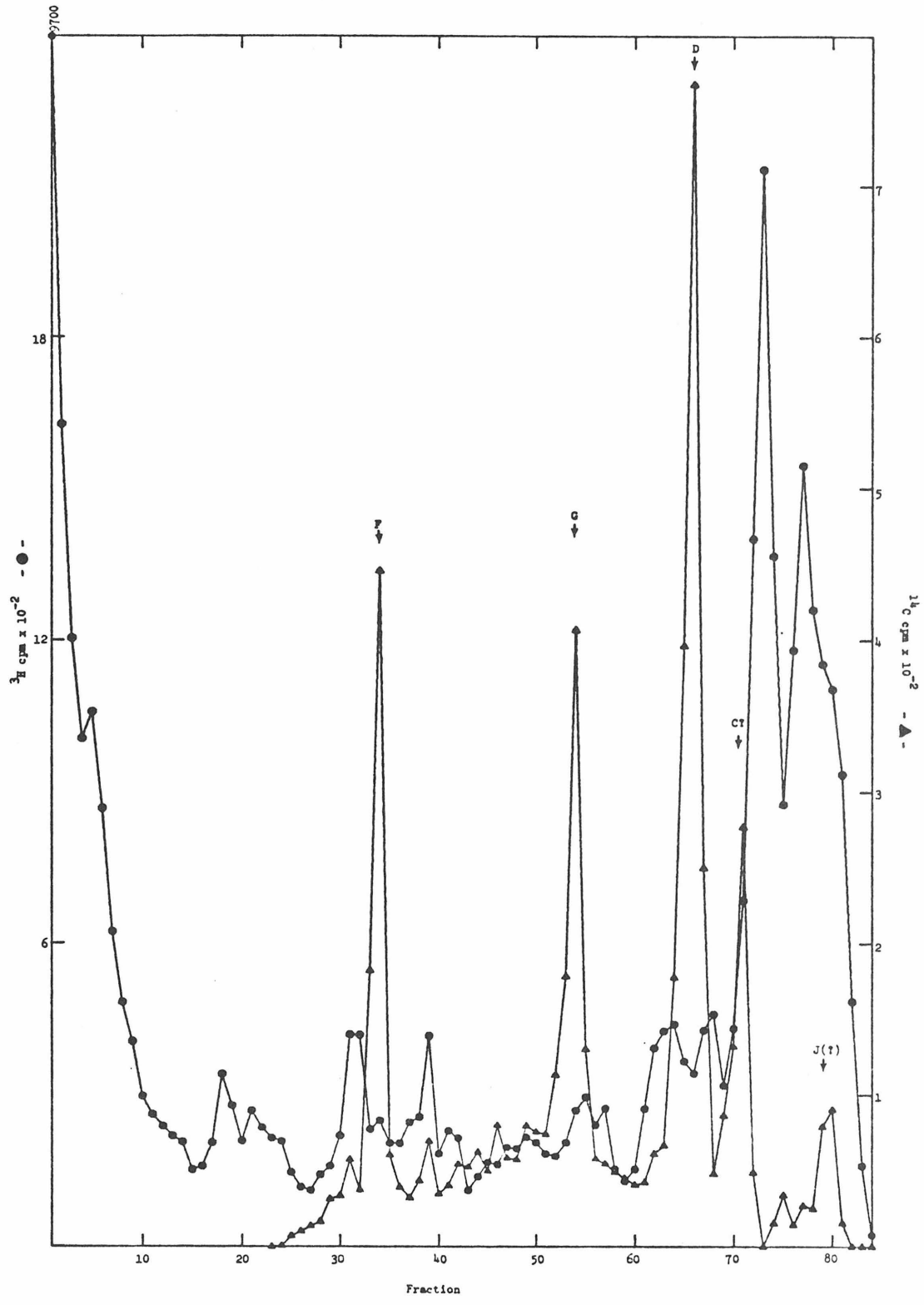

FIGURE 14. SDS-acrylamide gel electrophoresis of fraction B from Fig. 8(b).

250 µl and 100 µl aliquots of the pooled and dialysed, infected and uninfected material, respectively, from fraction B in Fig. 8(b) were mixed, concentrated and electrophoresed as described in the legend to Fig. 13.

● ^{3}H-leucine, uninfected; ^{3}H-thymidine, infected

▲ Δ^{14}C-leucine

FIGURE 15

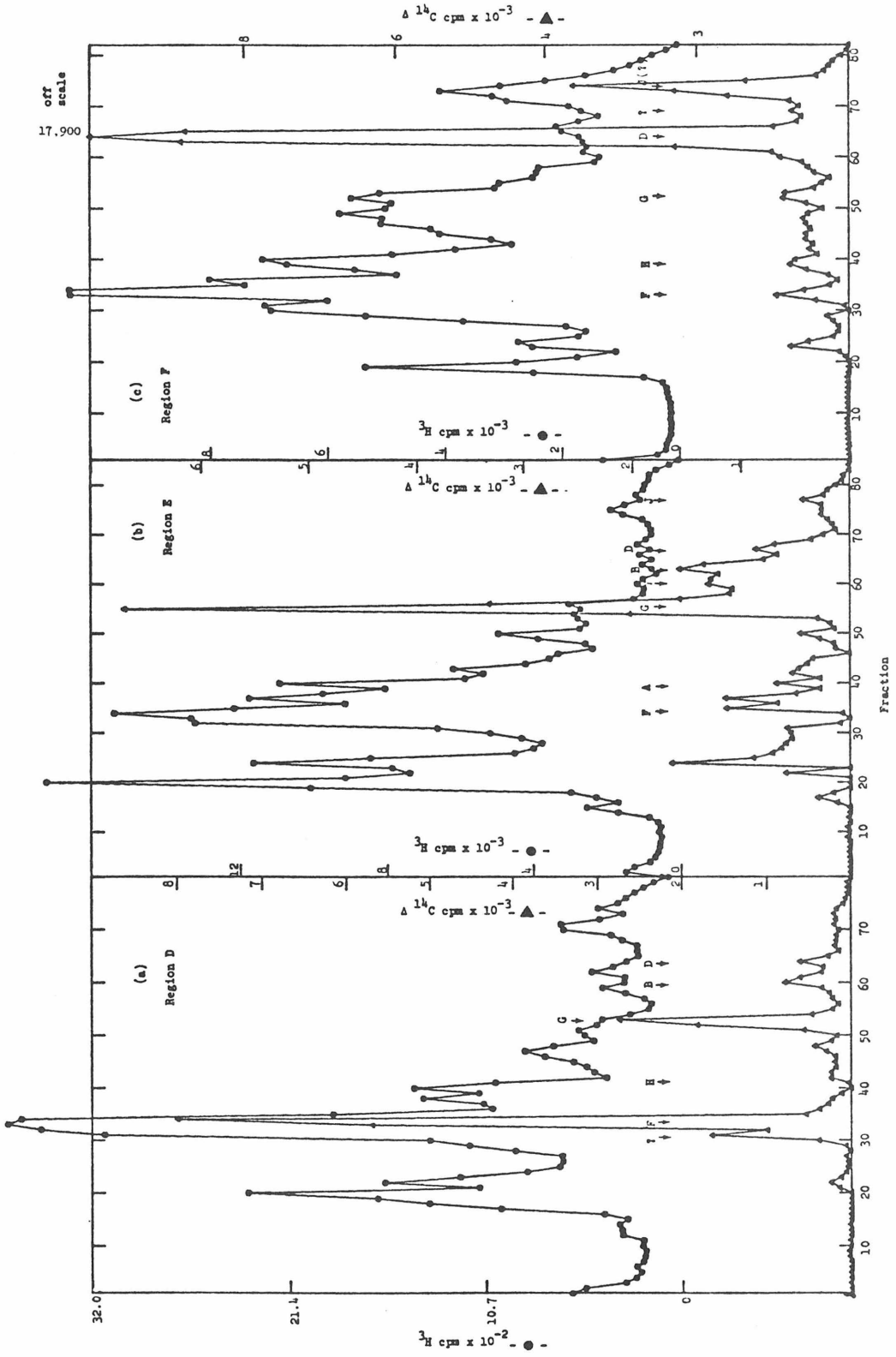
off scale
17,900
Δ 14C cpm x 10-3 - ▲ -
3H cpm x 10-3 - ● -
(c) Region F
(b) Region E
(a) Region D
3H cpm x 10-2 - ● -
32.0
21.4
10.7
0
Fraction

FIGURE 15. SDS acrylamide gel electrophoresis of fractions D, E and F from Fig. 8(b).

Infected and uninfected fractions from D, E and F in Fig. 8(b) were separately pooled and dialysed as indicated in the legend to Fig. 13. In each case 300 µl of the infected material was mixed with 100 µl of the uninfected material, then concentrated, redissolved and electrophoresed as described for Fig. 13. The DNA in fraction F was found in the top few fractions of an infected only control gel.

(a) Fraction D

(b) Fraction E

(c) Fraction F - The peak of D protein is plotted off scale so that the minor components may be visualized.

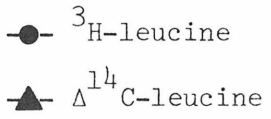

FIGURE 16

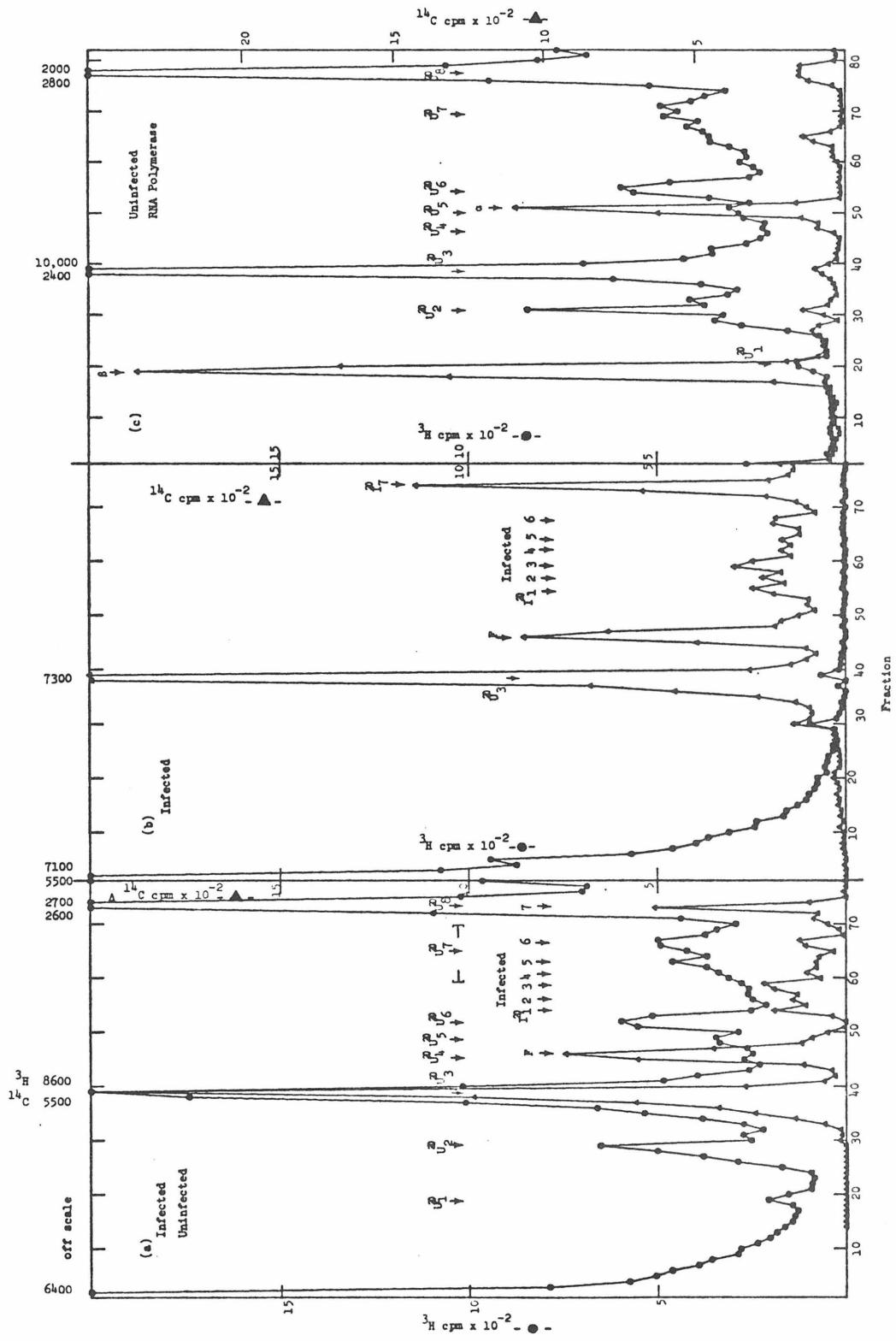
Uninfected
RNA Polymerase
(c)
(b) Infected
(a) Infected
Uninfected
Infected
off scale
Fraction
^{14}C cpm x 10^{-2}
^{3}H cpm x 10^{-2}
2000
2800
10,000
2400
7300
7100
5500
2700
2600
8600
6400

FIGURE 16. SDS acrylamide gel electrophoresis of fraction C from Fig. 8(b).

Fractions 25-30 including both the infected and uninfected "20S" sedimentation peaks in Fig. 8(b) were pooled separately and dialysed as described in the legend to Fig. 13. Sample (a) contained 250 µl and 150 µl of the infected and uninfected fraction C, respectively. Sample (b) contained 250 µl of the infected fraction C only. Sample (c) contained 150 µl of the uninfected fraction C mixed with 10 µl of a ^{14}C-leucine labeled, purified RNA polymerase marker prepared in collaboration with Lloyd Smith. The samples were concentrated and then electrophoresed on 7 x 110 mm 12% acrylamide gels according to procedure I in the Methods. The uninfected peaks are labeled U_1^{20}-U_8^{20} and the infected peaks I_1^{20}-I_6^{20} for reference purposes. The gene F assignment is made on the basis of the mobility of this peak and its comigration with F protein in other experiments. The alpha and beta RNA polymerase subunits are labeled. The Δ^{14}C calculation in (a) was performed utilizing the ratio observed under host peaks 2 and 6.

(a) Infected and uninfected 20S peak

● ^{3}H-leucine, uninfected; ^{3}H-thymidine, infected

▲ Δ^{14}C-leucine

(b) Infected 20S peak

● ^{3}H-thymidine

▲ ^{14}C-leucine

(c) Uninfected 20S peak and RNA polymerase marker

● ^{3}H-leucine, uninfected

▲ ^{14}C-leucine labeled RNA polymerase

FIGURE 17

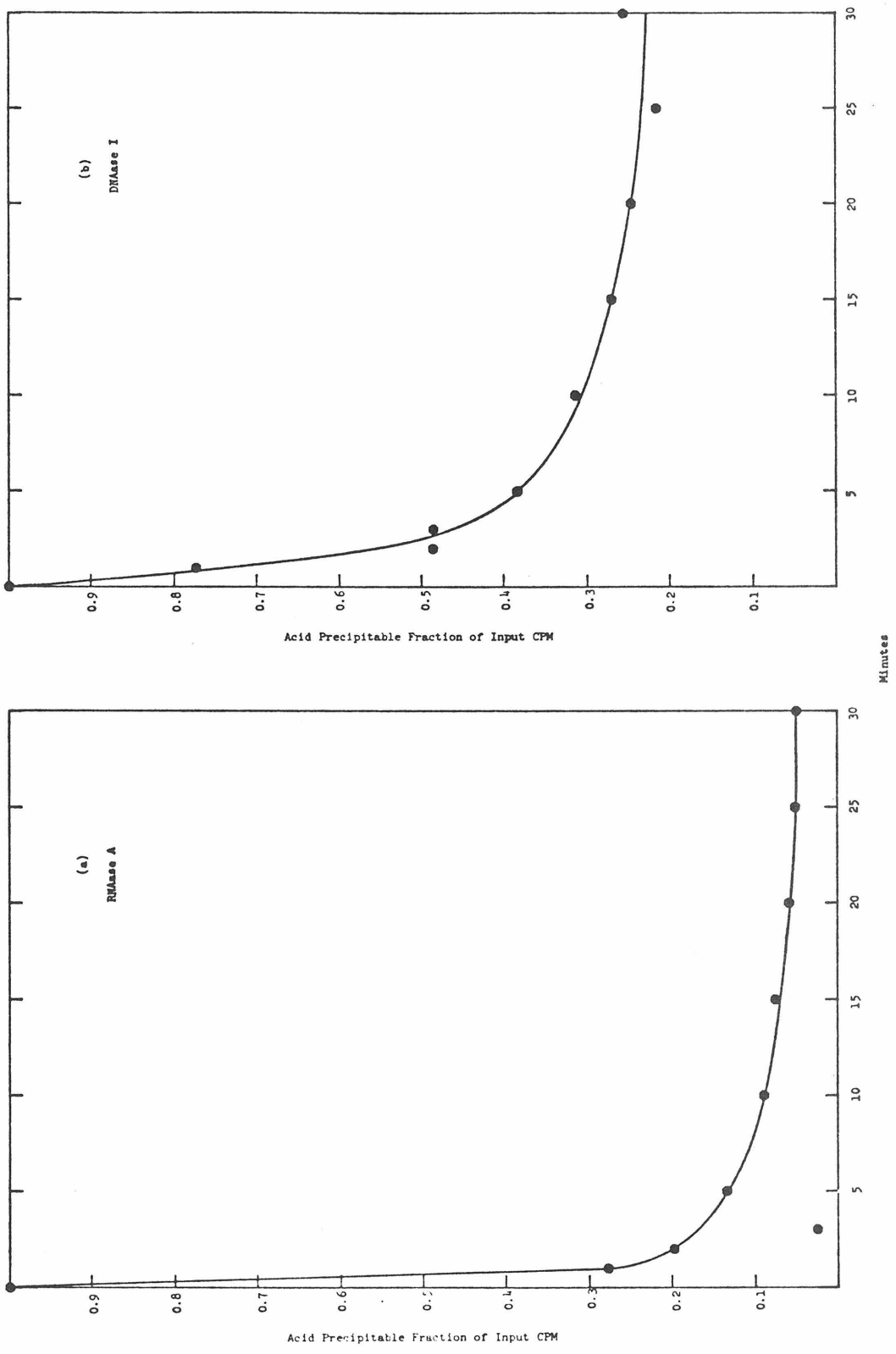
(b)
DNAse I
Acid Precipitable Fraction of Input CPM
0.9
0.8
0.7
0.6
0.5
0.4
0.3
0.2
0.1
5
10
15
20
25
30
Minutes
(a)
RNAse A
Acid Precipitable Fraction of Input CPM

FIGURE 17. Characterization of DNase I and RNase A nucleolytic activities in the presence of t-RNA and calf thymus DNA carriers.

(a) Purified ^{32}P labeled ϕX RF II DNA was brought to a final concentration of 20,000 cpm/50 µl in 600 µl of TM buffer containing 0.1% BSA, 0.001% calf thymus DNA carrier and 16.7 µg/ml t-RNA. After removing a zero time sample 12 µl of a 0.25 mg/ml stock solution of RNase free DNase I was added.

(b) Purified ^{3}H labeled mammalian ribosomal RNA was brought to a final concentration of 25,000 cpm/50 µl in 600 µl of TM buffer containing 0.1% BSA, 0.0% calf thymus DNA carrier and 16.7 µg/ml t-RNA. After removing a zero time sample 12 µl of a 1.0 mg/ml stock solution of heat treated RNase A was added.

Both mixtures were brought to 37°C before the addition of nuclease. Fifty lambda aliquots were then removed to 5 ml of 0°C 10% TCA at the times indicated. One drop of 1 mg/ml calf thymus carrier DNA was added to each sample, mixed, and the sample filtered through a GF/C glass filter. The filter was washed three times with 5 ml of 10% TCA and one time with 5 ml of 0°C 100% ethanol. The filters were dried and counted in TL.

(a) RNase A digestion

(b) Dnase I digestion

Percent input cpm that remain TCA precipitable

FIGURE 18

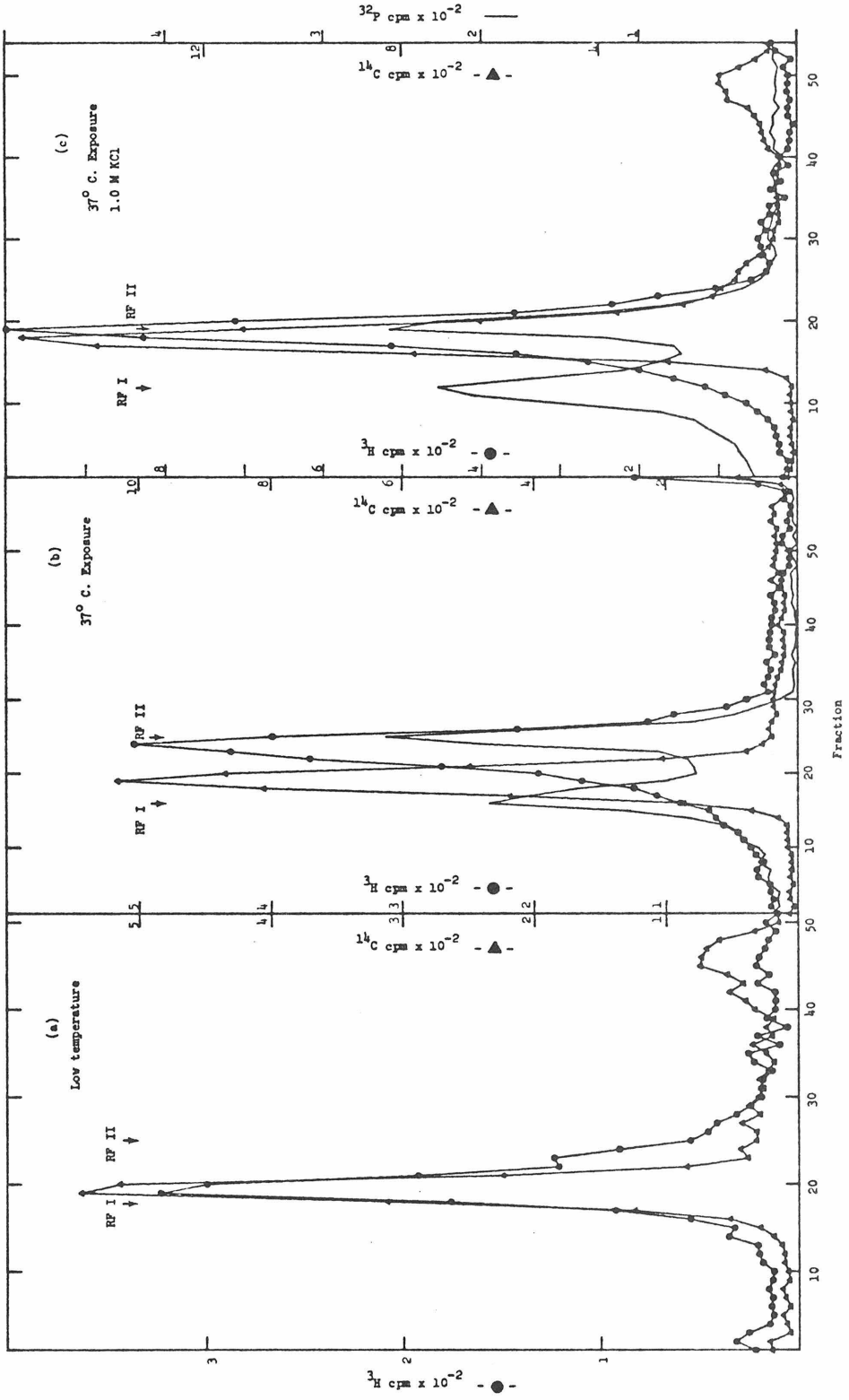
(a)
Low temperature
RF I
RF II
^{3}H cpm x 10^{-2} - ● -
(b)
37° C. Exposure
RF I
RF II
^{14}C cpm x 10^{-2} - ▲ -
^{3}H cpm x 10^{-2} - ● -
(c)
37° C. Exposure
1.0 M KCl
RF I
RF II
^{14}C cpm x 10^{-2} - ▲ -
^{3}H cpm x 10^{-2} - ● -
^{32}P cpm x 10^{-2} ——
Fraction

FIGURE 18. Resedimentation of the 20S peak from Fig. 8(b) after exposure to 37°C, EDTA and high ionic strength.

(a) A 100 µl aliquot of the pooled 20S peak from the infected gradient in Fig. 8(b) was brought to a final volume of 600 µl in TM buffer and to 0.1% BSA, 0.01% calf thymus DNA and 16.7 µg/ml t-RNA while taking care to keep the sample and buffers at $\leq$ 4°C. This sample was then layered onto a linear 10-30% sucrose gradient in TM buffer and sedimented under the same conditions employed in Fig. 19. The gradient was collected directly into scintillation vials and counted in a dioxane scintillator. The RF I and RF II positions indicated are derived from a parallel sedimentation of those marker DNAs in the same experiment and under identical buffer conditions.

The centrifugations in (b) and (c) were conducted in a separate experiment. In this case, 75 µl aliquots of the pooled 20S peak from the infected gradient in Fig. 8(b) were brought to a final volume of 400 µl in TM buffer and to 0.05% BSA, 9 µg/ml t-RNA and 50 µg/ml calf thymus DNA. One aliquot was kept at 4°C, another incubated at 37°C for 20 min (presented in (b)) and another titrated to 0.013 M-EDTA to give a final free EDTA concentration of 0.005M. All three samples gave a pattern like that presented in (b). Two aliquots were made 0.30 M in KCl and one of these was titrated with 0.013 M-EDTA. Both of these samples gave a pattern intermediate between those in (b) and (c) (see text). A final aliquot presented in (c) was made 1.0 M in KCl and 0.013 M in EDTA. 10 µl of ^{32}P labeled RF I and RF II DNA were added to each sample. Each sample was then layered onto an isokinetic sucrose gradient preformed in the homologous buffer (see Methods) and sedimented at 40,000 rpm for 12 hrs at 4°C in a SW40 rotor. Fractions were collected

directly into scintillation vials and counted in Aquasol. The isotopic composition of each fraction was computed by the TRIPSEP program.

(a) Resedimentation in TM buffer after no exposure to >4°C.

(b) Resedimentation in TM buffer after incubation at 37°C.

(c) Resedimentation in TM buffer substituted with 1.0 M-KCl, 0.013 M-EDTA after incubation at 37°C.

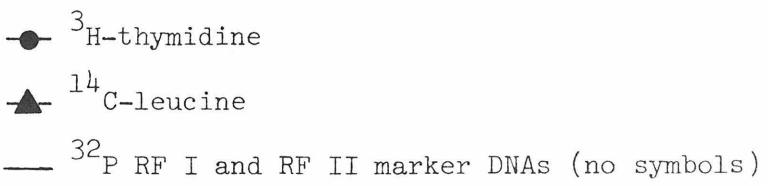

FIGURE 19

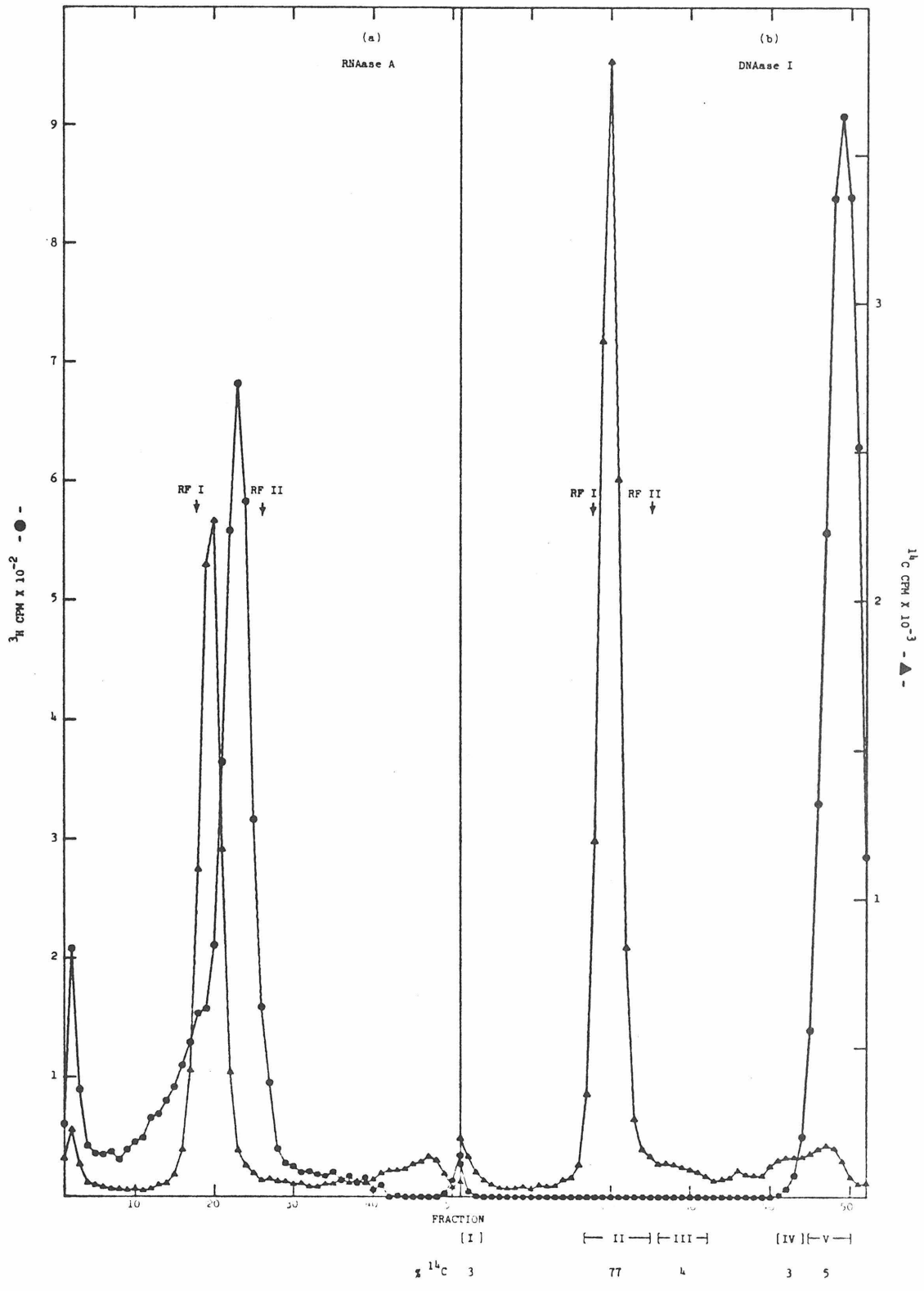
(a)
RNAase A
(b)
DNAase I
RF I
RF II
RF I
RF II
^{3}H CPM X 10^{-2} - ● -
^{14}C CPM X 10^{-3} - ▲ -
FRACTION
[I]
II
III
IV
V
% ^{14}C 3 77 4 3 5

FIGURE 19. The DNase and RNase sensitivity of the 20S peak from Figure 8b.

200 µl aliquots of the pooled 20S peak from the infected gradient in Fig. 8b were brought to final volumes of 600 µl in TM buffer and to the final concentrations of carrier molecules given in the legend to Fig. 17. These mixtures were brought to 37°C and heat treated RNase A or RNase free DNase I were added in (a) and (b), respectively. After a 20 min incubation at 37°C the entire samples were layered onto separate 10-30% sucrose gradients formed in TM buffer substituted with 0.01% BSA, 50 µg/ml t-RNA and 0.01 M NaN_3 over an underlayer of 0.3 ml of 50% Angio Conray and then centrifuged at 40,000 rpm for 12 h at 4°C in an SW 40 rotor. The gradients were collected into siliconized shell vials and 100 µl aliquots spotted onto paper filters, dried and counted in TL. The fractions indicated were pooled for later experiments. The RF I and RF II positions indicated were derived from a parallel sedimentation of marker DNAs in the same experiment and under the same buffer conditions.

(a) RNase A digestion

(b) DNase I digestion

-●- ^{3}H thymidine

-▲- ^{14}C leucine

FIGURE 20

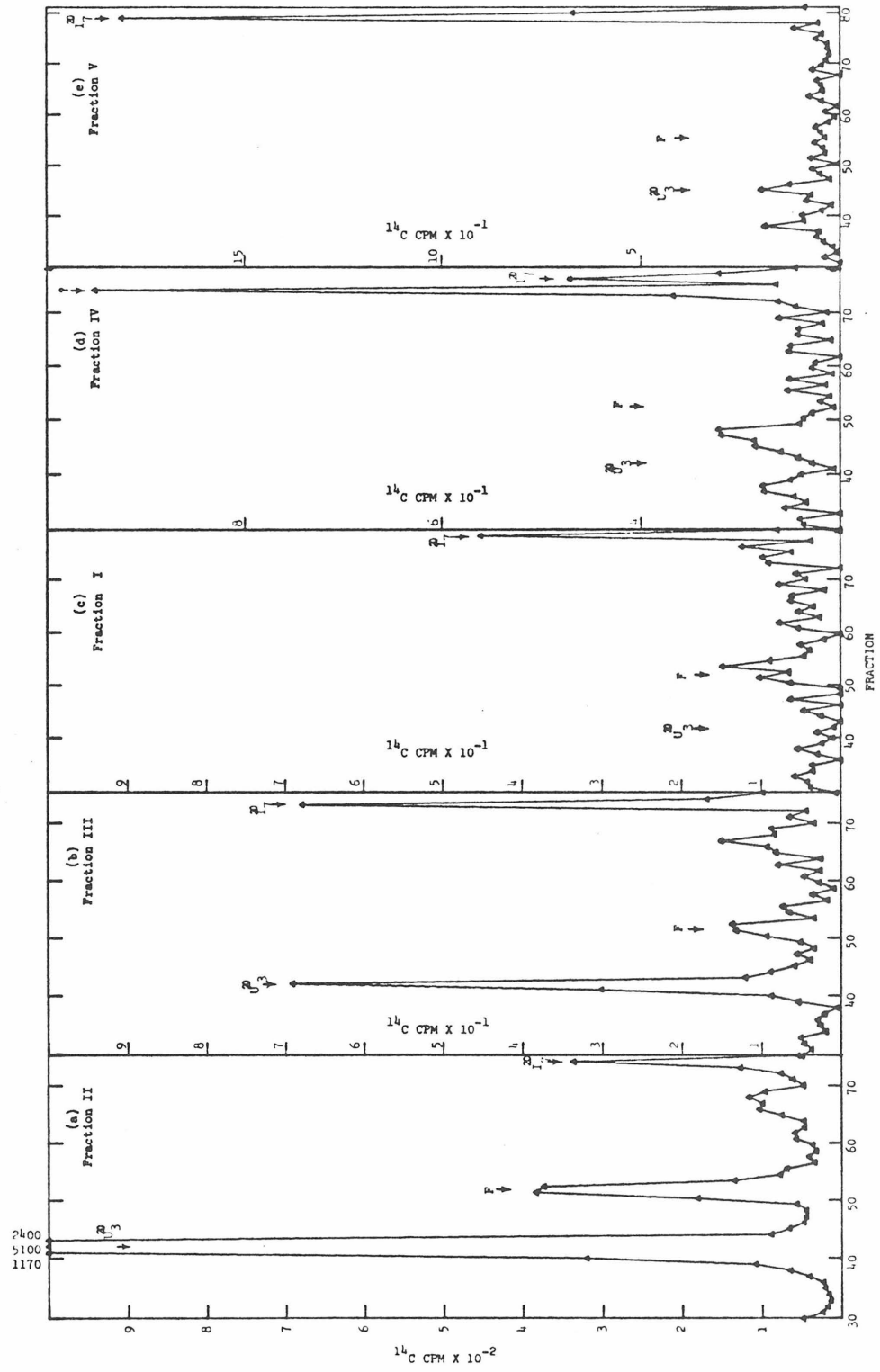
(a) Fraction II
(b) Fraction III
(c) Fraction I
(d) Fraction IV
(e) Fraction V
^{14}C CPM X 10^{-2}
^{14}C CPM X 10^{-1}
FRACTION
F
2400
5100
1170

FIGURE 20. SDS acrylamide gel electrophoresis of the protein peaks in Figure 19b.

The fractions indicated as I through V in the resedimentation gradient in Fig. 19b were pooled and dialysed against 0.01 M-Tris HCl, pH 7.2. The retentates were collected in siliconized glass vials and brought to dryness on the Evapo-Mix, then redissolved in 100 µl of 1% SDS, 1% ß-mercaptoethanol, 10% glycerol, and incubated for 2 min at 100°C. Merker dye was added and the samples layered onto 7 x 110 mm 12% acrylamide gels and electrophoresed according to procedure I in the Methods. Gels were fractionated into 1 mm slices with a Mickel Gel Slicer and counted in TLNCS. Although fractions were monitored for ^{3}H-thymidine as well as ^{14}C-leucine, no significant ^{3}H-thymidine incorporation was observed. Fractions 1-30 were not plotted as neither label was observed in them. Peak assignments were made by comparison with the gels in Fig. 16.

(a) 20S peak- fraction II

(b) Shoulder of the 20S peak- fraction III

(c) Bottom - fraction I

(d) Top - fraction IV

(e) Top - fraction V

-▲- ^{14}C-leucine

FIGURE 21

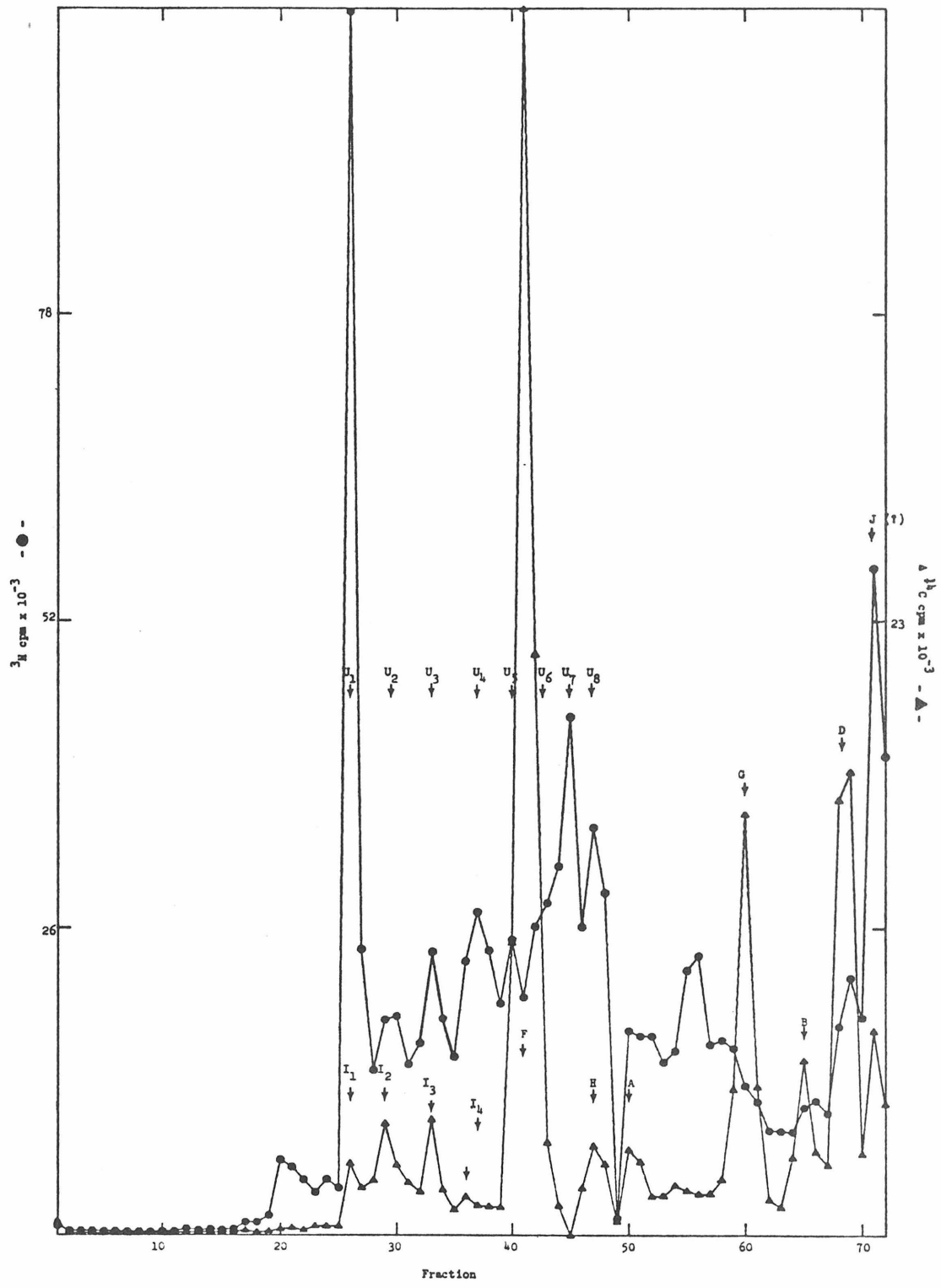
78
52
26
23
10
20
30
40
50
60
70
Fraction
^{3}H cpm x 10^{-3} - ● -
^{14}C cpm x 10^{-3} - ▲ -
U1
U2
U3
U4
U5
U6
U7
U8
I1
I2
I3
I4
F
H
A
G
D
B
J (T)

FIGURE 21. A comparison of the infection specific proteins and the host proteins from a whole lysate of a non-UV irradiated ϕXam3 infected H502 culture.

E. coli H502 was grown to 3 x 10^8 cells/ml in TPG supplemented with 1 µg/ml thymine and then split into two 15 ml aliquots. One portion was infected with ϕXam3 at a multiplicity of 7. 30 min later the uninfected culture was pulsed for 6 min with ^{3}H-leucine at a final concentration of 20 µc/ml and 2 c/mmole. 50 min after infection the infected culture was pulsed for 60 min with ^{14}C-leucine at a final concentration of 2 µc/ml and 312 mc/mmole. Both pulses were stopped by rapid cooling, thawed at 0°C, washed three times in equal volumes of TE-azide, and lysed by procedure I. The lysates were extensively dialysed against 0.05 M-Tris-HCl pH 7.6 and the retentates stored frozen in siliconized glass tubes.

10 µl of the infected an uninfected lysates were mixed, denatured and electrophoresed on 12% acrylamide gels as described in procedure I in the Methods. The electrophoresis was stopped when the marker dye was 2 cm from the bottom of the gel. The gel was then fractionated, counted, and the Δ^{14}C infection specific cpm computed as described in the Methods. ϕX proteins were assigned on the basis of Table I from the Introduction. The host proteins and the four high molecular weight infection specific proteins were numbered and lettered, respectively, to facilitate discussion.

-●- ^{3}H-leucine - uninfected

-▲- Δ^{14}C-leucine- infected

FIGURE 22

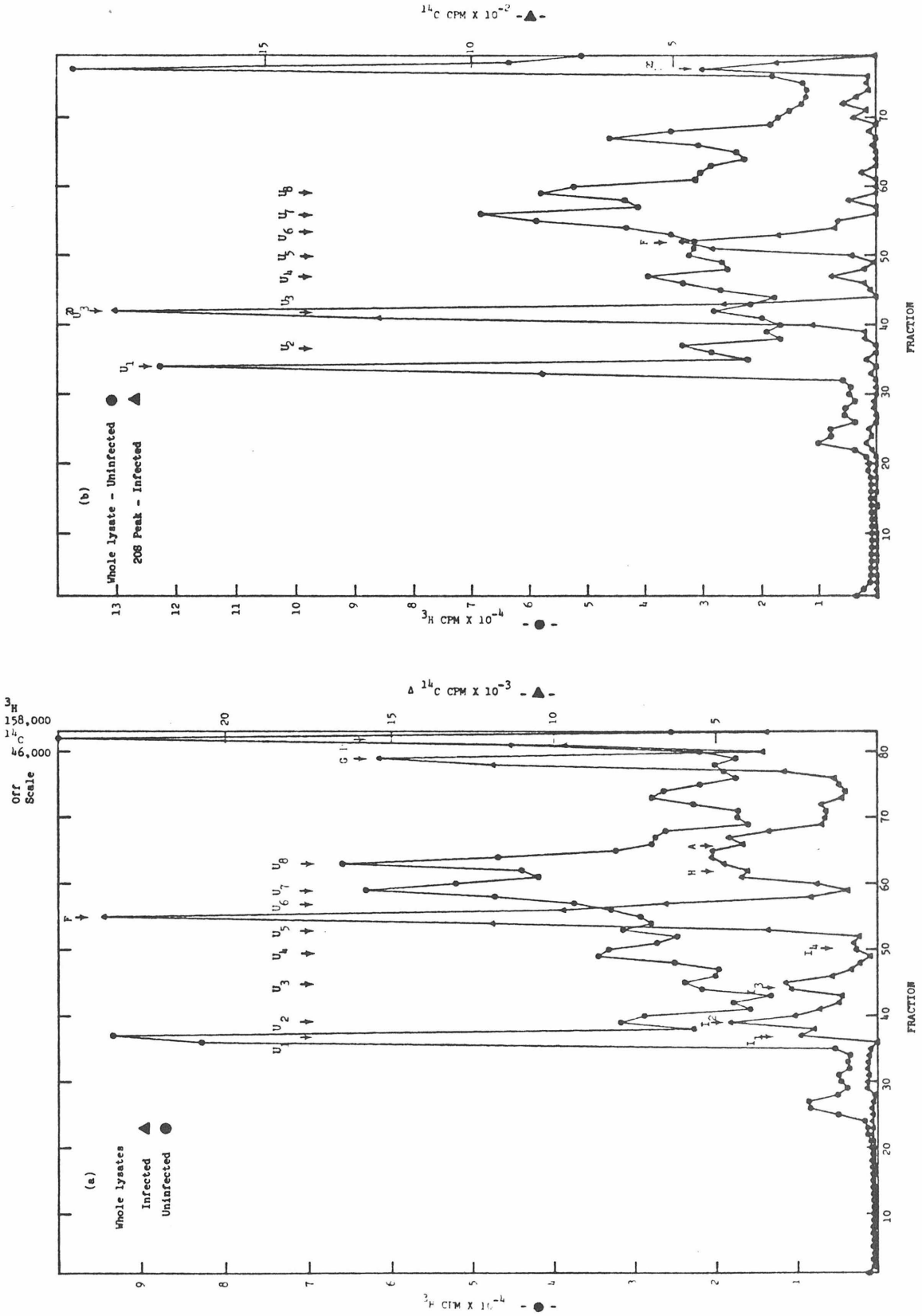
(a)
Whole lysates
Infected
Uninfected
Off Scale
^{3}H 158,000
^{14}C 46,000
^{3}H CPM X 10^{-4} - ● -
$\Delta\ ^{14}C$ CPM X 10^{-3} - ▲ -
FRACTION
(b)
Whole lysate - Uninfected
208 Peak - Infected
^{3}H CPM X 10^{-4} - ● -
^{14}C CPM X 10^{-2} - ▲ -
FRACTION

FIGURE 22. Assignment of host protein U_3 from the 20S peak to a host protein peak in the electrophoretic pattern of whole lysates of infected and uninfected cells.

The infected and uninfected lysates are those prepared in conjunction with the experiment in Fig. 21. Sample preparation, denaturation and electrophoresis are as in Fig. 21 except that the electrophoresis was not stopped until the marker dye was less than 1 cm from the bottom of the gel. Numberings and letterings are as in Fig. 21.

(a) 10 µl of the infected and uninfected lysates as in Fig.21.

-●- ^{3}H-leucine - uninfected

-▲- Δ^{14}C-leucine - infected

(b) 10 µl of the uninfected lysate mixed with 50 µl of the 20S peak from the infected gradient in Fig. 8b.

-●- ^{3}H-leucine - uninfected

-▲- ^{14}C-leucine - infected 20S peak

FIGURE 7.5

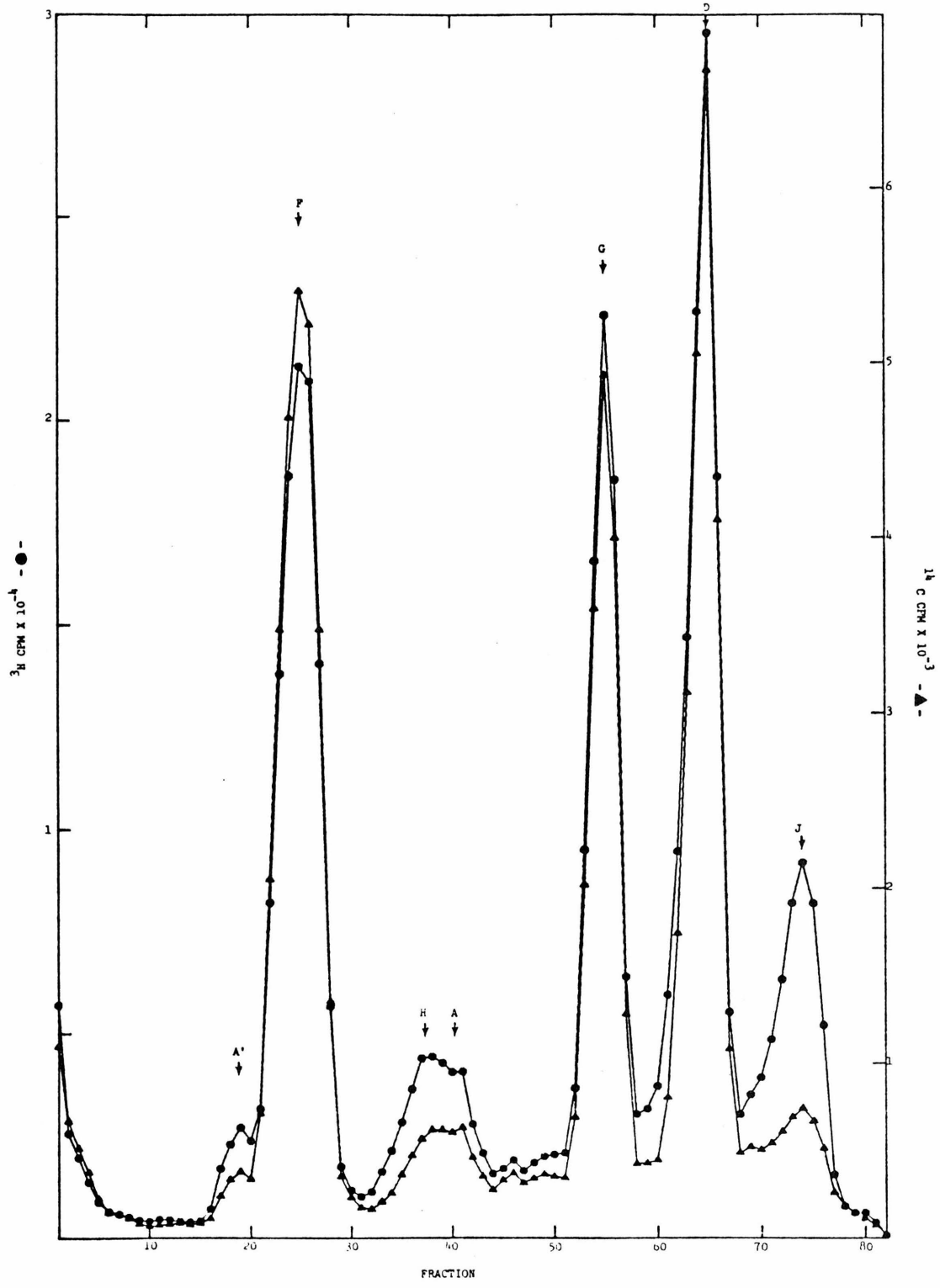

FIGURE 23. Comparison of leucine and lysine labels - Coelectrophoresis of ^{14}C-leucine and ^{3}H-lysine labeled lysates of ϕX174 wt infected, UV pretreated H502 host cells.

A 50 ml portion of a culture of H502 grown to 3 x 10^8 cells/ml at 37°C in TPG supplemented with 5 µg/ml thymine was UV irradiated for 5 min at room temperature and then aerated for 10 min at 37°C as described in the Methods. Two 5 ml aliquots were then infected with ϕX wt virus at a multiplicity of 10. The cultures were incubated with aeration at 37°C. At 30 min after infection ^{14}C-leucine was added to one culture at a final concentration of 2 µc/ml and 2 µg/ml. ^{3}H-lysine was added to the other culture at 20 µc/ml and 2 µg/ml. 90 min after infection both cultures were cooled to 0°C in an ice bath, washed once in TE buffer, resuspended in 150 µl of TE, and lysed by incubating at room temperature after the addition of 10 µl of a 1 µg/ml solution of lysozyme. The lysates were dialysed against 0.05 M-Tris-HCl pH 7.6 at 4°C. 25 µl portions of each retentate were then mixed, denatured, electrophoresed on 15% SDS acrylamide gels, fractioned and counted according to procedure I in the Methods. The isotopic composition of each fraction was determined with the CNTSEP program. Peaks are labeled according to Table 1 from the General Introduction.

-●- ^{3}H-lysine

-▲- ^{14}C-leucine

FIGURE 24

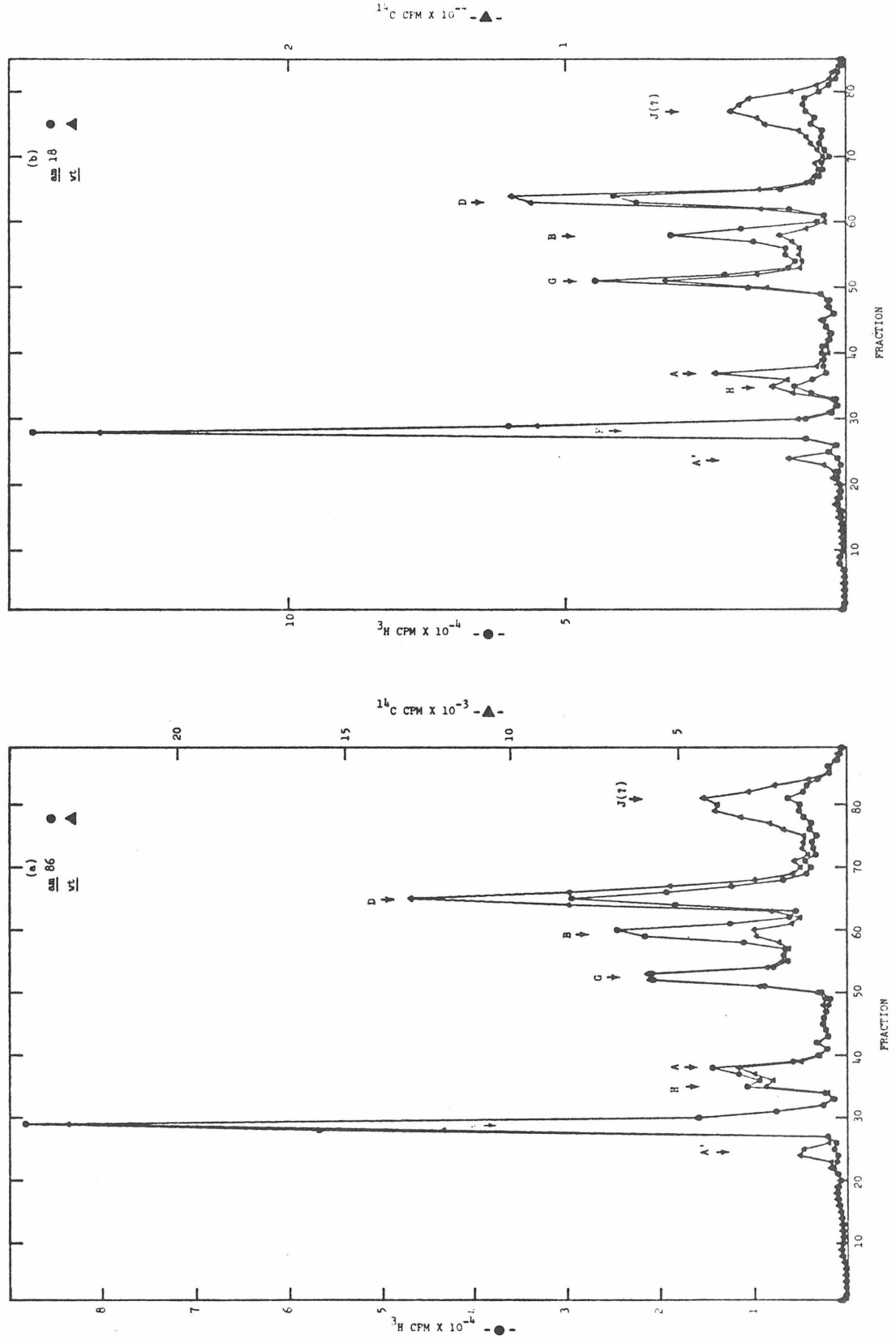
(a)
am 86
vt
(b)
am 18
vt
A'
H
A
G
B
D
J(?)
FRACTION
^{3}H CPM X 10^{-4} -●-
^{14}C CPM X 10^{-3} -▲-
^{14}C CPM X 10^{-4} -▲-

FIGURE 24. The effect of φX gene A mutations on the synthesis of φX proteins in UV irradiated host cells.

E. coli H502 was grown to 3 x 10^8 cells/ml at 37°C in TPG medium supplemented with 5 μg/ml thymidine. A 50 ml portion was UV irradiated for 7.5 min at room temperature, then aerated at 37°C for 10 min as described in the methods. Separate 5 ml aliquots were then infected with φX174 wt, am86 and am18 at multiplicities of infection of 12, 10 and 10, respectively. The infection was allowed to proceed for 30 min with aeration at 37°C before the addition of radioactive label. Then the wt culture was labeled with ^{14}C-lysine at final concentrations of 2.0 μc/ml and 2 μg/ml. The am86 and am18 cultures were labeled with ^{3}H-lysine at final concentrations of 20 μc/ml and 2 μg/ml. 90 min later all cultures were placed in an ice bath and cooled to 0°C. The cultures were washed once in TE buffer, resuspended in 150 μl of the same, and lysed by a brief incubation at room temperature after the addition of 10 μl of a 1 mg/ml lysozyme solution. The lysates were extensively dialysed against TP buffer at 4°C and the retentates transferred to siliconized glass tubes for storage. 20 μl aliquots of the wt lysate were then mixed with 50 μl aliquots of the am86 and am18 lysates in (a) and (b), respectively. These mixtures were then denatured, electrophoresed, fractionated, and counted as described in procedure II in the Methods. The peak assignments are based on Table 1 in the General Introduction.

(a) Am86 plus wt

(b) Am18 plus wt

-●- ^{3}H-lysine, am86 or am18

-▲- ^{14}C-lysine, wt

FIGURE 25

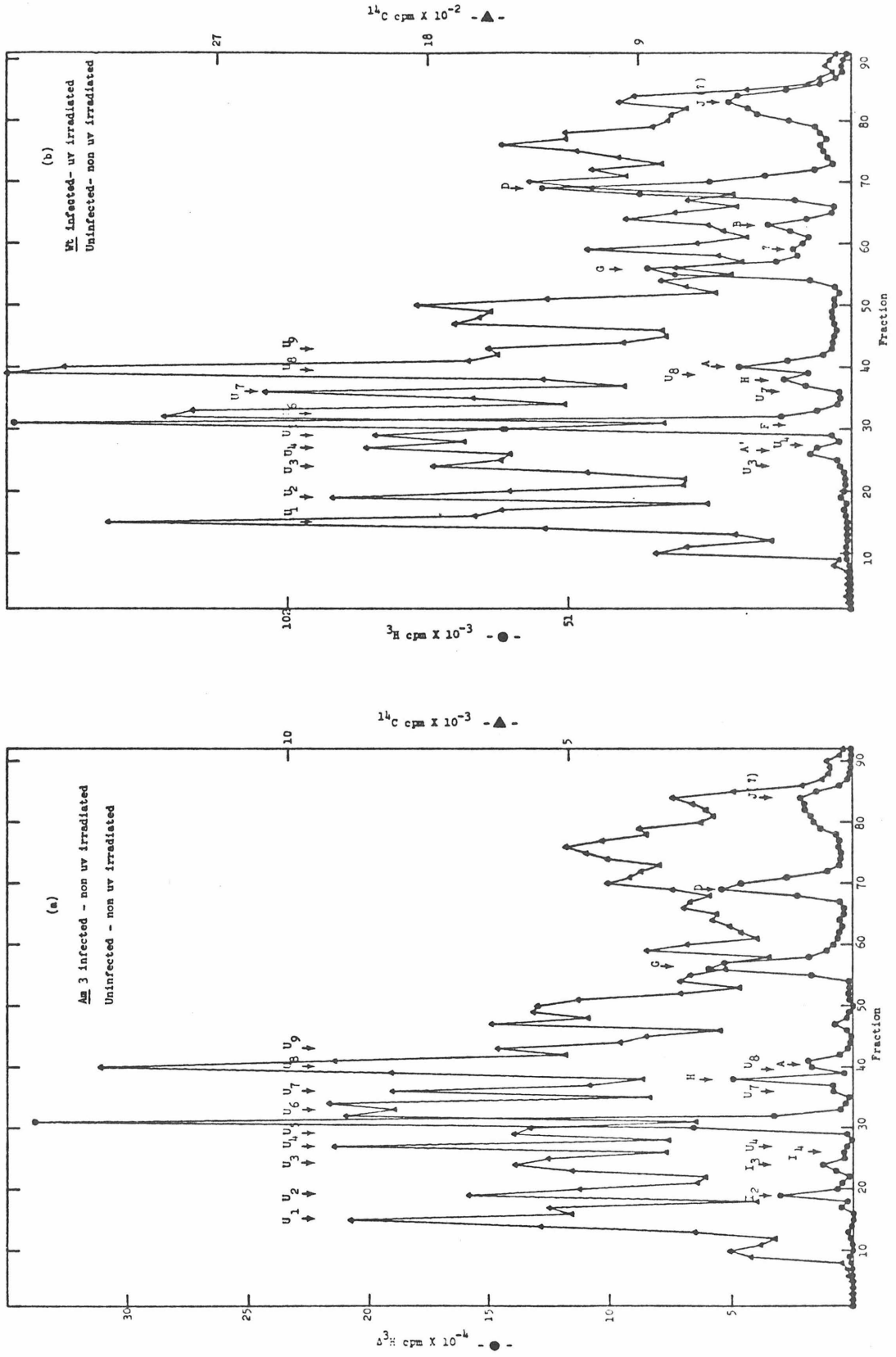
(a)
Am 3 infected - non uv irradiated
Uninfected - non uv irradiated
^{14}C cpm X 10^{-3} -▲-
^{3}H cpm X 10^{-4} -●-
Fraction
(b)
Wt infected- uv irradiated
Uninfected- non uv irradiated
^{14}C cpm X 10^{-2} -▲-
^{3}H cpm X 10^{-3} -●-
Fraction

FIGURE 25. Identification of the locus of the A' protein in the SDS acrylamide gel electrophoresis patterns of whole lysates of non-UV irradiated cells.

E. coli H502 was grown to 3 x 10^8 cells/ml at 37°C in TPG medium supplemented with 5 µg/ml thymidine and 0.2 M-$MgSO_4$ as described in the Methods. At time zero one 5 ml aliquot was infected with φXam3 at a multiplicity of infection of 10 and labeled with ^{3}H-lysine at final concentrations of 20 µc/ml and 2 µg/ml. An uninfected 5 ml aliquot was labeled with ^{14}C-lysine at final concentrations of 2 µc/ml and 2 µg/ml. The cultures were incubated for 140 min at 37°C then cooled to 0°C in an ice bath after addition of NaN_3 to a final concentration of 0.01 M. In (a), 2 ml of the am3 infected culture was mixed with 1 ml of the uninfected culture before lysis. In (b), 1 ml of the uninfected culture was lysed alone.

The respective samples, (a) and (b), were pelleted and then resuspended in 150 µl of 0.05 M sodium tetraborate, 0.05 M-EDTA, 10 µl of a 1 mg/ml solution of lysozyme and 10 µl of 1% SDS. They were then dialysed against TP buffer. Lysis occurred in the dialysis bags. The retentates were transferred to siliconized glass tubes. In (b) 25 µl of the uninfected lysate was mixed with 50 µl of a ^{3}H-lysine labeled lysate of φX wt infected UV irradiated cells prepared as in Fig. 24. This sample and a 75 µl aliquot of sample (a) were then denatured, electrophoresed, fractionated, and counted as described in procedure II in the Methods. The isotopic composition of each sample was computed with the CNTSEP program. In (a), the infection specific ^{3}H incorporation was computed as Δ^3H cpm. Host protein peaks were numbered

as in Fig. 22 and ϕX protein assignments were made according to Table 1 from the General Introduction.

(a) Non-UV irradiated lysates of ϕX<u>am</u>3 infected and uninfected cells.

-●- Δ^{3}H-lysine - infected

-▲- ^{14}C-lysine - uninfected

(b) UV irradiated lysate of ϕX <u>wt</u> infected cells and the non-UV irradiated uninfected lysate from (a).

-●- ^{3}H-lysine - infected

-▲- ^{14}C-lysine uninfected

FIGURE 26

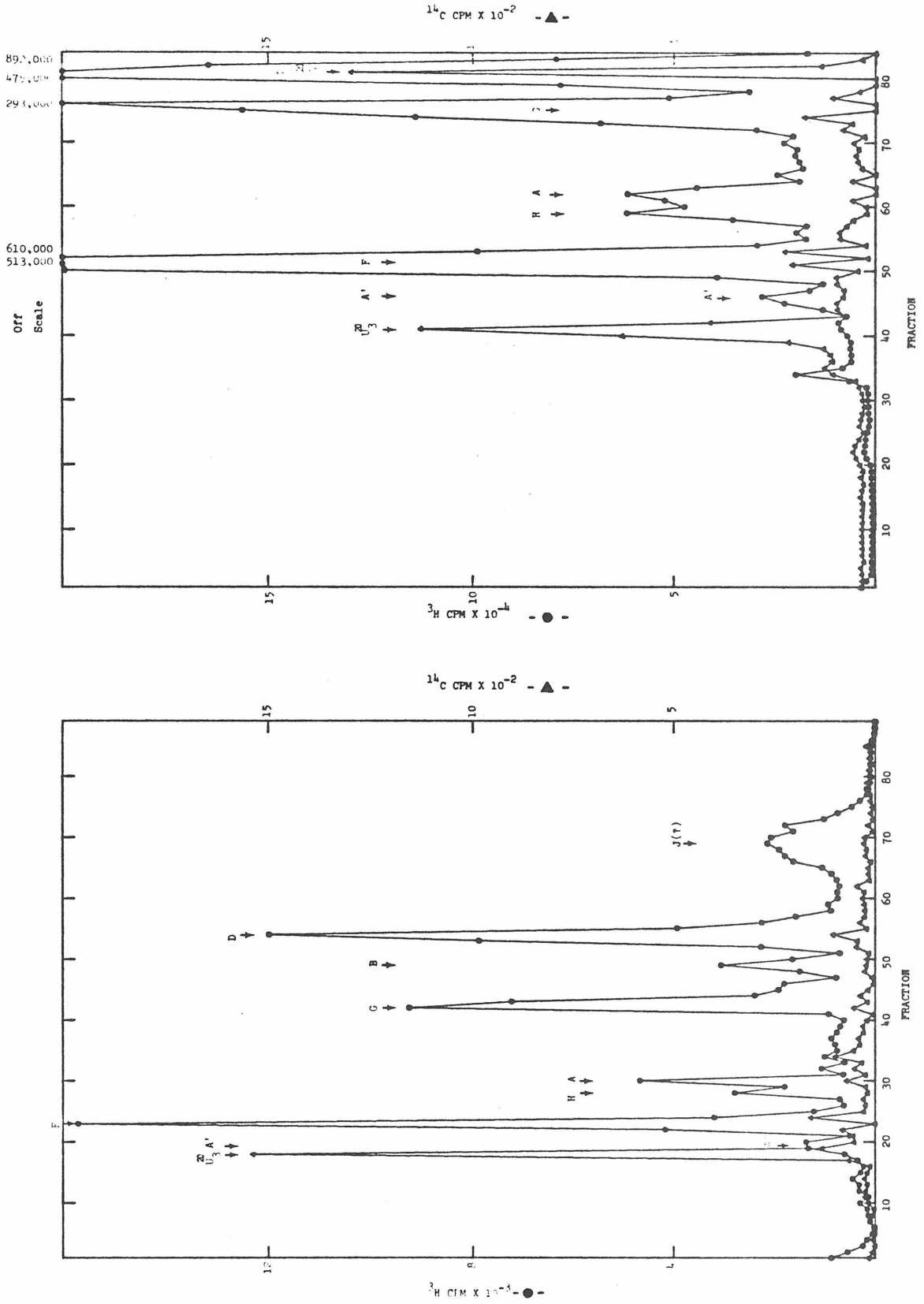
^{14}C CPM X 10^{-2} - ▲ -
610,000
513,000
Off Scale
H A
F
A'
U_3^R
FRACTION
^{3}H CPM X 10^{-4} - ● -
^{14}C CPM X 10^{-2} - ▲ -
J(?)
D
B
G
H A
U_3 A'
FRACTION
^{3}H CPM X 10^{-3} - ● -

FIGURE 26. The relative electrophoretic mobilities of ϕX174 A' protein and host protein U_3 from the 20S sedimentation peak of whole lysates.

25 µl aliquots of the ^{14}C-leucine labeled 20S sedimentation velocity peak from the ϕX infected lysate in Fig. 8b were mixed with one of two preparations of ^{3}H labeled whole lysates of ϕX wt infected, UV irradiated cells and electrophoresed according to two different procedures.

(a) The lysate of ϕX wt infected, UV irradiated cells is the same as that in Fig. 25b. A 10 µl aliquot was mixed with the 20S material, then denatured, electrophoresed, fractionated and counted as in Fig. 24.

(b) E. coli H502 was grown to 3 x 10^8 cells/ml at 37°C in TPG medium supplemented with 10 µg/ml thymine. A 50 ml portion was UV irradiated for 3.5 min at room temperature and then incubated for 10 min with aeration at 37°C as described in the Methods. A 10 ml aliquot was then infected with ϕX wt at a multiplicity of 10. ^{3}H-leucine was added at the same time to final concentrations of 20 µc/ml and 1.3 µg/ml. 90 min later the culture was cooled to 0°C in an ice bath, washed once in TE buffer supplemented with 0.01 M-NaN_3, resuspended in 150 µl of the same and lysed by a brief incubation at room temperature after the addition of 10 µl of a 1 mg/ml lysozyme solution. The lysate was dialysed against 0.05 M-Tris-HCl pH 7.6 at 4°C. Comparison of the ϕX wt infected culture with an uninfected, UV irradiated control labeled at the same time indicated that under these conditions irradiation suppressed uninfected incorporation only by a factor of two relative to infected incorporation. A 25 µl aliquot of the infected lysate was

mixed with the 20S material and brought to 1% SDS, 1% β-mercaptoethanol, 10% glycerol in a final volume of 100 µl then denatured and electrophoresed on 12% acrylamide gels according to procedure I in the Methods. The gel was fractionated and counted according to procedure II in the Methods.

Peak assignments were made by analogy to Fig. 16 and comparison to Table 1 from the General Introduction.

(a) and (b) ^{3}H-lysine labeled lysate of φX wt infected, UV irradiated cells plus the ^{14}C-leucine labeled 20S peak from the infected gradient in Fig. 8b.

(a) UV irradiation 7.5 min; 15% acrylamide

-●- ^{3}H-lysine, wt

-▲- ^{14}C-leucine, 20S

(b) UV irradiation 3.0 min; 12% acrylamide

-●- ^{3}H-leucine, wt

-▲- ^{14}C-leucine, 20S

FIGURE 27

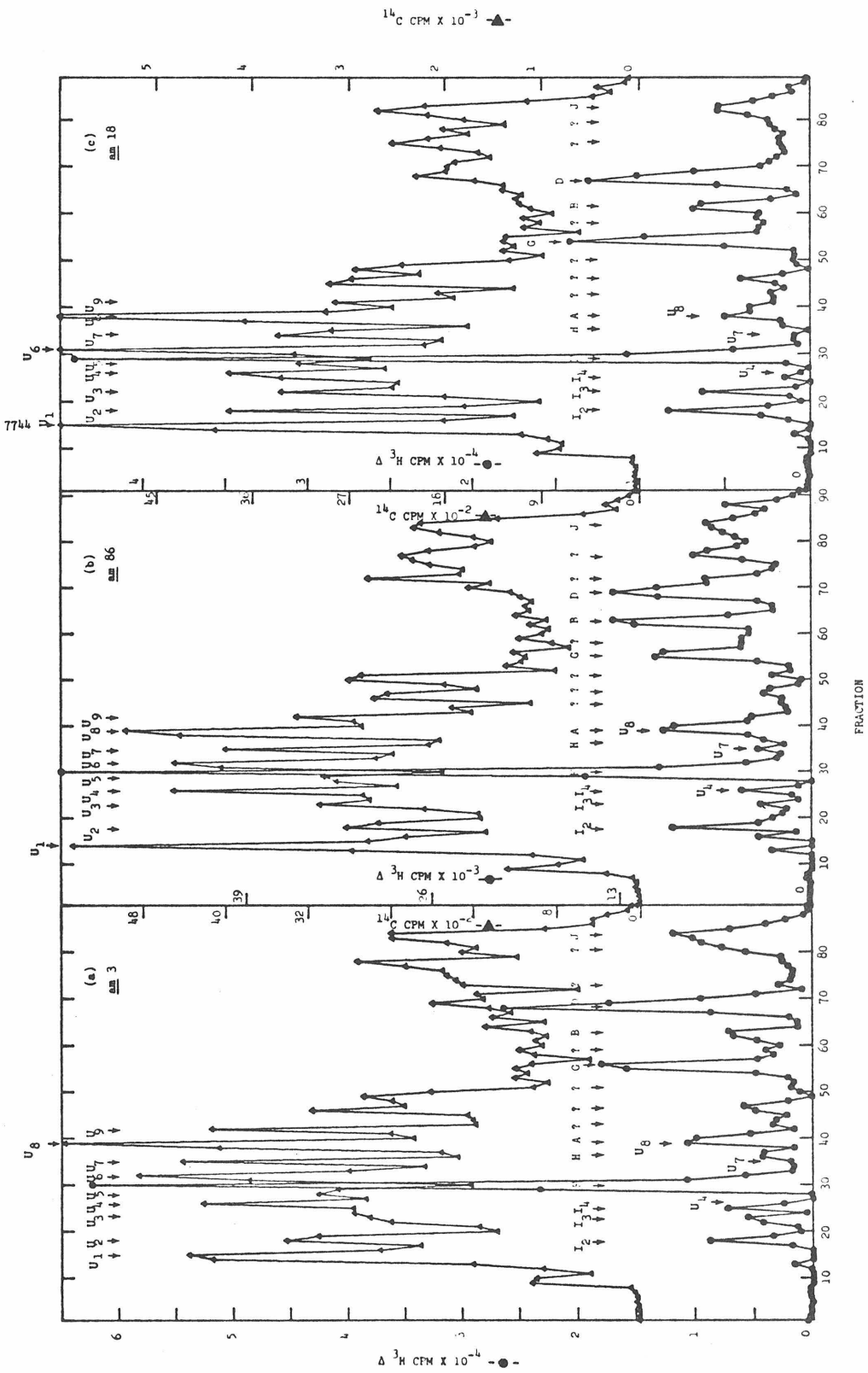
^{14}C CPM X 10^{-3}
(c)
am 18
Δ ^{3}H CPM X 10^{-4}
^{14}C CPM X 10^{-2}
(b)
am 86
Δ ^{3}H CPM X 10^{-3}
^{14}C CPM X 10^{-2}
(a)
am 3
Δ ^{3}H CPM X 10^{-4}
FRACTION

FIGURE 27. A comparison of the ϕX specific proteins in SDS acrylamide gel electrophoreses of whole lysates of ϕXam3, am86 and am18 infected, non-UV irradiated cells labeled for the first 18 min of infection.

E. coli H502 was grown to 3 x 10^8 cells/ml at 37°C in TPG medium supplemented with 5 µg/ml thymine. Three 5 ml aliquots were infected with ϕXam3, am86 and am18 at multiplicities of 10 and a fourth aliquot was uninfected. Radioactive lysine was added to each culture at the time of infection. ^{14}C-lysine was added to the uninfected culture at final concentrations of 2 µc/ml and 2 µg/ml. ^{3}H-lysine was added to the infected cultures at 20 µc/ml and 2 µg/ml. 18 min after infection the cultures were cooled to 9°C in an ice bath, then lysed, denatured, and electrophoresed on SDS stacking gels as described in procedure II of the Methods. In each case, 10 µl of the uninfected lysate was mixed with 50 µl of the infected lysate. Gels were fractionated and counted as described in the Methods. ϕX specific incorporation was computed as Δ^3H. Host peak assignments are as in Fig. 21 and ϕX assignments are taken from Table 1 of the General Introduction.

(a) Am3 infected lysate plus uninfected lysate

(b) Am86 infected lysate plus uninfected lysate

(c) Am18 infected lysate plus uninfected lysate

-●- Δ^3H-lysine, infection specific incorporation

-▲- ^{14}C-lysine, host incorporation

FIGURE 28

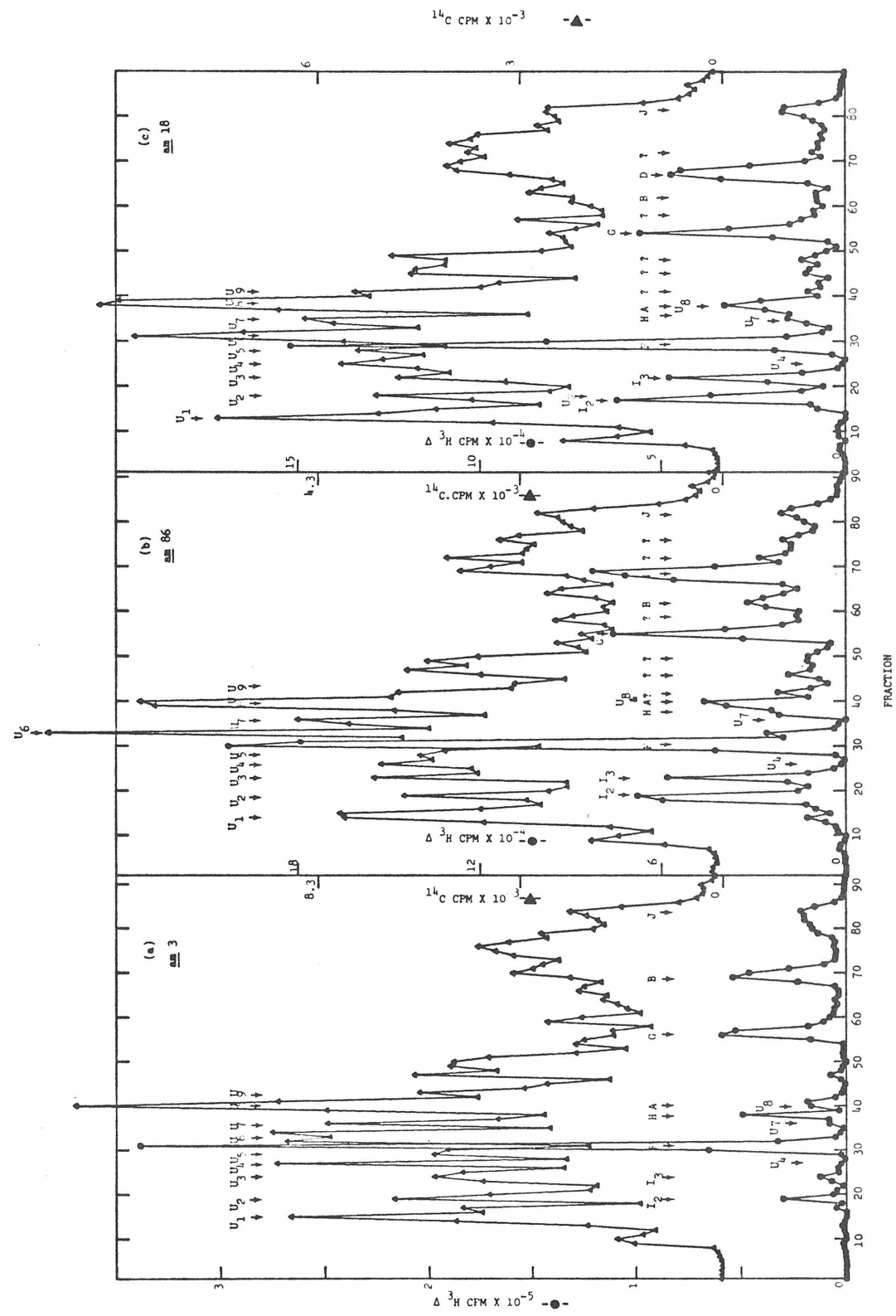
^{14}C CPM X 10^{-3}
(c)
an 18
(b)
an 86
(a)
an 3
Δ ^{3}H CPM X 10^{-4}
Δ ^{3}H CPM X 10^{-5}
FRACTION

FIGURE 28. A comparison of the ϕX specific proteins in SDS acrylamide gel electrophoresis of whole lysates of ϕXam3, am86 and am18 infected, non-UV irradiated cells labeled from 0-140 min after infection.

E. coli H502 was grown to 3 x 10^8 cells/ml at 37°C in TPG medium supplemented with 5 µg/ml thymidine and with 0.2 M-$MgSO_4$ as described in the Methods. At time zero 5 ml aliquots were infected with ϕXam3, am18 and am86 or left uninfected and then labeled with radioactive lysine as described for Fig. 27. The incorporation was terminated 140 min later by placing the cultures in an ice bath and adding NaN_3 to 0.01 M. Before lysis, one ml of the uninfected culture was mixed with 2 ml of each of the infected cultures. These mixtures were pelleted and resuspended in 150 µl of 0.05 M sodium tetraborate, 0.05 M-EDTA and 10 µl of a 1 mg/ml lysozyme solution and 10 µl of 1% SDS. Each mixture was then dialysed against TP buffer. Lysis occurred in the dialysis bag. 75 ml aliquots of each mixture were denatured and electrophoresed on SDS stacking gels as described in procedure II of the Methods. The gels were fractionated and counted according to the Methods and the ϕX specific incorporation, Δ^3H, computed with the CNTSEP program. Peak assignments are as in Fig. 27.

(a) Am3 infected lysate plus uninfected lysate

(b) Am86 infected lysate plus uninfected lysate

(c) Am18 infected lysate plus uninfected lysate

-●- ^3H-lysine, ϕX specific incorporation

-▲- ^{14}C-lysine, host incorporation

FIGURE 29a

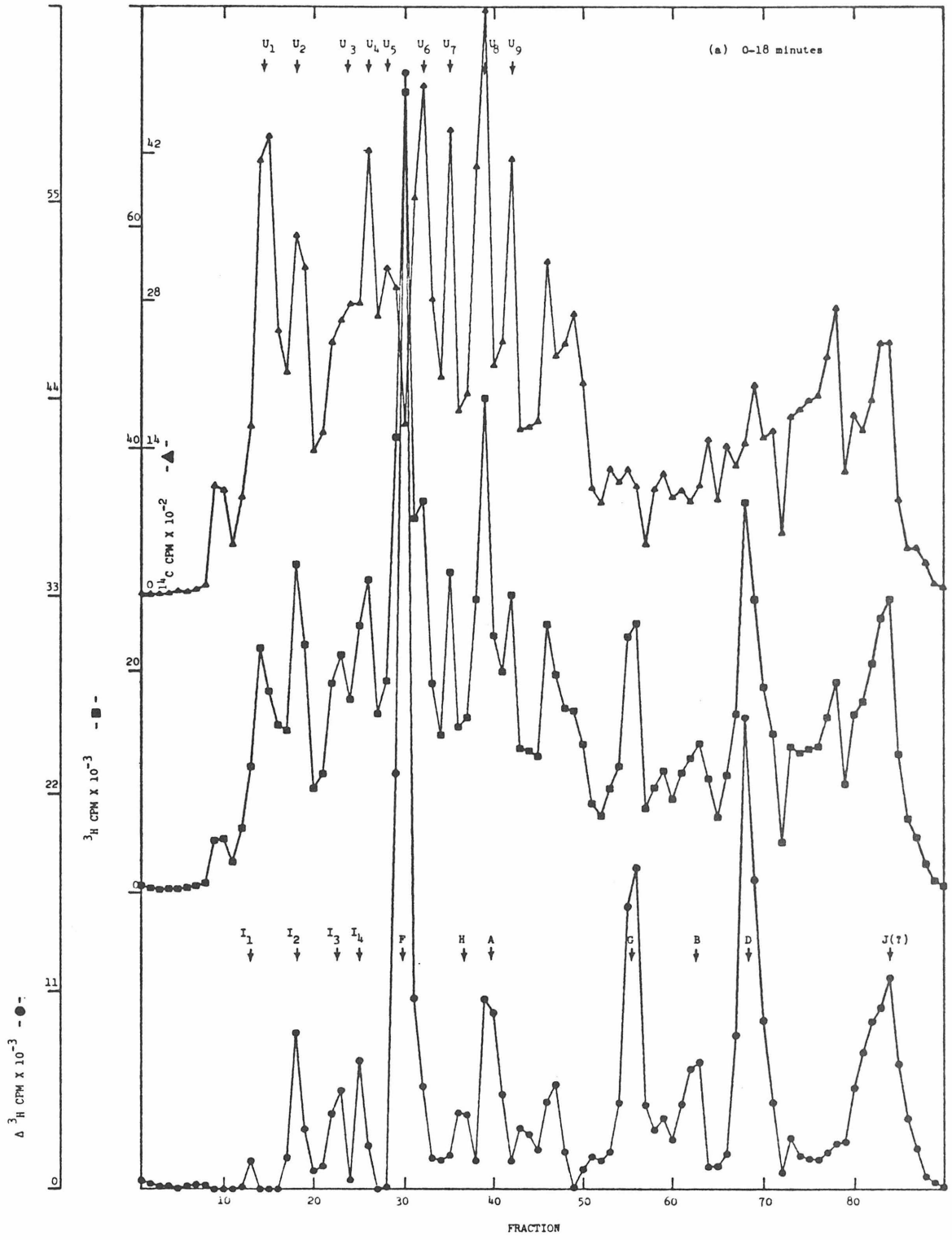
(a) 0-18 minutes
U1 U2 U3 U4 U5 U6 U7 U8 U9
I1 I2 I3 I4 F H A G B D J(?)
14C CPM X 10-2 -▲-
3H CPM X 10-3 -■-
Δ 3H CPM X 10-3 -●-
FRACTION

FIGURE 29b

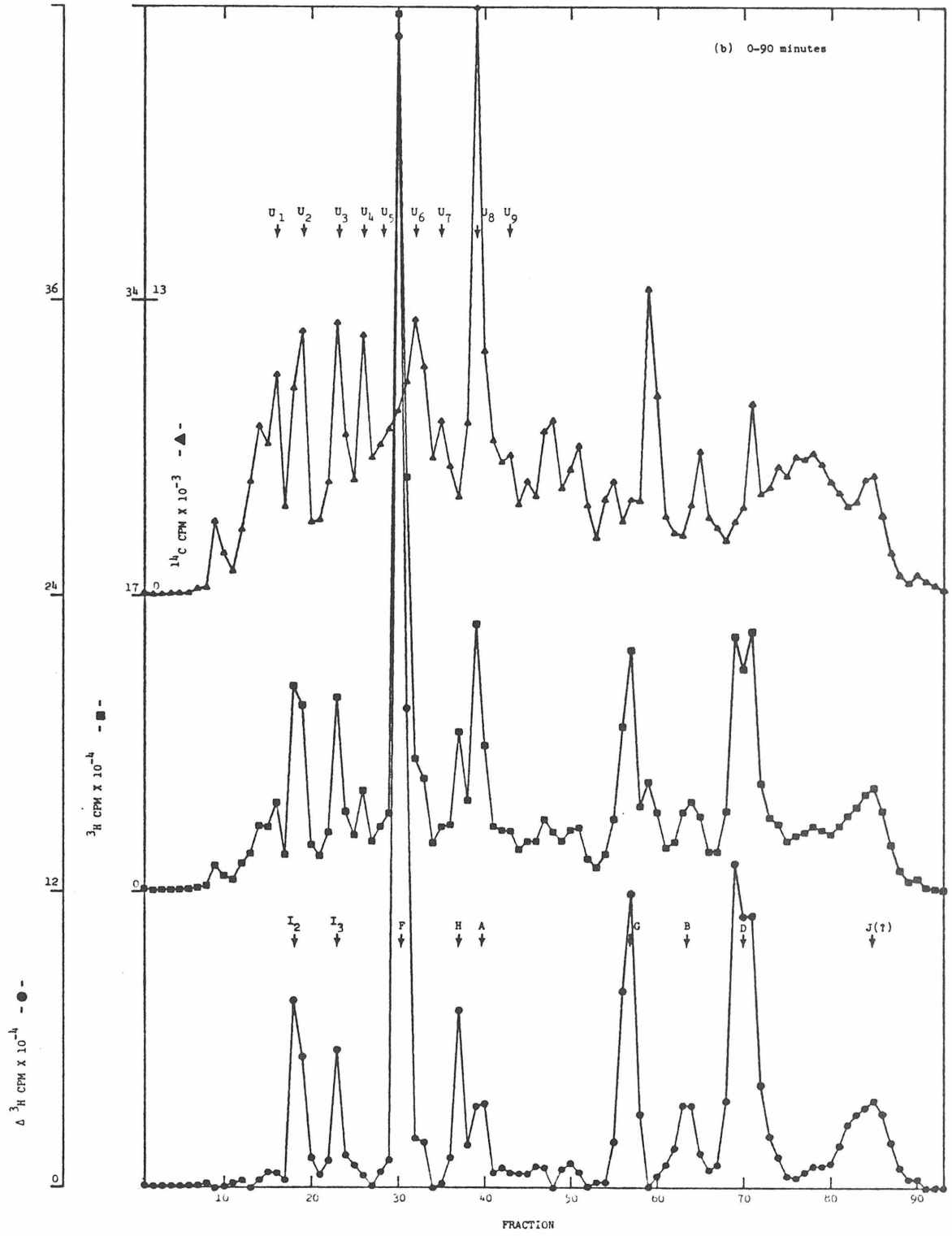
(b) 0-90 minutes
U1 U2 U3 U4 U5 U6 U7 U8 U9
36
34
13
24
17
0
12
0
0
14C CPM X 10-3 -▲-
3H CPM X 10-4 -■-
Δ 3H CPM X 10-4 -●-
I2 I3 F H A G B D J(?)
10 20 30 40 50 60 70 80 90
FRACTION

FIGURE 29c

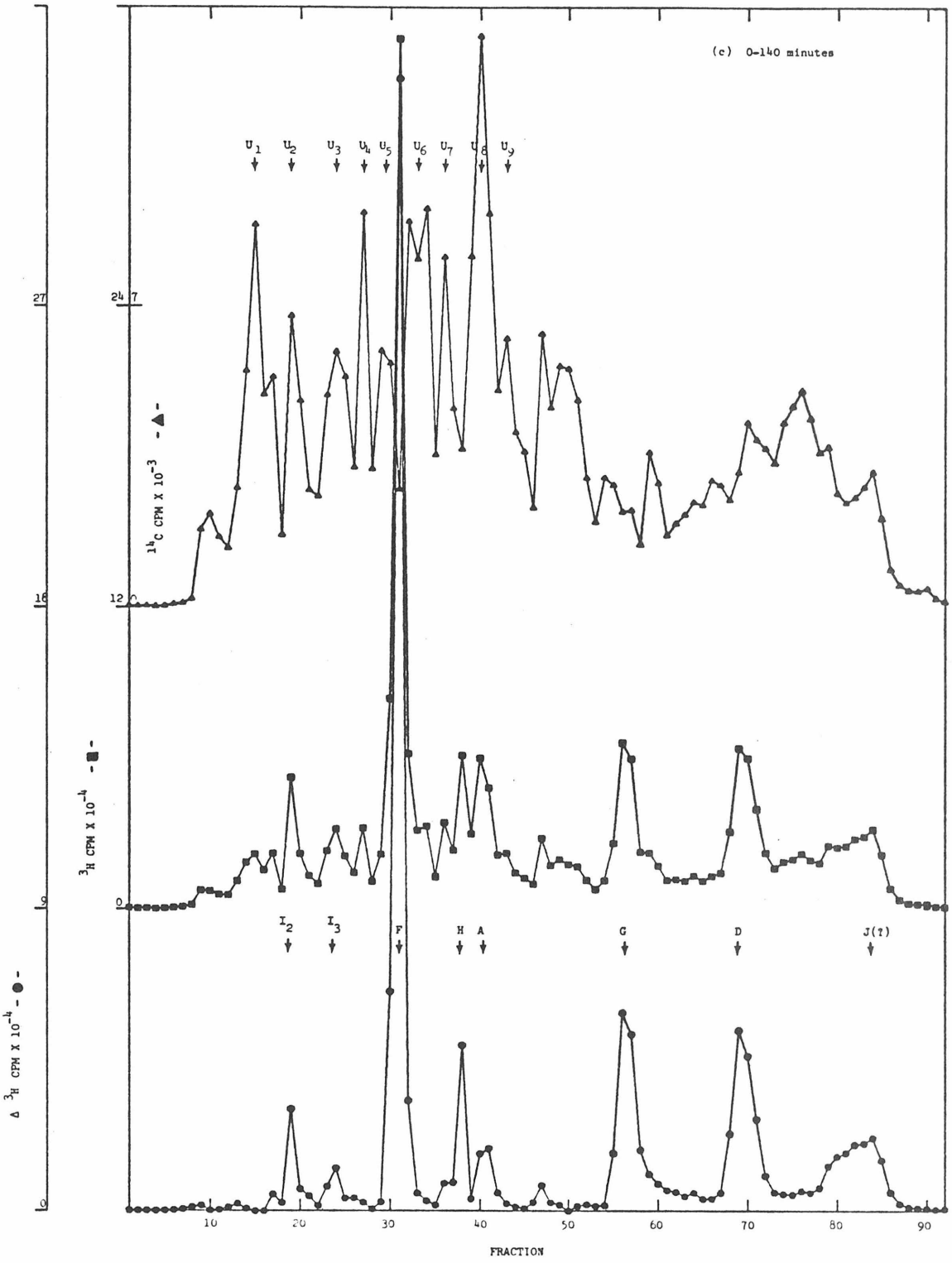
(c) 0-140 minutes
U1
U2
U3
U4
U5
U6
U7
U8
U9
I2
I3
F
H
A
G
D
J(?)
14C CPM X 10-3 - ▲ -
3H CPM X 10-4 - ■ -
Δ 3H CPM X 10-4 - ● -
FRACTION

FIGURE 29d

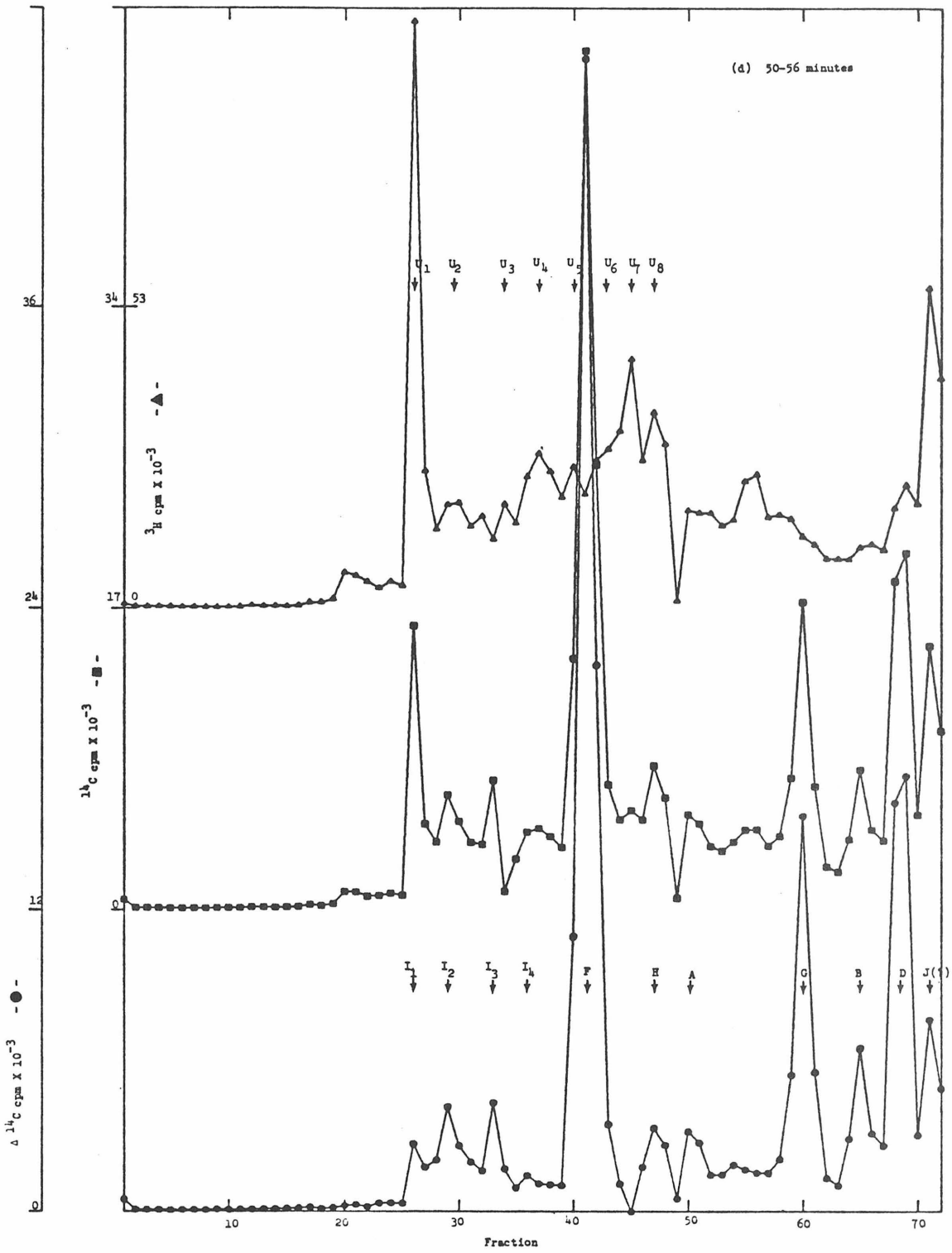
(d) 50-56 minutes
^{3}H cpm X 10^{-3} -▲-
^{14}C cpm X 10^{-3} -■-
Δ ^{14}C cpm X 10^{-3} -●-
U_1 U_2 U_3 U_4 U_5 U_6 U_7 U_8
I_1 I_2 I_3 I_4 F H A G B D J(1)
34 53
17 0
36
24
12
0
10 20 30 40 50 60 70
Fraction

FIGURE 29. Comparison of host, infected host, and infection specific protein labeling patterns in SDS acrylamide gels after labeling for different time periods in non-UV irradiated cells.

All experiments were conducted by the differential label technique in non-UV irradiated cells and with the am3 ϕX strain. In (a) the labeling period was 0-18 min after infection and this experiment is the same as that in Fig. 27a. In (b) the labeling period was from 0-90 min after infection. The experiment was otherwise performed as described in the legend to Fig. 28 except that the infected and uninfected cultures were lysed before mixing. In (c) the labeling period is from 0-140 min and the experiment is the same as that in Fig. 25a. Cultures (a), (b) and (c) were differentially labeled with ^{3}H- and ^{14}C-lysine. The cultures in (d) were labeled with ^{3}H- and ^{14}C-leucine from 50-56 min after infection and the experiment is the same as that in Fig.21.

In each graph the plots of the uninfected, infected and infection specific patterns have been displaced from each other along the vertical axis in order to aid in the interpretation of the results.

(a) Label 0-18 min, lysine

(b) Label 0-90 min, lysine

(c) Label 0-140 min, lysine

(d) Label 50-56 min, leucine

-●- Infection specific incorporation - $\Delta^{3}H$-lysine in (a), (b) and (c), ^{14}C-leucine in (d).

-■- Infected culture

-▲- Uninfected culture

FIGURE 30

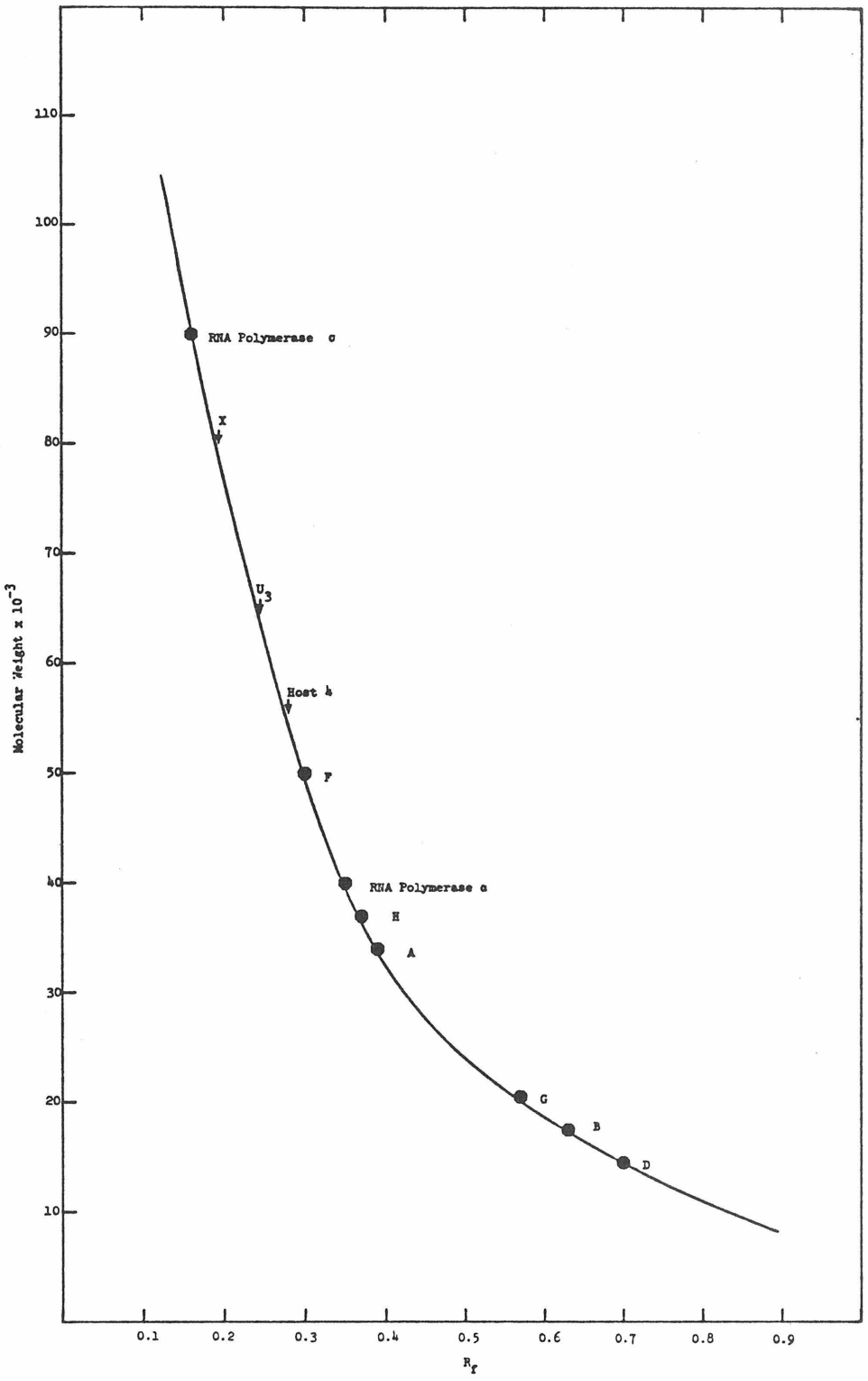
Molecular Weight x 10^{-3}
110
100
90
80
70
60
50
40
30
20
10
RNA Polymerase σ
X
U3
Host 4
F
RNA Polymerase α
H
A
G
B
D
0.1
0.2
0.3
0.4
0.5
0.6
0.7
0.8
0.9
R_f

FIGURE 30. Determination of the molecular weights of the ϕX174 infection specific host proteins from lysates of non-UV irradiated cells.

Data are from Fig. 29b. R_f is the relative mobility of the various proteins compared to a marker dye mobility of one. The ϕX174 protein molecular weights are from Table 1 of the General Introduction. The molecular weights of RNA polymerase subunits sigma and alpha are from Burgess (191). The molecular weight curve was established with ϕX proteins F, H, A, G, B and D, and with RNA polymerase subunits sigma and alpha. The R_f positions of infection specific peaks I_2 and (U_3, I_3, U_3^{20}) and host peak U_4 are indicated by arrows.

FIGURE 31

(a) Known Pathways Between ϕX174 Subviral Particles

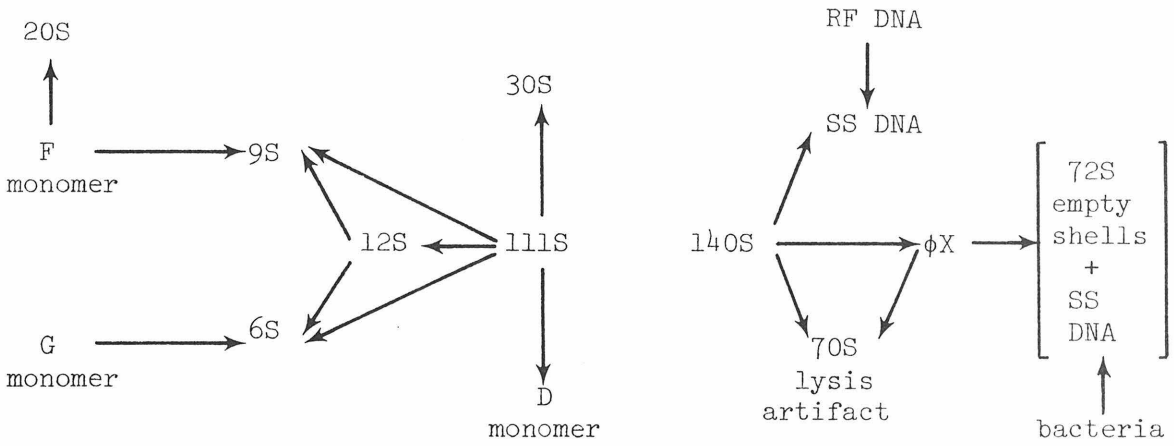

(b) Proposed Assembly Pathway - A Working Hypothesis

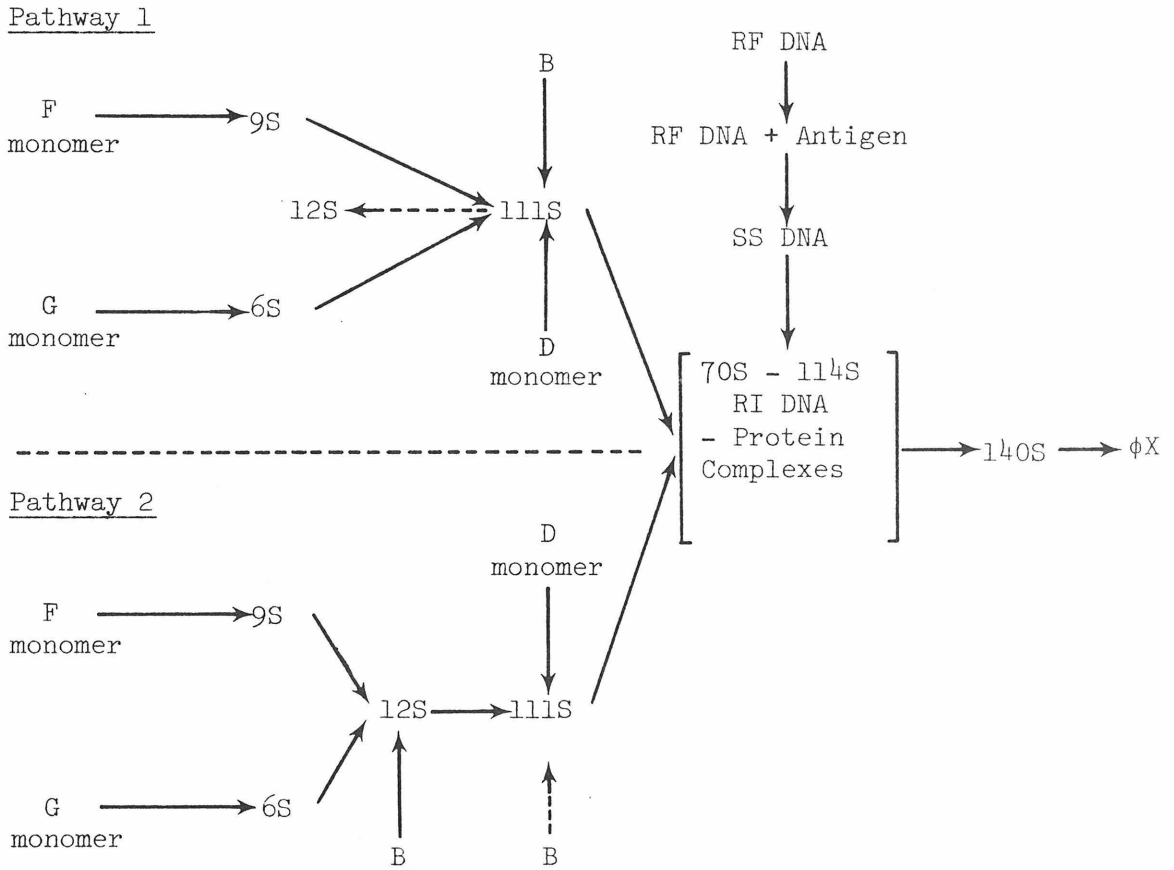

APPENDICES

APPENDIX A

Derivation of the standard deviation expressions for the computed isotopic composition of a radioactive sample containing three isotopes

I. Expressions for the computation of standard deviations

The symbol σ means "standard deviation of" the following subscripted variable. The statistical counting error inherent in all scintillation counter data is given by Equation 1.

Equation 1 $$\sigma_{(cpm)} = (\text{cpm observed/total counting time in minutes})^{1/2}$$

Standard deviations are propagated during calculations involving quantities with standard deviations according to the expressions below. Given the variables R_1 and R_2 with standard deviations σ_1 and σ_2, respectively, then:

$R_N = R_1 + R_2$ has a standard deviation σ_N given by

Equation 2 $$\sigma_N = (\sigma_1^2 + \sigma_2^2)^{1/2}$$

and $R_P = R_1 \cdot R_2$ has a standard deviation σ_P given by

Equation 3 $$\sigma_P = \left[\left(\frac{\sigma_1}{R_1}\right)^2 + \left(\frac{\sigma_2}{R_2}\right)^2 \right]^{1/2}$$

II. Definitions

The quantities H, C, P, D' and M_i, K_i, N_i, a_i, b_i, and c_i for $i = 1,2,3$ are defined in the text. Sigma, "σ", preceding any variable

means the standard deviation of that variable.

σ_{M_i} is given by Equation 1

σ_{K_i} is given by Equation 2

Equation 4 $\sigma_{N_i} = (\sigma_{M_i}^{2} + \sigma_{K_i}^{2})^{1/2}$

h_i is the count rate of the ^{3}H standard in channel i

c_i is the count rate of the ^{14}C standard in channel i

p_i is the count rate of the ^{32}P standard in channel i

S_{h_i}, S_{c_i}, and S_{p_i} are the count rates (corrected for background) of the ^{3}H, ^{14}C and ^{32}P standards, respectively, in channel i

$\sigma_{S_{h_i}}$, $\sigma_{S_{c_i}}$, and $\sigma_{S_{p_i}}$ are the standard deviations of S_{h_i}, S_{c_i} and S_{p_i}, respectively, computed as in Equation 4

σ_{a_i}, σ_{b_i}, and σ_{c_i} are computed in the same manner as σ_{a_2} given below:

$$a_2 = S_{h_2} / S_{h_1} \qquad \sigma_{a_2} = a_2 \left[\left(\frac{\sigma_{S_{h_1}}}{S_{h_1}}\right)^2 + \left(\frac{\sigma_{S_{h_2}}}{S_{h_2}}\right)^2 \right]^{1/2}$$

III. Derived expressions for σ_H, σ_C and σ_P

Repeated application of Equations 1, 2 and 3 to the expressions for H, C and P and substitution of the quantities defined above into the resultant equations leads to the following expressions:

$$\sigma_{D'} = \Bigg[\Bigg[a_2^2 b_1^2 \left[\left(\frac{\sigma_{a_2}}{a_2}\right)^2 + \left(\frac{\sigma_{b_1}}{b_1}\right)^2 \right] + a_3^2 c_1^2 \left[\left(\frac{\sigma_{a_3}}{a_3}\right)^2 + \left(\frac{\sigma_{c_1}}{c_1}\right)^2 \right]$$

$$+ b_3^2 c_2^2 \left[\left(\frac{\sigma_{b_3}}{b_3}\right)^2 + \left(\frac{\sigma_{c_2}}{c_2}\right)^2 \right] + a_3^2 b_1^2 c_2^2 \left[\left(\frac{\sigma_{a_3}}{a_3}\right)^2 + \left(\frac{\sigma_{b_1}}{b_1}\right)^2 + \left(\frac{\sigma_{c_2}}{c_2}\right)^2 \right]$$

$$+ a_2^2 b_3^2 c_1^2 \left[\left(\frac{\sigma_{a_2}}{a_2}\right)^2 + \left(\frac{\sigma_{b_3}}{b_3}\right)^2 + \left(\frac{\sigma_{c_1}}{c_1}\right)^2 \right] \Bigg]\Bigg]^{1/2}$$

$$\sigma_H = H \Bigg[\Bigg[\Bigg[\Bigg[\Bigg[\sigma_{N_1}^2 (1 - c_2 b_3)^2 + N_1^2 c_2^2 b_3^2 \left[\left(\frac{\sigma_{c_2}}{c_2}\right)^2 + \left(\frac{\sigma_{b_3}}{b_3}\right)^2 \right]$$

$$+ \sigma_{N_2}^2 (b_3 c_1 - b_1)^2 + N_2^2 b_3^2 c_1^2 \left[\left(\frac{\sigma_{b_3}}{b_3}\right)^2 + \left(\frac{\sigma_{c_1}}{c_1}\right)^2 \right]$$

$$+ N_2^2 \sigma_{b_1}^2 + \sigma_{N_3}^2 (b_1 c_2 - c_1)^2$$

$$+ N_3^2 b_1^2 c_2^2 \left[\left(\frac{\sigma_{b_1}}{b_1}\right)^2 + \left(\frac{\sigma_{c_2}}{c_2}\right)^2 \right] + N_3^2 \sigma_{c_1}^2 \Bigg]\Bigg] \div \Bigg[\Bigg[H \cdot D' \Bigg]\Bigg]^2$$

$$+ \left[\left[\frac{\sigma_{D'}}{D'} \right]\right]^2 \Bigg]\Bigg]^{1/2}$$

$$\sigma_C = C \left\| \left[\sigma_{N_1}^2 (c_2 a_3 - a_2)^2 + N_1^2 c_2^2 a_3^2 \left[\left(\frac{\sigma_{c_2}}{c_2}\right)^2 + \left(\frac{\sigma_{a_3}}{a_3}\right)^2 \right] + N_1^2 \sigma_{a_2}^2 \right.\right.$$

$$+ \sigma_{N_2}^2 (1 - a_3 c_1)^2 + N_2^2 a_3^2 c_1^2 \left[\left(\frac{\sigma_{a_3}}{a_3}\right)^2 + \left(\frac{\sigma_{c_1}}{c_1}\right)^2 \right]$$

$$+ \sigma_{N_3}^2 (a_2 c_1 - c_2)^2 + N_3^2 a_2^2 c_1^2 \left[\left(\frac{\sigma_{a_2}}{a_2}\right)^2 + \left(\frac{\sigma_{c_1}}{c_1}\right)^2 \right]$$

$$\left.\left. + N_3^2 \sigma_{c_2}^2 \right] \div \left[C \cdot D' \right]^2 + \left[\frac{\sigma_{D'}}{D'} \right]^2 \right\|^{1/2}$$

$$\sigma_P = P \left\| \left[\sigma_{N_1}^2 (a_2 b_3 - a_3)^2 + N_1^2 a_2^2 b_3^2 \left[\left(\frac{\sigma_{a_2}}{a_2}\right)^2 + \left(\frac{\sigma_{b_3}}{b_3}\right)^2 \right] + N_1^2 \sigma_{a_3}^2 \right.\right.$$

$$+ \sigma_{N_2}^2 (a_3 b_1 - b_3)^2 + N_2^2 a_3^2 b_1^2 \left[\left(\frac{\sigma_{a_3}}{a_3}\right)^2 + \left(\frac{\sigma_{b_1}}{b_1}\right)^2 \right] + N_2^2 \sigma_{b_3}^2$$

$$\left. + \sigma_{N_3}^2 (1 - a_2 b_1)^2 + N_3^2 a_2^2 b_1^2 \left[\left(\frac{\sigma_{a_2}}{a_2}\right)^2 + \left(\frac{\sigma_{b_1}}{b_1}\right)^2 \right] \right]$$

$$\div \left[P \cdot D' \right]^2 + \left[\frac{\sigma_{D'}}{D'} \right]^2 \Bigg\|^{1/2}$$

APPENDIX B

Problems associated with the use of a leucine pulse label as an indicator of the mass distribution of ϕX proteins

In the absence of continuous labeling data with a uniformly labeled carbon source or, alternatively, a method for monitoring the masses of the various ϕX specific infection components directly, one can only estimate in a crude way the mass distribution of the ϕX components in whole lysates. The limitations of such estimates, based upon the incorporation of radioactively labeled leucine during six minute pulses, is discussed below.

I. The mass distribution of leucine in ϕX proteins

In order for an amino acid label to reflect the relative masses of different proteins, it must constitute a constant proportion of the mass of each of the protein species compared. A comparison of the ϕX specific protein patterns observed in whole lysates of ϕX infected cells after a variety of labeling regimes suggests that leucine is distributed rather uniformly among the presently assayable ϕX proteins.

Godson (20) has observed that ϕX proteins from whole lysates are labeled in approximately the same relative proportions with either radioactive leucine or a uniformly labeled amino acid mixture. Gelfand & Hayashi (52) observed a similar distribution after labeling with a mixture of five amino acids. Table 17 (Results) presents the distributions of leucine and lysine labels among ϕX proteins from whole lysates. The only striking differences in incorporation of these two labels are in gene products A', A, and J. Several investigators

(8,11,20,65) have measured the relative proportions of radioactively labeled virion proteins with similar results for leucine, histidine, various amino acid mixtures, and glucose.

The fact that the patterns of incorporation of all of these amino acids, including leucine, are so similar indicates that all of the amino acids utilized so far, with the exception of lysine (see Results), are rather uniformly distributed. Nevertheless, it should be noted that the validity of these comparisons is weakest for minor and poorly resolved components of the infection. Thus the differences noted in the Results (Table 17) between the leucine and lysine labels might not have been observed had the differentially labeled lysates not been mixed and electrophoresed together. By comparison a 2.6 X increase (such as that observed for J protein) in lysine relative to leucine incorporation in F, G or D product would certainly have been noticed.

II. The temporal course of synthesis of ϕX proteins

In order for a pulsed amino acid label to serve as a relative mass indicator for a group of in vivo proteins, the proteins compared must be synthesized at the same relative rates at all times. In the case of ϕX, Godson has demonstrated the temporal uniformity of the leucine incorporation by showing that ϕX proteins as assayed by SDS acrylamide gel electrophoresis are made at the same relative rates throughout the infection. As discussed in the General Introduction, it is likely that this is true for all ϕX proteins.

III. The exchangeability of the ϕX precursor particle pools and the use of a leucine pulse label to determine protein stoichiometries

When the conditions in I and II are met, as seems to be the

case with a leucine label in the ϕX174 infection, it is possible to deduce the relative masses of the total *in vivo* proteins from the relative incorporation of the pulsed label into various proteins. The molecular weights of the proteins can then be used to compute the total intracellular stoichiometry.

However, the conditions in I and II are only necessary, but not sufficient, to accurately determine by pulse labeling the stoichiometries of the protein components of the viral or subviral particles as is desired in the Results. This is because the ϕX proteins presumably do not exchange freely between the various pools into which they are sequestered. For example, the F, G, H, and J proteins are obviously used up at the rate at which new phage are matured whereas proteins that function in some enzymatic way may be reusable and hence accumulate into ever larger pools as the infection proceeds. Thus a six minute amino acid pulse at late times may label relatively small pools of phage structural precursors compared to, for example, gene D protein. The stoichiometry computed for a precursor particle containing both virion proteins and reusable proteins would then reflect the relative pool sizes of the component proteins as well as the particle composition.

As a consequence, one would expect that a calculation of the protein stoichiometry of the 111S particle on the basis of pulse data would result in a minimum value for the proportion of D protein to the F and G proteins. The real value for D protein could be, depending upon its reusability and the time at which the pulse is begun, as much as an order of magnitude greater. The calculated relationship between the F and G proteins would also depend heavily upon the pool sizes of

the precursor particles. If the precursor pools are small enough to be labeled uniformly in the course of the pulse, then the composition of the particle assembled from those precursors can be obtained from the pulse data. However, it is not yet known whether or not this is true for the phage or 111S particle after a 6 minute leucine pulse.

APPENDIX C

The effects of ionic strength, Mg++ and dilute solutions on the stability of macromolecular associations

In the experimental design of the Results section the ribosome was used as a model protein-nucleic acid complex from which to obtain appropriate environmental conditions for the isolation of φX assembly intermediates. As a consequence the search for intermediates was conducted in TM buffer (0.05 M Tris-HCl, 0.05 M KCl, 0.008 M $MgSO_4$, pH 7.2). However, as elaborated below, these conditions are somewhat arbitrary and might not be appropriate for the visualization of some kinds of structures. The experimental methods employed also exposed the particle bearing lysates to dilute solutions which may also prevent the observation of some kinds of associations.

I. Ionic strength

In the selection of appropriate ionic strength conditions for the isolation of intermediates in viral assembly, one is confronted with a paradox. As evidenced by the ionic strength dependence of DNA affinity column chromatography (178), ribosome and polyribosome stability (200, 201), various enzymatic activities employing nucleic acid substrates, and other well characterized protein-DNA associations such as repressor binding (for an excellent review of DNA-protein interactions see 203), low ionic strength promotes and stabilizes the interactions of nucleic acids and protein. [It is essential for the stability of several well characterized spherical plant viruses (5).] On the other hand, low

ionic strength (0.05 M KCl) is decidedly non-physiological (203). Furthermore, the work of Lerman, Pettijohn, and others (166, 167, 168, 169) demonstrates that high ionic strength is essential for maintaining the in vivo conformation of nucleic acids.

The infectious 140S ϕX particle discovered by Weisbeek and Sinsheimer (165) is stabilized by high salt conditions, suggesting that high, rather than low, salt may be a more appropriate condition for the isolation of assembly intermediates. However the 140S particle, itself, can only be isolated from low salt EDTA lysates and is not observed after lysis in high salt.

It seems likely that two kinds of effects are at work in DNA-protein interactions. First there are the direct binding interactions of large or small, but usually small, protein complexes with nucleic acid molecules. These associations are promoted by low ionic strength conditions. (On the other hand, the specificity of many of these same reactions is often, though not always, increased by higher ionic strength conditions. Compare phage T_7 and E. coli RNA polymerases, reference 203. These increases in specificity are, however, often accompanied by decreases in total binding.) Second, there are the kinds of interactions proposed by Lerman (168) in which the self-repulsion of the DNA phosphate chain must be minimized by a high ionic strength environment. High ionic strength and isoelectric pH also promote the hydrophobic interactions which are generally (though not exclusively, e.g., the intercalation reaction is presumably a hydrophobic one) more characteristic of protein-protein interactions than of protein-DNA interactions (203). In as much as the relative importance of these various interactions on the structural stability of the ϕX174 maturation

intermediates is not yet known, the initial choice of low ionic strength conditions may, in fact, have been arbitrary.

II. Magnesium ion

The Mg++ ion at low concentrations has an almost universally stabilizing effect upon DNA-protein interactions (80, 203, 233). Its applicability to the ϕX system is indicated by its stabilizing effect on the infectious 140S particle (165), mediating its transformation to virions instead of noninfectious decomposition products, and its effect on the first sedimentation of 111S particles in whole lysates (Figures 10 and 11).

Several other isolation conditions might profitably be explored in future research. Thus the formation of the in vitro DNA-protein complexes observed by Takai (179) was highly dependent upon the presence of Ca++ or Zn++. The purified phage is extremely stable in pH 9.5 borate buffer (Results). It is not known whether this is an effect of the pH or the borate. ϕX174 is rather unstable in pH 7 Tris buffers (24, 32; Zuccarelli, A., personal communication; Rohwer, R., unpublished). Again it is not known whether this is a consequence of the buffer or the pH.

The instability of the 111S particle to resedimentation under conditions of both low and high ionic strength suggests that it may be separated from some stabilizing component during the first fractionation of the lysate. Alternatively, it may be extremely sensitive to the osmotic shock of either dialysis or dilution or it may degrade, as discussed below, due to exposure to dilute solution (regardless of the osmolarity).

III. Dilute solutions

In the experiments presented here sedimentation velocity was employed for the primary visualization of the ϕX174 lysates. This technique, as does any technique that exposes molecular complexes to dilute solution, places certain limitations on the kinds of intermediates that can be visualized. Many non-covalent, bimolecular associations will be lost simply due to the mass action equilibrium in dilute solution. As might be expected from the extremely high association constants and remarkable specificities of the E. coli lac (206) and phage λ (205) repressors, both of these molecules cosediment with their respective DNA substrates under conditions of low ionic strength and dilute solution. (However, in the case of both repressors, this ability is destroyed when the KCl concentration of the sedimentation buffer is raised to 0.15 M.) By comparison to the lac and λ repressors, the T4 gene 32 protein has a much lower, if much more general, affinity for DNA. In spite of its smaller association constant it binds quantitatively to, and cosediments with SS DNA at much higher ionic strengths than can be tolerated by repressor binding. This is most likely due to the cooperative nature of the gene 32 protein binding and reflects strong protein-protein as well as DNA-protein associations (207).

As evidenced by the gene 32 protein binding, the extracellular stability of many cellular particles often increases as the complexity of the particle increases and the total number of molecular interactions increases. Thus there are many examples of multi-component enzymes that are stable in dilute solution as well as even more complex particles such as ribosomes and polyribosomes. Perhaps the best examples of

extremely complex, non-covalent structures, that are nevertheless remarkably stable in dilute solution, are the viruses themselves. In this regard it should also be noted that many subviral particles, such as the F protein and G protein pentamers of ϕX174, also share this property.

It cannot be known in advance at what point the effects of mere dilution become important in the isolation of ϕX174 maturation intermediates. Nevertheless, recognition of these effects does lead one to the expectation that those structures which do survive sedimentation and storage in dilute solution will be complex multicomponent ones.

Abbreviations

SS DNA is single stranded. The plus or viral strand is the strand encapsulated in the virus. The minus strand is complementary to the plus strand. RF I DNA is a supercoiled covalently closed double stranded circle. RF II DNA is a double stranded circle in which one or both strands are nicked though not in the same place. RF III DNA is the double stranded linear molecule that results when both strands are nicked in the same place. RI DNAs are the replicative intermediates in DNA synthesis.

Abbreviations: RIA, radioimmunoassay; PDI, propidium diiodide; SDS, sodium lauryl sulphate; BSA, bovine serum albumin; TCA, trichloroacetic acid; silane, dichlorodimethylsilane; CAM, chloramphenicol; MW, molecular weight; UV, ultraviolet radiation of wavelength 260 nm; pfu, plaque forming unit; moi, multiplicity of infection.

BIBLIOGRAPHY

BIBLIOGRAPHY

1. Sinsheimer, R. L. (1959). Brookhaven Symposia in Biology 12, 27-34.
2. Sinsheimer, R. L., Hutchison III, C. A. and Lindquist, B. (1967). In The Molecular Biology of Viruses (Colter, J. S. & Paranchych, W., eds.), pp. 175-192, Academic Press, New York.
3. Sinsheimer, R. L. (1968). In Progress in Nucleic Acid Research and Molecular Biology (Davidson, J. N. & Cohn, W. E., eds.) Vol. 8, pp. 115-169, Academic Press, New York.
4. Eiserling, F. A., Dickson, R. C. (1972). Ann. Rev. Biochem. 41, 467-502.
5. Bancroft, J. B. (1970). Advan. Virus Res. 16, 99-135.
6. Casper, D. L. D., Klug, A. (1962). Cold Spr. Harb. Symp. Quant. Biol. 27, 1-24.
7. Siegel, J. E. D., Hayashi, M. (1969). J. Virol. 4, 400-407.
8. Mayol, R. F., Sinsheimer, R. L. (1970). J. Virol. 6, 310-319.
9. Hutchison III, C. A. (1969). Ph.D. Thesis, California Institute of Technology, Pasadena, California.
10. Krane, S. G. (1966). Ph. D. Thesis, California Institute of Technology, Pasadena, California.
11. Burgess, A. B. (1969). Proc. Nat. Acad. Sci. 64, 613-617.
12. Benbow, R. M., Mayol, R. F., Picchi, J. C., Sinsheimer, R. L. (1972) J. Virol. 10, 99-114.
13. Fiers, W., Sinsheimer, R. L. (1962). J. Mol. Biol. 5, 424-434.

14. Sinsheimer, R. L. (1959). J. Mol. Biol. 8, 43-53.

15. Benbow, R. M., Hutchison III, C. A., Fabricant, J. D., Sinsheimer, R. L. (1971). J. Virol. 7, 549-558.

16. Edgell, M. H., Hutchison III, C. A., Sinsheimer, R. L. (1969). J. Mol. Biol. 42, 547-557.

17. Maclean, E. C., Hall, C. E. (1962). J. Mol. Biol. 4, 173-178.

18. Hall, C. E., Maclean, E. C., Tessman, I. (1959). J. Mol. Biol. 1, 192-194.

19. Tromans, W. J., Horne, R. W. (1961). Virology 15, 1-7.

20. Godson, N. G. (1971). J. Mol. Biol. 57, 541-553.

21. Newbold, J. E. (1970). Ph. D. Thesis, California Institute of Technology, Pasadena, California.

22. Jazwinski, S. M., Marco, R., Kornberg, A. (1973). Proc. Nat. Acad. Sci. 70, 205-209.

23. Jazwinski, S. M. (1974). Presentation at the 1974 Small DNA Phage Meeting, University of California in Los Angeles Conference Center, Lake Arrowhead, California.

24. Dann-Markert, A., Deutsch, H. F., Zillig, W. (1966). Virology 29, 126-132.

25. Eigner, J., Stouthamer, A. H., van der Sluys, I., Cohen, J. A. (1963). J. Mol. Biol. 6, 61-84.

26. Eigner, J., Doty, P. (1965). J. Mol. Biol. 12, 549-580.

27. Bleichrodt, J. F., Knijnenburg, C. M. (1969). Virology 37, 132-161.

28. Bowman, B. U., Patnode, R. A. (1964). Proc. Soc. Exp. Biol. Med. 115, 338-341.

29. Bowman, B. U., Patnode, R. A. (1963). Virology 21, 506-508.

30. Bowman, B. U., Ornstein, S. M. (1965). Bioch. Biophys. Res. Comm. 21, 176-181.

31. Brown, D. T., MacKenzie, J. M., Boyer, M. E. (1971). J. Virol. 7, 836-846.

32. Newbold, J. E., Sinsheimer, R. L. (1970). J. Mol. Biol. 49, 49-66.

33. Guthrie, G. D., Sinsheimer, R. L. (1960). J. Mol. Biol. 2, 297-305.

34. Jeng, U., Gelfand, D., Hayashi, M., Shleser, R., Tessman, E. S. (1970). J. Mol. Biol. 49, 521-526.

35. Godson, G. N. (1973). J. Mol. Biol. 77, 467-477.

36. Compton, J. L. (1974). Ph. D. Thesis, California Institute of Technology, Pasadena, California.

37. Knippers, R., Hoffmann-Berling, H. (1966). J. Mol. Biol. 21, 305-312.

38. Miller, L. K., Sinsheimer, R. L. (1974). Manuscript in preparation.

39. Schekman, R., Ray, D. S. (1971). Nature New Biol. 231, 170-173.

40. Francke, B., Ray, D. S. (1972). Virology 9, 1027-1032.

41. Lytle, C. D., Ginoza, W. (1969). Virology 38, 152-165.

42. Zuccarelli, A. J. (1974). Ph. D. Thesis, California Institute of Technology, Pasadena, California.

43. Knippers, R., Salivar, W. O., Newbold, J. E., Sinsheimer, R. L. (1969). J. Mol. Biol. 39, 641-654.

44. Hutchison III, C. A., Sinsheimer, R. L. (1971). J. Virol. 8, 121-124.

45. Linney, E., Hayashi, M. (1973). Nature New Biol. 245, 6-8.

46. Linney, E., Hayashi, M. N., Hayashi, M. (1972). Virology 50, 381-387.

47. Francke, B., Ray, D. S. (1971). Virology 44, 168-187.

48. Francke, B., Ray, D. S. (1971). J. Mol. Biol. 61, 568-586.

49. Francke, B., Ray, D. S. (1972). Proc. Nat. Acad. Sci. 69, 475-479.

50. Henry, T. J., Knippers, R. (1974). Proc. Nat. Acad. Sci. 71, 1549-1553.

51. Van der Mei, D., Zandberg, J., Jansz, H. S. (1972). Biochim. Biophys. Acta 287, 312-321.

52. Gelfand, D. H., Hayashi, M. (1969). J. Mol. Biol. 44, 501-516.

53. Burgess, A. B., Denhardt, D. T. (1969). J. Mol. Biol. 44, 377-386.

54. Edgell, M. H., Hutchison III, C. A., Sclair, M. (1972). J. Virol. 9, 574-582.

55. Weisbeek, P. J., Van de Pol, J. H. (1970). Biochim. Biophys. Acta 244, 328-338.

56. Lee, A. S., Sinsheimer, R. L. (1974). Proc. Nat. Acad. Sci. 71, 2882-2886.

57. Levine, A. J., Sinsheimer, R. L. (1969). J. Mol. Biol. 39, 619-639.

58. Tessman, E. (1965). Virology 25, 303-321.

59. Yarus, J. M., Sinsheimer, R. L. (1967). J. Virol. 1, 135-144.

60. Knippers, R., Sinsheimer, R. L. (1968). J. Mol. Biol. 34, 17-29.

61. Siden, E., Hayashi, M. (1974). J. Mol. Biol., in press.

62. Borrás, M. T., Vanderbilt, A. S., Tessman, E. S. (1971). Virology 45, 802-803.

63. Lindquist, B., Sinsheimer, R. L. (1967). J. Mol. Biol. 30, 69-80.

64. Weisbeek, P. J., Van de Pol, J. H., Van Arkel, G. A. (1973). Virology 52, 408-416.

65. Tonegawa, S., Hayashi, M. (1970). J. Mol. Biol. 48, 219-242.

66. Shleser, R., Tessman, E. S., Casaday, G. (1969). Virology 38, 166-173.

67. Funk, F. D., Sinsheimer, R. L. (1970). J. Virol. 6, 12-19.

68. Dowel, C. E., Sinsheimer, R. L. (1966). J. Mol. Biol. 16, 374-386.

69. Tessman, I., Ishiwa, W., Kumar, S., Baker, R. (1967). Science 156, 824-825.

70. Zahler, S. A. (1958). J. Bact. 75, 310-315.

71. Iwaya, M., Denhardt, D. T. (1971). J. Mol. Biol. 57, 159-175.

72. Sinsheimer, R. L., Starman, B., Nagler, C., Guthrie, S. (1962). J. Mol. Biol. 4, 142-160.

73. Levine, A. J., Sinsheimer, R. L. (1968). J. Mol. Biol. 32, 567-578.

74. Levine, A. J., Sinsheimer, R. L. (1969). J. Mol. Biol. 39, 655-668.

75. Hutchison III, C. A., Sinsheimer, R. L. (1963). J. Mol. Biol. 7, 206-208.

76. Hutchison III, C. A., Sinsheimer, R. L. (1963). J. Mol. Biol. 18, 429-447.

77. Zuccarelli, A. J., Benbow, R. M., Sinsheimer, R. L. (1972). Proc. Nat. Acad. Sci. 69, 1905-1910.

78. Fujimura, R., Kaesberg, P. (1962). Biophys. J. 2, 433-449.

79. Markert, A., Zillig, W. (1965). Virology 25, 88-97.

80. Lerman, M. A., Spirin, A. S., Gabrilova, L. P., Golov, V. F. (1966). J. Mol. Biol. 15, 268-281.

81. Gschwender, H. H., Hofschneider, P. H. (1969). Biochim. Biophys. Acta 190, 454-459.

82. Iwaya, M., Denhardt, D. T. (1973). J. Mol. Biol. 73, 291-305.

83. Bradley, D. E. (1968). J. Gen. Virol. 3, 141-143.

84. Newbold, J. E., Sinsheimer, R. L. (1970). J. Virol. 5, 427-431.

85. Hutchison III, C. A., Edgell, M. H., Sinsheimer, R. L. (1967). J. Mol. Biol. 23, 553-575.

86. Greenlee, L. L., Sinsheimer, R. L. (1968). J. Mol. Biol. 32, 303-320.

87. Tessman, E. S. (1966). J. Mol. Biol. 17, 218-236.

88. Stone, A. B. (1967). Biochem. Biophys. Res. Comm. 26, 247-254.

89. Cairns, J., Denhardt, D. T. (1968). J. Mol. Biol. 36, 335-342.

90. Lindquist, B. H., Sinsheimer, R. L. (1967). J. Mol. Biol. 28, 87-94.

91. Morishima, I., Komono, T., Onodera, K. (1971). Agr. Biol. Chem. 55, 1899-1905.

92. Stone, A. B. (1970). Virology 42, 171-181.

93. Knippers, R., Razin, A., Davis, R., Sinsheimer, R. L. (1969). J. Mol. Biol. 45, 237-263.

94. Incardona, N. L., Selvidge, L. (1973). J. Virol. 11, 775-782.

95. Newbold, J. E., Sinsheimer, R. L. (1970). J. Mol. Biol. 49, 23-47.

96. Sinsheimer, R. L., Knippers, R., Komono, T. (1968). Cold Spr. Harb. Symp. Quant. Biol. 33, 443-447.

97. Komono, T., Knippers, R., Sinsheimer, R. L. (1968). Proc. Nat. Acad. Sci. 59, 911-916.

98. Knippers, R., Sinsheimer, R. L. (1968). J. Mol. Biol. 35, 591-605.

99. Denhardt, D. T., Sinsheimer, R. L. (1965). J. Mol. Biol. 12, 647-662.

100. Lindquist, B. H., Sinsheimer, R. L. (1968). J. Mol. Biol. 32, 285-302.

101. Dressler, D. H., Denhardt, D. T. (1968). Nature 219, 346-351.

102. Gilbert, W., Dressler, D. (1968). Cold Spr. Harb. Symp. Quant. Biol. 33, 473-484.

103. Yokoyama, Y., Komono, T., Onodera, K. (1971). Agr. Biol. Chem. 35, 1353-1362.

104. Yokoyama, Y., Ohtaki, M., Komono, T., Onodera, K. (1971). Agr. Biol. Chem. 35, 1803-1805.

105. Johnson, P. H., Sinsheimer, R. L. (1974). J. Mol. Biol. 83, 47-61.

106. Razin, A., Sinsheimer, R. L. (1970). Proc. Nat. Acad. Sci. 66, 646-650.

107. Campbell, J. L., Soll, L., Richardson, C. C. (1972). Proc. Nat. Acad. Sci. 69, 2090-2094.

108. Hirota, Y., Gefter, M., Mindich, L. (1972). Proc. Nat. Acad. Sci. 69, 3238-3242.

109. DeLucia, P., Cairns, J. (1969). Nature 224, 1164-1166.

110. Knippers, R. (1970). Nature 228, 1050-1053.

111. Moses, R., Richardson, C. C. (1970). Biochim. Biophys. Res. Comm. 41, 1565-1571.

112. Kornberg, T., Gefter, M. L. (1971). Proc. Nat. Acad. Sci. 68, 761-764.

113. Carl, P. L. (1970). Mol. Gen. Genet. 109, 107-122.

114. Wechsler, J., Gross, J. D. (1971). Mol. Gen. Genet. 113, 273-284.

115. Gefter, M. L., Hiroto, Y., Kornberg, T., Wechsler, J. A., Barnoux, C. (1971). Proc. Nat. Acad. Sci. 68, 3150-3153.

116. Schekman, R., Wickner, W., Westergaard, O., Brutlag, D., Geider, K., Bertsch, L. L., Kornberg, A. (1972). Proc. Nat Acad. Sci. 69, 2691-2695.

117. Wickner, R. B., Wright, M., Wickner, S., Hurwitz, J. (1972). Proc. Nat. Acad. Sci. 69, 3233-3237.

118. Hiroto, Y., Ryter, A., Jacob, F. (1968). Cold Spr. Harb. Symp. Quant. Biol. 33, 677-693.

119. Bonhoeffer, F. (1966). Z. Vererbungsal. 98, 141-149.

120. Wickner, S., Wright, M., Hurwitz, J. (1974). Proc. Nat. Acad. Sci. 71, 783-787.

121. Tabak, H. F., Griffith, J., Geider, K., Schaller, H., Kornberg, A. (1974). Proc. Nat. Acad. Sci., submitted for publication.

122. Taketo, A. (1973). Mol. Gen. Genet. 122, 15-22.

123. Dumas, L. B., Miller, C. A. (1973). J. Virol. 11, 848-855.

124. Kranias, E. G., Dumas, L. B. (1974). J. Virol. 13, 146-154.

125. Schuback, W. H., Whitmer, J. D., Davern, C. I. (1973). J. Mol. Biol. 74, 205-221.

126. Greenlee, L. L. (1973). Proc. Nat. Acad. Sci. 70, 1757-1760.

127. Steinberg, R. A., Denhardt, D. T. (1968). J. Mol. Biol. 37, 525-528.

128. Nusslein, V., Otto, B., Bonhoeffer, F., Schaller, H. (1971). Nature New Biol. 234, 285-286.

129. Salivar, W. O., Sinsheimer, R. L. (1969). J. Mol. Biol. 41, 39-65.

130. Weisbeek, P. J., Van de Pol, J. H., Van Arkel, G. A. (1972). Virology 48, 456-462.

131. Kornberg, A. (1969). Science 163, 1410-1418.

132. Lee, A. S. (1974). Ph. D. Thesis, California Institute of Technology, Pasadena, California.

133. Wickner, W., Schekman, R., Geider, K. Kornberg, A. (1973). Proc. Nat. Acad. Sci. 70, 1764-1767.

134. Kornberg, T., Gefter, M. (1972). J. Biol. Chem. 247, 5369-5375.

135. Wickner, R. B., Ginsberg, B., Hurwitz, J. (1972). J. Biol. Chem. 247, 498-504.

136. Baas, P. D., Jansz, H. S. (1972). J. Mol. Biol. 63, 557-568.

137. Baas, P. D., Jansz, H. S. (1972). J. Mol. Biol. 63, 569-576.

138. Truffaut, N., Sinsheimer, R. L. (1974). J. Virol. 13, 818-827.

139. Sinsheimer, R. L. (1969). J. Cell Physiol. 74, 21-32.

140. Schröder, C., Kaener, H. C. (1971). FEBS Letters 19, 38-44.

141. Wechsler, J. A. (1973) in press. (From reference 114).

142. Dressler, D. (1970). Proc. Nat. Acad. Sci. 67, 1934-1942.

143. Jacob, F., Brenner, S., Cuzin, F. (1963). Cold Spr. Harb. Symp. Quant. Biol. 28, 329-348.

144. Ganesan, A. T., Lederberg, J. (1965). Biochem. Biophys. Res. Comm. 18, 824-835.

145. Denhardt, D. T., Sinsheimer, R. L. (1965). J. Mol. Biol. 12, 663-673.

146. Denhardt, D. T., Sinsheimer, R. L. (1965). J. Mol. Biol. 12, 674-694.

147. Denhardt, D. T., Silver, R. B. (1966). Virology 30, 10-19.

148. Datta, B., Poddar, R. K. (1970). J. Virol. 6,583-588.

149. Iwaya, M., Denhardt, D. T. (1973). J. Mol. Biol. 73, 279-290.

150. Schröder, C. H., Erben, E., Kaener, H. C. (1973). J. Mol. Biol. 79, 599-613.

151. Denhardt, D. T., Sinsheimer, R. L. (1965). J. Mol. Biol. 12, 641-646.

152. Knippers, R., Komono, R., Sinsheimer R. L. (1968). Proc. Nat. Acad. Sci. 59, 577-581.

153. Funk, F., Sinsheimer, R. L. (1970). J. Virol. 5, 282-288.

154. Burton, A., Sinsheimer, R. L. (1965). J. Mol. Biol. 14, 327-347.

155. Denhardt, D. T. (1972). J. Theor. Biol. 34, 487-508.

156. Okazaki, R., Okazaki, T., Sakabe, K., Sugimoto, K., Kainuma, R., Sugino, A., Swatsuki, N. (1968). Cold Spr. Harb. Symp. Quant. Biol. 33, 129-143.

157. Kozinski, A. W. (1969). Biochem. Biophys. Res. Comm. 35, 294-299.

158. Eisenberg, S., Denhardt, D. T. (1974). Proc. Nat. Acad. Sci. 71, 984-988.

159. Puga, A., Borrás, M. T., Tessman, E. S., Tessman, I. (1973). Proc. Nat. Acad. Sci. 70, 2171-2175.

160. Razin, A., Sedat, J., Sinsheimer, R. L. (1970). J. Mol. Biol. 53, 251-259.

161. Razin, A., Sedat, J., Sinsheimer, R. L. (1970). J. Mol. Biol. 78, 417-425.

162. Razin, A. (1973). Proc. Nat. Acad. Sci. 70, 3773-3775.

163. Goulian, M., Kornberg, A., Sinsheimer, R. L. (1967). Proc. Nat. Acad. Sci. 58, 2321-2328.

164. Iwaya, M., Eisenberg, S., Bartok, K., Denhardt, D. T. (1973). J. Virol. 12, 808-818.

165. Weisbeek, P. J., Sinsheimer, R. L. (1974). Proc. Nat. Acad. Sci. 71, 3054-3058.

166. Worcel, A., Burgi, E. (1974). J. Mol. Biol. 82, 91-105.

167. Stonington, O. G., Pettijohn, D. E. (1971). Proc. Nat. Acad. Sci. 68, 6-9.

168. Lerman, L. S. (1971). Proc. Nat. Acad. Sci. 68, 1886-1890.

169. Pettijohn, D. E., Hecht, R. M., Stonington, O. G., Stamato, T.D. (1973). Steenbock Symp. on DNA synthesis in vitro. University Park Press.

170. Fong, P. J. (1967). J. Theor. Biol. 15, 230-235.

171. Kilkson, R., Maestre, M. F. (1962). Nature 195, 494-495.

172. Maniatis, T., Venable, J. H., Lerman, L. S. (1974). J. Mol. Biol. 18, 37-64.

173. Richards, K. E., Williams, R. C., Calendar, R. (1973). J. Mol. Biol. 78, 255-259.

174. Greenlee, L. L. Sinsheimer, R. L. (1968). J. Mol. Biol. 32, 321-326.

175. Warner, J. R., Knopf, P. M., Rich, A. (1963). Proc. Nat. Acad. Sci. 49, 122-129.

176. Kuff, E. L., Roberts, N. E. (1967). J. Mol. Biol. 26, 211-225.

177. Godson, G. N., Sinsheimer, R. L. (1967). Biochim. Biophys. Acta 149, 489-495.

178. Alberts, B., Herrick, G. (1971). Methods Enzymol. 21, 198-217.

179. Takai, M. (1966). Biochim. Biophys. Acta 119, 20-28.

180. Catt, K., Tregear, G. W. (1967). Science 158, 1570-1571.

181. Sinsheimer, R. L. (1959). J. Mol. Biol. 1, 37-42.

182. Martin, R. G., Ames, B. N. (1961). J. Biol. Chem. 236, 1372-1379.

183. Denhardt, D. T. (1969). J. Biol. Chem. 244, 2710-2715.

184. Rachmeler, M., Gerhart, J., Rosner, J. (1961). Biochim. Biophys. Acta 49, 225-228.

185. Rahmanian, M., Oxender, D. L. (1972). J. Supramolecular Struc. 1, 55-59.

186. Burns, R. O., Calvo, J., Margolin, P., Umbarger, H. E. (1966). J. Bact. 91, 1570-1576.

187. Calvo, J. M., Freundlich, M., Umbarger, H. E. (1969). J. Bact. 97, 1272-1282.

188. Kohlhaw, G., Leary, T. R., Umbarger, H. E. (1969). J. Biol. Chem. 244, 2218-2225.

189. Somers, J. M., Amzallag, A., Middleton, R. B. (1973). J. Bact. 113, 1268-1272.

190. Yang, H. L., Kessler, D. P. (1974). J. Bact. 117, 63-72.

191. Burgess, R. R. (1971). Ann. Rev. Biochem. 40, 711-740.

192. Yamamoto, K. R., Alberts, B. M., Benzinger, R., Lawhorne, L., Treiber, G. (1970). Virology 40, 734-744.

193. Gschwender, H. H., Haller, W., Hofschneider, P. H. (1969). Biochim. Biophys. Acta 190, 460-469.

194. Burgess, R. R., Travers, A. A. (1971). Prog. Nuc. Acid Res. 2, 851-863.

195. Noll, H. (1969). Tech. in Prot. Biosynth. 2, 101-179.

196. Noll, H. (1967). Nature 215, 360-363.

197. Laemmli, U. K., Favre, M. (1973). J. Mol. Biol. 80, 575-599.

198. Barner, H. D., Cohen, S. S. (1954). J. Bacteriol. 68, 80-88.

199. Kato, A. C., Bartok, K., Fraser, M. J., Denhardt, D. T. (1973). Biochim. Biophys. Acta 308, 68-78.

200. Attardi, G. (1967). Ann. Rev. Microbiol. 21, 383-416.

201. Spitnik-Elson, P., Atsmon, A.(1969). J. Mol. Biol. 45, 113-124.

202. Soloman, A. K. (1962). Biophy. J. 2, 79-95.

203. Von Hippel, P. H., McGhee, J. D. (1972). Ann. Rev. Biochem. 26, 231-300.

204. Bauer, D. J.(1972). Chemotherapy of Virus Diseases 1, Pergamon Press.

205. Ptashne, M. (1967). Nature 214, 232-234.

206. Gilbert, W., Müller-Hill, B. (1967). Proc. Nat. Acad. Sci. 58, 2415-2521.

207. Albert, B. M. (1971). In Nucleic Acid-Protein Interactions and Nucleic Acid Synthesis in Viral Infection (Ribbons, D. W., Woessner, J. F., Schultz, J., eds). pp. 128-243, Amsterdam, North Holland.

208. Kelley Jr., T. J., Smith, H. O. (1970). J. Mol. Biol. 51, 393-409.

209. Wilson, D. A., Thomas, C. A. (1974). J. Mol. Biol. 84, 115-144.

210. Szybalski, W., Iyer, V. N. (1967). Antibiotics 1, 211-245.

211. Laemmli, U. K. (1970). Nature 227, 680-685.

212. Dickson, R. C., Barnes, C. L., Eiserling, F. A. (1970). J. Mol. Biol. 53, 461-474.

213. Hosoda, J., Cone, R. (1970). Proc. Nat. Acad. Sci. 66, 1275-1281.

214. Kellenberger, E., Kellenberger-Van der Kamp, C. (1970). FEBS Letters 8, 140-144.

215. Lengyel, J. A., Goldstein, R. N., Marsh, M., Sunshine, M. G., Calendar, R. (1973). Virology 53, 1-25.

216. Georgopoulos, C. P., Hendrix, R. W., Casjens, S. R., Kaiser, A. D., (1973). J. Mol. Biol. 76,45-60.

217. Hendrix, R. W., Casjens, S. R. (1974). Manuscript on protein fusion.

218. Hendrix, R. W., Casjens, S. R. (1974). Manuscript on protein fission.

219. Botstein, D., Waddell, C. H., King, J. (1973). J. Mol. Biol. 80, 669-695.

220. King, J., Lenk, E. U., Botstein, D. (1973). J. Mol. Biol. 80, 697-731.

221. Kaiser, D., Masuda, T. (1973). Proc. Nat. Acad. Sci. 70, 260-264.

222. Kerr, C., Sadowski, P. D. (1974). In press.

223. Hohn, B., Wurtz, M., Klein, B., Lustig, A., Hohn, T. (1974). In press.

224. Serwer, P. (1972). Ph. D. Thesis, Harvard University, Cambridge, Massachusetts.

225. Clements, J. B., Sinsheimer, R. L. (1974). J. Virol. In press.

226. Hayashi, Y., Hayashi, M. (1970). Cold Spr. Harb. Symp. Quant. Biol. 35, 171-177.

227. Pettijohn, D. E. (1974). Seminar, California Institute of Technology, Pasadena, California.

228. Radloff, R., Bauer, W., Vinograd, J. (1967). Proc. Nat. Acad. Sci. 57, 1514-1521.

229. Hudson, B., Upholt, W. B., Devinny, J., Vinograd, J. (1969). Proc. Nat. Acad. Sci. 62, 813-820.

230. Fukuda, A., Sinsheimer, R. L. (1973). Manuscript in preparation.

231. Hanawalt, P. C., Ray, D. S. (1964). Proc. Nat. Acad. Sci. 52, 125-132.

232. Ben-Porat, T., Stere, A., Kaplan, A. S. (1962). Biochim. Biophys. Acta 61, 150-152.

233. Kushner, D. J. (1969). Bacteriol. Rev. 33, 302- 345.

234. Uhr, J. W., Dancis, J., Franklin, E. C., Finkelstein, M. S., Lewis, E. W. (1962). J. Clin. Invest. 41, 1509-1513.